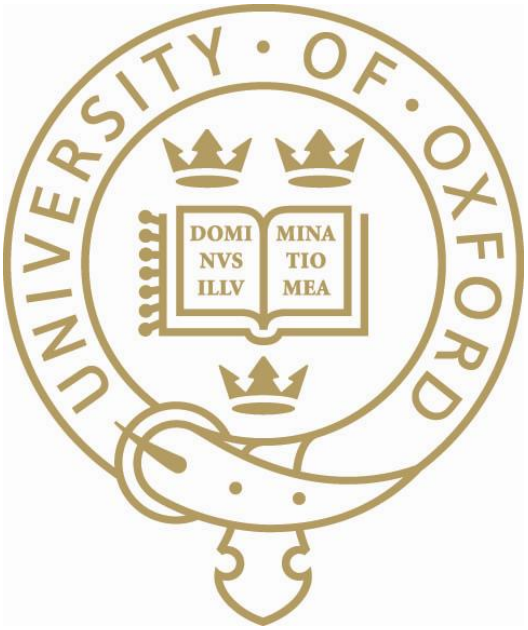

Investigating the Role of the Fat Mass and Obesity Associated Gene (*Fto*) in Obesity

Fiona McMurray

DPhil Candidate

Department of Biochemistry,
Wolfson College, University of Oxford

Genetics of Type 2 Diabetes,
MRC Mammalian Genetics Unit, Harwell

MRC Mammalian Genetics Unit

Investigating the Role of the Fat Mass and Obesity Associated Gene (*Fto*) in Obesity

Fiona McMurray

Department of Biochemistry, Wolfson College, University of Oxford

Genetics of Type 2 Diabetes, MRC Mammalian Genetics Unit, Harwell

A thesis presented for the degree of Doctor of Philosophy, Trinity Term, 2013

Abstract

In 2007, a genome wide association study identified a SNP in intron 1 of *FTO* with increased BMI. Homozygous risk allele carriers are on average three kg heavier than those homozygous for the protective allele. Mouse models have been made, including a conditional knockout, which is lean when globally expressed, as well as a conditional overexpression allele, which has increased body weight when globally expressed. The results from these and other studies suggest that the *FTO* SNPs lead to weight gain by increasing FTO activity and/or expression.

Adult inactivation of *Fto* using the tamoxifen inducible Cre demonstrated that removal of *Fto* may be as deleterious as overexpression, with the adult knockout mice having increased fat mass and decreased lean mass. It also supported the role FTO plays in development as adult inactivation of *Fto* did not increase mortality rates as seen in the global $Fto^{-/-}$ pups. This study also revealed the importance of effective energy expenditure analysis in the mouse.

I have confirmed a link between $Fto^{-/-}$ and increased mortality, which may be caused by alterations to developmental processes. $Fto^{-/-}$ reduces cilia formation in MEFs and results in dysregulated cilia formation in specific tissues in $Fto^{-/-}$ embryos. Levels of FTO also appear to affect adipogenic differentiation, which could be due to altered WNT/β-CATENIN signalling.

Pharmacological inhibition of FTO was a success *in vitro* and a compound screen identified FG2216, which could be used *in vivo* to inhibit FTO. The *in vivo* effects of FG2216 at 60 mg/kg/2days did not affect body weight or composition in the mouse.

My research suggests that there is dysregulation of gut hormones and neuronal signalling pathways in the FTO overexpression mice, which could cause the hyperphagia and increased body weight.

These studies add to our current knowledge of FTO function, and suggest a role for FTO in control of body composition, development, and satiety signalling.

Publications arising from work presented in this thesis:

McMurray F, Church CD, Larder R, Nicholson G, Wells S, Teboul L, Tung YCL, Rimmington D, Bosch F, Jimenez V, Yeo GSH, O'Rahilly S, Ashcroft FM, Coll AP, Cox RD. Adult onset global loss of the *Fto* gene alters body composition and metabolism in the mouse. *PLOS Genetics* 2013 January; 9(1):e1003166.

Osborn DPS, Roccasecca RM, **McMurray F**, Hernandez-Hernandez V, Mukherjee S, Barroso I, Stemple D, Cox RD, Beales PL, Christou-Savina S. Loss of FTO anatagonises Wnt signalling and leads to developmental defects associated with ciliopathies. (Manuscript in preparation)

Publications arising from DPhil:

Church C, Moir L, **McMurray F**, Girard C, Banks GT, Teboul L, Wells S, Brüning JC, Nolan PM, Ashcroft FM, Cox RD. Overexpression of Fto leads to increased food intake and results in obesity. *Nature Genetics*, 2010 December; 42(12):1086-92.

McMurray F and Cox RD. Mouse Models and Type 2 Diabetes: Translational Opportunities. *Mammalian Genome*. 2011 August; 22(7-8):390-400.

McMurray F, Moir L and Cox RD. From Mice to Humans. *Current Diabetes Reports*. 2012 December; 12(6): 651–658

Acknowledgements

I am grateful to my supervisor Professor Roger Cox for his help and support during my time at MRC Harwell. Your experience, gentle guidance, and open office door, have helped me to develop my ideas. I would also like to thank all of the members of the Cox Group, past and present, including Lee Moir, Alison Hough, Elizabeth Bentley, Michelle Goldsworthy, Christopher Church, Daniel Andrew, Thomas Agnew, Nor Muhsin, and Sneha Anand for all of their help in the lab, supportive coffee breaks and making the lab a welcoming and enjoyable place to be. I would also like to thank the extended members of the group, Myrte Merkestein and Lukasz Stasiak; you are wonderful people and have been fantastic additions to the FTO team. During my DPhil I have had a number of fantastic opportunities to collaborate with labs in Oxford, MRC Harwell and beyond. I would especially like to thank Professor Frances Ashcroft and Professor Christopher Schofield and their lab members including Sheena Lee, Holger Kramer, James McTaggart, Wei Shen Aik and Michael McDonough for supporting my research into FTO.

I have thoroughly enjoyed my time at MRC Harwell over the last five years. I would like to thank Dr. Charlotte Dean for taking me on as a graduate intern, and Laura Yates for helping me find my feet in the lab and Oxford all those years ago. You were both very patient with me and provided fantastic support and advice. During my time here I have made full use of the facilities including histology, clinical chemistry, bioimaging, necropsy, transgenics and gene targeting, proteomics, bioinformatics and GEMS. I am also indebted to the members of the Mary Lyon Centre, in particular Ward 4, including Sara Wells, Lucie Vizor, Lisa Ireson and Tamzin Osborne for supporting my research and carrying out essential animal work.

I would like to thank my supportive parents Alan and Bridget McMurray, without your love and encouragement I would not be where I am today. I hope you can be proud of my research and I dedicate this thesis to you. I would also like to thank the rest of my family and my brother Iain for always being there. I also thank all of the fantastic friends I have made whilst at MRC Harwell and the University of Oxford, especially Sarah Rollauer, Eachan Johnson, David Marshall, Louise Walport, Anne Grijzenhout, Jerome Ma, Hannah Long, Christopher Jones, Elizabeth Milway, and Laura Molloy, and one of my oldest friends Kelly Evans, you have helped to keep me sane during the last few years, and made my time in Oxford unforgettable. I also want to thank my partner Dan Murrin for your love, patience and always brightening my day. I hope we will have an incredible time together in Canada.

I would like to thank the Medical Research Council for funding this research and my DPhil.

Table of Contents

Table of Figures

Table of Tables

Abbreviations

1-meA	1-Methyladenine
1-meG	1-Methylguanidine
2OG	2-Oxoglutarate
3-meC	3-Methylcytosine
3-meT	3-Methylthymine
3-meU	3-Methyluracil
3'UTR	3' Untranslated Region
4E-BP1	Eukaryotic Initiation Factor 4E-Binding Protein 1
6-meA	N6-Methyladenine
A	Adrenaline
AAV	Adeno-Associated Virus
AARS	Aminoacyl-tRNA synthetase
ABH	AlkB Homologue
ACC	Acetyl CoA Carboxylase
ADP	Adenosine-5'-Diphosphate
AgRP	Agouti-Related Protein
AMP	Adenosine Monophosphate
AMPK	Adenosine Monophosphate-Activated Kinase
AmpR	Ampicilin Resistant
ANOVA	Analysis of Variance
AP	Area Postrema
ARC	Arcuate Nucleus
ATG	Autophagy-Related
ATP	Adenosine-5'-Triphosphate
AUC	Area Under the Curve
AVP	Vasopressin
BAT	Brown Adipose Tissue
BBB	Blood-Brain-Barrier
BBS	Bardet-Biedel Syndrome
BMD	Bone Mineral Density
BMI	Body Mass Index
BP	Blood Pressure
BSA	Bovine Serum Albumin
CAMKKβ	Calmodulin-Dependent Protein Kinase Kinase β
cAMP	Cyclic AMP
CART	Cocaine and Amphetamine-Regulate Transcript
CCK	Cholecystokinin
CCK1R	CCK 1-Receptor
CCK2R	CCK 2-Receptor
CNR1	Cannabinoid Receptor 1
CNS	Central Nervous System
CPT1	Carnitine Palmitoyltransferase-1
CREB	cAMP Response Element-Binding Protein
CRF	Corticotrophin-Releasing Hormone

CRTC2	CREB-Regulated Transcription Coactivator 2
CT	Computed Tomography
CUTL1	Cut-Like Homeobox 1 Protein
CUX1	Cut-Like Homeobox 1 Gene
CV	Caloric Value
DEXA	Dual-Energy X-ray Absorptiometry
DIO	Diet Induced Obesity
DMH	Dorsomedial Hypothalamus
DMOG	Dimethyloxalylglycine
DRD2	Dopamine Receptor D2
DRN	Dorsal Raphe Nucleus
dsDNA	Double Stranded DNA
E	Embryonic Day
ECAR	Extracellular Acidification Rate
E.coli	*Escherichia coli*
EnR	Energy Restriction
ENU	N-Ethyl-N-Nitrosourea
ER	Endoplasmic Reticulum
ES cells	Embryonic Stem Cells
ESRD	End Stage Renal Disease
FIP200	200 kDa FAK Family Kinase-Interacting Protein
fMRI	Functional Magnetic Resonance Imaging
FOXO	Forkhead Box Protein O
Ft	Fused Toes
FTO	Fat Mass and Obesity Associated
GHRH	Growth Hormone Releasing Hormone
GHS-R1a	Growth Hormone Secretagogue Receptor-1a
GIANT	Genetic Investigation of ANthropometric Traits
GIP	Gastric Inhibitory Polypeptide
GIRK	G protein-Coupled Inwardly-Rectifying Potassium Channel
GLP-1	Glucagon-Like Peptide 1
GLUT4	Glucose Transporter Type 4
GS	Glycogen Synthase
GWAS	Genome-Wide Association Study
HDAC	Histone Deacetylase
HDL	High Density Lipoprotein
H&E	Haematoxylin and Eosin
HFD	High Fat Diet
HIF	Hypoxia-Inducible Factor
HR	Homologous Recombination
HTR2C	Serotonin Receptor 2C
IL	Interleukin
IP	Intraperitoneal
IPGTT	Intraperitoneal Glucose Tolerance Test
IRS1	Insulin Receptor Substrate 1
KHB	Krebs Henseleit Buffer
KO	Knockout
LB	Luria Bertani

LD	Linkage Disequilibrium
LDL	Low Density Lipoprotein
LH	Lateral Hypothalamus
LKB1	Liver Kinase B1
LNAAs	Large Neutral Amino Acids
LRS	Leucyl-tRNA Synthetase
MCH	Melanin-Concentrating Hormone
MEFs	Mouse Embryonic Fibroblasts
min	Minute
MRI	Magnetic Resonance Imaging
MS	Mass Spectrometry
MSC	multi-synthetase complex
mTOR	Mammalian Target of Rapamycin
mTORC	Mammalian Target of Rapamycin Complex
NA	Noradrenaline
NAcc	Nucleus Accumbens
NAD^+	Nicotinamide Adenine Dinucleotide
NMR	Nuclear Magnetic Resonance
NPY	Neuropeptide Y
NTS	Nucleus of the Solitary Tract
ob	Obese
OCR	Oxygen Consumption Rate
OXM	Oxyntomodulin
OXT	Oxytocin
P	Postnatal Day
PCOS	Polycystic Ovaries Syndrome
PCR	Polymerase Chain Reaction
PDK1	3-Phosphoinositide-Dependent Protein Kinase 1
PFK2	Phosphofructokinase 2
PGC1α	Peroxisome Proliferator-Activated Receptor-γ Coactivator 1α
PHD	Prolyl Hydroxylase
PHI	Prolyl Hydroxylase Inhibitor
PI3K	Phosphoinositide 3-Kinase
POMC	Pro-Opiomelanocortin
PP	Pancreatic Polypeptide
PPARγ	Peroxisome Proliferator-Activated Receptor-γ
PrRP	Prolactin-Releasing Peptide
PTEN	Phosphatase and Tensin Homolog
PVN	Paraventricular Nucleus
PYY	Peptide-Tyrosine-Tyrosine
QTLs	Quantitative Trait Loci
RBL2	Retinoblastoma Like 2
RER	Respiratory Exchange Ratio
Rheb	Ras Homolog Enriched in Brain
RPGRIP1L	Retinitis Pigmentosa GTPase Regulator-Interacting Protein 1-like
S6K	Ribosomal S6 Kinase
SD	Standard Diet
SEM	Standard Error of the Mean

SGBS	Simpson-Golabi-Behmel Syndrome
SHH	Sonic Hedgehog
SIRT	Sirtuin
SNP	Single Nucleotide Polymorphism
SON	Supraoptic Nucleus
SREBP	Sterol Regulatory Element-Binding Protein
ssDNA	single stranded DNA
T2DM	Type 2 Diabetes Mellitus
TAK1	TGF-β-Activated Kinase 1
TALENs	Transcription Activator Like Effector Nucleases
TGF-β	Transforming Growth Factor-β
TRH	Thyrotropin-Releasing Hormone
TNFα	Tumor Necrosis Factor-α
TSC1/2	Tuberous Sclerosis 1/2
ULK	UNC-51-Like Kinase
UV	Ultra-Violet
v-ATPase	Vacuolar H^+-Adenosine Triphosphatase
VCO_2	Carbon Dioxide Production
VMN	Ventromedial Nucleus
VO_2	Oxygen Consumption
VTA	Ventral Tegmental Area
WAT	White Adipose Tissue
WHR	Waist Hip Ratio
Y1R	Neuropeptide Y Receptor 1
Y2R	Neuropeptide Y Receptor 2
Y5R	Neuropeptide Y Receptor 5
ZFNs	Zinc Finger Nucleases

Chapter 1:

Introduction

1.1 Obesity

The incidence of obesity has reached epidemic proportions; 33 % of the world's adult population were overweight or obese in 2005, and if this trend continues 57.8 % could be overweight or obese by 2030 (Kelly *et al*., 2008). Excessive weight can lead to morbidity and premature mortality, as it predisposes to type 2 diabetes mellitus (T2DM), cardiovascular disease and many forms of cancer (Kopelman, 2007).

The terms overweight and obese refer to a subject who has abnormal or excessive fat accumulation that may impair their health. There are several ways of classifying these patients. The most common is by using body mass index (BMI). This is simple to measure and is calculated by weight in kilograms divided by height in meters (kg/m^2). Adiposity and BMI generally have a high correlation, and those with a BMI of ≥ 25 are considered overweight with an increased risk of co-morbidities, and ≥ 30 as obese with a moderate risk of co-morbidities (WHO, 2000). These standards are based on Europids and may not be accurate at assessing morbidities in other ethnic groups (WHO, 2000).

The distribution of fat is an important factor to consider and BMI does not always reflect abdominal obesity. Abdominal obesity can be estimated easily using waist measurements (WHO, 2008a). Waist circumferences should be measured in the midpoint between the lower margin of the last palpable rib and the top of the iliac crest, and hip circumference around the widest portion of the buttocks (WHO, 2008b). In Caucasians a waist circumference of more than 88 cm increases risk of morbidity and mortality, such as cardiovascular disease (Han *et al*., 1995, James, 1996). Using the waist and hip measurements to calculate a waist hip ratio (WHR) >1.0 for men and

>0.85 in women indicate abdominal fat accumulation (James, 1996). Fat distribution can be measured most accurately using serial magnetic resonance imaging (MRI), computed tomography (CT), or by dual-energy X-ray absorptiometry (DEXA), or just a single CT or MRI scan at lumbar region 3/4 (WHO, 2000). The amount of fat in the area can then be assessed and in Caucasians those with less than 110 cm^2 are classified as low risk, and those with fat levels greater than 130 cm^2 have an increased risk of cardiovascular disease and or other morbidities (WHO, 2000).

1.1.1 Obesity and Energy Homeostasis

Increased weight gain occurs when energy input exceeds energy output. Modern lifestyles with an abundance of palatable energy-rich foods and lack of physical activity can result in a metabolic imbalance, increasing the risk of obesity (Swinburn *et al*., 2011). Numerous feedback loops exist in the body to regulate energy balance and food intake. Various genetic studies in the mouse and man have demonstrated the importance of the brain in the control of energy intake and body weight (Schwartz and Porte, 2005, Yeo and Heisler, 2012). An overview of the neuroendocrine system regulating food intake can be seen in **Figure 1.1**. The various nuclei and their connections involved in food intake in relation to energy homeostasis and reward behaviour are highlighted.

When there is an imbalance in energy homeostasis, and energy intake exceeds energy expenditure this can activate a response in multiple cells-types, such as: endothelial cells, hepatocytes, myocytes, adipocytes and immune cells (Wisse *et al*., 2007). Increased nutrients lead to increases in reactive oxygen species (ROS) levels, which can cause oxidative damage to cellular structures and trigger an inflammatory response (Hotamisligil, 2006). Nutrient excess can also cause endoplasmic reticulum (ER) stress, activating a response where unfolded or misfolded proteins accumulate in the ER, the unfolded protein response (Hotamisligil, 2006). This halts translation and activates signalling pathways which increase production of molecular chaperones to improve protein folding. If the stress is not resolved this can lead to apoptosis and stimulation of inflammatory signalling pathways.

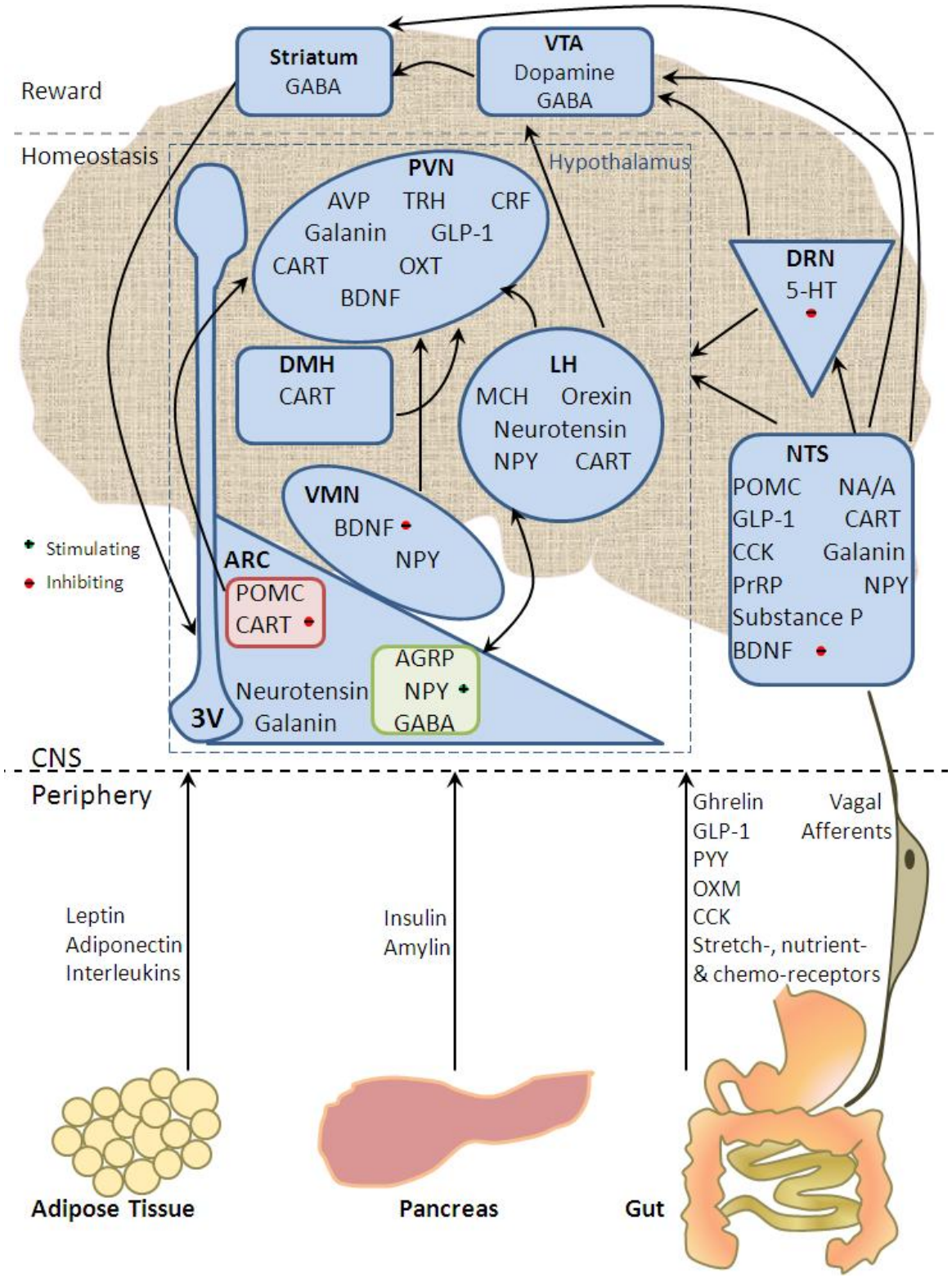

Figure 1.1 Schematic Representation of Regions Involved in Regulation of Energy Intake. Brain Regions: PVN, paraventricular nucleus; DMH, dorsomedial hypothalamus; VMN, ventromedial nucleus; LH, lateral hypothalamus; ARC, arcuate nucleus; VTA, ventral tegmental area; DRN, dorsal raphe nucleus; NTS, nucleus of the solitary tract. Signalling molecules: AGRP, Agouti-related protein; CART, cocaine and amphetamine-regulate transcript; CRF, corticotrophin-releasing hormone; GLP-1, glucagon-like peptide 1; MCH, melanin-concentrating hormone; OXT, oxytocin; AVP, vasopressin; TRH, thyrotropin-releasing hormone; NPY, Neuropeptide Y; NA, noradrenaline; A, adrenaline; POMC, Pro-opiomelanocortin; PrRP, prolactin-releasing peptide; PYY, Peptide-tyrosine-tyrosine; OXM, oxyntomodulin; CCK, cholecystokinin. Projections between nuclei in the central nervous system (CNS) are indicated by arrows. Sites of action of neuropeptides and neurotransmitters inhibiting (-) or stimulating (+) food intake are shown [Adapted from (Rask-Andersen *et al*., 2010) and (Yeo and Heisler, 2012)].

Sufficient nutrient levels are important for growth, development and maintenance throughout the organism. Therefore several homeostatic signalling networks have evolved to monitor energy status (summarised in **Figure 1.2**). Hydrolysis of adenosine-5'-triphosphate (ATP) to adenosine-5'-diphosphate (ADP) and phosphate (or adenosine monophosphate (AMP) and pyrophosphate) allows energy consuming processes to take place within the cell. ATP is generated by oxidising metabolites such as glucose, fatty acids and amino acids. Adenosine monophosphate-activated kinase (AMPK) senses the ratios of ATP to ADP and AMP in the cell. AMPK, which is ubiquitously expressed, allows the cell to react to increased energy demands and when active promotes catabolic pathways to produce more ATP, such as increased glucose transporter translocation and mitochondrial biogenesis, and antagonises anabolic pathways which consume and store energy, such as synthesis of glycogen and fatty acids (Yuan *et al*., 2013).

The ubiquitously expressed mammalian target of rapamycin (mTOR) is a serine/threonine kinase which monitors cellular amino acid levels and influences cell growth. Two different protein complexes contain mTOR, mTORC1 and mTORC2. These are distinguishable by the complex containing Raptor and Rictor accessory proteins respectively. Amino acid levels affect mTORC1; however mTORC2 is regulated by insulin, growth factors, serum, and nutrient levels (Zoncu *et al*., 2011, Kim *et al*., 2012). Feeding raises levels of amino acids and glucose, which converge to activate both of the mTORCs. Activation of mTORC1 leads to an increase in translation, lipogenesis and inhibits autophagy, and mTORC2 promotes glucose import and glycogen synthesis [**Figure 1.2** (Yuan *et al*., 2013)]. In the fasted state, when nutrient levels are decreased, mTORC activation decreases and levels of autophagy, gluconeogenesis and lipolysis can increase. This leads to an increase in free metabolites which can be used to generate ATP. Unlike AMPK, mTOR activation increases anabolic processes, such as protein synthesis, to increase growth.

Along with downregulating mTOR calorie restriction has been shown to activate the sirtuin (SIRT) class of proteins, and increase longevity in some species (Cohen *et al*., 2004, Wood *et al*., 2004). These proteins are nicotinamide adenine dinucleotide (NAD^+)-dependent deacetylases and mono-ADP-ribosyl transferases which can regulate processes involved in metabolism and stress

responses (Michan and Sinclair, 2007). When activated SIRT1 can promote fat mobilisation, decrease glycolysis and induces oxidative phosphorylation genes and mitochondrial biogenesis (Michan and Sinclair, 2007). SIRT3 and SIRT4 are found in the mitochondria and SIRT3 has been shown to decreases membrane potential and the generation of reactive oxygen species, whilst increasing cellular respiration (Shi *et al*., 2005). SIRT4 can downregulate glutamate dehydrogenase to decrease the amino-acid-stimulated insulin secretion in pancreatic *β*-cells (Haigis *et al*., 2006).

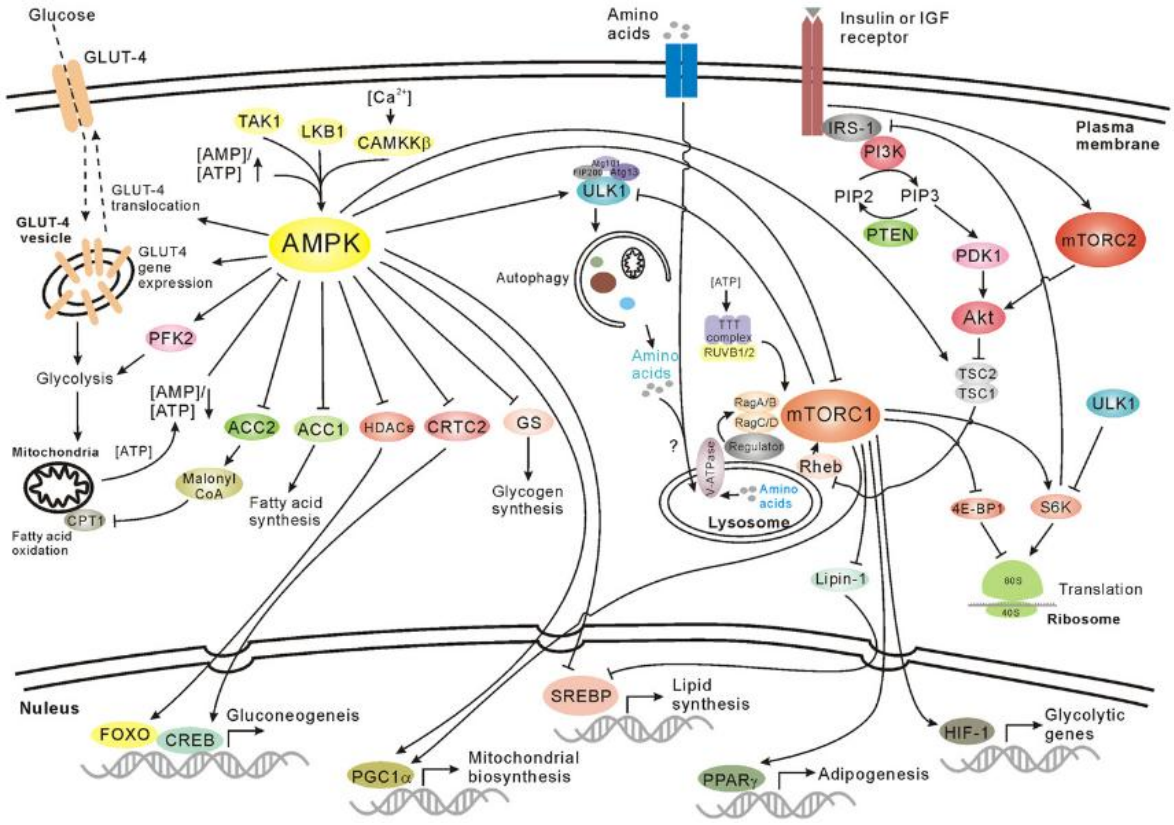

Figure 1.2 Nutrient-Sensing and Metabolism Pathways. AMP-activated kinase (AMPK) is activated by energy stress and promotes catabolic pathways to produce ATP while switching off ATP-consuming anabolic pathways. In contrast, mammalian target of rapamycin complex 1 (mTORC1) activation under nutrient sufficiency leads to significant elevation of anabolic processes, such as protein and lipid synthesis. Abbreviations: GLUT4, glucose transporter type 4; CPT1, carnitine palmitoyltransferase-1; TAK1, TGF-β-activated kinase 1; LKB1, liver kinase B1; CAMKKβ, calmodulin-dependent protein kinase kinase β; ACC, acetyl CoA carboxylase; PFK2, phosphofructokinase 2; GS, glycogen synthase; HDACs, histone deacetylases; CRTC2, CREB-regulated transcription coactivator 2; FOXO, forkhead box protein O; CREB, cAMP response element-binding protein; ULK, UNC-51-like kinase; FIP200, 200 kDa FAK family kinase-interacting protein; ATG, autophagy-related; PI3K, phosphoinositide 3-kinase; IRS1, insulin receptor substrate 1; PTEN, phosphatase and tensin homolog; PDK1, 3-phosphoinositide-dependent protein kinase 1; TSC1/2, tuberous sclerosis 1/2; Rheb, Ras homolog enriched in brain; v-ATPase, vacuolar H^+-adenosine tri-phosphatase; 4E-BP1, eukaryotic initiation factor 4E-binding protein 1; S6K, ribosomal S6 kinase; Ragulator, a protein complex responsible for lysosomal recruitment and activation of Rag GTPases; PGC1α, peroxisome proliferator-activated receptor-γ coactivator 1α; PPARγ, peroxisome proliferator-activated receptor-γ; SREBP, sterol regulatory element-binding protein; HIF, hypoxia-inducible factors. Stimulatory interactions are indicated with ↑, and inhibitory interactions are indicated with ⊤. Image taken from (Yuan *et al*., 2013).

1.1.2 Adiposity signals

Adipose tissue stores fat, and normally its mass is maintained within a narrow range by homeostatic mechanisms. White adipose tissue (WAT) is used to store excess fat, and insulate the organs, whilst brown adipose tissue (BAT) is primarily for generating heat and is derived from the same lineage as muscle (Timmons *et al*., 2007). There is also a third type of fat which has been called 'beige' or 'brite' (brown in white) or 'inducible' to distinguish brown adipocytes that appear in WAT after permanent thermogenic induction or pathways that elevate intracellular cyclic AMP (cAMP) (Wu *et al*., 2012). In adult humans the BAT is composed of these beige/brite cells (Wu *et al*., 2012).

As well as storing energy, adipose tissue also communicates to the body the level of fat stored by secreting various adipokines, this allows coordination between energy intake and expenditure to regulate body weight. These adipokines include leptin, adiponectin, resistin and a variety of interleukins (ILs) as indicated in **Figure 1.1**.

Leptin levels correlate closely with the levels of adipose tissue (Maffei *et al*., 1995). Leptin acts on leptin receptors present in the hypothalamus, stimulating POMC and inhibiting AgRP and NPY expressing neurons, causing satiety (Farooqi and O'Rahilly, 2008). Leptin receptors are also expressed in many other tissues and the leptin-melanocortin pathway has been shown to be involved in energy homeostasis, glucose metabolism, reproduction, angiogenesis, immunity, gastrointestinal function, wound healing, bone remodelling and cardiovascular function (Lancha *et al*., 2012). A mutation in the leptin gene is responsible for the phenotype of the obese (*ob/ob*) mice (Friedman *et al*., 1991, Zhang *et al*., 1994). The homozygote animals become progressively overweight, hyperphagic and developed severe insulin resistance (Ingalls *et al*., 1950, Garthwaite *et al*., 1980). These mice and others with similar mutations in leptin [for example (Hong *et al*., 2010)] are leptin deficient. Leptin deficient mutations do also occur in some obese human patients, although these mutations are rare in the general population (Farooqi and O'Rahilly, 2008).

Unlike leptin serum levels of adiponectin have been shown to be inversely proportional to BMI (Arita *et al*., 1999). Adiponectin knockout mice exhibit severe diet induced insulin-resistance, increased inflammatory markers and impaired fatty acid clearance levels (Maeda *et al*., 2002). Adiponectin administration in rodent models of obesity-associated diabetes lowers blood glucose and improves insulin sensitivity (Berg *et al*., 2001, Combs *et al*., 2002). These and other studies have demonstrated the importance of adiponectin and its protective effect in developing insulin resistance. In obesity WAT has been shown to produce inflammatory cytokines such as tumour necrosis factor-α (TNFα), IL-6 and transforming growth factor-β (TGF-β) in mice and man. These inflammatory processes are linked with metabolic dysfunction, and can be reversed with weight loss (Hotamisligil *et al*., 1993, Hotamisligil *et al*., 1995, Samad *et al*., 1997, Fried *et al*., 1998, Esposito *et al*., 2003). Taken together WAT appears to have an important role in food intake, and development of metabolic dysfunction.

1.1.3 Pancreatic Signalling

Glucose homeostasis is maintained by the pancreas, and dysfunction can result in Diabetes. Increased glucose levels cause secretion of insulin from the β-cells. Insulin acts on tissues to increase glucose uptake, allowing the excess glucose to be stored as glycogen and triglyceride. As well as these peripheral effects, insulin can also act on the brain to reduce food intake, and insulin receptor deficiency results in increased food intake (Bruning *et al*., 2000).

Glucagon, which is secreted from α-cells has catabolic effects, such as gluconeogenesis and glycogenolysis and opposes the actions of insulin. It also reduces food intake by acting as a satiety signalling factor in the brain (Habegger *et al*., 2010). The pancreas also produces amylin and pancreatic polypeptide (PP), which both have been shown to reduce gastric emptying and food intake (Lancha *et al*., 2012).

1.1.4 Gut hormones

The gastrointestinal tract is responsible for breaking down the food we ingest into the nutrients we need and excreting the indigestible parts. It is therefore not surprising that it also produces a variety of hormones and neural signalling to inform the body that food has been ingested, which effect feeding behaviour.

Ghrelin is the only orexigenic gut peptide and is secreted from the stomach, whereas the others CCK, gastric inhibitory polypeptide (GIP), GLP-1, OXM and PYY are all anorexigenic (Karra and Batterham, 2009). An overview of each of these peptides action and secretion site is shown in **Table 1.1**.

Table 1.1 Summary of Gut Hormone Function and Site of Action. Abbreviations: CCK1R, CCK 1-receptor; CCK2R, CCK 2-receptor; GHS-R1a, Growth hormone secretagogue receptor-1a; GIPR, gastric inhibitory polypeptide receptor; GLP-1R, GLP-1 receptor; Y1R, neuropeptide Y receptor 1; Y2R, neuropeptide Y receptor 2; Y5R, neuropeptide Y receptor 5; SON, supraoptic nucleus; GHRH, Growth hormone releasing hormone. (Karra and Batterham, 2009, Lancha *et al*., 2012).

Hormone	Effect	Origin	Receptor	Site of Action
CCK	Anorexigenic	I-cells in the mucosal epithelium of the small intestine.	CCK1R, CCK2R	Vagus nerve, brain-stem, hypothalamus
Ghrelin	Orexigenic	X/A-like cells of the gastric oxyntic glands of the stomach	GHS-R1a	NPY/AgRP within the ARC, pituitary gland, brain-stem. GHRH neurons
GIP	Anorexigenic	K cells of the duodenum and jejunum	GIPR	Pancreas; ARC, PVN, SON and brainstem
GLP-1	Anorexigenic	Intestinal L-cells	GLP-1R	Pancreas; CNS ARC, PVN, SON and brainstem
OXM	Anorexigenic	Intestinal L-cells	GLP-1R	ARC, GI tract, Pancreas
PYY	Anorexigenic	Intestinal L-cells	Y1R,Y2R, Y5R	NPY/AgRP within the ARC

1.1.5 Pharmacological and Surgical Intervention

Increased physical activity and decreased energy intake can have a positive effect on weight loss, although these lifestyle changes require a lifelong commitment to maintain a healthy weight. A variety of pharmacological interventions have been trialled, but with limited success. In the U.K. over 120 medications have been tested in clinic trials, however only Orlistat has made it to the

market and not been withdrawn due to concern over side-effects (Hainer and Hainerova, 2012, NHS UK, 2012). Orlistat is a reversible inhibitor of gastrointestinal lipase, reducing the amount of dietary fat broken down and absorbed. It is also thought to improve release of gut hormones increasing satiety (Olszanecka-Glinianowicz *et al*., 2013). There are several emerging medications that may aid in the treatment of obesity such as Lorcaserin, a $5HT_{2C}$ receptor agonist, and Phentermine-topiramate, a combination of an amphetamine (Phentermine) and an anti-convulsant (Topiramate), which has weight-loss side-effects (Taylor *et al*., 2013).

There is extensive evidence that bariatric surgery is safe and highly effective in reducing weight, obesity-associated co-morbidities, and mortality (Buchwald *et al*., 2004, Sjostrom *et al*., 2012). Several different procedure options are available which are classed as either restrictive or mal-absorptive (Kissler and Settmacher, 2013). Adjustable gastric banding and sleeve gastrectomy are classed as restrictive. Roux-en-Y gastric bypass is a more complex mixture of the two effecting gut hormone responses to food intake, and bilio-pancreatic diversion with or without duodenal switch is mainly mal-absorptive with a minor restrictive component. (Kissler and Settmacher, 2013). Some of these surgical approaches, such as Roux-en-Y can also reverse T2DM and hyperlipidaemia (Berthoud, 2013).

A greater understanding of the causes and complications of obesity are needed so that future therapies can be efficacious.

1.2 Genetics of Obesity

The modern obesity epidemic may have an evolutionary origin. Man may have evolved to take advantage in times of plenty to survive in times of adversity, which due to modern lifestyles has resulted in the obesity epidemic. In 1962 Neel proposed this "thrifty" genotype hypothesis, that the modern environment was responsible for the increased levels of T2DM (Neel, 1962). This suggests that we have evolved a genetic tendency to rapidly deposit fat in times of plenty, which would have been advantageous when food was in short supply. John Speakman has counter-proposed a 'drifty' gene hypothesis which argues that genes predisposing to fat gain have arisen through random drift

following release from the threat of predation (Speakman, 2008). These theories both indicate a strong genetic cause for the current obesity epidemic.

As with other diseases, twin studies have been used to assess whether obesity has a genetic factor. The strong concordance rate for developing obesity between monozygotic twins supports the contribution of genetic predisposition to the development of obesity. The first links showing obesity had a genetic component were from twin and adoption studies, starting in the 1970s (Feinleib *et al*., 1977, Stunkard *et al*., 1986, Koeppen-Schomerus *et al*., 2001). These findings strongly support the concept that genes play a central role in body weight and obesity.

1.2.1 Monogenic Obesity

The discovery of mutations underlying rodent models of obesity led to the known monogenic forms of human obesity (Farooqi and O'Rahilly, 2005) and understanding of the leptin-melanocortin system. These monogenic mutations are rare in the general population, and therefore do not explain the rise in obesity generally, but they have allowed us to understand the mechanisms that control food intake and metabolism.

As mentioned earlier the *ob/ob* mice have a mutation in the gene leptin (Friedman *et al*., 1991, Zhang *et al*., 1994). Mutations in the leptin gene in man are rare but the obesity caused by congenital leptin deficiency can be successfully treated with leptin administration (Montague *et al*., 1997, Farooqi *et al*., 1999, Farooqi *et al*., 2002). Mutations in other genes in the leptin-melanocortin pathway, such as the leptin receptor, POMC and MC4R can also cause monogenic obesity (Clement *et al*., 1998, Krude *et al*., 1998, Farooqi *et al*., 2000, Farooqi *et al*., 2003). These mutations and others are rare, but when severe early-onset obesity is diagnosed, genome sequencing is valuable in determining how to treat these patients.

1.2.2 Polygenic Obesity

As severe monogenic obesity cases are rare, common obesity in the general population is likely to be influenced by more than one gene, and so be polygenic. Each polygene only contributes a small amount to the development of obesity, and each 'risk' allele would occur more frequently in the obese than in the non-obese subjects. These alleles require identification and validation by statistical analyses (Hinney and Hebebrand, 2008).

Candidate genes implicated in rarer monogenic obesity or from other biological evidence have been studied to assess their involvement in common obesity. Sequence variants in leptin have been shown to be associated with an increased BMI and obesity (Li *et al*., 1999, Jiang *et al*., 2004). Polymorphisms in other genes including *PPARγ*, dopamine receptor D2 (*DRD2*), serotonin receptor 2C (*HTR2C*) and cannabinoid receptor 1 (*CNR1*) have also been associated with obesity and T2DM by this technique (Deeb *et al*., 1998, Thomas *et al*., 2000, Pooley *et al*., 2004, Benzinou *et al*., 2008).

Human quantitative trait loci (QTLs) are stretches of DNA which underlie quantifiable traits, and can be identified by genome-wide linkage studies. Many of these studies have also been carried out to identify loci associated with obesity, and have been successful when looking at the monogenic Mendelian disease (Hirschhorn and Daly, 2005). However when looking at diseases with non-Mendelian characteristics this technique has only achieved limited success, due to small sample sizes, difficulties in refining the linkage signal to a gene or variant, and a failure to replicate loci (Altmuller *et al*., 2001, Hirschhorn and Daly, 2005).

Recently the genome-wide association study (GWAS) approach has superseded these techniques. GWASs are high-throughput, and allow researchers to scan a dense set of single nucleotide polymorphism (SNP) markers (0.1~5 million SNPs) in an unbiased manner (Xia and Grant, 2013). The SNPs are not considered causal but rather tag the regions with the associated trait. Mapping of the SNPs requires extensive knowledge of the genome of the organism of interest, and is therefore difficult to perform in species that have not been well studied or do not have well-annotated

genomes. The HapMap project, a large-scale effort to develop a haplotype map of the human genome, describes the common patterns of sequence variation and linkage disequilibrium (LD) (The International HapMap Consortium, 2005). This has aided in interpreting GWAS by determining patterns of LD (Hirschhorn and Daly, 2005). Thousands of GWASs have already been performed for a range of diseases (Hindorff *et al*., 2009). Several factors have made GWASs successful: subjects do not need to be related, high-density scans, large sample size, and the two stage study design (Loos, 2012). The two stage design involves detecting loci for which associations reach high significance levels; these are then tested in an independent series of samples. Loci are considered significant if associations reaches $<5 \times 10^{-8}$ in the meta-analysis of the first and second stage results, generating highly credible results (Loos, 2012).

1.2.3 Obesity Gene Discovery through GWAS

GWASs have been employed to explore phenotypes related to adiposity and metabolic dysfunction. Four waves of large-scale high-density GWAS for BMI have identified 32 loci that successfully reached genome-wide significance (Loos, 2012). These four waves are represented in **Figure 1.3** (Loos, 2012). The first wave consisted of two independent studies each with ~4800 white European individuals, which identified variants in the first intron of the fat mass and obesity associated gene (*FTO*) associated with BMI (Frayling *et al*., 2007, Scuteri *et al*., 2007). For the second wave of studies an international consortium, Genetic Investigation of ANthropometric Traits (GIANT) was formed. This enabled study sizes to increase and over 16,000 Europeans from seven separate GWAS for BMI were analysed (Loos *et al*., 2008), confirming the *FTO* SNP and a new locus near *MC4R*. This was also confirmed in a GWAS in Indian Asian subjects looking at waist circumference and other measures of adiposity (Chambers *et al*., 2008). For the third wave the GIANT consortium sample size increased to over 32,000 participants of white European descent, and identified six new loci associated with BMI (Willer *et al*., 2009). A similar sized GWAS was carried out by deCODE genetics on participants mainly from Iceland and identified a further seven new loci associated with BMI, four of which were in common with the GIANT study

[**Figure 1.3** and **Figure 1.4** (Thorleifsson *et al*., 2009)]. Finally the fourth wave comprised of over 120,000 participants from 46 populations of white European descent (Speliotes *et al*., 2010). In this study they were able to confirm all of the previously identified BMI-loci whilst also uncovering 20 more loci associated with BMI.

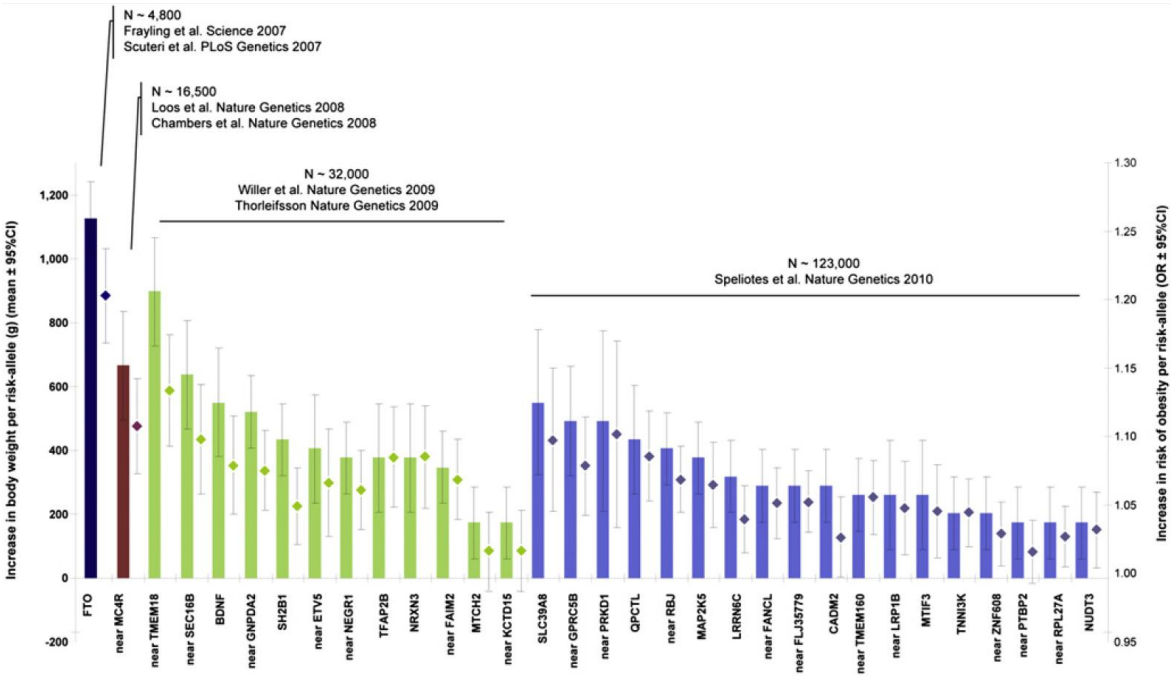

Figure 1.3 Per-allele effect of BMI-associated loci on body weight (left axis) and obesity risk (right axis). Loci are sorted by wave of discovery (first wave in dark blue, second in red, third in green, and fourth in light blue) and subsequently by effect on body weight. Graph taken from (Loos, 2012).

BMI is one of the most commonly used markers for adiposity used in obesity GWAS [**Figure 1.4** (Loos, 2012)]. Others measures include waist circumference, WHR, body fat percentage and extreme obesity [for example early onset before the age of six and adults with a BMI $\geq$ 40 kg/m^2 (Meyre *et al*., 2009)].

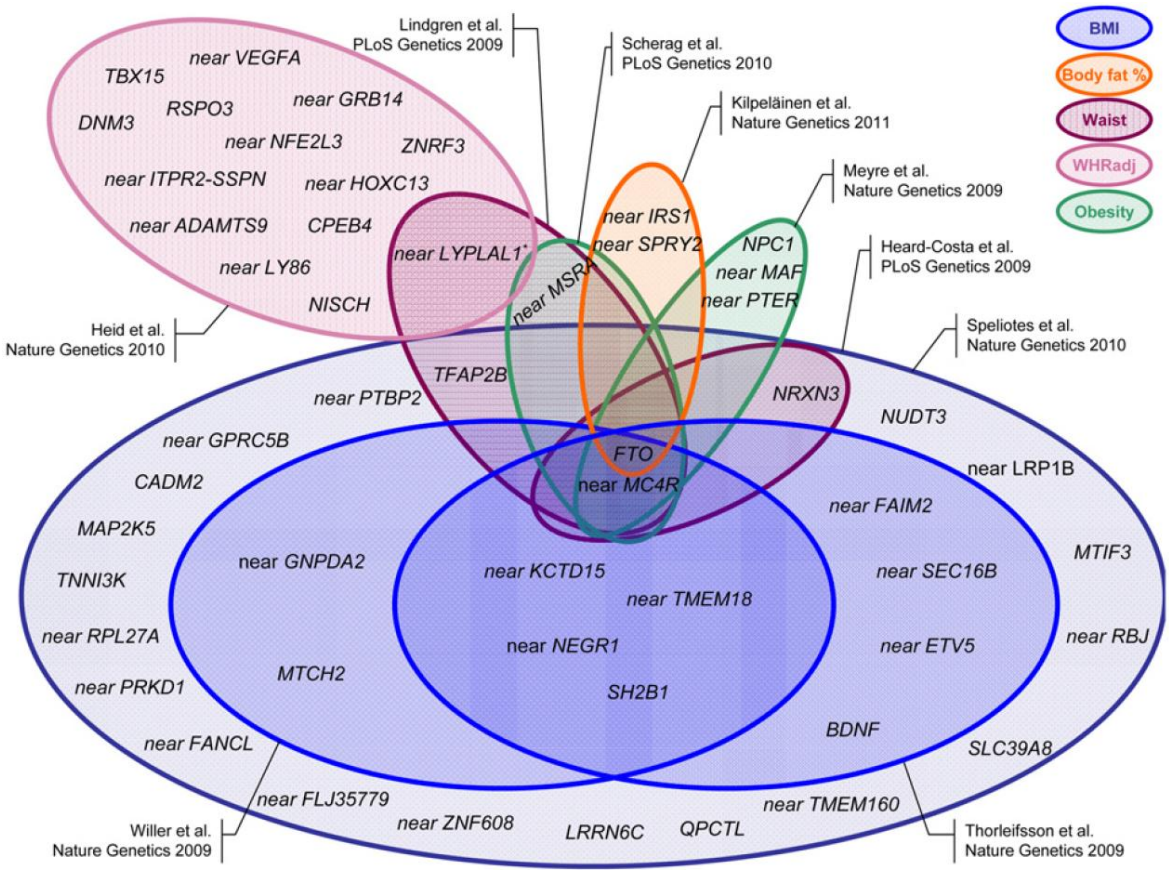

Figure 1.4 Obesity-susceptibility loci discovered in four waves of GWAS for BMI [blue (Frayling *et al.*, 2007, Scuteri *et al.*, 2007, Loos *et al.*, 2008, Chambers *et al.*, 2008, Thorleifsson *et al.*, 2009, Willer *et al.*, 2009, Speliotes *et al.*, 2010)], in one genome-wide meta-analysis for body fat percentage [orange, (Kilpelainen *et al.*, 2011a)], in two waves of GWAS for waist circumference and WHR [pink, (Lindgren *et al.*, 2009, Heard-Costa *et al.*, 2009, Heid *et al.*, 2010)], and in two GWAS for extreme and early-onset of obesity [green, (Meyre *et al.*, 2009, Scherag *et al.*, 2010)]. Each Venn-diagram represents the loci of one paper, except for papers that discovered only one locus, i.e. the *FTO* (Frayling *et al.*, 2007, Scuteri *et al.*, 2007) and the near-MC4R loci (Farooqi *et al.*, 2003, Loos *et al.*, 2008) for which no Venn-diagram was drawn. Image taken from (Loos, 2012).

1.3 FTO and GWAS

The *FTO* locus was the first obesity gene identified by GWAS and still has the highest causal effect [**Figure 1.3** (Frayling *et al.*, 2007, Loos, 2012)]. This SNP (A-allele variant rs9939609) in intron one of *FTO* has a modest effect on BMI, with those homozygous for the risk allele weighing approximately three kg more than case controls with the 'protective' allele (Frayling *et al.*, 2007). The risk allele frequency is high in populations of European descent with approximately 63 % of the population carrying at least one copy of the risk allele and 16 % being homozygous (Dina *et al.*, 2007, Frayling *et al.*, 2007).

Table 1.2 FTO GWAS. Studies listed here include only those attempting to assay at least 100,000 SNPs in the initial stage. Table adapted from search for 'FTO' in the (National Human Genome Research Institute, 2013).

Reference	Date	Population	Disease/Trait	Strongest SNP-Risk Allele	Context	p-Value
(Frayling *et al*., 2007)	12/04/2007	White European	Body mass index	rs9939609-A	Intron 1	2E-20
(Scott *et al*., 2007)	26/04/2007	Finnish	Type 2 diabetes	rs8050136-A	Intron 1	1E-12
(Zeggini *et al*., 2007)	26/04/2007	European ancestry	Type 2 diabetes	rs8050136-A	Intron 1	7E-14
(Wellcome Trust Case Control Consortium, 2007)	07/06/2007	British Caucasian	Type 2 diabetes	rs9939609-A	Intron 1	2E-7
(Scuteri *et al*., 2007)	20/07/2007	Sardinian and Americans: African, European & Hispanic	Obesity-related traits, Body mass index	rs9930506-A	Intron 1	9E-7
(Scuteri *et al*., 2007)	20/07/2007	Sardinian and Americans: African, European & Hispanic	Obesity-related traits, Hip circumference	rs9930506-A	Intron 1	3E-8
(Scuteri *et al*., 2007)	20/07/2007	Sardinian and Americans: African, European & Hispanic	Obesity-related traits, Weight	rs9930506-A	Intron 1	9E-7
(Hinney *et al*., 2007)	26/12/2007	Early Onset Obesity, German	Obesity (early onset extreme)	rs1121980-T	Intron 1	1E-7
(Zeggini *et al*., 2008)	30/03/2008	White European	Type 2 diabetes	rs8050136-A	Intron 1	7E-6
(Loos *et al*., 2008)	04/05/2008	White European	Body mass index	rs1121980-?	Intron 1	4E-8
(Timpson *et al*., 2009)	03/12/2008	European ancestry	Type 2 diabetes	rs8050136-?	Intron 1	2E-17
(Thorleifsson *et al*., 2009)	14/12/2008	European ancestry & African Americans	Body mass index	rs6499640-A	Intron 1	4E-13
(Thorleifsson *et al*., 2009)	14/12/2008	European ancestry & African Americans	Body mass index	rs8050136-A	Intron 1	1E-47
(Thorleifsson *et al*., 2009)	14/12/2008	European ancestry & African Americans	Weight	rs6499640-A	Intron 1	6E-14
(Thorleifsson *et al*., 2009)	14/12/2008	European ancestry & African Americans	Weight	rs8050136-A	Intron 1	5E-36
(Willer *et al*., 2009)	14/12/2008	European ancestry	Body mass index	rs9939609-A	Intron 1	4E-51
(Meyre *et al*., 2009)	18/01/2009	European ancestry	Obesity	rs1421085-C	Intron 1	1E-28
(Cho *et al*., 2009)	26/04/2009	East Asian	Biomedical quantitative traits	rs9939609-A	Intron 1	2E-7
(Cotsapas *et al*., 2009)	24/06/2009	White European	Obesity (extreme)	rs9941349-T	Intron 1	6E-12
(Heard-Costa *et al*., 2009)	26/06/2009	Caucasian	Waist circumference	rs1558902-?	Intron 1	5E-19
(Scherag *et al*., 2010)	22/04/2010	Early Onset Obesity, European	Obesity (extreme)	rs1558902-A	Intron 1	7E-13

		ancestry				
(Voight *et al*., 2010)	27/06/2010	European ancestry	Type 2 diabetes	rs11642841-A	Intron 1	3E-8
(Speliotes *et al*., 2010)	10/10/2010	European ancestry	Body mass index	rs1558902-A	Intron 1	5E-120
(Wan *et al*., 2011)	29/10/2010	European ancestry	Body mass in chronic obstructive pulmonary disease	rs8050136-A	Intron 1	4E-8
(Elks *et al*., 2010)	21/11/2010	European ancestry	Menarche (age at onset)	rs9939609-A	Intron 1	3E-8
(Dorajoo *et al*., 2012)	19/04/2011	Singaporean Chinese, Malay and Asian-Indian	Obesity	rs1558902-T	Intron 1	1E-7
(Wang *et al*., 2011a)	28/04/2011	non-Hispanic Caucasians	Obesity	rs17817449-?	Intron 1	2E-12
(Kilpelainen *et al*., 2011b)	26/06/2011	White European and Indian-Asian Ancestry	Adiposity	rs8050136-C	Intron 1	3E-26
(Okada *et al*., 2012)	19/02/2012	Japanese and European Ancestry	Body mass index	rs12149832-A	Intron 1	5E-22
(Kristiansson *et al*., 2012)	07/03/2012	Finnish	Metabolic syndrome	rs9940128-A	Intron 1	2E-9
(Fox *et al*., 2012)	10/05/2012	European Ancestry	Subcutaneous adipose tissue	rs9922619-T	Intron 1	6E-8
(Fox *et al*., 2012)	10/05/2012	European Ancestry	Subcutaneous adipose tissue	rs1421084-A	Intron 1	3E-6
(Perry *et al*., 2012)	31/05/2012	European Ancestry	Type 2 diabetes	rs9939609-A	Intron 1	1E-20
(Prescott *et al*., 2012)	04/06/2012	Postmenopausal with and without cancer	Sex hormone-binding globulin levels	rs12596210-C	Intron 8	9E-6
(Zeggini *et al*., 2012)	02/07/2012	European ancestry	Osteoarthritis	rs8044769-C	Intron 1	4E-6
(Yang *et al*., 2012)	12/09/2012	White European	Body mass index	rs7202116-G	Intron 1	2E-10
(Tabassum *et al*., 2013)	03/12/2012	Indian-Asian	Type 2 diabetes	rs8050136-A	Intron 1	6E-6
(Iles *et al*., 2013)	03/03/2013	White European	Melanoma	rs16953002-A	Intron 8	4E-12
(Berndt *et al*., 2013)	07/04/2013	European ancestry	Body mass index	rs11075990-G	Intron 1	2E-51
(Berndt *et al*., 2013)	07/04/2013	European ancestry	Obesity	rs8043757-T	Intron 1	5E-110
(Berndt *et al*., 2013)	07/04/2013	European ancestry	Obesity	rs7185735-G	Intron 1	1E-79
(Berndt *et al*., 2013)	07/04/2013	European ancestry	Obesity	rs1421085-C	Intron 1	6E-39
(Berndt *et al*., 2013)	07/04/2013	European ancestry	Obesity	rs1558902-A	Intron 1	2E-81
(Monda *et al*., 2013)	14/04/2013	African ancestry	Body mass index	rs17817964-T	Intron 1	1E-10
(Tanaka *et al*., 2013)	01/05/2013	European ancestry	Higher protein intake	rs1421085-C	Intron 1	1E-9

Since the discovery of this SNP many other GWAS studies have confirmed the effect of various intronic SNPs in FTO on various measures of adiposity and in a variety of populations worldwide (**Figure 1.4** and **Table 1.2**). These obesity associated SNPs are mainly found in intron one, however they have also been identified in intron two (Bollepalli *et al*., 2010, Hassanein *et al*., 2010, Zhang *et al*., 2010), intron three (Tonjes *et al*., 2010) and intron eight (Adeyemo *et al*., 2010) and in multiple populations world-wide (**Table 1.2**). The proximity of intron one SNPs to the transcriptional start site of *FTO* may suggest a regulatory function for the control of *FTO* expression. The additional linkage in intron three and intron eight may suggest additional regulatory regions and will require the investigation of population-specific SNPs (i.e. rs7191513) and their effect on *FTO* expression and the further characterisation of enhancer or repressor elements for *FTO* or nearby genes.

The increase in fat mass associated with the *FTO* risk allele manifests from seven years of age (Frayling *et al*., 2007). If the weight of the child is corrected for height, a distinctive peak can be seen at nine to twelve months old [**Figure 1.5** (Frayling and Ong, 2011, Sovio *et al*., 2011)]. There is an inverse correlation between BMI and the risk 'A' allele before two and a half years of age and then those with the risk allele have an earlier adiposity rebound. It has been previously observed that when the adiposity rebound occurs before 5.5 years of age it is considered a risk for obesity in later life (Rolland-Cachera *et al*., 1984, Williams *et al*., 1999). This has been shown to be true with those with the risk alleles weighing on average 1.5 kg more for each copy they possess (Frayling *et al*., 2007). An early adiposity rebound is also associated with early puberty (Williams and Goulding, 2009, Sovio *et al*., 2011), and indeed the rs9939609 A allele has been shown to associate with early menarche in girls (Elks *et al*., 2010). The strong association in childhood and adolescence appears to weaken with age (Jacobsson *et al*., 2009, Hardy *et al*., 2010, Jacobsson *et al*., 2011). A study looking at FTO in an elderly population (more than 55 years old, mean age 69) has shown that SNP genotype does not associate with obesity (Hardy *et al*., 2010). Another looking in Swedish adult males found no significant association from 50-82 years of age, they did however find an association between physical activity and the effect of the FTO genotype on BMI levels

suggesting that lack of physical activity is a requirement for an association of FTO gene variants to obesity (Jacobsson *et al*., 2009).

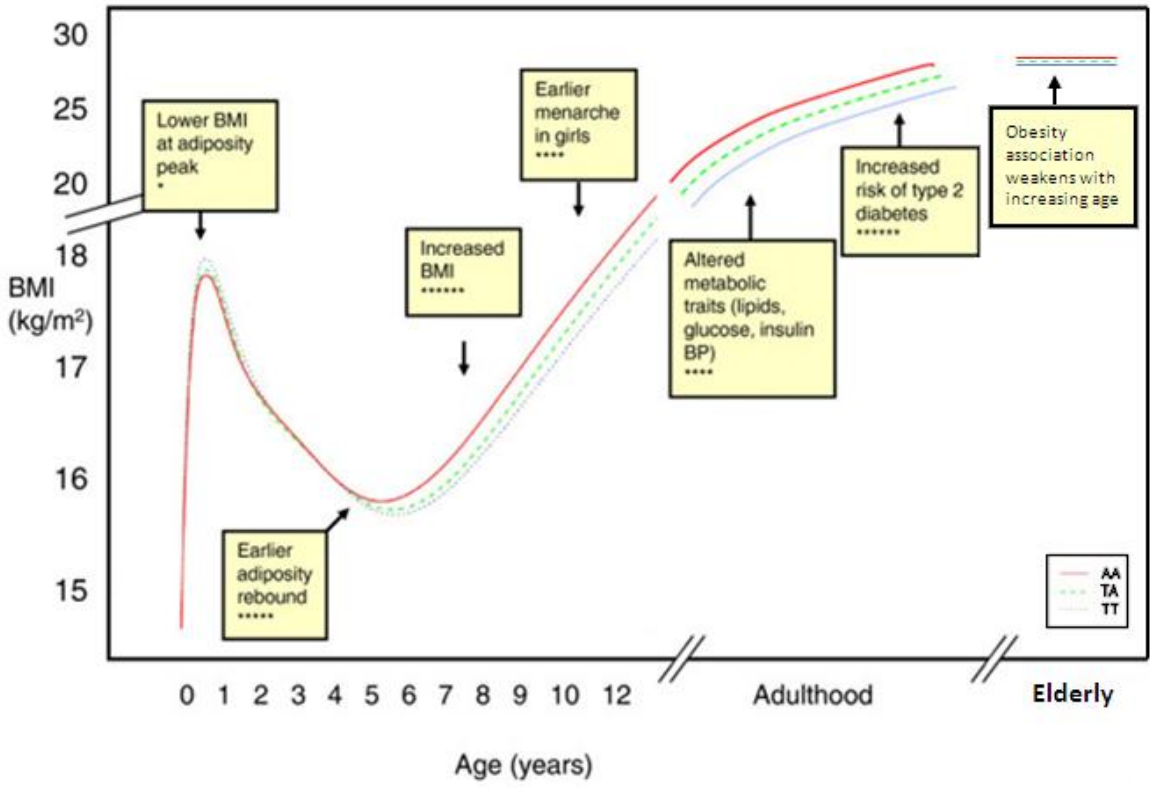

Figure 1.5 BMI throughout childhood and adulthood in individuals of different *FTO* genotypes. The A allele genotype is the minor 'fat' allele AT rs9939609. The figure was adapted from (Frayling and Ong, 2011, Sovio *et al*., 2011) and is based on real association data in childhood and a schematic of the association in adulthood (BP, blood pressure). Boxes describe associations with the minor 'fat' allele and stars are indicative of the statistical confidence of the association.

Physical activity has been shown to blunt the effect of SNP genotype, and emphasise the importance of carrying out regular exercise (Andreasen *et al*., 2008, Rampersaud *et al*., 2008, Kilpelainen *et al*., 2011a). *FTO* genotype itself has not been associated with level of physical activity carried out by adults (Kilpelainen *et al*., 2011a). This association has also been observed in adolescent males, but not females, with the obesogenic influence of *FTO* largely confined to inactive males (Scott *et al*., 2010). There is a study in Scandinavian adults however which does not support the hypothesis that exercise can modulate the effect of *FTO* genotype (Jonsson *et al*., 2009).

Studies have shown that the polymorphisms in *FTO* are associated with increased energy intake rather than an alteration in energy expenditure (Speakman *et al*., 2008, Haupt *et al*., 2009). Adults

and children homozygous for the risk A allele rs9939609 have been shown to not only have an increased food intake but also a preference for food with a higher energy and fat content (Cecil *et al*., 2008, Speakman *et al*., 2008, Timpson *et al*., 2008, Tanofsky-Kraff *et al*., 2009, Wardle *et al*., 2009, Sonestedt *et al*., 2009). Children and adults with the risk allele have also been shown to have diminished satiety responses compared with this with the T allele (Wardle *et al*., 2008, den Hoed *et al*., 2009). Recently Karra and colleagues have also observed attenuated post-prandial responses in AA carriers in terms of hunger and circulating acyl-ghrelin levels. Subjects also underwent functional MRI (fMRI) scans which revealed that *FTO* genotype modifies responses to food images in homeostatic and reward regions in the brain, such as the hypothalamus and VTA (Karra *et al*., 2013).

FTO has also been associated with other conditions. Some such as T2DM, hyperlipidaemia, hypertension and increased risk of cardiovascular disease (Frayling *et al*., 2007, Ahmad *et al*., 2010) which are directly associated with the increased risk of obesity. Although a study which pooled ten data sets for cardiovascular disease risk has shown a significant association of the rs9939609 *FTO* SNP independent of BMI and other conventional risk factors (Liu *et al*., 2013). Obesity is often observed as a co-morbidity with osteoarthritis, and *FTO* genotype has been shown as a risk for this condition (Zeggini *et al*., 2012, Elliott *et al*., 2013). Adjustment for BMI attenuated this osteoarthritis signal, indicating that the primary association is with BMI (Zeggini *et al*., 2012, Elliott *et al*., 2013). A longitudinal study of Danish adult males has demonstrated increased all-cause mortality associated with the minor allele of rs9939609 independent of BMI, which suggests *FTO* may exert its effects in ways that are incompletely assessed by current disease-defining measures (Zimmermann *et al*., 2009).

FTO has also been shown to be associated with cognitive decline, reduced brain volume in the elderly and increased risk of Alzheimer's disease (Ho *et al*., 2010, Reitz *et al*., 2012, Bressler *et al*., 2013). Brain volume differences of ~8 % in the frontal lobes and 12 % in the occipital lobes were observed, which were not attributable to differences in cholesterol levels, hypertension, or the volume of white matter hyperintensities; which were not detectably higher in *FTO* risk allele

carriers versus non-carriers (Ho *et al*., 2010). Obesity, hyperinsulinaemia, T2DM, cardiovascular disease and low levels of inflammation are all risk factors for Alzheimer's disease, and cognitive decline later in life, so whether this is as a result of increased BMI or a true association with neurodegeneration requires further investigation (Profenno *et al*., 2010, Hildreth *et al*., 2012). The rs9939609 A allele may be associated with a lower risk of depression independent of its effect on BMI (Samaan *et al*., 2012), and depression has been previously linked increased risk of dementia (Kessing, 2012, Gao *et al*., 2013).

Cancer risk also increases with obesity, and *FTO* genotype has been shown to be associated with melanoma and breast cancer, but showed no link with endometrial cancer (Gaudet *et al*., 2010, Kaklamani *et al*., 2011, Iles *et al*., 2013). The SNPs associated with breast cancer are found in intron one (Kaklamani *et al*., 2011), however the SNPs associated with melanoma are found in intron eight (Iles *et al*., 2013). Intron eight SNPs have been shown to be associated with obesity in African American and West African subjects. The Adeyemo *et al.* study did not find association with BMI and SNPs in intron 1, this may be due to differences in sample size, allele frequency differences, or different LD patterns in European and African individuals (Adeyemo *et al*., 2010). A GWAS of circulating sex hormone levels did show an increase of sex hormone-binding globulin levels increased with a SNP in intron eight (rs12596210), although they concluded that as levels of this are known to be negatively correlated with BMI, this may be the result of residual confounding (Prescott *et al*., 2012).

Polycystic ovaries syndrome (PCOS) is a common endocrine disorder, and women with the syndrome are at increased risk for obesity, insulin resistance and T2DM (Barber *et al*., 2006). There have been several studies which show a link between *FTO* genotype and PCOS (Barber *et al*., 2008, Kowalska *et al*., 2009, Wehr *et al*., 2010, Ewens *et al*., 2011, Wojciechowski *et al*., 2012, Li *et al*., 2013). It is likely that this association is due to increased BMI (Barber *et al*., 2008, Ewens *et al*., 2011), although levels of circulating testosterone were significantly associated with the A allele of rs9939609, indicating that *FTO* may play a role hyperandrogenism in women with PCOS (Wehr *et al*., 2010).

Osteoarthritis in people of European ancestry has been shown to associate with SNPs in intron one (Zeggini *et al*., 2012) and bone mineral density (BMD) was shown to be significantly associated with SNPs in intron eight in a Chinese population, although this study showed no significant association in a Caucasian group (Guo *et al*., 2011). This association with *FTO* emphasises that loss of excess bodyweight is a clinical recommendation for symptom relief and avoidance of osteoarthritis (Zeggini *et al*., 2012).

Two studies have shown that *FTO* minor alleles at rs9939609 and rs8050136 lead to a decreased risk for symptoms of attention deficit hyperactivity disorder and better emotional control (Velders *et al*., 2012, Choudhry *et al*., 2013). This suggests that children with these SNPs are protected against attention deficit hyperactivity disorder; this is particularly interesting due to the hyperactivity symptoms, which could affect body weight, although physical activity was not directly measured in these studies. Adults diagnosed with attention deficit hyperactivity disorder as children are however at an increased risk of developing obesity in adulthood which does not agree with this observation (Cortese *et al*., 2013).

There have been mixed results when examining *FTO* genotype for addictive behaviours such as alcohol dependence and cigarette smoking. Food intake can be controlled by similar hedonistic pathways in the brain, and as mentioned previously food intake and a preference for high fat food has been shown to be associated with *FTO* genotype (Cecil *et al*., 2008, Speakman *et al*., 2008, Timpson *et al*., 2008, Tanofsky-Kraff *et al*., 2009, Sonestedt *et al*., 2009, Wardle *et al*., 2009). One study has found that rs9939609 AA genotype was associated with lower ethanol intake, and low levels of alcohol dependence (Sobczyk-Kopciol *et al*., 2011). Although another study has not been able to replicate this result (Hubacek *et al*., 2012a, Hubacek *et al*., 2012b).

Finally *FTO* has been positively associated with BMI in chronic obstructive pulmonary disease patients, and as BMI of less than 21 is associated with increased mortality it is likely that carrying the risk allele would be somewhat beneficial in these patients (Wan *et al*., 2011).

1.4 FTO

GWAS is a non-hypothesis-driven technique, and can be used to uncover new insight into the biology of a phenotype. When the SNPs in *FTO* were discovered it was "a gene of unknown function in an unknown pathway" (Frayling *et al*., 2007). The actual gene(s) or region(s) having an impact on body weight might be in the surrounding area or even in linkage somewhere else in the genome. Many investigations have since taken place to examine the effects of *FTO* to see if it could play a role in metabolic control and obesity.

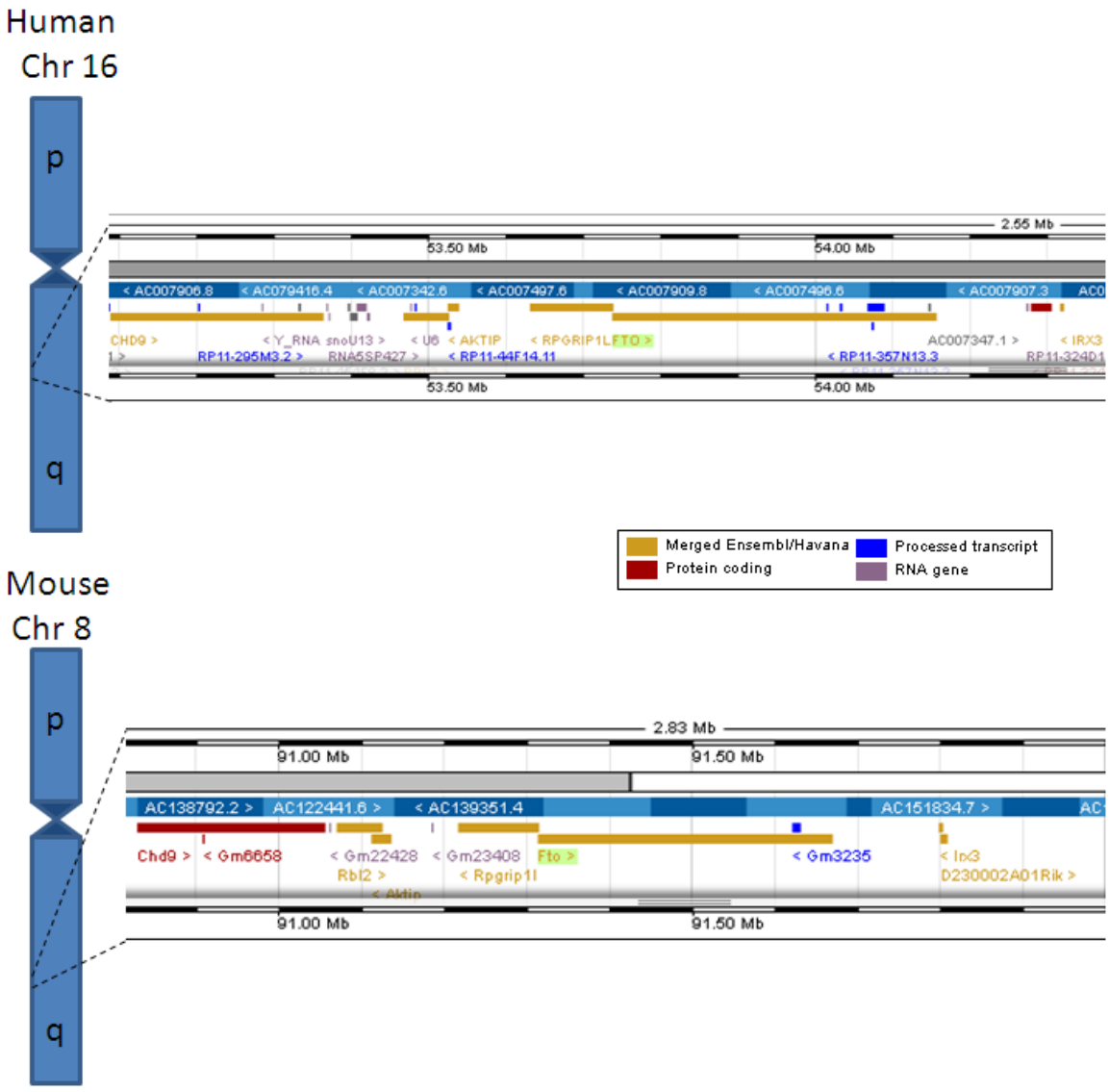

Figure 1.6 *FTO* Gene Location and surrounding region in man and mouse. Image adapted from Ensembl (Ensembl release 72). Chr, Chromosome; Mb, Megabase; p, petite arm; q, long arm.

1.4.1 FTO Knowledge Pre-GWAS

The *Fto* gene was first identified as part of a 1.6 Mb deletion in the *Fused toes* mouse mutant (*Ft*) characterised by fused toes on the fore limbs and a thymic hyperplasia (van der Hoeven *et al*., 1994, Peters *et al*., 1999). This region contains the Iroquois B cluster (*Irx3*, *Irx5*, and *Irx6*) as well as three other unknown genes which were called *Ft1* (now called *Aktip*), *Ftm* (now called *Rpgrip1l)* and *Fto* (Peters *et al*., 1999, Peters *et al*., 2002). *Fto* was originally named 'Fatso' as it was the biggest gene in the region, although apt this was changed to the 'Fat mass and obesity' gene when the SNPs in humans were discovered. The *Ft* mice have severe developmental disorders, such as neural tube defects, left-right asymmetry and defects in hypothalamus development, and are homozygous lethal with pups only surviving to embryonic day (E) 10 (van der Hoeven *et al*., 1994, Anselme *et al*., 2007).

Left-right asymmetry, neural tube patterning, and floor plate defects in the *Ft* mutant may be caused by the absence of *Ftm*, a regulator of sonic hedgehog (SHH) signalling expressed at the basal body of cilia (Vierkotten *et al*., 2007). *Ftm* has been renamed to retinitis pigmentosa GTPase regulator-interacting protein 1-like (*Rpgrip1l*). The heterozygous *Ft* mice did not present any metabolic defects, so it was still unclear if any of these genes were implicated in body weight in man.

FTO is coded by nine exons and spans more than 400 kb on human chromosome 16 and mouse chromosome 8 (**Figure 1.6**). The region is similar in man and mouse with *RPGRIP1L* (formerly *FTM*) close upstream (~3.4 kb) as well as *AKTIP*, *RBL2*, and *CHD9*. Downstream is *IRX3* and in the region are also *IRX5* and *IRX6*. The transcriptional start site of the adjacent gene *Rpgrip1l* is co-regulated with *Fto* in the mouse (Stratigopoulos *et al*., 2008).

1.4.2 FTO Structure and Function

Sequence analysis of FTO predicts that the protein would contain a double-stranded β-helix fold homologous to those of Fe(II) and 2-oxoglutarate (2OG) oxygenases, and may have a similar

function as these 2OG oxygenases (Gerken *et al*., 2007). Among this family of proteins FTO most closely resembles AlkB, a protein found in *Escherichia coli* (*E.coli)* (Gerken *et al*., 2007). AlkB is a DNA repair enzyme, capable of hydroxylating 1-methyladenine (1-meA) and 3-methylcytosine (3-meC). Although eukaryotes do not have the AlkB gene, they do possess AlkB homologues (ABHs). When FTO was classified two ABHs, ABH2 and ABH3 had already been identified and were known to be homologues of AlkB and can reverse 1-meA and 3-meC in DNA to adenine and cytosine by oxidative demethylation (Duncan *et al*., 2002, Aas *et al*., 2003). Gerken and colleagues then screened potential FTO substrates, and found that FTO could demethylate 1-meA, 3-meC and 3-methylthymine (3-meT) in single stranded DNA and exhibited a preference for 3-meT [(Gerken *et al*., 2007) **Figure 1.7**]. FTO also has a strong preference for demethylating 3-methyluracil (3-meU) and N6-methyladenine (6-meA) in single stranded nucleic acids [(Jia *et al*., 2008, Jia *et al*., 2011) **Figure 1.7**]. Other mammalian AlkB homologues have been identified and are summarised in **Table 1.3**, and a phylogenetic tree of the family can be seen in **Figure 1.8**. FTO is most closely related to ALKBH5, a family member which can also demethylate 6-meA.

Table 1.3 The known functions of AlkB and its human homologues. Abbreviations: KO, knockout; 1-meG, 1-methylguanidine; dsDNA, double stranded DNA; ssDNA, single stranded DNA.

Name	Activity	Mouse Model	Reference
AlkB (*E. coli)*	1-meA, 3-meC, 3-meT, 1-meG dsDNA, ssDNA, RNA	n/a	(Falnes *et al*., 2002, Trewick *et al*., 2002)
ALKBH1	3-meC, histone dioxygenase that acts specifically on histone H2A	KO: Developmental defects	(Westbye *et al*., 2008, Ougland *et al*., 2012)
ALKBH2	Lesions in DNA	KO: No phenotype, but accumulate 1-meA due to impaired DNA repair	(Aas *et al*., 2003, Ringvoll *et al*., 2006, Ringvoll *et al*., 2008)
ALKBH3	Lesions in ssDNA and 1-meA, 3-meC RNA	KO: No phenotype	(Aas *et al*., 2003, Ringvoll *et al*., 2006)
ALKBH4	Protein biding, Gene expression or chromatin state	-	(Bjornstad *et al*., 2012)
ALKBH5	6-meA RNA	KO: Normal, impaired spermatogenesis	(Zheng *et al*., 2013)
ALKBH6	Nucleic acid, unknown function	-	(Sedgwick *et al*., 2007)
ALKBH7	Protein binding, localized to mitochondrial matrix. A role in short chain fatty acid oxidation.	KO: Obese, altered fat metabolism	(Solberg *et al*., 2013)
ALKBH8	Hyper-modification of tRNA wobble uridines	KO: No phenotype	(Fu *et al*., 2010a, Fu *et al*., 2010b, Songe-Moller *et al*., 2010)

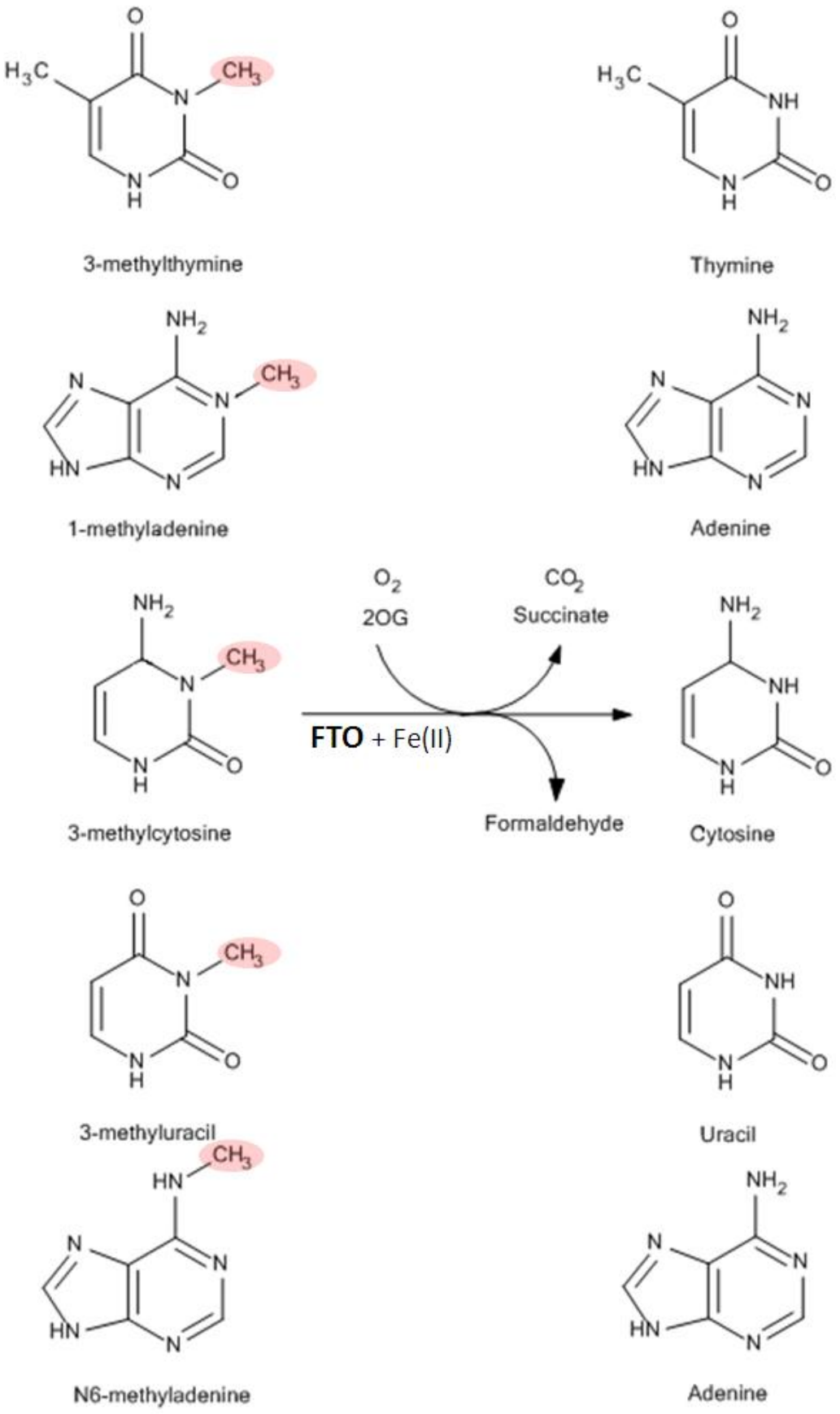

Figure 1.7 FTO substrates in demethylase reaction. FTO is a non-haem 2-oxoglutarate dependent dioxygenase and can demethylate 3-methylthymine, 1-methyladenine, 3-methylcytosine, 3-methyluracil and N6-methyladenine *in vitro*. Adapted from (Gerken *et al*., 2007, Gulati and Yeo, 2013).

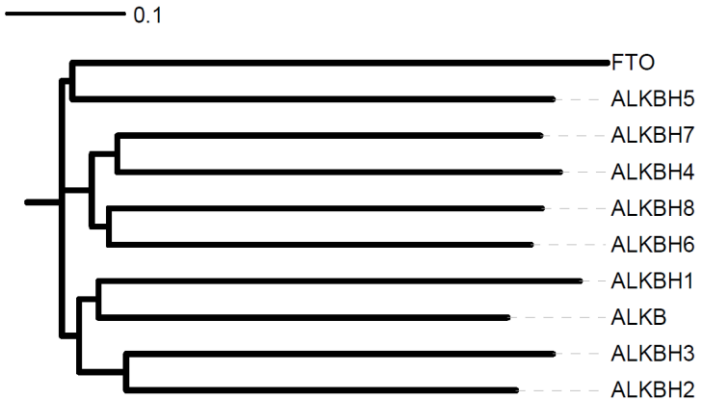

Figure 1.8 Phylogenetic Tree of Human FTO and ALKBH Family of Proteins and *E.coli* AlkB. Sequences downloaded from Ensembl release 73 and aligned with Muscle (multi sequence alignment tool). Phylogenetic tree then drawn using iTOL (interactive tree of life). Tree Scale shown at top.

2OG (also known as α-ketoglutarate) is a co-substrate of FTO, and an intermediate in the citric acid cycle. Ma and colleagues have measured the K_m of FTO for 2OG, and found it is 10-fold lower than the estimated intracellular concentrations of 2OG which means it is unlikely FTO is a sensor of intracellular 2OG levels.

FTO comprises of two domains, an N-terminal domain where the catalytic core is found, and a C-terminal domain of which the function is still unknown (Han *et al*., 2010). FTO also has a region referred to as 'Loop 1' which is highly conserved in FTO from different species but is not present in other ABHs. This loop is thought to give FTO its substrate preference for single-stranded nucleic acids (Han *et al*., 2010). The crystal structure of FTO validates that it binds 3-meT, and supports 3-meT and 3-meU as being FTO's primary substrates *in vitro* (Han *et al*., 2010). The crystal structure has aided our understanding of substrate specificity; however the *in vivo* substrate for FTO is still to be elucidated together with the link between FTOs catalytic activity and obesity.

1.4.3 FTO Expression

FTO is ubiquitously expressed, with the highest levels of expression in the hypothalamus and cerebellum (Gerken *et al*., 2007). The hypothalamus is an important brain region for control of energy homeostasis. There is some evidence that FTO is nutritionally regulated in the brain in mice

and rats by fasting, although upregulation (Fredriksson *et al*., 2008, Olszewski *et al*., 2009), downregulation (Gerken *et al*., 2007, Wang *et al*., 2011b) and no significant differences (McTaggart *et al*., 2011, Olszewski *et al*., 2011b) have all been reported (summarised in **Table 1.4**). In some of these studies animals were fasted for at least 40 hours, which would resemble a state of starvation, at least in the mouse. It should be taken into consideration that rats and mice are likely to have different sensitivities to fasting, therefore studies with a range of fasting periods are needed to investigate this more thoroughly.

Table 1.4 Summary of studies examining FTO expression and nutritional regulation. Abbreviations: ARC, arcuate nucleus; PVN, paraventricular nucleus; VMN, ventromedial nucleus; DIO, diet induced obesity; AAV, adeno-associated virus; SON, supraoptic nucleus; DMH, dorsomedial hypothalamus; NTS, Nucleus of the Solitary Tract; AP, area postrema; NAcc, nucleus accumbens; EnR, energy restriction.

Reference	Methods	Observations
(Gerken *et al*., 2007)	Mouse; 48 hour fast	ARC *Fto* ↓ 60 % by fasting, PVN and VMN unchanged
(Fredriksson *et al*., 2008)	Rat; 48 hour fast	48 hour fast ↑ *Fto* mRNA expression
(Stratigopoulos *et al*., 2008)	Mouse; A^y, Lep^{ob}, $Lepr^{db}$, Cpe^{fat}, *tub*, 4 weeks old and DIO 18 weeks old. 40 hour fast, and cold exposure examined	*Fto* and *Ftm* expression were ↓ by fasting in lean and obese animals and by cold exposure in lean mice
(Olszewski *et al*., 2009)	Mouse; 16 hour fast, 48 hour palatable food intake Organotypic hypothalamic cultures; leucine	16 hour fast ↑ *Fto*, palatable diet not effect expression. Leucine ↓ *Fto* expression
(Tung *et al*., 2010)	Rat; Stereotactic injection of AAV to increase and decrease *Fto* expression	Overexpression of *Fto* in the ARC ↓ food intake and ↑ *Stat3*, knocking-down *Fto* ↑ food intake
(McTaggart *et al*., 2011)	Mouse; 18 hour fast	No change in mRNA or protein expression in brain regions
(Olszewski *et al*., 2011b)	Rat; 16 hour fast and 16 hour fast with a 2 hour refeed	Feeding status did not affect expression in rat: ARC, PVN, SON, DMH, VMH, NTS, AP and Nacc
(Wang *et al*., 2011b)	Rat; 60 % ER for 8 or 50 weeks $Lepr^{db}$ mouse; 60 % EnR for 8 weeks	Rat; EnR ↓ mRNA and protein expression in hypothalamus and brainstem but not in periphery. $Lepr^{db}$; response impaired and no weight reduction
(Vujovic *et al*., 2013)	Rat; 48 hour fast	↑ protein and mRNA expression in the hypothalamus

FTO expression is downregulated *in vitro* by removal of glucose or total amino acid levels from the tissue culture media, and when nutrients are replaced FTO expression levels are restored

(Cheung *et al*., 2013). Gulati and colleagues have also shown that FTO may play a role in nutrient sensing and have described a role for FTO in the coupling of amino acid levels to mammalian target of rapamycin complex 1 signalling (Gulati *et al*., 2013). One study has found an inverse relationship between FTO and satiety, and that *Fto* levels in the hypothalamus were reduced *in vitro* after the addition of leucine, which *in vivo* reduces feeding and activates anorexigenic neurons synthesizing POMC (Olszewski *et al*., 2009).

FTO and *RPGRIP1L* transcription start sites are in close proximity to each other, and both could potentially be affected by altered enhancers in intron 1 or 2 of *FTO*. *Fto* is expressed at higher levels than *Rpgrip1l*, with for example hypothalamic expression levels ~6 fold higher than *Rpgrip1l* (Stratigopoulos *et al*., 2008). Stratigopoulos and colleagues reported that Cut-like homeobox 1 (*CUX1*) regulates expression of *Fto* and *Rpgrip1l*, and that the risk allele (A) of SNP rs8050136 preferentially bound to the transcription factor CUTL1 protein (transcribed from *CUX1*) in human fibroblast DNA (Stratigopoulos *et al*., 2008). Knockdown of *CUX1* by 70 % decreased *FTO* and *RPGRIP1L* expression by 90 and 65 %, respectively, indicating that it is needed for *FTO* and *RPGRIP1L* transcriptional activation (Stratigopoulos *et al*., 2008).

Berulava and Horsthemke have shown that the SNPs in *FTO* can impact on its transcription, and that increased BMI associated with increased expression of *FTO* (Berulava and Horsthemke, 2010). Although they only had a small sample size and examined blood cells and fibroblasts, which are unlikely to have a strong role in the obesity phenotype (Berulava and Horsthemke, 2010). Increased expression of the risk allele agrees with the results of Stratigopoulos and colleagues (Stratigopoulos *et al*., 2008). Karra and colleagues have also shown that rs9939609 AA subjects had increased *FTO* mRNA abundance compared with TT subjects in peripheral blood cells (Karra *et al*., 2013).

Several other studies have failed to reveal any influence of the *FTO* genotype on total mRNA level of *FTO* or *RPGRIP1L*. One group examined expression levels in subcutaneous and omental adipose tissue they found no difference in *FTO* expression between individuals from different

genotype groups, but did see an increase in the obese individuals (Wahlen *et al*., 2008). They did observe an increase in adipocyte lipolytic activity both *in vivo* and *in vitro* in subjects with the protective rs9939609 SNP (Wahlen *et al*., 2008). Another study in adipose tissue found no association between *FTO* or *RPGRIP1L* expression and the rs8050136 SNP (Kloting *et al*., 2008), however they observed decreased expression of *FTO* in obese patients in visceral and subcutaneous adipose tissue (Kloting *et al*., 2008). Expression of *FTO* in skeletal muscle is also not correlated with genotype for risk of obesity (Grunnet *et al*., 2009b). Finally a study looking at SNP genotype and *FTO* expression in lymphocytes, found no association with *FTO* and SNP genotype, however the retinoblastoma like 2 (*RBL2)* a gene which ~270 kb away showed an association (Jowett *et al*., 2010). *RBL2* binds members of the DNA binding E2F transcription factor family that regulate transcription of many genes associated with cell cycle progression and cellular differentiation, and so could be a candidate (Jowett *et al*., 2010).

An increase in body weight has been observed in a patient with an extra copy of *FTO* due to a partial trisomy of 16q (van den Berg *et al*., 2010). This subject had a duplication of 11.45 Mb presented with included obesity, severe anisomastia, moderate to severe mental retardation, attention deficit hyperactivity disorder, dysmorphic facies, and contractions of the small joints (van den Berg *et al*., 2010). Analysis of *FTO* expression in the patient's immortalised lymphocytes however revealed no increase in expression due to the trisomy, which they speculate may be due to maternal imprinting of the *FTO* locus (van den Berg *et al*., 2010).

Humans homozygous with catalytically inactive FTO have a range of lethal developmental disorders [(Boissel *et al*., 2009) summarised **Table 1.5**]. This mutation changes one of the arginine residues in the catalytic domain for a glutamine (R316Q). These arginine residues are critical for substrate binding and when replaced FTO is catalytically null with no demethylase activity. Body weight data from heterozygous relatives is unavailable.

Finally a study examining mutations in *FTO* in severely obese patients and lean individuals reveal that heterozygous, loss-of-function mutations in *FTO* exist, and are found in both lean and obese

subjects (Meyre *et al*., 2010). It therefore appears that loss of one functional copy of *FTO* in humans is compatible with being either lean or obese.

1.4.4 Mouse models of FTO

In order to understand the role the obesity SNPs plays *in vivo* several different mouse models of FTO and other genes in the region have been developed. As discussed the homozygous *Ft* mice present with several developmental problems and do not survive post E13.5 (van der Hoeven *et al*., 1994). Mice where *Rpgrip1l* (*Ftm*) is inactivated died around birth, and had micropthalmia, preaxial polydactyly in the fore and hind limbs, craniofacial malformations, exencephaly and disruption of left-right patterning (Vierkotten *et al*., 2007). *Rpgrip1l* is located at the basal body of the cilia, and its presence is necessary to elicit a quantitative SHH response (Vierkotten *et al*., 2007). This suggests that *Rpgrip1l* is required for several processes during embryonic development, and could be the cause of the developmental abnormalities in the *Ft* mice; however the *Rpgrip1l*$^{-/-}$ did not have fused toes.

One study has suggested that the SNPs in *FTO* are in fact in LD with *IRX3*, and may alter *IRX3* expression (Ragvin *et al*., 2010). Knockdown of its orthologue *irx3a* in zebrafish disrupted proper pancreas development (Ragvin *et al*., 2010) but this is yet to be fully investigated in mice. Mice with loss of *Irx3* have however been shown to have disruption to the regulation of intercellular gap junction coupling and impulse propagation in the heart (Zhang *et al*., 2011). *Irx5* and *Irx6* are both required for retinal development. *Irx5* is required for proper development of the retinal cone bipolar cells (Cheng *et al*., 2005), and *Irx6* is required downstream of bipolar cell specification for terminal differentiation of type 2, type 3a and possibly type 6 bipolar cells (Star *et al*., 2012). The final gene in the region *Aktip* has so far not been investigated, but targeted and gene trapped cell lines are available to generate the mice. The phenotypes of the mice discussed so far do not suggest an appreciable role for these genes in control of body weight. I shall now discuss the findings revealed by the various mouse models of *Fto*.

1.4.4.1 Global and Tissue Specific Knockout of *Fto*

The Rüther laboratory generated a gene trap knockout mouse line to further study FTO function [(Fischer *et al*., 2009) summarised in **Table 1.5**]. FTO protein was successfully removed, and levels of *Rpgrip1l* mRNA were unaffected in all tissues examined (Fischer *et al*., 2009). Homozygous *Fto*$^{-/-}$ mice did not present with any developmental abnormalities at birth; however after postnatal day (P) 2 mice had a significantly lower bodyweight than controls and increased postnatal lethality (Fischer *et al*., 2009). The *Fto*$^{-/-}$ mice also have a reduced body length, a reduction in adipose tissue and lean mass, increased energy expenditure, increased sympathetic nervous system activity, relative hyperphagia and reduced spontaneous locomotor activity (Fischer *et al*., 2009). The *Fto*$^{+/-}$ mice did not have an increased postnatal lethality and were not growth retarded, but were protected from diet-induced obesity following 12 weeks of high fat diet (HFD) feeding. This demonstrated the first direct evidence that FTO is involved in metabolism and that the loss of *FTO* expression or FTO function may protect from obesity.

A group from Baylor College of Medicine generated a conditional *Fto* knockout line (Gao *et al*., 2010). When they cross this conditional line with a *Meox2*-Cre mouse line to generate whole body deletion of *Fto*, these animals like the gene trap knockout, had postnatal growth retardation and only 50 % survived to weaning (Gao *et al*., 2010). They also observed that these mice had lower serum IGF-1, lower BMD, and were relatively hyperphagic. They did not see any significant difference in adipose tissue mass in male *Fto*$^{-/-}$ *mice*, and a significant increase in female *Fto*$^{-/-}$ mice, lean mass was significantly lower in both *Fto*$^{-/-}$ sexes. When they tested their mice with a HFD their *Fto*$^{-/-}$ mice were not protected from diet-induced obesity (Gao *et al*., 2010).

Gao and colleagues then used their conditional knockout line to generate a neural *Fto*$^{-/-}$ mouse line using a *Nestin-Cre*. They found that these mice recapitulated the phenotypes of the global *Fto*$^{-/-}$ mice, suggesting that the neuronal removal of FTO is crucial for the phenotype of the global *Fto*$^{-/-}$ mice (Gao *et al*., 2010).

A final study has examined the role of FTO in regulation of dopaminergic signalling. Hess and colleagues found that global *Fto*$^{-/-}$ mice showed attenuated activation of G protein-coupled inwardly-rectifying potassium (GIRK) channel conductance by cocaine and quinpirole (Hess *et al*., 2013). They were able to replicate this finding in mice where *Fto* was conditionally inactivated in dopaminergic neurons by using a *Dat*-Cre line, and found that these mice had increased basal locomotor activity similar to mice lacking D2 autoreceptors (Hess *et al*., 2013). This suggests that FTO is involved in reward pathway signalling and regulation.

1.4.4.2 FTO^{I367F}

Mice with a dominant ENU induced point mutation in *Fto* were identified from the ENU mutation archive at MRC Harwell [(Church *et al*., 2009) summarised in **Table 1.5**]. This point mutation replaces an isoleucine with a phenylalanine at position 367 (I367F). This may modify FTO function by altering its dimerisation state (Church *et al*., 2009) although this residue is buried in the structure so may alter the function in an as yet undetermined way (Han *et al*., 2010). Mice which carry this mutation are protected from obesity and have increased energy expenditure compared to controls. They do not show perinatal lethality or any developmental growth abnormalities (Church *et al*., 2009). This model may therefore be a better model of the effect of human *FTO* variants.

1.4.4.3 FTO Overexpression

Church and colleagues generated a mouse which can conditionally overexpress *Fto* from the *Rosa26* locus under control of the strong *CAGGS* promoter [(Church *et al*., 2010) **Table 1.5**]. Overexpression of *Fto* leads to a dose-dependent increase in body and fat mass on both a standard and HFD. These mice are also hyperphagic compared to control animals despite having decreased leptin levels relative to their increased body weight, and when on a HFD develop glucose intolerance (Church *et al*., 2010).

Table 1.5 Comparison of the effects of *FTO* variants in mouse and human [adapted from (Fawcett and Barroso, 2010)]. Abbreviations: BW, body weight; SD, standard diet; HFD, high fat diet; epi, epigonadal; sub, subcutaneous; FTO-4, mice which have 2 additional copies of *Fto*; HDL, high density lipoprotein; LDL, low density lipoprotein.

Phenotype	**Mouse Model or Human Case Study**			
	***Fto*$^{-/-}$ mouse** (Fischer *et al*., 2009)	***Fto* I367F mouse** (Church *et al*., 2009)	***Fto* Overexpression mouse** (Church *et al*., 2010)	***FTO* R316Q in human** (Boissel *et al*., 2009)
Pre- and post-natal body weight	No effect on pre-natal; ↓ BW apparent from early age, ↓ fat mass more pronounced than ↓ in lean mass; ↓ weight gain on HFD	No effect pre-natal; Males exhibit maturity-onset ↓ in BW, due to ↓ fat mass; ↓ weight gain on HFD	Maturity-onset ↑ in BW, most pronounced in females, and further ↑ on HFD	All show failure to thrive postnatally, and 3 individuals show intrauterine growth retardation; No data for relatives
Postnatal death	↑ frequency	None	None	Death from intercurrent infection or an unidentified cause occurred within 30 months of age
Growth retardation	From postnatal day 2	None	None	All affected individuals had postnatal growth retardation
Developmental Abnormalities	No other gross developmental abnormality	No gross developmental abnormality	None	In all: microcephaly, severe psychomotor delay, functional brain deficits, and facial dysmorphism. In some: cardiac defects, structural brain malformations, genital abnormalities, and cleft palate.
Adipose tissue mass and adipokines	↓ in adipose tissue mass; ↓ leptin; ↑ adiponectin	↓ in adipose tissue mass; ↑ leptin secretion/unit of body fat; No difference in adiponectin	↑ in adipose tissue mass; ↑ adipocyte size ↓ circulating leptin at 8 weeks, no difference at 20 weeks; mRNA ↑ epi and sub WAT, ↓ ab WAT at 20 weeks; Hom and het Females ↓, and ↑ in males	No difference reported
***FTO* expression and function**	Abolished expression in all tissues tested	↓ expression in mammalian cells; Disrupted dimerisation and catalytic activity of FTO	↑ expression, dose related to number of *Fto* genes in tissues tested	FTO R316Q is catalytically inactive, but mutation does not affect nuclear localisation
Sex differences	↓ BW more pronounced in males; *Fto*$^{+/-}$ only females showed ↓ BW at 20 weeks	Only male mice exhibit reduced BW at 12 weeks	↑ BW more pronounced in females	No difference reported

Energy intake	↑ food intake relative to lean mass	No difference in food intake	↑ food intake, even when normalised to body weight	No difference reported
Energy expenditure	↑ energy expenditure	↑ energy expenditure	FTO-4 on HFD mice showed ↓ in O_2 consumption and CO_2 production during light and dark periods relative to BW	No difference reported
Physical activity	↓ physical activity	No difference	No significant difference in locomotion, but female FTO-4 mice showed ↑ anxiety	No difference reported
Glucose tolerance and insulin sensitivity	Mild improvement in insulin sensitivity (probably as a consequence of leanness)	No convincing difference	No significant on SD, except ↓ fasting glucose in FTO-4 mice. On HFD FTO-4 have ↓ in glucose tolerance; Insulin: SD no change, HFD ↑ fasting insulin FTO-4 at 16 weeks	No difference reported
Lipids	No difference reported	Triglycerides and HDL cholesterol increased	↑ HDL; ↓ LDL	No difference reported
Other gene expression	*Npy* mRNA induction was blunted and *Pomc* mRNA repression exaggerated in fasted -/- mice	Altered expression of some genes involved in inflammation, fatty acid catabolism and synthesis, carbohydrate metabolism and the ER stress response in mutant mice; *Npy* expression was ↓ in fed mutant mice	↑ hypothalamic *AgRP* after fasting	No difference reported

1.4.5 FTO and nutrient sensing

FTO expression in mouse and human cell lines has been shown to be regulated by nutrient availability (Cheung *et al*., 2013). Depriving the cells of glucose and total amino acids decreases FTO protein and mRNA expression after 6 hours, which can be reversed by nutrient replacement. When examining which amino acids influenced the decrease in expression; essential amino acids, methionine and cysteine, and glutamine were found to effect FTO expression on their own (Cheung *et al*., 2013). These findings suggest that FTO could be involved in cellular nutrient sensing.

Building on these results the group then went on to investigate if FTO plays a role in cell growth and translation, processes regulated by nutrient availability (Gulati *et al*., 2013). They found that *Fto*$^{-/-}$ mouse embryonic fibroblasts (MEFs) exhibited a slower rate of growth and had reduced mRNA translation compared to wild-type MEFs. They then were able to demonstrate that FTO is necessary for normal mTORC1 signalling in response to amino acid deprivation, and by using catalytically inactive FTO they demonstrated that the demethylase activity is necessary for this response (Gulati *et al*., 2013).

Recently another group have been able to demonstrate that there is a link between FTO, ghrelin and impaired brain food-cue responses (Karra *et al*., 2013). They found that subjects homozygous for the risk A rs9939609 polymorphism have dysregulated circulating levels of the orexigenic hormone acyl-ghrelin and had an attenuated postprandial appetite reduction (Karra *et al*., 2013). In cells they were able to show that 6-meA levels were reduced on ghrelin mRNA by overexpression of FTO, causing an increase in ghrelin mRNA and protein levels. They went on to show that this was also mirrored in AA human subjects, as they had increased *FTO* mRNA, decreased ghrelin mRNA 6-meA levels and increased abundance of ghrelin mRNA compared to TT subjects (Karra *et al*., 2013).

1.4.6 FTO and methylation levels

Although a large number of modifications including 6-meA are found in RNA their roles are poorly understood. Recently a number of studies have examined 6-meA levels in human and mouse transcripts to understand how common this methylation mark is, and if it could play a role in gene expression.

Dominissini and colleagues used a 6-meA sequence technique to examine the presence of this modification in the transcriptome of humans and mice (Dominissini *et al*., 2012). They found over 12,000 6-meA sites in the transcripts of more than 7000 coding and non-coding genes in man. These sites correlated highly with stop codons and within long internal exons, which may indicate a role in the control of translation or splicing, and this was found to be significantly conserved between humans and mice (Dominissini *et al*., 2012). They went on to silence a 6-meA transferase (*METTL3*) in HepG2 cells and demonstrated that this significantly affects gene expression and alternative splicing patterns, modulating p52 signalling and apoptosis (Dominissini *et al*., 2012).

A second study using the same technique was also published around the same time (Meyer *et al*., 2012). Meyer and colleagues identified over 7000 genes with the methylation mark in mice, and found that the mark exhibits tissue-specific regulation and is markedly increased throughout brain development (Meyer *et al*., 2012). They found associations with the mark in stop codons and in the RNA three prime untranslated region (3'UTR), and that the 3'UTR sites associate with miRNA binding sites (Meyer *et al*., 2012). They then went on to overexpress FTO in HEK293T cells, which caused a decrease in 6-meA levels in the transcriptome (Meyer *et al*., 2012).

Previously FTO has been shown to co-localise with nuclear splicing speckles, these speckles have been shown to function in spliceosome assembly or post-transcriptional splicing of pre-mRNAs (Jia *et al*., 2011). This would agree with these 6-meA results, suggesting that FTO could be involved with demethylating this modification and be implicated in control of translation and splicing. They then went on to knockdown and overexpress FTO in HeLa cells. Knockdown of

FTO increased 6-meA levels in extracted mRNA by 23 %, and overexpression decreased mRNA methylation of 6-meA by 18 % (Jia *et al*., 2011).

Another group examined the consequence of altered FTO levels in cultured cells and mouse brain (Berulava *et al*., 2013). They also found that FTO co-localises with nuclear speckles, and to lesser extent in the nucleoplasm and nucleoli. Total brain RNA was analysed for modifications in wild-type and *Fto*$^{-/-}$ mice, loss of FTO increases the ratio of 3-meU/U and decreases ratio of pseudouridine/U, but has no effect on 6-meA/A or 3meC/C (Berulava *et al*., 2013). Total RNA is mainly composed of rRNA, so this may be predominantly due to changes in rRNA rather than mRNA, and FTO may act on multiple substrates *in vivo*.

6-meA has also been examined in RNA from midbrain and striata from control and *Fto*$^{-/-}$ mice (Hess *et al*., 2013). The *Fto*$^{-/-}$ mice had 5000 more 6-meA peaks than control samples, suggesting that FTO may play a role in demethylation of this substrate (Hess *et al*., 2013). Analysis of the transcripts methylated specifically in the *Fto*$^{-/-}$ mice revealed that they are disproportionately linked to synaptic transmission and cell-cell signalling, which suggests FTO may target a specific set of transcripts (Hess *et al*., 2013).

In MGN3-1 and HEK293T cells FTO has been shown to regulate levels of ghrelin (Karra *et al*., 2013). Examination of the ghrelin mRNA in these cell lines reveals that FTO reduces ghrelin pre-mRNA 6-meA specific methylation (Karra *et al*., 2013).

Another AlkB homolog ALKBH5 (**Table 1.3**) can also demethylate 6-meA. In ALKBH5 deficient cells cytoplasmic RNA is increased, due to increased export from the nucleus (Zheng *et al*., 2013). They also observed decreased RNA stability and differential gene expression. Their data suggest that the 6-meA modification is important in RNA export, metabolism and gene-expression. *Alkbh5*$^{-/-}$ mice are viable and have a normal appearance and no body weight phenotype, however they do have a spermatogenic defect which may be explained by its function and high expression in the testis (Zheng *et al*., 2013).

Taken together the results from these studies suggest that 6-meA has a role in regulation of gene expression, and that FTO may affect methylation levels of 6-meA and uridine *in vivo* which alters gene and protein expression.

1.4.7 FTO and other functions

Several other studies have also suggested other putative functions of FTO. Leptin has been shown to downregulate FTO expression *in vitro* in mouse hypothalamic cultures by activating the STAT3 signalling pathway (Wang *et al*., 2011b). Leptin however has also been shown to upregulate FTO expression *in vitro* in neonatal rat cardiomyocytes by activation of JAK2/STAT3 activation, which was dependent on CUTL1 upregulation (Gan *et al*., 2013). FTO may have tissue-specific functions, and so differential effects on its expression could link in with these results. This study also supports the role of CUTL1 in FTO expression (Stratigopoulos *et al*., 2008).

Fto$^{-/-}$ mice have higher expression of UCP-1 in their epigonadal and inguinal WAT compared to control littermates (Tews *et al*., 2013). They found that FTO deficient adipocytes also had increased expression of UCP-1 and that these cells differentiated as readily as controls, but they had lower levels of *de novo* lipogenesis. UCP-1 is an uncoupling protein, and FTO deficient adipocytes had increased mitochondrial uncoupling, suggesting increased energy expenditure in FTO deficient adipocytes (Tews *et al*., 2013).

Olszewski and colleagues have shown that the majority of neurons containing oxytocin, a neuronal satiety mediator, also express FTO (Olszewski *et al*., 2011a). They also showed that although oxytocin does not affect FTO expression, increased FTO cause increased levels of oxytocin.

Skeletal muscle from patients with T2DM has higher FTO expression than controls, which could be reduced by treatment with the insulin sensitiser rosiglitazone (Bravard *et al*., 2011). Bravard and colleagues then went on to show that increased FTO expression in myotubes caused enhanced lipogenesis and reduced mitochondrial oxidative function leading to enhanced oxidative stress.

1.5 The Mouse as a model

Obesity is a complex multi-organ disease, with interactions between the pancreas, liver, skeletal muscle, adipose tissue, gut, and brain, and consequently requires a mammalian species such as the mouse for complete analysis. Lower organisms are valuable for some aspects of the biology as many of the pathways are highly conserved and have precursors in lower organisms. Benefits to using mice are that they have a fairly short gestation; they are small, which allows maintenance to be relatively easy and cost effective; and they have a relatively short life span allowing investigation of aging phenotypes. The environment they are housed in can be well regulated, allowing this effect to be examined or minimised so that the environment–gene interactions can be fully scrutinised. Rats are also regularly used to model human disease and have the advantage of being larger than mice, making some physiological procedures easier, but until recently genetic manipulation of the rat genome has not been possible (Zan *et al*., 2003, Kitada *et al*., 2007, Geurts *et al*., 2009). Manipulation of the mouse genome has been possible for over 20 years (Capecchi, 1989), and as such a huge range of resources are available for investigations using the mouse.

Standardized protocols for mouse phenotyping are available to help laboratories characterize their models in a comparable way (EMPReSS http://empress.har.mrc.ac.uk/, IMPReSS http://www.mousephenotype.org/impress/, EUMORPHIA http://www.eumorphia.org/). Precise diagnostic criteria that are used to identify the disease in man are not used in the mouse; instead wild-type and mutant mice (age- and sex-matched individuals, which are ideally littermates) are compared with one another. Similar diagnostic tests as those used in human patients have been established in the mouse, this allows phenotyping results to be at least partly comparative between mouse models and human studies, leading to stronger translatable results.

When using animal models, the strain is important to consider. Phenotypic traits such as weight, length, spontaneous activity, and insulin resistance are polygenic and different mouse strains vary from each other in these phenotypic traits. Some of these characteristics have been mapped to specific loci in certain strains, adding to any observed phenotype seen. These QTLs should be considered when planning which strain to use [for some examples see (Reed *et al*., 2003, Almind

and Kahn, 2004, Ishimori *et al*., 2004, Biddinger *et al*., 2005)]. An important example of strain differences can be seen with the insulin receptor knockout mouse. It has been shown that 85 % of C57BL/6 mice heterozygous for the insulin receptor knockout (*Insr*$^{+/-}$) and heterozygous for the insulin receptor substrate-1 (*Irs1*$^{+/-}$) are overtly diabetic by 6 months, whereas 129Sv and DBA mice with the same mutations show a much lower rate of 2 and 64 %, respectively (Kulkarni *et al*., 2003). Genetic background can be used to exacerbate the phenotype of interest, but it can also obscure underlying differences; therefore, strain choice should be planned carefully and appropriate controls used when using a mixed genetic background.

1.5.1 Genetic manipulation of the Mouse

Humans have been breeding mice for the last 3000 years (Beck *et al*., 2000). Inbred mice are strains that have undergone at least 20 intercross matings. By 20 generations 98.6 % of the loci in each mouse are homozygous. Each inbred strain is considered isogenic because all individuals trace back to a common ancestor in the twentieth or a subsequent generation (Beck *et al*., 2000). Using these inbred strains minimises background effects allowing us to observe phenotypic differences caused only by the desired genetic manipulations.

Induced random mutations are also valuable for uncovering novel genes involved in disease. Mouse mutagenesis strategies include gene-trapping, which induces random loss-of-function mutations [reviewed in (Stanford *et al*., 2001)]; N-ethyl-N-nitrosourea (ENU), which produces point mutations that can result in a variety of different alleles (Quwailid *et al*., 2004, Acevedo-Arozena *et al*., 2008), X-rays; chlorambucil; and insertional mutagenesis using retroviral infection. Spontaneous mutations also occur at a rate of approximately 5 x 10^{-6} per locus, but these are detected only if there is a visible phenotype.

1.5.1.1 ENU Mutagenesis

ENU is a powerful alkylating agent which mutagenises highly the spermatogonial germ cells routinely causing single base-pair changes with a preference for A-T/T-A tranversion (Justice *et*

al., 1999). ENU has been used successfully in many mutagenesis programmes worldwide to identify novel genes of human diseases (Acevedo-Arozena *et al*., 2008). The major problem with ENU has always been the time and cost of mapping any mutations generated, but with the cost of next generation sequencing almost reaching the targeted '$1000 genome', this step will be considerably quicker. This will allow easy identification of potential novel genes for research.

ENU mutagenesis screens, such as those performed at MRC Harwell, are also available for screening archived DNA for the generation of novel mice. Although loss-of function mutations are valuable, an important advantage of chemical mutagenesis is that it generates allelic series, possibly generating a range of phenotypes from mutations in the same gene (Coghill *et al*., 2002, Quwailid *et al*., 2004).

1.5.1.2 Mouse Transgenics

Targeted manipulation of the mouse genome has been possible for over 20 years (Capecchi, 1989), and as such a huge range of resources are available for investigations using the mouse. Gene targeting involves the introduction of foreign DNA at a specific locus by homologous recombination (HR) in embryonic stem (ES) cells (Smithies *et al*., 1984, Smithies *et al*., 1985, Thomas *et al*., 1986). HR can generate any sort of genetic modification you can imagine, such as gene knockout, overexpression, point mutations, splice variants and conditional alleles. Conditional mutagenesis allows mutations to be selectively targeted to a specific tissue, cell type and/or developmental stage. The most commonly used method for this is the Cre/*LoxP* system [reviewed in (Kos, 2004, Ray *et al*., 2000, Brault *et al*., 2007, Sauer, 1998), of which many Cre lines are accessible at The Jackson Laboratory (http://cre.jax.org/index.html]. Other site-specific recombinase systems are available such as Flp/*FRT*, φC31/*att*, and Dre/*Drox* (Kilby *et al*., 1993, Feng *et al*., 1999, Bode *et al*., 2000, Anastassiadis *et al*., 2009).

These conventional gene targeting strategies use HR and have been very successful but they can often take over a year to generate mice on the correct background ready to begin exploring the effect of the altered gene. More recently zinc finger nucleases (ZFNs) and Transcription activator

like effector nucleases (TALENs) have proven to be useful additions to the transgeneticist's toolbox.

Zinc finger nucleases (ZFNs) are manmade scissors that are capable of inducing double stranded breaks at a prescribed locus. TALENs are very similar to ZFNs binding to particular DNA sequence and then causing a double stranded break, and then utilising HR to introduce specific mutations or in the absence of a donor sequence non-homologous end-joining (Christian *et al*., 2010). Unlike traditional HR which requires ES cells, ZFNs and TALENs have the ability to be used in a wide variety of organisms from plants to large domestic animals for which ES cells were not available. They are also quicker and simpler than HR, and can bypass the tedious work of constructing large constructs.

1.5.1.3 Mouse Resources

There are a number of resources available to the research community to provide mice for their studies. The Federation of International Mouse Resources (FIMRe) is a collaborating group of mouse repository and resource centres worldwide (**Table 1.6**) that archive and provide strains of mice as cryopreserved embryos and gametes, ES cell lines, and live breeding stock (http://www.fimre.org/).

Table 1.6 Members of the Federation of International Mouse Resources (FIMRe).

Member	Link
The Jackson Laboratory (TJL)	http://www.jax.org/
Mouse Mutant Resource Regional Centres (MMRRC)	http://www.mmrrc.org/
Mouse Models of Human Cancer Consortium (MMHCC)	http://emice.nci.nih.gov/
Canadian Mouse Consortium (CMC)	http://www.mousecanada.ca/
Canadian Mouse Mutant Repository (CMMR)	http://www.cmmr.ca/
European Mouse Mutant Archive (Karra *et al*.)	http://www.emmanet.org/
RIKEN BioResource Center (RBRC)	http://www.brc.riken.jp/lab/animal/en/
Center for Animal Resources and Development (CARD)	http://card.medic.kumamoto-u.ac.jp/
Australian Phenomics Network (APN)	http://www.australianphenomics.org.au/

Following on from the completion of the mouse genome sequence, that in principal identified every gene in the genome, the International Knockout Mouse Consortium was developed to systematically generate null mutant ES cells that provide "knockout first" alleles that can then be converted into conditional alleles (alleles that are null only from specific time points and/or specific tissues) for every protein coding gene (20,000 plus genes) in the mouse genome [(Skarnes *et al*., 2011) **Table 1.7**]. These resources are readily available to the research community (Ringwald *et al*., 2011). Exploiting the knockout mouse resource the International Mouse Phenotyping Consortium (http://www.mousephenotype.org/) has been established and funded to create mouse lines from each targeted ES cell and to determine the phenotype of the resulting mutant mice (Gates *et al*., 2011, Brown and Moore, 2012). Through high-throughput phenotyping of each line, using pipelines already established by pilot programs such as EUMODIC (http://www.eumodic.eu/), functional information can be attached to every gene in the mouse genome (Brown and Moore, 2012). This should provide novel genes and models for translational research for human diseases including T2DM.

Table 1.7 Members of the International Knockout Mouse Consortium (IKMC)

Member	Role
International Knockout Mouse Consortium (IKMC) http://www.knockoutmouse.org/	Incorporates all the members. Enables the IKMC database to be searched for gene of interest by gene symbols, gene IDs or genome location. Provides information on availability of Knockout Attempts and other resources.
NIH Knockout Mouse Project (KOMP) http://www.nih.gov/science/models/mouse/knockout/	Incorporates KOMP-CSD and KOMP-Regeneron, Inc. Utilise different strategies. KOMP-CSD use promoterless and promoter-driven targeting cassettes for the generation of a 'Knockout-first allele' to produce frame shift mutations of a 'critical' exon. KOMP-Regeneron constructs generate complete null alleles that delete the entire protein coding sequence of the target gene. Provides central database resource through the Knockout Mouse Project Data Coordination Centre (KOMP DCC). KOMP Repository to archive, maintain and distribute KOMP products.
The European Conditional Mouse Mutagenesis Program (EUCOMM) www.eucomm.org/	Largest contributor. Uses conditional approaches, conditional gene trapping – a random approach for expressed genes, conditional targeted trapping – a directed approach, for expressed genes, conditional gene targeting - a directed approach, for non-expressed genes.
North American Conditional Mouse Mutagenesis project	Utilises a combination of gene trap random mutagenesis and systematic high-throughput targeting of remaining untrapped

(NorCOMM) http://www.norcomm.org/index.htm	genes.
Texas A&M Institute for Genomic Medicine (TIGM) http://www.tigm.org/	Maintains the world's largest C57BL/6N gene trap library, containing over 350,000 cell lines representing more than 10,000 unique genes. Has access to a privately held 129/SvEvBrd gene trap library, containing more than 270,000 sequence-tagged embryonic stem cell clones.

1.6 Thesis Aims and Objectives

This thesis aims to understand the role that FTO plays in obesity. To achieve this, the following approaches have been taken:

- Conditional deletion of FTO in six week old mice to understand the role FTO plays in the adult mouse, and circumvent any deleterious developmental effects.
- *In vitro* analysis of FTO to examine the role FTO plays in amino acid sensing, development and adipogenesis.
- Utilise a gene-driven approach to identify novel ENU induced mutations in Exon 5 of FTO to examine the catalytic function of FTO *in vivo*.
- Generate a targeted conditional overexpression allele of *Fto* without catalytic activity to examine the effect of catalytically inactive FTO *in vivo*.
- Pharmacological inhibition of FTO to examine the effect of inhibiting the catalytic function of FTO *in vivo*.
- Analysis of FTO overexpression mice to understand why they are hyperphagic.

Chapter 2:

Materials and Methods

This chapter describes the general materials and methods used in this thesis. More specific methods can be found within the relevant chapter.

2.1 General Reagents and Solutions

Chemicals were purchased from Sigma-Aldrich (Dorset, U.K.) unless stated otherwise. Restriction endonucleases were purchased from New England Biolabs (NEB, Massachusetts, U.S.A.) unless stated otherwise. Synthetic oligonucleotides and primers were designed using Primer3 (http://frodo.wi.mit.edu/primer3/) or VectorNTI (Invitrogen, California, U.S.A.) and synthesised by Eurogentec (Hampshire, U.K.).

Standard solutions (**Table 2.1**) were prepared using ddH_2O unless specified otherwise according to (Sambrook *et al*., 1989).

Table 2.1 Standard Solutions

Reagent	Composition
ES Cell Lysis Buffer	10 mM Tris (pH 7.5), 10 mM EDTA (pH 8), 10 mM NaCl, 0.5 % Sarcosyl, and 1 mg/ml Proteinase K (added fresh)
Krebs Henseleit Buffer (5 X)	555 mM NaCl, 23.5 mM KCl, $MgSO_4$ 10 mM, Na_2HPO_4 6 mM, filter sterilised
Luria Bertani (LB) Broth	10 g/l Bactotryptone, 5 g/l Bactoyeast extract, 5 g/l NaCl, pH 7.0 at 25 ºC
Loading Buffer (Agarose Gel)	500 ml glycerol, 200 ml 0.5 mM EDTA, 200 ml ddH_2O and 2 g xylene orange for 1 litre
PBST	0.1 % Tween-20 in 1 X PBS
SSC Solution (20 X)	0.3 M $Na_3citrate_2H_2O$, pH 7.0, 3 M NaCl
TAE (10 X)	48.4 g of Tris base tris(hydroxymethyl)aminomethane], 11.4 ml of glacial acetic acid (17.4 M), 3.7 g of EDTA, disodium salt, deionized water to 1 l
TBST	0.1 % Tween-20 in 1 X TBS

TBSTM	5 % milk powder (Marvel, Premier Brands. Ltd., Birmingham, U.K.) 0.1 % Tween-20 in 1 X TBS
TBSTBSA	5 % Bovine Serum Albumin powder 0.1 % Tween-20 in 1 X TBS
TE	10 mM Tris, 1 mM EDTA (pH 8.0)
Transfer Buffer (Immunoblot)	25 mM Tris-Base, 192 mM Glycine, 20 % methanol

2.2 DNA methods

2.2.1 Polymerase Chain Reaction

The polymerase chain reaction (PCR), originally pioneered by (Saiki *et al*., 1985), was used to specifically amplify DNA sequences of interest. A master stock of primers (100 µM) was diluted to a working stock of 10 µM with nuclease free water (ddH_2O). PCR was routinely performed according to the following protocols:

<u>High Fidelity Phusion Polymerase (Finnzymes, Espoo, Finland)</u>

5 µl Template DNA (typically 5 ng/µl)

4 µl 10X Buffer (High Fidelity Buffer)

0.4 µl 10 mM dNTPs (Invitrogen)

0.5 µl Forward amplification primer (10 µM)

0.5 µl Reverse amplification primer (10 µM)

0.2 µl 1x Phusion High-Fidelity DNA Polymerase

9.4 µl ddH_2O

In a total volume of 20 µl.

PCR thermocycling was carried out using the following program as an example:

Initial denaturing step 95 ºC for 45 seconds,

35 cycles of

Denaturing Step 95 ºC for 20 seconds,

Annealing Step *T for 20 seconds

Extension Step 72 ºC for 30 seconds (30 seconds per Kb of genomic DNA amplicon)

Final extension step 72 ºC for 10 min.

Specific primers and information are listed below in **Section 2.6.1 Genotyping**.

*Primer annealing temperatures were estimated using the Finnzymes TM calculation (http://www.finnzymes.fi/tm_determination.html) according to a modified method of Breslauer's thermodynamics (Breslauer *et al*., 1986).

2.2.2 Gel Electrophoresis

DNA fragments were resolved by agarose gel electrophoresis using 0.6-4 % (w/v) 1 X TAE (Tris-acetate; 40 mM Tris acetate and 1 mM EDTA) gels containing 0.001 % (w/v) ethidium bromide with 1 x TAE running buffer using standard techniques (Sambrook *et al*., 1989). DNA was mixed for loading with 10 % (w/v) loading buffer. DNA fragments were visualised using a ultra-violet (UV) transilluminator with the quantity one basic software (Molecular Imager Gel Doc XR System, BioRad, Hertfordshire, U.K.). DNA fragment sizes were estimated next to known DNA ladders including the 100 bp ladder (100 bp-2072 bp, Invitrogen), Lambda (λ) DNA-HindIII Digest (129 bp – 23,130 bp, NEB) or 1 Kb Plus DNA ladder (100 bp-12,000 bp, Invitrogen).

2.2.3 Bacterial Culture

Bacteria (*Escherichia coli, E.coli*) were routinely cultured in liquid media in a shaking incubator (200-250 rpm) or on solid media plates in a static incubator, with the addition of ampicilin (Amp) at a concentration of 50 µg/ml overnight for 12 hours (LB broth, prepared by Laboratory Services at MRC Harwell). Both solid and liquid media were incubated at 37 ºC. Bacteria were pelleted from liquid media (typically 1-2 ml) by centrifugation for 1 min at 13,000 rpm (13,200 xg) using a Biofuge Pico microcentrifuge (Thermo Fisher Scientific-Heraeus, Loughborough, U.K.). Bacteria used include DH5α (sub-cloning efficiency™ DH5α™ Competent Cells, Invitrogen) and XL-10 (XL10-Gold Ultracompetent Cells, Agilent, California, U.S.A.).

2.2.4 Plasmid Isolation and Purification from Bacterial Culture

Plasmid DNA from ampicilin resistant (AmpR) bacterial (*E.coli*) colonies were isolated and purified using the Qiagen Miniprep kit (Qiagen Inc, California, U.S.A.), following the manufacturer's instructions using a method originally developed by (Birnboim and Doly, 1979). In a high salt buffer plasmid DNA binds to the silica membrane. Following a series of alcohol washes, the plasmid DNA is eluted from the column in 50 µl of TE buffer or ddH_2O. Plasmid minipreparations (minipreps) were checked by restriction digest pattern analysis upon separation by agarose gel electrophoresis and sequencing.

2.2.5 Determination of Nucleic Acid Concentrations

The concentration of purified plasmid DNA and genomic DNA was determined using a Nanodrop 8000 spectrophotometer (Thermo Fisher Scientific-Heraeus). Approximately 2 µl of nucleic acid solution was placed on the Nanodrop 8000 spectrophotometer that subsequently transmits UV light through the sample and measures absorbance using a photo detector. Based on the absorbance, according to the Beer Lambert Law, the concentration of nucleic acids is determined. For DNA a 260/280 nm ratio of ~1.8 is generally accepted as "pure" and a ratio of ~2.0 is generally accepted as "pure" for RNA. For RNA the 260/230 nm ratio can be additionally used to check purity, with a range of 2.0-2.2 for "pure" RNA.

2.2.6 Large Scale Plasmid DNA Purification

Plasmids were amplified by inoculating 250 ml of LB broth containing Amp (50 µg/ml) overnight for 12-16 hours at 37 ºC. Plasmid DNA was purified using an EndoFree Plasmid Maxi kit (Qiagen) to yield approximately 500 µg of transfection grade, gram-negative bacteria endotoxin free, plasmid DNA following the manufacturer's instructions.

2.2.7 Restriction Endonuclease Digests

Restriction endonucleases (restriction enzymes) were purchased from NEB unless stated otherwise and used with the recommended buffer and incubation temperature using the rule that 1 unit of restriction enzyme fully digests 1 µg of DNA within 1 hour. Restriction enzyme digestion of plasmid DNA, for the isolation of DNA fragments, plasmid composition analysis or restriction enzyme pattern analysis, was routinely performed according to the following protocol:

5 µl Purified miniprep DNA (~200 ng/µl)

5 µl 10 X Specified Restriction enzyme buffer

1 µl Restriction enzyme (10 U/µl)

39 µl ddH_2O

Total reaction volumes of 50 µl.

Reactions were incubated for 1 hour at 37 ºC unless stated otherwise. The quantity of DNA, concentration of restriction enzymes and sample volume were adjusted according to amount required. DNA fragments were resolved by agarose gel electrophoresis. **Table 2.2** describes the restriction enzymes and conditions required for the restriction enzyme digestion of DNA.

Table 2.2 - Restriction Endonuclease Reactions. Restriction enzyme digests were incubated for 1 hour for plasmid DNA and overnight for genomic DNA at 37 ºC unless stated otherwise.

DNA	Enzyme	NEB Buffer	BSA	Units / µl
Plasmid	*AscI*	4	-	10
Plasmid	*AsiSI*	4	BSA	10
Plasmid	*BamHI*	3	BSA	20
Plasmid	*EcoRI*	NEBuffer EcoRI	-	20
Genomic DNA	*Eco*RI (5 X Concentration)	NEBuffer EcoRI	-	50
Plasmid	*EcoRV*	4	BSA	4
Plasmid	*HindIII*	2	-	20
Genomic DNA	*HindIII (5 X Concentration)*	2	-	50

2.2.8 Isolation and Purification of DNA fragments

DNA fragments generated by PCR or restriction digestion were purified by one of two methods. Both methods utilise a silica membrane in the presence of buffers with a high salt concentration to enable DNA binding, following a series of alcohol washes, the DNA fragment is eluted in 25-40 µl ddH_2O:

QiaQuick Gel Extraction Kit (Qiagen)

Agarose gel slices containing DNA fragments were excised using a scalpel blade over a UV transilluminator removing the minimum amount of surrounding agarose. The gel slice was transferred to a 1.5 ml tube and dissolved in high salt buffer by incubation at 50 ºC. The DNA was isolated using the QiaQuick Gel extraction kit (Qiagen) according to the manufacturer's instructions.

QiaQuick PCR Purification Kit (Qiagen)

DNA fragments resolved by agarose gel electrophoresis, with no additional DNA fragments, were isolated using the QiaQuick PCR purification kit (Qiagen) according to the manufacturer's instructions.

2.2.9 Plasmid Linearisation

Plasmids for the insertion of DNA fragments or oligonucleotides were prepared by restriction enzyme digest of approximately 1 µg of plasmid DNA in a 50 µl total volume. The linear plasmid (vector) DNA was extracted by phenol/chloroform extraction to remove proteins. One volume of phenol:chloroform:isoamylalcohol (25:24:1; Fisher Chemicals, Thermo Fisher Scientific-Heraeus) was added to the restriction enzyme reaction, followed by vortexing for 2 min. The emulsion reaction mixture was fractionated at 3000 rpm (800 xg) for 2 min using a Biofuge Pico microcentrifuge (Thermo Fisher Scientific-Heraeus). The top aqueous layer was removed and ethanol precipitated using 2.2 volumes of absolute ethanol, 0.1 volumes of sodium acetate (NaOAC; pH 5.2) and 1 µl glycogen (as a carrier). The reaction mixture was placed on ice for 30

min and spun at 13,000 rpm (13,200 xg) at 4 °C for 20 min using a Biofuge pico-microcentrifuge. The pellet was rinsed with 70 % ethanol and air dried. Finally the pellet was re-suspended in ddH_2O or TE.

2.2.10 Dephosphorylation of Vector DNA

To prevent DNA strands from self-ligating, by self-circularisation and concatenation, and to aid ligation efficiency, 5' phosphates were removed from DNA ends by dephosphorylation using a recombinant rAPid alkaline phosphatase (from bovine intestine expressed in *Pichi pastoris*, Roche, West Sussex, U.K.*)* following the manufacturer's instructions:

5 µl Purified vector DNA (~200 ng/µl)

2 µl 10 X rAPid Alkaline Phosphatase Buffer

1 µl rAPid Alkaline Phosphatase (1 U)

12 µl ddH_2O

Total reaction volume to 20 µl.

Reactions were incubated at 37 °C for 10 min for 5' overhang DNA ends or 20 min for blunt DNA ends. rAPid Alkaline Phosphatase was inactivated by incubating the reaction for 2 min at 75 °C and returned to room temperature. Dephosphorylated vector DNA was subsequently used for ligation.

2.2.11 Ligation of Vector and Insert

Positive and negative control ligation reactions were performed alongside each ligation reaction. Ligation reactions were performed using an approximate molar ratio of 3:1 insert fragment to vector using the T4 DNA ligase (Roche) following the manufacturer's instructions:

1 µl Vector DNA (50 ng/µl)

6 µl Insert Fragment DNA (25 ng/µl)

2 µl 5X DNA Dilution Buffer (Roche)

10 µl 2X T4 DNA Ligation Buffer (Roche)

1 µl T4 DNA Ligase (5 Units) (Roche)

Total reaction volume to 20 µl.

Ligation reactions were incubated at room temperature for 15 min for sticky 5' overhang DNA ends and for 1 hour at room temperature for blunt DNA ends.

2.2.12 Bacterial Transformations by Heat Shock

DH5α chemically competent (by CaCl2) cells (sub-cloning efficiency™ DH5α™ Competent Cells, Invitrogen) XL-1 Blue (XL1-Blue Competent Cells, Stratagene, California, U.S.A.) or XL-10 (XL10-Gold Ultracompetent Cells, Agilent) were used for transformations. For DH5α chemically competent cells transformation was performed by incubating the ligation mixture (5 µl) or purified plasmid DNA (1 µl) with 50 µl of ice cold chemically competent cells for 20 min on ice. The transformation reaction was incubated for exactly 20 seconds at 42 °C in a water-bath, and then placed immediately on ice for 2 min. Subsequently, the transformation reaction was recovered by adding 900 µl of liquid LB media (without antibiotic) or SOC liquid media (Invitrogen) pre-warmed to 37 °C and incubated for 1 hour shaking at 250 rpm at 37 °C. The transformation reaction was then centrifuged at 3000 rpm (800 xg) using a Biofuge Pico microcentrifuge (Thermo Fisher Scientific-Heraeus) for 3 min to pellet the bacteria. The supernatant was removed by pouring, leaving approximately 50 µl of LB media. The bacterial pellet was re-suspended in approximately 50 µl of liquid LB media and added to solid LB media 10 cm^2 petri dishes containing Amp (50 µg/µl when in molten form). Solid LB media plates were incubated overnight for 16 hours and bacterial colonies were picked using a sterile P10 pipette tip for inoculation.

2.2.13 Genomic DNA Extraction

Genomic DNA was extracted from cells and mouse tissues by two main methods for genotyping or Southern blotting/hybridisation analysis:

2.2.13.1 DNeasy Genomic DNA Extraction (Qiagen)

Genomic DNA was extracted from mouse ear and tail tissues using a DNeasy blood and tissue kit (Qiagen) according to the manufacturer's instructions. The tissue was directly lysed in 180 µl of tissue lysis buffer (ATL) with 20 µl of proteinase K (PK, 600 mAU/ml solution). The lysate was bound to a silica-based DNA purification spin-column. Contaminants and enzyme inhibitors are removed in two wash steps (with AW1 and AW2). The DNA was then eluted in H_2O or AE buffer (ear tissue, 100 µl; tail tissue, 200 µl).

2.2.13.2 Extraction of Genomic DNA from ES cells

Frozen ES cells were provided in 96-well plates or as cell pellets in 15 ml tubes (Transgenics and Gene Targeting, MRC Harwell). ES cells from 96-well plates were incubated in 50 µl of ES cell lysis buffer (**Table 2.1**) at 55 °C overnight in a humidified chamber. The following day the DNA was precipitated by adding 100 µl of 75 mM NaCl in ice-cold absolute ethanol. The 96-well plates were incubated for 30 min on ice with nucleic acids precipitating as a filamentous network. The 96-well plates were centrifuged at 3000 rpm (845 xg) using a Beckman-Coulter Allegra 6KR centrifuge (Beckman-Coulter, California, U.S.A.) at 4 °C for 45 min to ensure all DNA was attached to the plastic base. The cell suspension solution was decanted and the plate gently tapped dry on tissue. The plates were washed twice with 200 µl of 70 % ethanol with 5 min centrifugation steps at 3000 rpm (845 xg) in between (Beckman-Coulter Allegra 6KR centrifuge). The solution was decanted by inverting the plate and the DNA left to air dry. The ES cell DNA was dissolved in 20 µl of TE or directly used for restriction enzyme digestion (see **section 2.2.7**, **Table 2.2**). ES cell pellets in 15 ml tubes were lysed with 5 ml of ES cell lysis buffer and incubated at 55 °C overnight. Phenol/chloroform was used to extract and purify the DNA (**section 2.2.9**).

2.2.14 Sequence Analysis

Purified PCR amplification products and plasmids were sent for Sanger sequencing (Sanger *et al*., 1977) to either GATC Biotech (Konstanz, Germany), Geneservice (Cambridge, U.K.), or Source Bioscience (Oxford, U.K.) and analysed using Vector NTI advance 10-Contig Express (Invitrogen) or DNASTAR Seqbuilder and Seqman (Lasergene 7 DNASTAR Inc, Wisconsin, U.S.A.). Samples were sent with 10 µM of sequencing primers.

2.2.15 Southern Blotting

Ten micrograms of genomic DNA was digested with the appropriate restriction endonuclease in a total volume of 50 µl (**Section 2.2.7**, **Table 2.2**). The genomic DNA was fractionated by gel electrophoresis (0.5-1 % agarose gel at 100 V) in 1 x TAE for 4 hours. Once the DNA fragments had been resolved sufficiently the agarose gel was photographed against a ladder with known DNA size markers and a ruler on a UV transilluminator. The agarose gel was placed in a tray containing denaturing solution (1.5 M NaCl, 0.5 M NaOH) for 1 hour at room temperature on an orbital shaker (Stuart Scientific, 3D rocking platform STR9, Essex, U.K.). The gel was rinsed in ddH_2O and placed in neutralising solution (1.5 M NaCl, 0.5 M Tris-HCl, pH 7.5) for 1 hour at room temperature on a STR9 orbital shaker. Finally the gel was placed into 20 X SSC solution for 20 min at room temperature. Genomic DNA was transferred from the agarose gel overnight to a charged nitrocellulose membrane (Hybond-N+, Amersham, GE Healthcare, Buckinghamshire, U.K.) through capillary action using 20 X SSC. The following day the well positions were marked on the membrane in pencil. The membrane was subsequently washed for 5 min in a 2 X SSC solution at room temperature on a STR9 orbital shaker. The DNA was fixed to the membrane (filter) by UV crosslinking with a Stratalinker UV Crosslinker using the automatic cross link function (Stratagene).

2.2.16 Southern Hybridisation

Each membrane was placed in a hybridisation tube with prewarmed (65 °C) pre hybridisation solution (approximately 10-15 ml, QuickHyb; Stratagene) at 68 °C for 1 hour. Twenty-five nanograms of purified DNA fragment were labelled with [32P]α-dCTP (Perkin Elmer Massachusetts, U.S.A.) using the Rediprime II random primer labelling system (GE Healthcare) according to the manufacturer's instructions to generate the radioactively labelled probe. The probe was purified from non-incorporated [32P]α-dCTP nucleotides by illustra Sephadex G-50 DNA Nick columns (Amersham; GE Healthcare). The probe was eluted in 400 µl of TE, and 100 µl of sonicated salmon sperm DNA (Stratagene) was added to the reaction to reduce non-specific binding of the probe.

The purified probe was denatured at 100 ºC for 5 min, placed on ice for 5 min, and added to the hybridisation tube (Hybaid, Thermo Fisher Scientific-Heraeus). The membrane and probe were incubated in a rotating hybridisation oven at 68 °C for a minimum of 3 hours or overnight. The filter was washed with an increasing stringency consisting of different concentrations of SSC starting at 2 X to 0.1 X with 0.1 % SDS. The membrane was then placed in a cassette at -70 ºC and exposed to autoradiography film (Amersham, GE Healthcare). Visualisation of probe hybridisation on autoradiography film was developed using the Compact X4 imaging system (Xograph Imaging Systems Ltd, Gloucestershire, U.K.).

2.3 RNA Methods

2.3.1 RNA Extraction

Mouse tissues including brain, liver, pancreas, skeletal muscle and adipose tissue were homogenised using ceramic beads in 2 ml tubes (Stretton Scientific Ltd, Derbyshire, U.K.), with a Precellys-24 automated homogeniser (Bertin Technologies, Montigny-le-Bretonneux, France). Total RNA from individual mouse tissues were prepared for qRT-PCR. RNA was purified using an

RNeasy Plus Mini Kit for liver and hypothalamus, RNeasy fibrous Mini Kit for skeletal muscle or Lipid Tissue Mini Kit for white adipose tissue (WAT) and brown adipose tissue (BAT) (Qiagen) following the manufacturer's instructions. On-column DNase digestion was performed with the RNeasy Mini, fibrous and lipid kit whereas a genomic eliminator column was provided with the RNeasy Plus mini kit. RNA concentration and integrity were assessed using a NanoDrop spectrophotometer (**section 2.2.5**, Thermo Fisher Scientific-Heraeus) and an Agilent 2100 BioAnalyser (Agilent Technologies) respectively. Extracted RNA was stored at -80 °C.

2.3.2 cDNA Synthesis

Based on the RNA concentration, cDNA was generated by reverse transcription SuperScript III reverse transcriptase (Invitrogen) according to the manufacturer's instructions. Typically 1-3 µg of total RNA was reverse transcribed in a 20 µl total reaction volume.

2.3.3 Reverse Transcription and Real Time qRT-PCR

cDNA was analysed by separate quantitative PCR using real-time detection of accumulated fluorescence with TaqMan Gene Expression Assay reagents and TaqMan FAM dye-labelled probes (Applied Biosystems, Invitrogen, U.S.A.) using an ABIPRISM 7500 Fast Real-Time PCR System (Applied Biosystems). Taqman assay identification's for each Taqman probe are provided in the relevant chapter. Each individual sample and gene was tested in duplicate to achieve a cycle threshold (CT) value below 30 with the appropriate cDNA concentration (15-50 ng per reaction). All data was normalised to expression of the endogenous house-keeping gene *glyceraldehyde 3-phosphate dehydrogenase* (*GAPDH*) and/or *β-Actin* and analysed by the comparative ΔΔCT method to determine the difference in sample groups relative to control animals.

2.4 Protein Methods

2.4.1 Protein Extraction

Mouse tissues including brain, liver, pancreas, skeletal muscle and adipose tissue were homogenised using ceramic beads in 2 ml tubes (Stretton Scientific Ltd), with a Precellys-24 automated homogeniser (Bertin Technologies). Tissues were lysed in the CelLytic MT Mammalian Tissue Lysis/Extraction Reagent (Sigma-Aldrich, 1 ml buffer to 1 mg tissue) with 1 X complete protease inhibitor cocktail (1 µl / 100 µl lysis buffer, Sigma-Aldrich) and 1 X PhosStop phosphatase inhibitor cocktail (1 µl / 100 µl lysis buffer, Sigma-Aldrich). Lysates were placed on ice for 1 hour and cellular debris removed by centrifugation for 15 min at 13,000 rpm (865 xg, Beckman-Coulter Allegra 25R, TA-15 rotor) at 4 °C. The supernatant was removed to a pre-chilled 1.5 ml tube and stored at -80 °C.

Cultured adherent cells were trypsinised, washed with DPBS (Dulbecco's Phosphate Buffered Saline, Gibco, Invitrogen) and resuspended in pre-chilled 1.5 ml eppendorfs. Cells were resuspended in minimal CelLytic M Cell Lysis/Extraction Reagent (Sigma-Aldrich, approximately 125 µl for 10^6-10^7 of suspended cells) with 1 X complete protease inhibitor cocktail (1 µl / 100 µl lysis buffer, Sigma-Aldrich) and 1 X PhosStop phosphatase inhibitor cocktail (1 µl / 100 µl lysis buffer, Sigma-Aldrich). Tubes were left to lyse on an orbital shaker (Stuart Scientific) 15-20 min at room temperature. Cellular debris removed by centrifugation for 15 min at 13,000 rpm (865 xg, Beckman-Coulter Allegra 25R, TA-15 rotor) at 4 °C.

The protein concentrations of the extracted lysates were determined using the BCA (bicinchoninic acid) Protein Assay Reagent (BioRad,). Protein lysates were read against a known bovine serum albumin (BSA) standard curve (serial dilution of 10, 5, 2.5, 1.25, 0.625, 0.313, 0.156, and 0 µg/µl). Five microlitres of lysate or known standards were prepared and pipetted into a 96 well flat-bottomed plate. Twenty-five microlitres of reagent A' followed by 200 µl reagent B were added to each well, mixed for 10 min at room temperature on the STR9 orbital shaker (Stuart Scientific) and

the absorbance measured at 750 nm on a Spectra Max 190 spectrometer (MDS Analytical Technologies Ltd, Berkshire, U.K.). Protein lysates were immediately prepared for immunoblotting or stored at -80 °C.

2.4.2 Protein Electrophoresis and Blotting

Protein was separated by gel electrophoresis and transferred on to a membrane by one of two different systems.

BioRad

Protein samples were denatured by heating for 10 min at 70 ºC in Laemmli sample buffer. Protein lysates (mass loaded, 25-60 µg) were separated using a 4-15 % linear gradient Tris-HCl ready polyacrylamide gel with 1 X Tris/Glycine/SDS electrophoresis buffer (BioRad) at 200 V and 200 mA for 60 min using a mini-protean electrophoresis tank (BioRad). Proteins were size-separated by electrophoresis alongside a "Precision Plus Protein Standard" (250 kDa to 10 kDa, BioRad) or "SeeBlue Plus 2 standard (188 kDa to 3 kDa Invitrogen) protein ladders to allow molecular weights to be estimated.

Electrotransfer was performed using a mini-Transblot SD system (BioRad) by passing 100 V and 250 mA across the membrane/gel for 1 hour onto a polvinylidene difluoride (PVDF) membrane (Hybond-P Amersham, GE Healthcare) in chilled transfer buffer.

Invitrogen NuPAGE Novex Bis-Tris Gels

Protein samples were mixed with LDS sample buffer and reducing agent and denatured by heating at 70 ºC for 10 min. Protein Lysates (mass loaded, 10-60 µg) were separated using a 4-12 % linear gradient Bis-Tris ready polyacrylamide gel with 1 X MOPS or MES electrophoresis running buffer (Invitrogen) at 200 V for 50 min using a XCell Surelock Mini Cell tank (Invitrogen). Proteins were size-separated by electrophoresis alongside a "Precision Plus Protein Standard" (250 kDa to 10 kDa, Invitrogen) or "SeeBlue Plus 2 standard (188 kDa to 3 kDa Invitrogen) protein ladders to allow molecular weights to be estimated.

Electrotransfer was performed using a XCell II Blot Module (Invitrogen) by passing 30 V and across the membrane for one hour onto a nitrocellulose membrane (0.2 μm or 0.45 μm pore size) (Invitrogen) in transfer buffer (10 % methanol for 1 gel, 20 % methanol for 2 gels).

2.4.3 Immunoblotting

The membranes were washed with TBS for five min. Antibody incubation and washes were performed with an STR9 orbital shaker (Stuart Scientific) in TBS containing 0.1 % Tween and either 5 % non-fat milk (TBSTM) or 5 % Bovine Serum Albumin (TBSTBSA). Membranes were blocked for 1 hour at room temperature with TBSTM or TBSTBSA. Membranes were probed with a primary antibody overnight at 4 ºC in TBSTM or TBSTBSA. Each membrane was rinsed briefly and subsequently washed for 3 times for five min at room temperature with TBSTM or TBSTBSA.

Membranes were incubated with primary antibodies of interest; details of antibodies are within relevant chapters. Protein presence by binding of primary antibody was than detected by one of two methods:

Enhanced Chemiluminescense (ECL)

The membranes were incubated with a secondary horseradish peroxidise (HRP) conjugated anti-source primary antibody (1:1000; BioRad) for one hour at room temperature. The membrane was rinsed briefly and subsequently washed for four times for five min at room temperature with TBSTM or TBSTBSA. A final wash was performed with TBS for one min.

Membranes were incubated with Enhanced Chemiluminescence Plus (ECL plus; Amersham, GE Healthcare) according to the manufacturer's instructions with five min incubation at room temperature in complete darkness. Excess fluid was drained and the membrane wrapped in Clingfilm ready for exposure to Hyperfilm ECL autoradiography film (Amersham, GE Healthcare). Visualisation of protein on Hyperfilm ECL was developed using the Compact X4 imaging system (Xograph Imaging Systems Ltd). Membranes were re-blocked for 1 hour at room temperature before re-probing with a loading control antibody incubated overnight at 4 ºC with

TBSTM or TBSTBSA followed by a secondary HRP-conjugated goat anti-mouse IgG antibody (1:1000, 1 hour at room temperature, BioRad).

Fluorescent-conjugated Secondary Antibody

The membranes were incubated with a secondary fluorescent (IRDye 800CW or IRDye 680RD conjugated anti-source primary antibody (1:15,000; LI-COR, Nebraska, U.S.A.) for one hour at room temperature in complete darkness. The membranes were rinsed briefly and subsequently washed for four times for five min at room temperature with TBSTM or TBSTBSA in complete darkness. A final wash was performed with TBS for one min. Membranes were drained of excess fluid and left to dry in white tissue/filter paper at room temperature in complete darkness. Detection of secondary was performed using the Odyssey SA Infrared Imaging System (LI-COR Biosciences, Cambridge, UK).

2.5 Cell Biology

2.5.1 Cell Culture and Transient Transfection

C2C12 [muscle myoblast cells derived from C3H mouse (Yaffe and Saxel, 1977)] and HEPA1-6 [hepatoma cells derived from BW7756 tumour in a C57L mouse (Darlington *et al*., 1980)] cell lines were used for experiments.

Cell culture was performed following aseptic guidelines in a Class II vertical laminar-flow biological cabinet. Cells were incubated at 37 °C in a humidified 5 % CO_2 atmosphere. Cell culture media and associated solutions were purchased from Gibco, Invitrogen. Cell culture media consisted of DMEM (31966-021), 1 X Penicillin/Streptomycin (15070-063), and 10 % fetal bovine serum (FBS) (10500-064).

Cells were cultured in 25 cm^2 flasks or 75 cm^2 flasks (Greiner Bio One, Frickenhausen, Germany) until approximately 80-90 % confluent. Cells were washed with DPBS (14190-094, calcium and magnesium free) and detached from the flask or dish by incubating with 300 µl of TrypLE Express

for 4-5 min at 37 °C. Cell culture media was added to the cells to inactivate the trypsin and the homogenous solution was centrifuged at 1200 rpm (167 xg) for two min in a 15 ml tube. Media was removed and the cell pellet resuspended in sufficient cell culture media to split the cells to an appropriate density. Cells were counted using a haemocytometer counting chamber (Hawksley, Sussex, U.K.).

Gene knockdown was achieved by treating C2C12 cells with siRNA. Cells were plated in antibiotic free media [DMEM (31966-021), 10 % FBS (10500-064)] and left to seed overnight. When cells are 30-50 % confluent they are ready for treatment. Lipofectamine 2000 (Invitrogen) was added to Opti-Mem serum-free media (31985-062) 10 µl lipofectamine/1 ml media. The mixture was incubated at room temperature for 5 min. Whilst incubating the siRNA was diluted in Opti-Mem (10-50 pmol/50 µl), I used 40 pmol in 50 µl (0. 4 µM solution), so that when we combine the incubated lipofectamine solution and diluted siRNA the final concentration is 20 pmol/50 µl (0.2 µM solution). This was incubated at room temperature for 20 min. Media was removed and cells were washed with DPBS. Oligomer-lipofectamine complexes were added to each well/flask, and placed back into the tissue culture incubator. After 4-6 hours this was topped up with antibiotic free media. After 24 hours media was aspirated and replaced with regular growth media.

2.5.2 Generation of Mouse Embryonic Fibroblasts (MEFs)

Timed matings were set up and plug checked. Females were sacrificed and embryos collected at E12.5-14.5. The head, the liver and any blood clots were removed from the embryos, and the liver used for DNA extraction for genotyping. Each individual embryo was then placed in a separate well of a 6 well plate in DPBS. When all embryos are prepared DPBS is removed and each well filled with 1.5 ml of dissociation reagent (0.25% Trypsin (1X) , 25050-014). Embryos were pulled apart and minced with dissection scissors, and incubated at 37 °C for five min. Tissue was further homogenised by passing through a 21 gauge x1.5’ needle (microlance, Becton Dickinson, New Jersey, U.S.A.) on a 1 ml syringe until the solution was cloudy. To each well 5 ml MEF media

[DMEM (31966-021) 1 X NEAA (Sigma-Aldrich M7145) 1 X Penicillin/Streptomycin (15070-063) 50 µM 2-mercaptoethanol (31350-010) 10 % FBS (10500-064)] was added to deactivate the trypsin and cells left to adhere. When confluent, MEFs were split into T25 flasks and split every 2-3 days when confluent.

2.5.2.1 Adipogenic Differentiation of Mouse Embryonic Fibroblasts

MEFs were plated into 35 mm dishes or six well plates, and allowed to become confluent. Two days post confluency cells were treated with growth media [DMEM (31966-021) 1 X NEAA (Sigma-Aldrich M7145) 1 X Penicillin/Streptomycin (15070-063) 50 µM 2-mercaptoethanol (31350-010)] containing 1 µM dexamethasone (Sigma-Aldrich), 0.5 mM methylisobutylxanthine (Sigma-Aldrich), 5 µg/µl insulin (Sigma-Aldrich), and 0.5 µM BRL49653 (Rosiglitazone, Sigma-Aldrich). As a control 0.1 % DMSO can be used in place of BRL49653. After two days the media was changed for growth media containing 5 µg/µl insulin and 0.5µM BRL49653, and the media was refreshed on the cells every other day, until 10-12 days had passed.

2.5.3 Immunocytochemistry

Cells were cultured on glass coverslips or in clear bottom 35mm fluorodishes (World Precision Instruments, Florida, U.S.A.). Cells were fixed for 15 min with 4 % paraformaldehyde in growth media and permeabilised for five min in ice-cold acetone. Cells were washed three times with TBS and blocked for 30 min at room temperature with TBS 5 % Goat Serum. A custom polyclonal rabbit anti-FTO antibody (Eurogentec) was diluted 1 in 400 in TBST and incubated for one hour at room temperature. After washing an Alexa Fluor® 488 Goat Anti-Rabbit IgG (H+L) secondary antibody (Invitrogen) was diluted 1 in 200 and incubated for one hour at room temperature. After washing if in dishes leave in PBS to image or if on coverslips mount on to slides with fluorescence mounting medium (Dako, Tokyo, Japan).

2.5.4 Histochemical Cell Staining

To visualise neutral lipids the lysochrome Oil red O stain was used. Cell cultures were rinsed with DPBS and fixed with 4 % paraformaldehyde at room temperature for 30 min. Oil red O stain was prepared by weighing out 300 mg of Oil Red O powder (Sigma-Aldrich) to 100 ml 99 % isopropanol, this stock solution is stable for 1 year. During the last 15 min of 4 % paraformaldehyde fixation 15 ml Oil red O stock was mixed with 10 ml ddH_2O (3:2).The diluted stain was incubated for 10 min at room temperature and filtered into a fresh tube with Whatman filter paper (GE Healthcare, Buckinghamshire, U.K.) this solution is stable for two hours. The fixative was removed and cells rinsed twice with ddH_2O. To each well 1.5 ml 60 % isopropanol was added and incubated at room temperature for 5 min. This was then removed and 1.5 ml Oil red O working solution was added to cover the entire monolayer, and incubated at room temperature for five min. This was removed and cells were washed with room temperature tap water until the water rinsed off clear. Optionally the nuclei were stained with 1 ml haematoxylin for one min at room temperature. This was removed and cells rinsed with room temperature tap water until the water rinsed off clear. Cells were then imaged in DPBS or mounted on to slides.

2.5.5 Microscopy

Light microscopy of cells and tissues was performed on the Axio-Observer Z1 microscope (Zeiss, Göttingen, Germany) with the AxioVision Imaging System (Zeiss), or on the Leica M216F dissection microscope with fluocombi III (Leica, Wetzlar, Germany).

Fluorescently labelled cells and tissues were visualised by confocal imaging using the LSM 700 inverted confocal (Zeiss), which is equipped with 4 lasers: Blue near UV diode 405 nm; Blue 488 nm; Green 561 nm; and Red 633 nm, and Zen imaging software; or on the Axio-Observer Z1 microscope (Zeiss) with the AxioVision Imaging System (Zeiss).

Image analysis was carried out using Volocity 5 (Perkin Elmer) or the NanoZoomer slide scanner software (Hamamatsu, Hamamatsu, Japan).

2.5.6 Live Dead Cell Staining

Cells were counted and plated into 12-well, 24-well (Nunc, Thermo Fisher Scientific-Heraeus) or seahorse 24-well plates (Seahorse Bioscience Inc, North Billerica, MA, U.S.A.). C2C12 and HEPA1-6 Cells were treated with siRNA or MEFs were left untreated unless specified in the relevant chapter (See **section 2.5.1**). Cells were washed with DPBS and Live/Dead stain [(Invitrogen) 2 μM Calcein AM and 4 μM EthD-1] was added and incubated with the cells at room temperature for 20-40 min protected from light. The plate was read on the Optima Plate reader (BMG labtech, Offenburg, Germany), with filters for Live (calcein) excitation 485-12 and emission 520-10 and Dead (EthD-1) excitation 520-10 and emission 650-10.

2.5.7 Seahorse Extracellular Flux Analysis

The Seahorse XF24 flux analyzer (Seahorse Bioscience) is capable of simultaneously measuring changes in pH and oxygen levels from cells seeded on 24-well plates. Oxygen consumption rate (OCR) was measured by monitoring the concentrations of dissolved oxygen by the XF24 Analyzer solid state sensor probes above the cell monolayer. The extracellular acidification rate (ECAR) was also assessed by the extracellular changes in pH, an indirect measurement of lactic acid production from cellular anaerobic glycolysis. Since carbon dioxide produced by cells also acidifies the culture medium, glycolysis accounts for approximately 80 % of the ECAR, and has been shown to be consistent with the amount of lactate measured in cells (Wu *et al*., 2007b, Xie *et al*., 2009).

Cells were plated on to seahorse 24-well plates, treated with siRNA if required and analysed within 24-48 hours. XF assays require a non-buffered media to accurately measure proton production rate and extra cellular acidification rate. On the day of the assay one of two medias were prepared, Krebs Henseleit Buffer (KHB) (**Table 2.1**) was diluted to 1 X with ddH_2O and glucose 2.5 mM and carnitine 0.5 mM were added, pH was measured and adjusted to pH 7.4 at 37 °C; or for XF Assay Media glutamax 2 mM, sodium pyruvate 2 mM, and glucose 10 mM were added, pH was measured and adjusted to pH 7.4 at 37 °C. Cells were then washed with the assay media, and assay media was added to the cells. The cell plate was then placed at 37 °C in a CO_2 free incubator for 30

min (XF assay) or 60 min (KHB assay) to acclimatise the cells. The cartridge was loaded with the compounds to test (details of compounds are within relevant chapters) and the XF24 instrument calibrated before running the assay.

2.5.8 Stable Isotope Labelling by Amino Acids in Cell Culture

Prepare two bottles of SILAC media, one which contains 'light' L-Lysine and L-Arginine and one which contains 'heavy' L-Lysine and L-Arginine.

To 500 ml SILAC DMEM media (PN89985, Fisher Scientific) add:

- 50 ml dialysed fetal calf serum (PN89986, Fisher Scientific)
- Appropriate Arginine 50 mg (Heavy 13C615N4 L-Arginine, PN89990, Fisher Scientific; Light L-Arginine, PN89989, Fisher Scientific)
- Appropriate Lysine 50 mg (Heavy 13C6 15N2 L-Lysine, PN88209, Fisher Scientific; Light L-Lysine, PN89987, Fisher Scientific).

5 ml Penicillin-Streptomycin (15070-063, Invitrogen)

Cell Dissociation buffer (Part number 13151-014, Invitrogen) was used when passaging the cells. Trypsin-EDTA should not be used as it may contain non-isotopically labelled amino acids.

C2C12 cells were grown in the media, one group 'heavy', one group 'light'. Cells were passaged five times to ensure proteins were fully labelled in 75 cm^2 flasks, as outlined in **Figure 2.1**. 'Heavy' labelled cells were then treated with FTO siRNA and 'light' labelled cells were treated with a negative control scrambled siRNA with a similar GC content, for 24 hours (please see **section 2.5.1**). Cells were then trypsinised using Cell Dissociation buffer, pelleted at 1200 rpm (167 xg) for two min in a 15 ml tube. Cells were resuspended in DPBS and counted using a cell counter (Scepter™ 2.0: Precision in Cell Counting, Millipore, Massachusetts, U.S.A.). From both the 'light' (Wellcome Trust Case Control Consortium) and 'heavy' (*Fto* siRNA) group 1 x 10^6 cells were combined to give a total of 2 x 10^6. Cells were then fractionated using NE-PER Nuclear and Cytoplasmic Extraction Reagents (Thermo Fisher Scientific-Heraeus) according to the

manufacturer's instructions. Mass spectrometry (MS) analysis was conducted at the Welcome Trust Centre for Human Genetics.

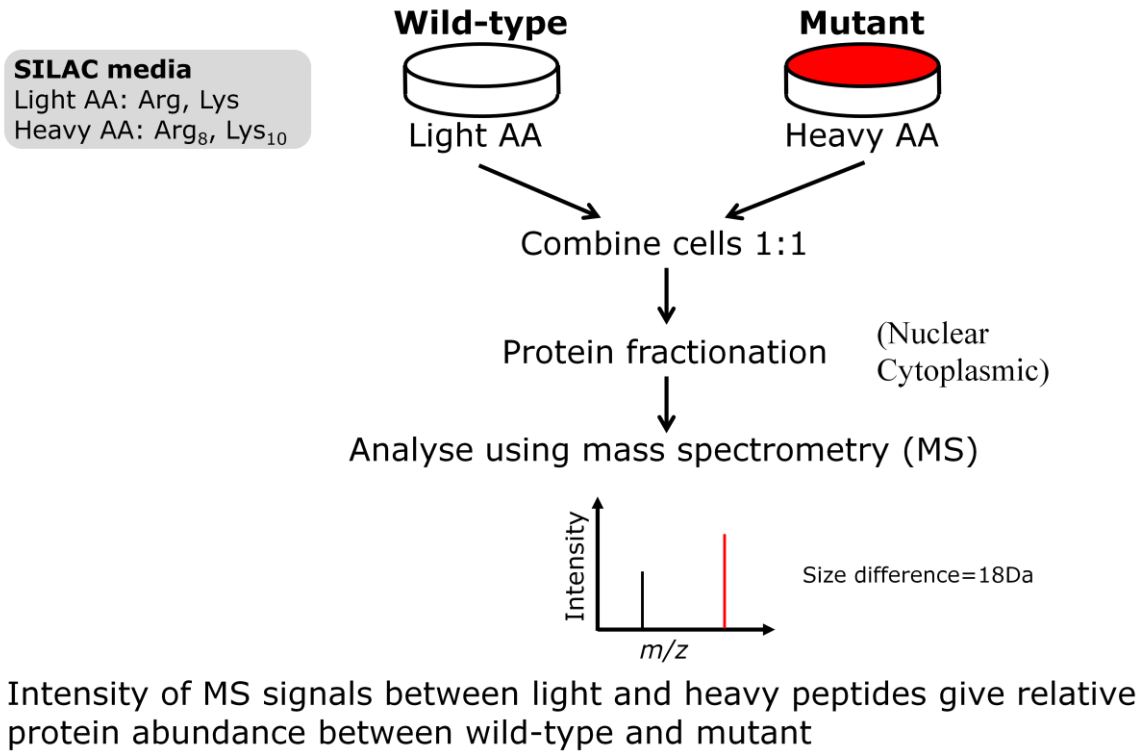

Figure 2.1 Stable Isotope Labelling by Amino Acids in Cell Culture.

2.6 Animal Husbandry and Metabolic Phenotyping

Animal studies were carried out under the guidance issued by the MRC; Responsibility in the Use of Animals for Medical Research (July 1993) and Home Project Licence Nos. 30/2642. Mice were kept in accordance with U.K. Home Office welfare guidelines and project license restrictions under controlled light (12 hr light and 12 hr dark cycle), temperature (21 °C ± 2 °C) and humidity (55 % ± 10 %) conditions. They had free access to water (25 ppm chlorine) and were fed *ad libitum* on a commercial diet (SDS maintenance chow, RM3, 3.6 kcal/g, Essex, U.K.). Where indicated, mice were maintained *ad libitum* on a HFD (D12451, Research Diets, New Brunswick, NJ, U.S.A.) containing 45 kcal % fat, 20 kcal % protein and 35 kcal % carbohydrate (4.7 kcal/g) from weaning.

2.6.1 Genotyping

Ear and tail tissue was taken from mice post weaning (approximately 3-4 weeks of age). DNA was extracted (**section 2.2.13**) and individual genotyping assays performed.

The following mouse lines were genotyped using a Fast SYBR Green (Applied Biosystems) real time PCR assay with their respective primers on the ABIPRISM 7500 Fast Real-Time PCR System (Applied Biosystems) using the standard Fast PCR programme. Each sample is run in duplicate for each assay, along with positive controls for each genotype. Using the Ct values we then can call the genotype, pass Ct <30, fail Ct >30.

SYBR Green (Applied Biosystems):

10 µl Fast SYBR green mastermix

4 µl DNA (approximately 5 ng/µl)

1.2 µl Forward Primer (5 µM)

1.2 µl Reverse Primer (5 µM)

3.6 µl ddH_2O

Total volume 20 µl

FTO-Rosa26-Overexpression-B6:

R26FTO	5’-TTATGGCGCGCCTAATGC-3’
R26FTOR	5’-TCTTAGCTTCCCGCTCTCGTT-3’
R26WTF	5’-TTCCCTCGTGATCTGCAACTC-3’
R26WTR	5’-CCTTTAAGCCTGCCCAGAAGA-3’

Fto Knockout Exon 3:

KOSF	5’-CTGGCAAGGTAAGAACCCTATAACTT-3’
KOR	5’-CCGCTCTAGAACTAGTGGATCCA-3’
FTOWTF	5’-GGTTTGTTTTTTAGACTGGCAAGGT-3’
FTOWTR	5’-TTCCAATAGTCTGTTTTCTTTCATAGAGTAC-3’

Cre Containing Lines

R26WTF (positive control)	5’-TTCCCTCGTGATCTGCAACTC-3’
R26WTR (positive control)	5’-CCTTTAAGCCTGCCCAGAAGA-3’
CreSybrF	5’-GGCAGTAAAAACTATCCAGCAACA-3’
CreSybrR	5’-CCCGGACCGACGATGAA-3’

Floxed FTO-Rosa26-Overexpression-B6:

R26WTF	5’-TTCCCTCGTGATCTGCAACTC-3’
R26WTR	5’-CCTTTAAGCCTGCCCAGAAGA-3’
NEOSYBRF	5’-CGACAAGACCGGCTTCCA-3’
NEOSYBRR	5’-AAGCGAAACATGGCATCGA-3’
ROSAFLXsybrF	5’-TTATGGCGCGCCTAATGC-3’
ROSAFLXsybrR	5’-TCTTAGCTTCCCGCTCTCGTT-3’

The following lines were genotyped using High Fidelity Phusion Polymerase (Finnzymes, Espoo, Finland) as in **section 2.2.1**.

Conditional Knockout Floxed Exon 3:

The Flx Knockout line was genotyped using the primers:

FLPeDELF	5’-GCATGCTCGATGGCAGTGTG-3’
FLPeDELR	5’-GTGAGACCGGCCAGGAAAGGAA-3’

A band at 300 bp indicated the presence of the floxed exon and a band at 100 bp indicated the presence of a wild-type gene.

Fto Knockout Exon 3:

FTOKOF	5’-AGCGCTCACTGGAGAGTGTCTG-3’
FTOKOR	5’-GAGCCAGAGAGGATTTAGATGGG-3’

A band at 237 bp indicates the recombined *Fto* KO allele, a band at 989 bp indicates the wild-type allele, and a band at 1184 bp indicate the floxed allele which is not recombined. Annealing 66 °C with an extension time of 1min to g*et al*l products, a 1.5 % gel may resolve the 989 and 1184 bp.

Reporter 26R:

The Reporter line was genotyped using the primers:

oIMR8545 5'- AAAGTCGCTCTGAGTTGTTAT-3'

oIMR8546 5'- GGACGGGAGAAATGGATATG-3'

oIMR4982 5'-AAGACCGCGAAGAGTTTGTC-3'

A band at 320 bp indicated the mutant and a band at 600 bp indicated the wild-type.

2.6.2 Embryo Collection

Timed matings were set up and plug checked. Pregnant female mice were killed at the desired age E8.5-18 according to Home Office guidelines. The abdomen was opened and uteri containing the embryos removed. Embryos were dissected in ice-cold PBS under a Zeiss Stemi 1000 dissection microscope and examined morphologically. Embryos were terminated by decapitation or immersion in 4 ºC fixative (Schedule 1) under Home Office guidelines.

2.6.3 Adult Tissue Collection for RNA, DNA and Protein Extraction

Tissue was collected from adult mice; brain, hypothalamus, liver, kidneys, heart, skeletal muscle, WAT, BAT and were snap frozen in liquid nitrogen using 2 ml cryotubes (Nunc, Thermo Fisher Scientific-Heraeus) and stored below -70 ºC.

2.6.4 Haematoxylin and Eosin (H&E) Analysis of Tissues

Liver, Epigonadal WAT, Kidney, BAT and gastrocnemius muscle were dissected and fixed in neutral buffered formaldehyde (Surgipath Europe Ltd, U.K.). Paraffin-embedded sections of the tissues were stained with haematoxylin and eosin (performed by the histology department, MRC Harwell). Images were captured by either the NanoZoomer Digital Pathology slide scanner

(Hamamatsu) or the Axio-Observer Z1 microscope (Zeiss) with the AxioVision Imaging System (Zeiss).

2.7 Metabolic Phenotyping

Phenotyping tests were performed according to EMPReSS (European Phenotyping Resource for Standardised Screens from EUMORPHIA; Brown *et al*., 2005; Mandillo *et al*., 2008). Standard operating procedures are described at http://empress.har.mrc.ac.uk.

2.7.1 Food and Water Consumption

Food and water consumption was measured by weighing and recording the food and water in the feeder chamber at the start and 24 hours after the mice have been placed into metabolic Techniplast cages (Buggeggiate, Italy). Urine was collected over 24 hours and the volume measured. Urine creatinine was measured on an AU400 (Olympus), as described (Hough *et al*., 2002). Urinary catecholamines were measured using a 3-CAT Epinephrine, Norepinephrine, Dopamine ELISA (Demeditec, Kiel-Wellsee, Germany) and normalised to urinary creatinine.

2.7.2 Body Composition

Body mass was measured each week from weaning on scales calibrated to 0.01 g. Body length was measured with a ruler in mm. Body composition was measured by DEXA (PIXImus, Wisconsin, U.S.A.) which can quantify fat mass, lean mass and bone mineral content (BMC) and density (BMD) (Nagy and Clair, 2000). DEXA uses an X-ray generator of high stability to produce photons over a broad spectrum of energy levels. The count data is transformed by software into bone and non-bone components, thus generating the bone density values together with soft tissue values.

Mice were placed into the DEXA apparatus following a lethal dose of anaesthetic (Euthatal 200mg/ml solution at a dose of approximately 150mg/kg) administered by intraperitoneal injection (IP).

Body composition was also measured using Nuclear Magnetic Resonance (NMR) (Echo-MRI-100, Echo-MRI, Texas, U.S.A.). NMR instruments for composition analysis create contrast between soft tissues by taking advantage of the differences in relaxation times of the hydrogen proton spins in different environments. Radio pulses cause proton spins to precess and emit radio signals which are then received and analysed. The amplitude, duration, and spatial distribution of these signals are related to properties of the material scanned. The high contrast between fat, muscle tissue, and free water is further enhanced by application of specially composed radio pulse sequences. Mice are not anaesthetised but are restrained in a tube and inserted into the instrument.

2.7.3 Indirect Calorimetry Oxymax

Oxymax indirect calorimetry (VO_2 /VCO_2 Oxymax System, Columbus Instruments, Ohio, U.S.A.) was used to simultaneously measure the metabolic performance of 16 individual mice in separate chambers. The Oxymax system measures or calculates VO_2 (oxygen consumption), VCO_2 (carbon dioxide production) RER (respiratory exchange ratio) and Heat (calculated value of the CV (caloric value) x VO_2) using the following equations:

$VO_2 = ViO_2i - VoO_2o$

$VCO_2 = ViCO_2i - VoCO_2o$

$RER = VCO_2 / VO_2$

$Heat = CV \times VO_2$

$CV = 3.815 + 1.232 \times RER$

CV, is a calorific value based on RER.

2.7.4 Blood Collection and Intraperitoneal Glucose Tolerance Test (IPGTT)

Each mouse was weighed and fasted overnight (16 hours) to establish the baseline glucose level "T0" (time zero). Mice were weighed again, and a blood sample was collected from the tail vein

after administration of local anaesthetic (EMLA cream, Eutectic Mixture of Local Anaesthetics, Lidocaine/Prilocaine, AstraZeneca, U.K.) using Lithium-Heparin microvette tubes (CB300, Sarstedt, Nümbrecht, Germany). Each mouse then received an IP injection of 2 g glucose / kg body weight (20 % glucose in 0.9 % NaCl). Subsequent blood samples were taken (at 60 and 120 min or at 10, 20 and 30 min) after glucose injection. AUC analysis was performed using GraphPad Prism version 5.02 for Windows. Fasted blood samples were taken at 8 weeks of age from the tail vein as described for the IPGTT.

2.7.5 Terminal Blood Collection

Mice were given a lethal dose of anaesthetic (**Section 2.7.2**) and terminal blood samples were taken by cardiac puncture; once fully anaesthetised a 22 G needle was inserted through the chest wall into the heart and blood drawn up into a 1 ml syringe. The needle was removed and the blood drawn from the syringe, by capillary action, into a Lithium-Heparin microvette tubes (Sarstedt).

2.7.6 Plasma Analysis

Following the collection of blood samples each microvette tube was centrifuged using a Biofuge Pico microcentrifuge (Thermo Fisher Scientific-Heraeus) at 3000 rpm (800 xg) for 10 min at room temperature. The supernatant (plasma) was removed leaving the red blood cells in the microvette tube. The plasma was transferred into 1.5 ml tubes and stored at -20 °C before testing. Plasma glucose was measured using an Analox Glucose Analyser GM9 (London, U.K.). Separate insulin levels were measured using an ultra-sensitive Mouse Insulin ELISA kit (Mercodia, Sweden). Plasma leptin, insulin, adiponectin and glucagon levels were measured using a mouse endocrine MILLIPLEX kit (MILLIPLEX MAP, Millipore) and a Bio-Plex 200 system (BioRad). Following the addition of dipeptidyl peptidase IV (DPP-4) inhibitor (Millipore) and serine protease inhibitor mix (Sigma-Aldrich) to plasma, amylin (active), ghrelin (active), GIP (total), GLP-1 (active), and PYY (total) were measured using a MILLIPLEX MAP mouse gut hormone panel kit (Millipore) with a Bio-Plex 200 system (BioRad). The plasma concentrations of glucose, ions (Na, K, Cl, Ca,

P), urea, creatinine, total protein, albumin, total bilirubin, total cholesterol, high density lipoprotein (HDL), low density lipoprotein (LDL), triglyceride, free fatty acids, glycerol, total bile acid, ALT, AST, ALP, and CK and urine creatinine were measured on an AU400 (Olympus U.K.), as described by (Hough *et al*., 2002).

2.7.7 Behavioural Analysis

The open field arena was defined with an 8 cm periphery zone and a centre zone (40 % of the total arena area) according to the standard operating procedure (http://empress.har.mrc.ac.uk). The total distance travelled in the arena and time spent in each zone was analysed using the video-tracking EthoVision software (Noldus Information Technology, Version 3.1). At the start of the test each mouse was placed at the centre of the arena. Measurements were taken for five min time bins for a total testing period of 30 min.

2.8 Statistical Analysis

Results are expressed as mean ± standard error of the mean (SEM). One or two way analysis of variance (ANOVA) was used to compare the means of genotype groups, followed by post hoc Bonferroni multiple comparison testing between all genotype groups using GraphPad Prism Software, version 5.02. The comparisons of genotype groups, for longitudinal body weight analysis, were performed using an ANOVA with repeated measures, followed by Bonferroni's post hoc tests to compare individual means from genotype groups. Area under the curve (AUC) analysis was performed using GraphPad Prism and compared using one way ANOVA with Bonferroni post hoc testing using GraphPad Prism 5.02. The Students *t*-test was used to investigate the difference between the means of two genotype groups. Significance was assigned to results that occurred with less than 5 % probability, $P<0.05$. The significance levels between genotype groups are indicated by asterisks in each figure above the bars: *P<0.05; **P<0.01; ***P<0.001. I thank Dr. George Nicholson for statistical advice and analysis.

Chapter 3:

Inactivation of *Fto* in the Adult Mouse

3.1 Introduction

The strongest BMI–associated GWAS locus in humans is the *FTO* gene. In the mouse, two constitutive knockout alleles have been reported (Fto^{tm1Urt} and $Fto^{tm1.1Pzg}$), both of which cause postnatal growth retardation and high postnatal mortality rates (Fischer *et al*., 2009, Gao *et al*., 2010). In one of these studies there was significant reduction in adipose tissue and lean body mass that was attributed to increased energy expenditure despite relative hyperphagia (Fischer *et al*., 2009). Deletion of *Fto* in neurons (using Nestin-Cre) caused a similar phenotype, demonstrating a neuronal role for FTO in postnatal growth (Gao *et al*., 2010). The phenotypes observed in loss of expression studies are complex with perinatal lethality, stunted growth from weaning, and significant alterations in body composition.

A third loss-of-function mouse model comprising a dominant missense mutation in the C-terminal of the mouse *Fto* gene resulted in reduced weight and fat mass and increased energy expenditure without the increased perinatal death and growth retardation (Church *et al*., 2009). In contrast, a mouse model that globally overexpressed FTO showed increased food intake, body weight and fat mass (Church *et al*., 2010).

These animal models clearly indicate a role for *Fto* in energy metabolism, but many questions remain unresolved, including whether there is any effect on energy expenditure, what the role of *Fto* is in early life and in the adult, which tissues are involved, and which regions of the brain contribute to the phenotype.

In order to investigate the function of the *Fto* gene in the mouse we constructed mice carrying a LoxP-flanked (floxed) exon 3 frame-shift allele [**Figure 3.1** (McMurray *et al*., 2013)]. Cre mediated excision of exon 3 will disrupt the catalytic double-stranded β-helix by generating a frame-shift null allele (after residue 41). Our global *Fto* germline knockout exhibits many similarities to the two other published *Fto* knockouts (Fischer *et al*., 2009, Gao *et al*., 2010). However, as all these models show considerable perinatal lethality and growth restriction it is difficult to determine the precise role of FTO in body composition and metabolism. In order to circumvent early postnatal and developmental effects that lead to lethality and growth restriction as a result of FTO loss, we therefore inactivated *Fto* in adult mice. This work has been published in collaboration with Professor Frances Ashcroft (University of Oxford), Dr. Giles Yeo (University of Cambridge) and Dr. Tony Coll (University of Cambridge) (McMurray *et al*., 2013). In this chapter my aim was to examine the effect of global removal of FTO in the adult mouse.

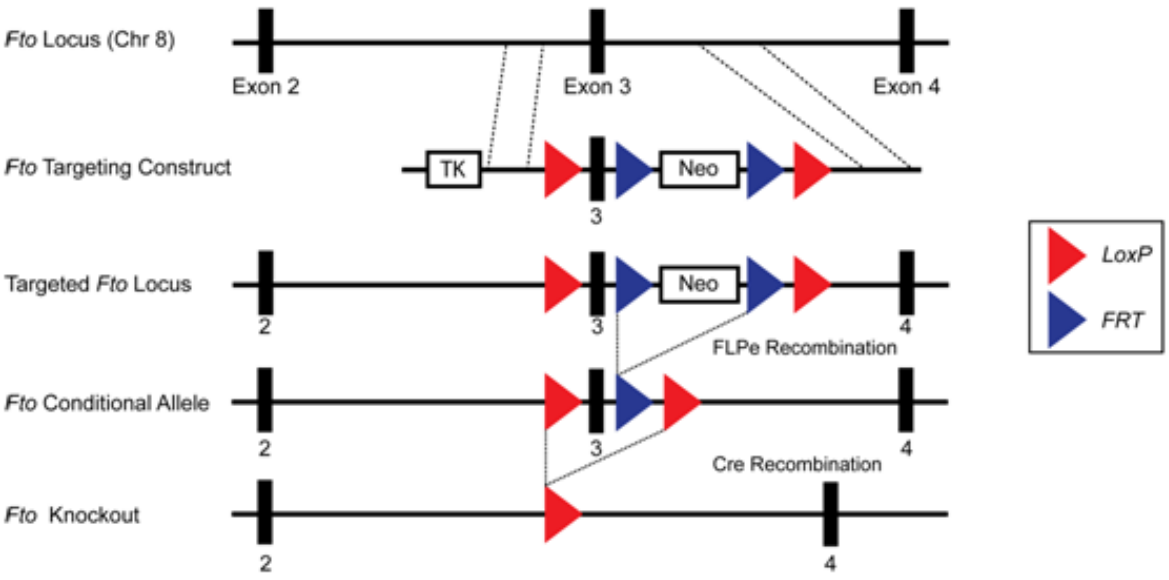

Figure 3.1 Schematic of the generation of the conditional knockout (*Neo* removed by Flpe recombination; $Fto^{+/Flox}$) and knockout (exon 3 deletion; $Fto^{-/-}$) mice.

3.2 Methods

General methods are described in **Chapter 2**; this section describes the specific methods used to characterise the *Fto* adult knockout mouse.

3.2.1 Generation of the Global Adult Knockout and Control Mice

The *Fto* conditional floxed allele (**Figure 3.1**) was crossed with a tamoxifen inducible Cre line from the Jackson laboratories (B6.Cg-Tg(UBC-Cre/ESR1)1Ejb/J). Tamoxifen free base (MP Biomedicals) was dissolved in corn oil and 2 % ethanol to produce a final 30 mg/ml solution. The mixture was shaken at 37 °C overnight to dissolve the Tamoxifen and the solution stored at 4 °C protected from light.

At 6 weeks of age male mice were treated with either 200 mg/kg tamoxifen free base solution (MP Biomedicals, Santa Ana, CA) dissolved in corn oil 2 % ethanol solution, or an equivalent amount of vehicle by oral gavage for 5 consecutive days using a 4.5 fg (fine-gauge) × 60 mm length PVC dosing catheter (VetTech solutions).

3.2.2 X-Gal Staining

Mice were perfusion fixed with 4 % paraformaldehyde and tissues collected and put into PBS at 4 ºC. Tissues were then transferred into fixative containing 4 % paraformaldehyde, 0.3 % glutaraldehyde, 2 mM $MgCl_2$, 5mM EGTA, 0.02 % NP-40 and fixed on ice on a rocking platform for 30 min. Samples were washed three times for five min with PBS 0.02 % NP-40. Tissues were then stained overnight at room temperature protected from light with BATGAL stain (5 mM $K_3Fe(CN)_6$, 5 mM $K_4Fe(CN)_6$, 2 mM $MgCl_2$, 0.01 % Deoxycholate, 0.02 % NP-40, 1 mg/ml X-GAL in PBS). Tissues were washed three times for five min in PBS and imaged.

3.2.3 Phenotyping Pipeline

Mice were weighed each week from weaning, and from 8 weeks mice were characterised using a standardised metabolic phenotyping pipeline (**Figure 3.2**). Phenotyping tests were performed according to EMPReSS (European Phenotyping Resource for Standardised Screens from EUMORPHIA) standardized protocols as described at http://empress.har.mrc.ac.uk.

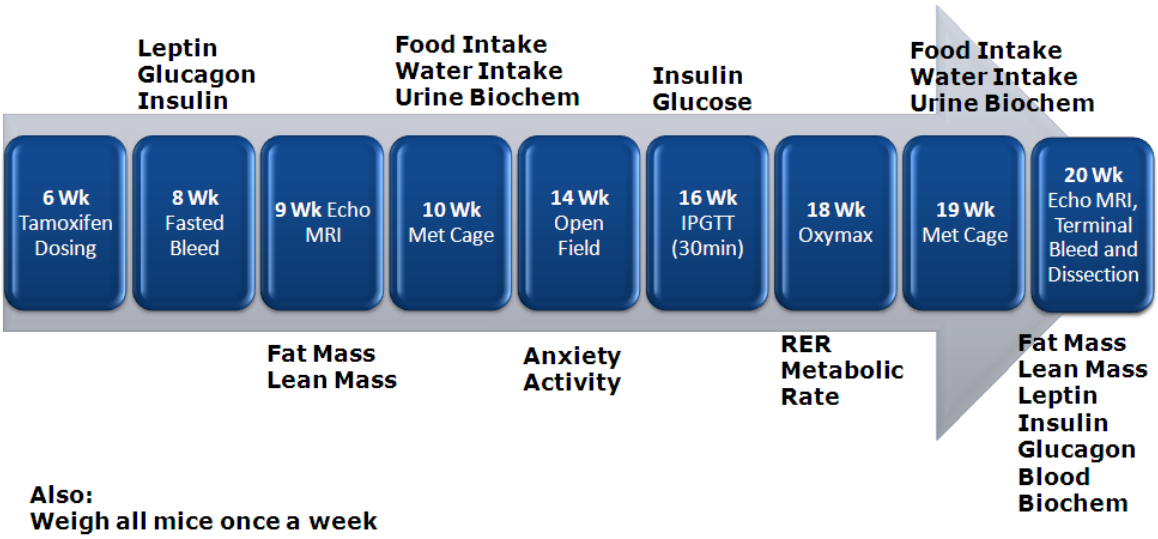

Figure 3.2 Metabolic Phenotyping Pipeline. Abbreviations: Met Cage, metabolic cage; IPGTT, Intraperitoneal glucose tolerance test; RER, Respiratory exchange ratio; Biochem, Biochemistry.

3.2.4 Statistical Analysis

Correction for body size:

When comparing some phenotypes across (treatment-genotype) groups, adjustment was made for variation in lean mass using multiple linear regression analysis (ANCOVA). Phenotypes for which this adjustment was made were: VO_2 consumed, VCO_2 produced, and energy expenditure (EE). The linear model used was:

$$y_i = \beta_{g(i)} + \gamma l_i + \varepsilon_i$$

where:

- $i = 1,\ldots,n$ indexes mouse,
- y_i denotes the phenotype of mouse i,
- $g(i) \in \{A,B\}$ denotes the (treatment-genotype) group of mouse i,

- the $\beta_{g(i)}$ denote the main group effects
- l_i is the lean mass of mouse i, where l has been centred to have zero mean ($\sum_{i=1}^{n} l_i = 0$)
- γ is the coefficient for lean mass in the linear model
- the ε_i are mutually independent identically distributed zero-mean Gaussian random measurement errors.

Table 3.4 (indirect calorimetry analysis) and **Figure 3.10** (indirect calorimetry scatter plot data) show estimates for β_A, β_B, and $\beta_B - \beta_A$, as well as a *p*-value for the test of the hypothesis $\beta_B = \beta_A$. For the corrected phenotypes, the points plotted in **Figure 3.10** (indirect calorimetry scatter plot data) are lean mass corrected using the least-squares estimate of γ (i.e. the points $y_i - \hat{\gamma} l_i$ are plotted).

This approach was also applied to lean and fat mass adjustment for body weight (**Table 3.3**).

Repeated-measures ANOVA:

Time-course data were analysed using the repeated-measures ANOVA model (Diggle *et al*., 2002):

$$y_{it} = \alpha + \beta_{g(i)} + \delta_{[g(i),t]} + u_i + \varepsilon_{it}$$

where:

- $i = 1,\ldots,n$ indexes mouse,
- $t = 1,\ldots T$ indexes time point,
- y_{it} denotes the phenotype of mouse i at time point t,
- α denotes an intercept term
- $g(i) \in \{A,B\}$ denotes the (treatment-genotype) group of mouse i,
- the $\beta_{g(i)}$ denote the main group effects (with the constraint $\beta_A \equiv 0$)
- the $\delta_{[g(i),t]}$ denote interactions between group and time (with the constraints $\delta_{[A,t]} \equiv 0$ and $\sum_{t=1}^{T} \delta_{[g(i),t]} \equiv 0$),
- u_i is the random effect for mouse i (these random effects model the correlation between repeated measures), with the u_i mutually independent identically distributed zero-mean Gaussian random variables, and

- the ε_{it} are mutually independent identically distributed zero-mean Gaussian random measurement errors.

The model was fitted using the lmer() function in the lme4 R package (Pinheiro and Bates, 2000). The null hypothesis of no main genotypic effect (i.e. that $\beta_A = \beta_B = 0$ for both groups) was tested against the alternative hypothesis under which β_B was unconstrained. The test was based on the asymptotic χ^2_1 null distribution of $-2 \log \Lambda$, where Λ denotes the likelihood ratio. To supplement the repeated-measures analysis, Welch t-tests were performed separately at each time point (**Table 3.2**). I thank Dr. George Nicholson (University of Oxford, Department of Statistics) for statistical advice and assistance with this analysis.

3.3 Results

3.3.1 Global Germline Knockout Results in Unchanged Energy Expenditure

As previously described the global germline *Fto*$^{-/-}$ mice weigh significantly less than controls, have reduced fat and lean mass and are growth retarded (Fischer *et al*., 2009). These mice are also reported to have increased energy expenditure (Fischer *et al*., 2009).

There has been much discussion in the literature of the correct way to normalise energy expenditure data for *Fto*$^{-/-}$ mice (Speakman, 2010). As our *Fto*$^{-/-}$ mice are substantially lighter than their wild-type littermates, as observed by Fischer and colleagues we compared linear regression and ratio normalisation methods with these mice.

To illustrate the differences between these two methods, we plotted energy expenditure against lean mass (**Figure 3.3A**). When energy expenditure data are not corrected (**Figure 3.3B**), wild-type mice exhibit higher mean energy expenditure than *Fto*$^{-/-}$ mice (although the difference is not statistically significant with our sample size). However, as **Figure 3.3A** shows, wild-type mice have higher lean mass, and lean mass positively correlates with energy expenditure. Consequently the difference in energy expenditure disappears upon regression adjustment for lean mass (**Figure 3.3C**). The difference in regression-adjusted energy expenditure in **Figure 3.3C** is the vertical distance between the two lines in **Figure 3.3A**. The traditional ratio-normalisation approach (**Figure 3.3D,E**) over-corrects for the effects of lean mass, leading to artificial inflation of ratio-adjusted energy expenditure in *Fto*$^{-/-}$ mice relative to wild-type mice.

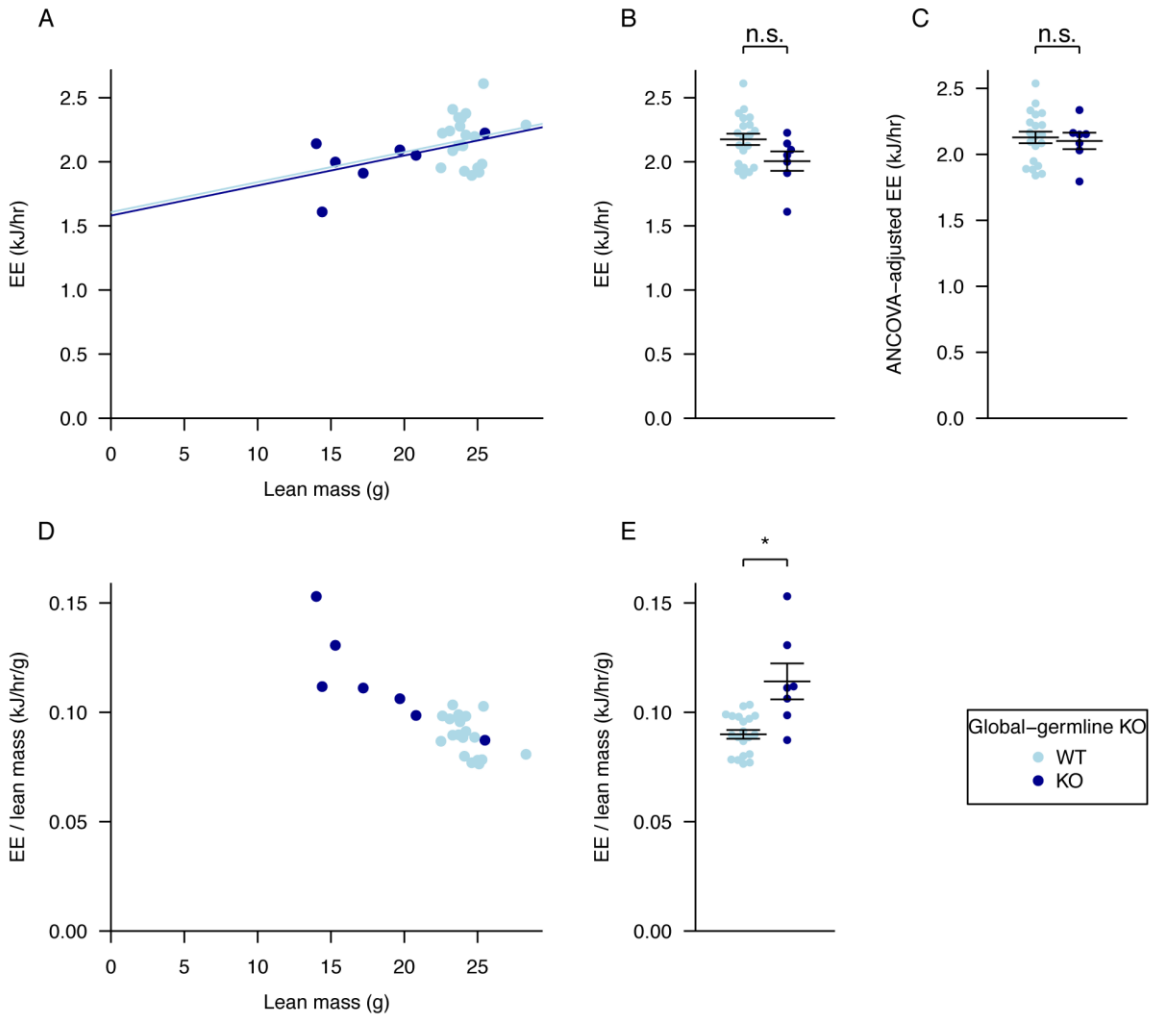

Figure 3.3 Adjustment of energy expenditure for lean mass, regression analysis compared to ratio adjustment. A, regression of energy expenditure against lean mass with lines of best fit with a function of group and lean body mass using , **B**, average energy expenditure, **C**, energy expenditure values adjusted for lean mass using ANCOVA, **D**, values for energy expenditure divided by lean mass and plotted against lean mass to show the effect of ratio adjustment, E, average energy expenditure divided by lean mass. Data for dark phase. The p-values in B,E were calculated using a Welch *t*-test of the null hypothesis of no difference between genotypic groups. For lean mass adjustment in **C**. *P<0.05. Data are expressed as mean ± SEM and individual data points are shown.

3.3.2 Charactering Tamoxifen Inducible Ubiquitin-Cre

A reporter line was used to check the expression of the tamoxifen-inducible Cre line. Mice carrying a tamoxifen-inducible ubiquitin-Cre recombinase were crossed with a LacZ reporter line (Gt(ROSA)26Sor^{tm1Sor}), producing heterozygous mice which do and do not carry Cre. Mice carrying the LacZ reporter were also crossed with the β-Actin-Cre recombinase line (Jackson Laboratory: Stock name Tg(ACTA1-Cre)79Jme/J) as a positive control. At six weeks of age tamoxifen-inducible ubiquitin-Cre mice were treated with tamoxifen for five days to investigate the

expression of the inducible Cre recombinase in our hands. All mice were sacrificed at approximately eight weeks of age and tissue collected for X-gal staining (**Figure 3.4**). All the cells expressing the lacZ transgene should present β-galactosidase activity. Five days of tamoxifen dosing by oral gavage was sufficient to induce expression of the Cre-recombinase, causing expression of β-galactosidase. We were able to show that tamoxifen was also able to cross the blood-brain-barrier (BBB) causing expression in the brain, although staining was not as global as in the positive control tissue (**Figure 3.4**). We could also see successful expression of the reporter line in the other tissues we examined, liver, kidney, gastrocnemius muscle and lungs at similar levels to the positive control (**Figure 3.4**).

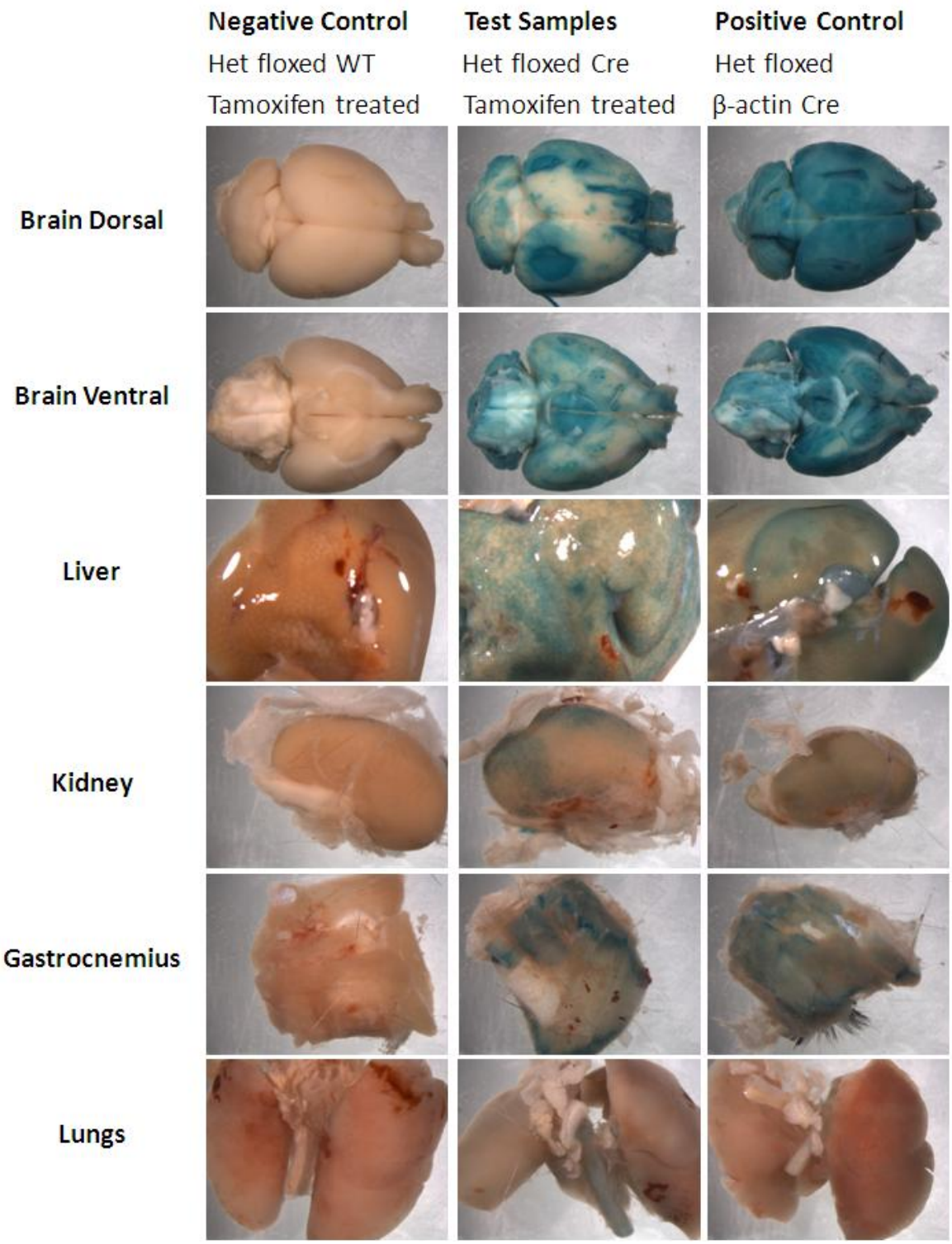

Figure 3.4 X-Gal Staining using a LacZ reporter line. Brain, liver, kidney, gastrocnemius and lungs were collected 2 weeks after 5 days of tamoxifen dosing and stained to examine expression of the tamoxifen-inducible ubiquitin-Cre recombinase. B-Actin-Cre crossed with the LacZ reporter line was used as a positive control.

3.3.3 Adult *Fto* Knockout

Mice carrying the conditional floxed *Fto* allele were crossed with mice carrying a tamoxifen-inducible ubiquitin-Cre recombinase and the resulting heterozygous mice carrying Cre recombinase intercrossed to generate homozygous floxed *Fto* mice and homozygous mice carrying both floxed *Fto* and Cre recombinase. Mice carrying Cre recombinase alone were bred from the heterozygote population by crossing with wild-type mice. All mice were on a congenic C57BL/6J background. Mice of all genotypes (**Table 3.1**) were treated with tamoxifen or vehicle at 6 weeks of age (around the time of sexual maturity) by oral gavage daily for five days. This led to global (as ubiquitin is expressed in most, if not all, tissues **Figure 3.4**) deletion of *Fto* in mice carrying both floxed *Fto* and Cre recombinase: we refer to these as adult onset KO mice. A PCR for genotyping $Fto^{-/-}$ mice was performed on DNA extracted from whole brain and whole liver of tamoxifen and vehicle dosed mice (**Figure 3.5**). Some background recombinase activity was seen in vehicle dosed animals, whereas no floxed band was seen in tamoxifen dosed animals. Inactivation of the *Fto* gene and loss of FTO protein was demonstrated by immunoblotting for FTO (**Figure 3.6**).

Table 3.1 Genotype Groups used in Adult onset FTO KO study

Genotype	Treatment	Effect
$Fto^{Flox/Flox};Cre$	Tamoxifen	Adult onset FTO Knockout
$Fto^{Flox/Flox};Cre$	Vehicle	Background Recombination Control
$Fto^{+/+};Cre$	Tamoxifen	Tamoxifen dosing and Cre activation control

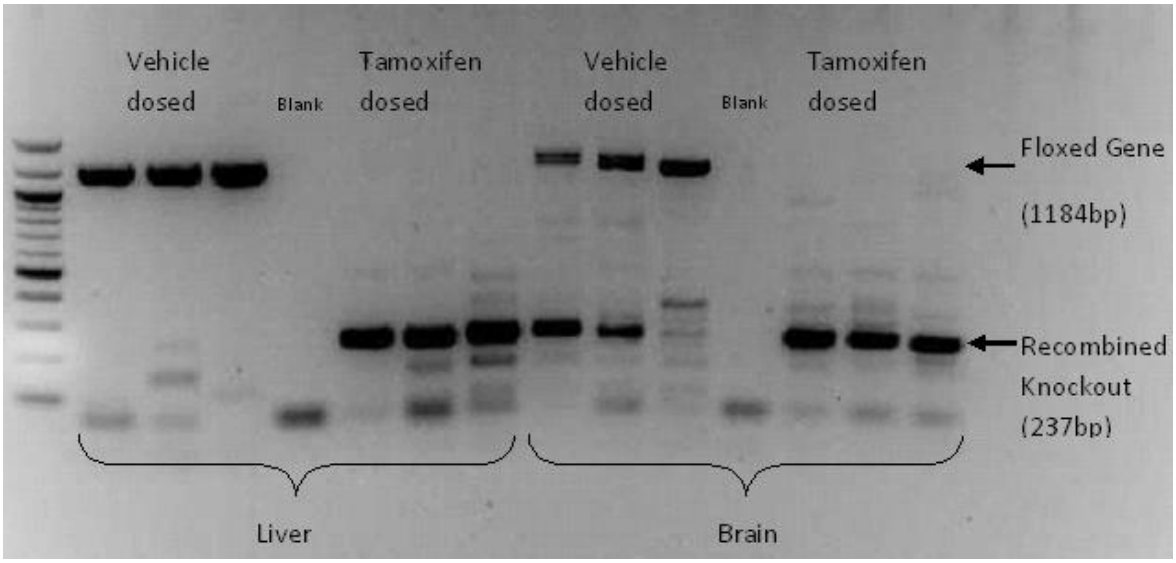

Figure 3.5 FTO KO genotyping PCR performed on DNA extracted from Liver and Brain from tamoxifen and vehicle treated mice homozygous for the floxed gene and heterozygous for the tamoxifen-inducible ubiquitin-Cre recombinase. Some background recombination is observed in brains of vehicle dosed mice. Vehicle control (n=3) and Tamoxifen Dosed (n=3).

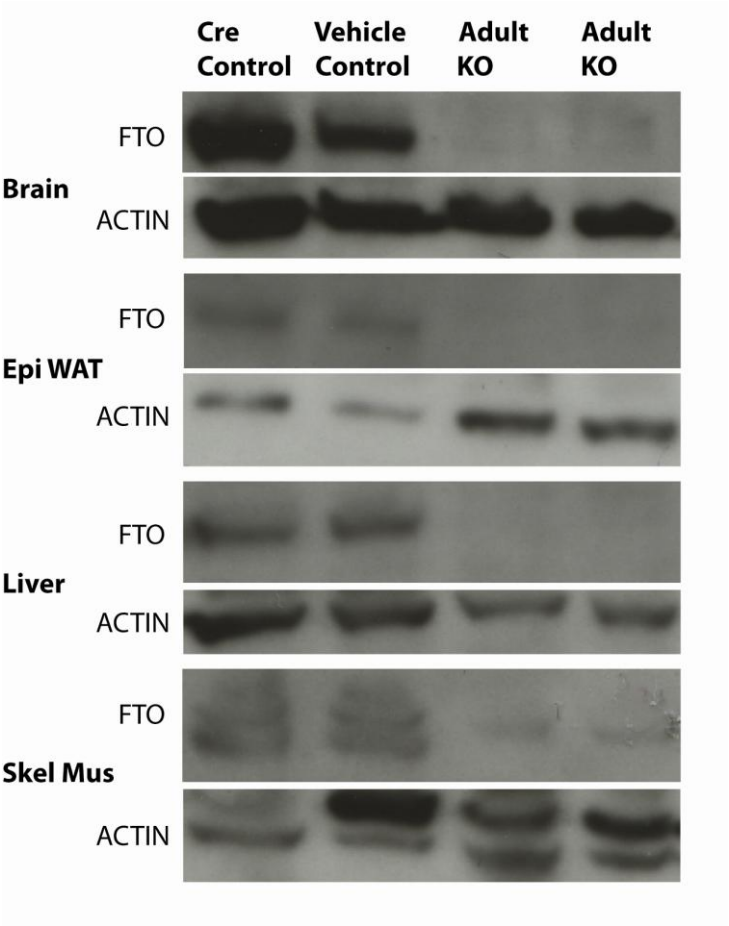

Figure 3.6 Loss of FTO in global adult onset KO mice. (a) FTO levels in brain, epigonadal white adipose tissue (Epi WAT), liver and calf muscle (skel Mus) of Cre control, Vehicle control and *Fto* adult KO mice.

3.3.4 The Severe Lethality Seen with Germline Fto KO Is Not Seen in Adult Onset Loss

There were three unexplained deaths out of 25 adult onset KO mice (12 %) over the 14 weeks after tamoxifen treatment, and one death in the vehicle control group (n=11, 9 %). This indicates substantially improved viability compared with germline KO mice (45 % lethality). Whether the three deaths in adult KO onset mice are related to *Fto* deletion or are chance events is unknown.

Repeated measures analysis comparing post-treatment body weight data from vehicle-treated mice carrying both Cre and floxed *Fto* alleles (Vehicle) and tamoxifen-treated Cre mice (Tamoxifen) did not show significant differences in weight (P=0.89 **Figure 3.7A**). No significant differences between the body length, or body composition of Vehicle and Cre control mice were observed (**Figure 3.7B,C,D**). We therefore present below only data on male mice carrying both the floxed *Fto* allele and Cre recombinase, which have either been treated with tamoxifen (Adult onset KO) or with the corn oil and 2 % ethanol vehicle (Wellcome Trust Case Control Consortium).

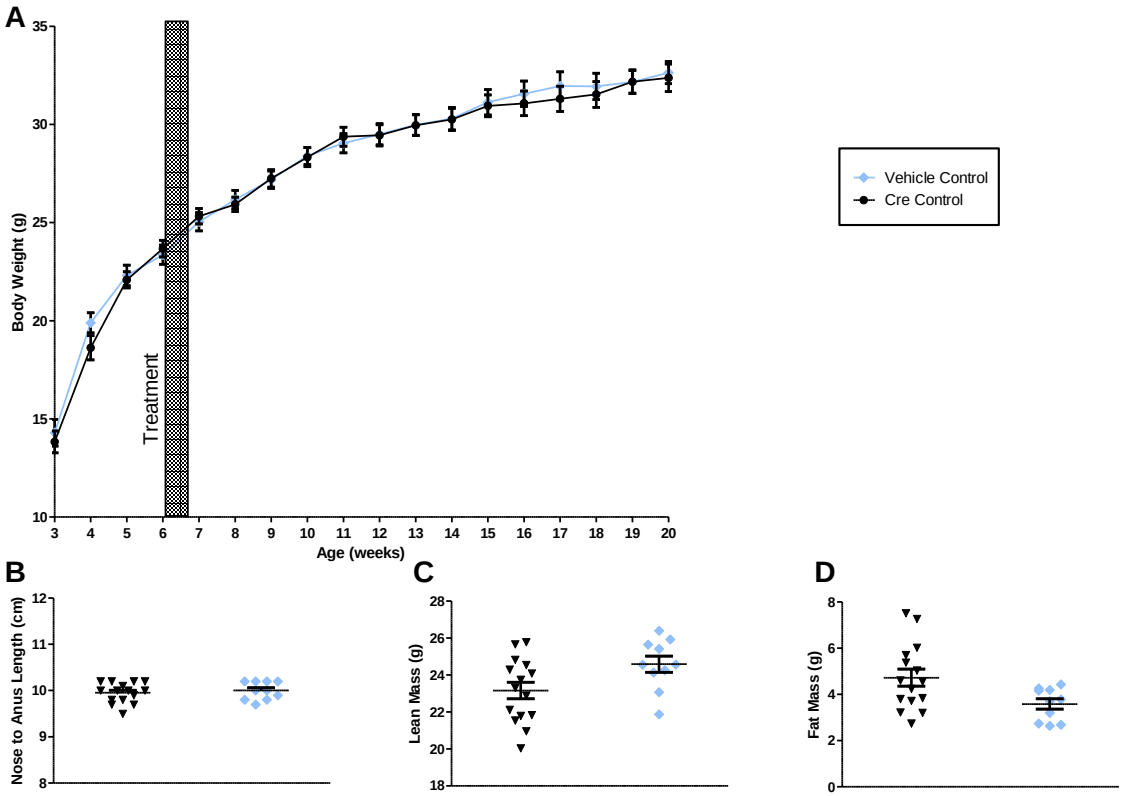

Figure 3.7 Body weight, and body composition of the Vehicle and Cre control mice. A, No significant differences were observed in the weekly body weights **B**, terminal body lengths, **C**, 20 week lean mass or **D** 20 week fat mass of vehicle control (n=10) and Cre control (n=15) mice. Data are expressed as mean ± SEM. In **B-D**, individual data points are shown. Time-course data were analysed using the repeated-measures ANOVA model, see Methods (**A**). The other comparison p-values (**B-D**) correspond to a Welch *t*-test of the null hypothesis of no difference between genotypic groups. *P<0.05, **P<0.01, ***P<0.001.

3.3.5 Adult KO Mice Have Reduced Body Weight and No Growth Retardation

To investigate body mass mice were weighed weekly from weaning at three weeks of age. In the weeks prior to treatment (weeks three to six) there was no statistical difference between groups (**Figure 3.8A, Table 3.2**). Mice were treated with tamoxifen or vehicle at 6 weeks of age. During weeks seven to nine, the average rate of weight gain of adult onset KO mice was slower than that of control mice, leading to a lower mean weight of KO mice that persisted over the next 12 weeks (**Figure 3.8A**). Repeated-measures ANOVA indicated statistically significant inter-group differences, with reduced KO body mass relative to controls (P=0.0043). Weekly inter-group differences were statistically significant throughout weeks eight to 18 (two to 14 weeks after

treatment started (Time-by-time ANOVA P<0.05; **Table 3.2**). There was no change in body length when measured in sacrificed animals at 20 weeks of age (**Figure 3.8B**).

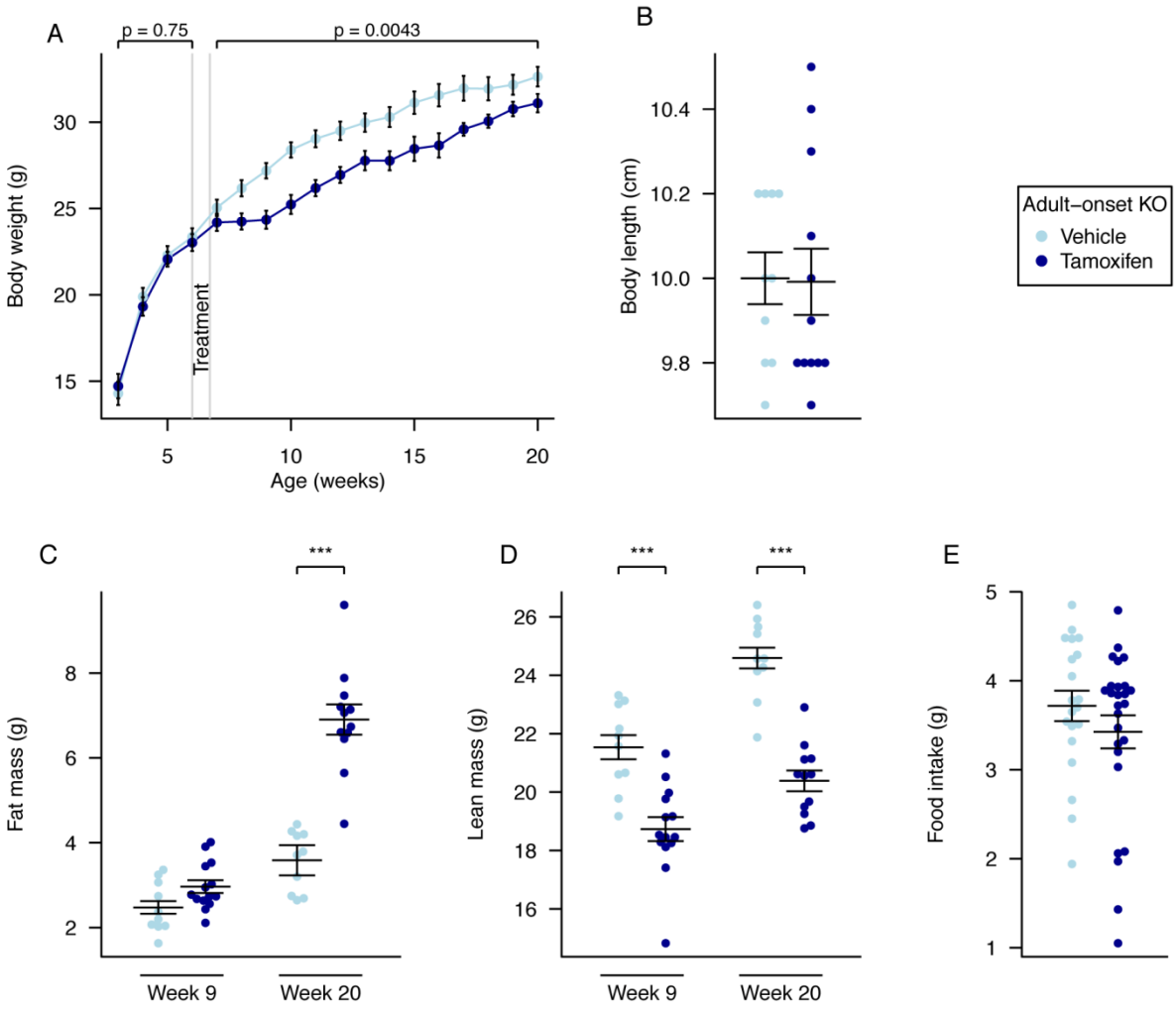

Figure 3.8 Body weight, body composition and food intake of global adult onset KO mice. A, Weekly body weight of adult onset KO (n=15) and vehicle-treated control mice (n=10), **B**, Nose-to-anus body length of control (n=10) and adult onset KO mice (n=12) at 20 weeks of age, **C**, Fat mass was increased in adult onset KO mice (n=14) compared to controls (n=10) in 9-week old mice (P=0.05) and further increased in adult onset KO mice (n=12) compared to controls (n=10) at 20 weeks, **D**, Lean mass was reduced in adult onset KO mice (n=14 and n=12) compared to controls (n=10 and n=10) at both 9 weeks and 20 weeks of age, **E**, Food intake at 10 weeks of age during a 24-hour period in metabolic cages, control (n=10) and adult onset KO mice (n=14). Data are expressed as mean ± SEM. In **B-E**, individual data points are shown. Time-course data were analysed using the repeated-measures ANOVA model, see Methods (**A**). The other comparison p-values (**B-E**) correspond to a Welch *t*-test of the null hypothesis of no difference between genotypic groups. *P<0.05, **P<0.01, ***P<0.001.

Table 3.2 Time by time ANOVA analysis of weight in global adult onset KO mice. SEM standard error

Week	Vehicle mean (SEM)	Tamoxifen mean (SEM)	p value
3	14.3 (0.7)	14.7 (0.7)	0.67
4	19.9 (0.5)	19.3 (0.5)	0.45
5	22.3 (0.5)	22.1 (0.4)	0.73
6	23.4 (0.5)	23.0 (0.5)	0.64
7	25.0 (0.5)	24.2 (0.5)	0.22
8	26.2 (0.5)	24.2 (0.5)	0.0082
9	27.2 (0.4)	24.3 (0.5)	0.00043
10	28.4 (0.4)	25.2 (0.5)	0.00019
11	29.0 (0.5)	26.2 (0.5)	0.00041
12	29.5 (0.5)	26.9 (0.5)	0.0019
13	30.0 (0.5)	27.8 (0.6)	0.0098
14	30.3 (0.6)	27.8 (0.6)	0.0047
15	31.1 (0.6)	28.5 (0.7)	0.011
16	31.6 (0.6)	28.7 (0.7)	0.0063
17	32.0 (0.7)	29.6 (0.4)	0.011
18	31.9 (0.7)	30.1 (0.4)	0.029
19	32.2 (0.6)	30.8 (0.4)	0.066
20	32.6 (0.6)	31.1 (0.5)	0.062

3.3.6 Adult KO mice have increased fat and decreased lean mass

To further understand the differences in body weight we used quantitative NMR to determine lean and fat mass weights at nine and 20 weeks of age (three and 14 weeks after treatment started, **Figure 3.8C,D**). At nine weeks of age there was a significant reduction in lean mass (P=0.00017), a fall in lean mass as a proportion of body weight (P=8.9E-05), a trend for increased fat mass (P=0.050), and a significant increase in fat mass as a proportion of body weight (P=0.0047), in KO mice compared to controls **Figure 3.8** and **Table 3.3**.

Using multiple linear regression to better take account of the body weight differences, lean mass was significantly decreased (P=0.0011) and fat mass was increased (P=0.024; **Table 3.3**). These differences were considerably larger at 20 weeks of age (Body weight adjusted ANCOVA: lean mass P=2.0E-09, fat mass P=5.9E-10, **Figure 3.8C,D**). At 20 weeks of age, when the mice were culled, liver weight was not significantly different (**Figure 3.9A**). The epigonadal WAT weight was significantly higher in adult KO mice than vehicle treated controls (P=4.98E-07 **Figure 3.9B**). H&E staining revealed that the adult KO mice did not have fatty livers (**Figure 3.9C**) and H&E

staining of the epigonadal fat pads revealed that this increase in mass was due to increased adipocyte size in the adult KO mice (P=4.83E-07) (**Figure 3.9C,D**).

Table 3.3 Analysis of fat and lean mass data either as raw data, data normalised by multiple linear regression (ANCOVA) for body weight or by % of body weight. SEM, standard error.

Age (weeks)	Trait (g)	Method	Estimate	SEM	t value	Pr(>|t|)
9	fat	Raw	0.491	0.237	2.072	0.05
9	fat	ANCOVA	0.682	0.28	2.433	0.024
9	fat	% of BW	0.028	0.009	3.142	0.0047
9	lean	Raw	-2.805	0.622	-4.513	0.00017
9	lean	ANCOVA	-1.014	0.268	-3.78	0.0011
9	lean	% of BW	-0.041	0.008	-4.783	8.90E-05
20	fat	Raw	3.318	0.442	7.508	3.10E-07
20	fat	ANCOVA	3.859	0.338	11.422	5.90E-10
20	fat	% of BW	0.115	0.011	10.344	1.80E-09
20	lean	Raw	-4.206	0.554	-7.588	2.60E-07
20	lean	ANCOVA	-3.402	0.32	-10.628	2.00E-09
20	lean	% of BW	-0.102	0.01	-9.949	3.40E-09

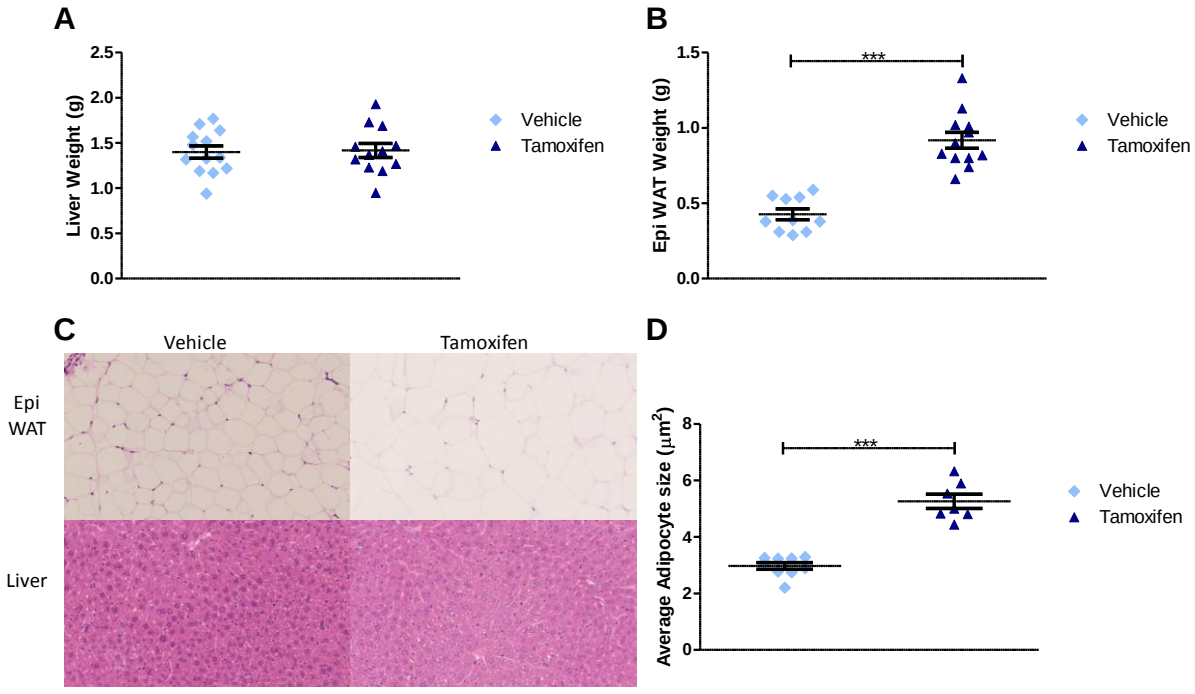

Figure 3.9 Liver and Epigonadal fat pad (Epi WAT) analysis from control and Adult KO mice. A, Liver weights from 20 week old mice (Vehicle n=10, Adult KO n=12). **B**, Epigonadal Fat pad weight from 20 week old mice (Vehicle n=10, Adult KO n=12). **C**, H&E staining of 10 % formalin fixed Epigonadal WAT (Epi WAT) and Liver at x20 magnification. **D**, Average Cell size from x10 magnification H&E stained section counts (Vehicle n=9, Adult KO n=7 sections). One way ANOVA bonferroni corrected for multiple comparisons. *P<0.05, **P<0.01, ***P<0.001. Data are expressed as mean ± SEM.

3.3.7 Adult KO mice do not have increased energy expenditure but do show altered metabolism

To further understand the cause of the differences in body composition and weight gain we measured food intake and energy expenditure.

There were no significant differences in 24 hour food intake measurements in metabolic cages at either ten (**Figure 3.8E**) or 19 weeks (data not shown) of age. Adult onset KO mice were subjected to 24 hour indirect calorimetry at 18 weeks of age and showed unchanged oxygen consumption and decreased carbon dioxide output (when adjusted for lean body mass **Figure 3.10A,B**; **Table 3.4**). Energy expenditure adjusted for lean mass was not significantly different during either light or dark periods (**Figure 3.10C**, **Table 3.4**) The RER of adult KO mice was significantly reduced during both periods and overall (**Figure 3.10D**, **Table 3.4**).

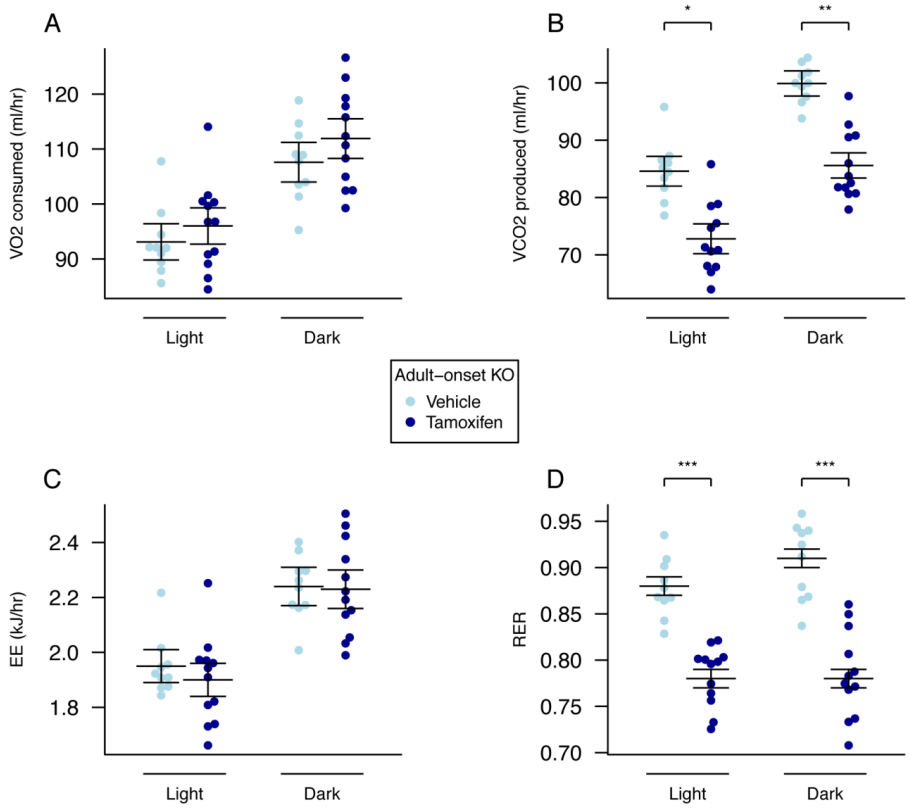

Figure 3.10 Energy expenditure and metabolism of global adult onset KO mice. A, VO_2 consumed, **B**, VCO_2 produced, and **C**, energy expenditure (EE), adjusted for variation in lean mass using multiple linear regression (ANCOVA). **D**, respiratory exchange ratio (RER). Adult onset KO mice (n=12) control mice (n=10). Measurements were made over a 22-hour period during the dark and light phases in 18-week old mice. Data are expressed as mean ± SEM and individual data points are shown. For details of the lean-mass adjustment made in panels **A, B, C**, see Materials and Methods, *P<0.05, **P<0.01, ***P<0.001.

Table 3.4 Energy expenditure phenotypes across groups, with the exception of RER, adjustment was made for variation in lean mass using multiple linear regression (ANCOVA). Light or dark phase; day or night, Tam; Tamoxifen, SEM standard error.

Parameter	Time	A	A mean (SEM)	B	B mean (SEM)	B-A mean (SEM)	P-value
VO2	Light	Vehicle	93.1 (3.8)	Tam	96.0 (3.3)	2.9 (6.3)	0.65
VO2	Dark	Vehicle	107.6 (4.1)	Tam	111.9 (3.6)	4.3 (6.9)	0.54
VCO2	Light	Vehicle	84.6 (3.0)	Tam	72.8 (2.6)	-11.9 (5.0)	0.027
VCO2	Dark	Vehicle	99.9 (2.6)	Tam	85.6 (2.2)	-14.3 (4.3)	0.0035
RER	Light	Vehicle	0.88 (0.01)	Tam	0.78 (0.01)	-0.10 (0.01)	8.10E-07
RER	Dark	Vehicle	0.91 (0.01)	Tam	0.78 (0.01)	-0.12 (0.02)	3.10E-06
EE	Light	Vehicle	1.95 (0.07)	Tam	1.90 (0.06)	-0.05 (0.12)	0.7
EE	Dark	Vehicle	2.24 (0.08)	Tam	2.23 (0.07)	-0.01 (0.13)	0.96

Open Field analysis showed no significant difference in cumulative distance or time moving over a 30 minute trial, although there was a trend for increased movement in the Adult KO mice (**Figure 3.11**). There was also no significant difference between the Adult KO and vehicle treated mice occupancy of the centre or peripheral areas of the arena (data not shown), which suggests that the adult KO mice do not have an anxiety phenotype.

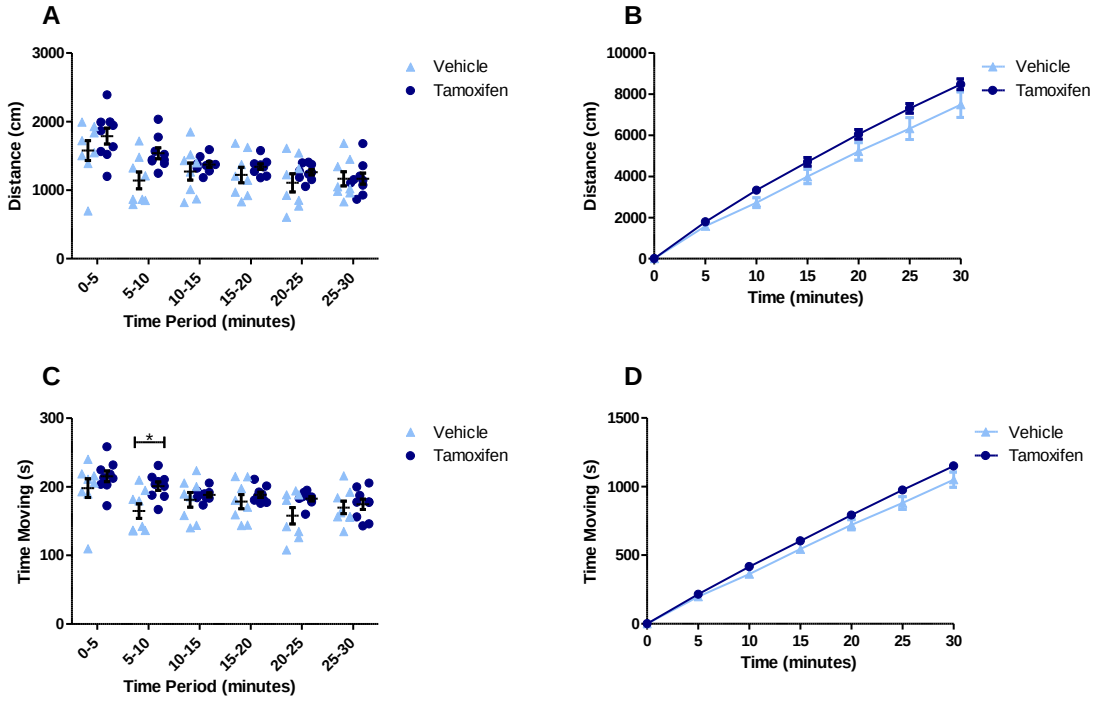

Figure 3.11 Open Field analysis of Adult KO and vehicle treated mice for 30 minutes. A, Total distance moved in the arena in each 5 minute interval. **B**, Cumulative distance moved in the arena in each 5 minute interval. **C**, Time moving in the arena in each 5 minute interval **D**, Cumulative time moving in the arena in each five min interval. Two-way ANOVA corrected for multiple comparisons. *P<0.05, **P<0.01, ***P<0.001. Data are expressed as mean ± SEM.

3.3.8 Altered Hormone and Biochemistry in Adult KO mice

No significant difference was seen in plasma insulin, glucagon, or leptin at eight weeks of age (**Figure 3.12A,B,C**). At 20 weeks of age Adult KO mice showed a trend for decreased insulin, but this was not significant **Figure 3.12A**), glucagon analysis unfortunately failed in most of the samples tested **Figure 3.12B**) and leptin levels were significantly higher in adult KOs (P=0.0424).

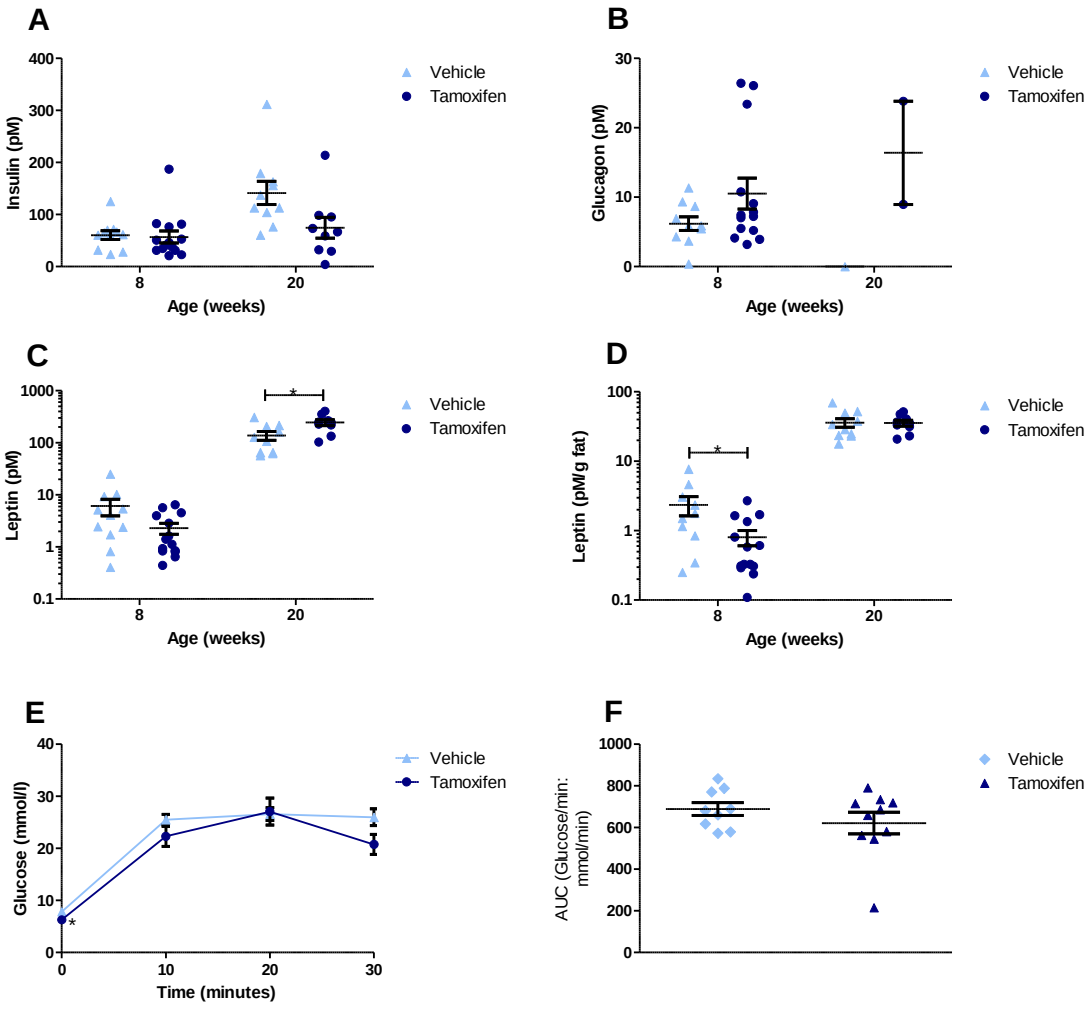

Figure 3.12 Twenty week Plasma insulin, glucagon and leptin analysis and 16 week 30 minute Intraperitoneal glucose tolerance test (IPGTT). A, Plasma insulin. **B**, Plasma glucagon. **C**, Plasma Leptin. **D**, Plasma Leptin corrected for fat mass (Echo MRI data **Figure 3.8**). **E**, Intraperitoneal glucose tolerance test (IPGTT) at 16 weeks of age (students t-test at T0 p=0.0434). **F**, Area Under the Curve (AUC) analysis of 30 minute IPGTT. One way ANOVA bonferroni corrected for multiple comparisons. *P<0.05, **P<0.01, ***P<0.001. Data are expressed as mean ± SEM.

This hyperleptinaemia is likely due to the adult KO mice having significantly higher adipose tissue mass at 20 weeks old (**Figure 3.8C** Figure **3.9B,D**). When leptin levels are corrected for the

amount of fat mass (**Figure 3.12D**) the significance at 20 weeks is lost, however at eight weeks of age this correction shows that the Adult KO mice were secreting less leptin per gram of fat than control mice (P=0.017). Plasma adiponectin and thyroxine (T4) were also analysed and were not significantly different in Adult KO mice (data not shown). Urinary adrenaline, noradrenaline and dopamine were analysed in 10 week old mice, these were also not significantly different from controls (data not shown).

IPGTT performed at 16 weeks of age with time points at 10, 20 and 30 minutes showed no significant difference between adult KO and vehicle treated groups (**Figure 3.12E,F**) however at T0 there was a trend for a hypoglycaemia in the Adult KO mice (adult KO 6.26±0.54 SEM and vehicle 7.81±0.45 SEM mmol glucose P=0.0434 students t-test).

Table 3.5 Adult KO and Vehicle Urine Biochemistry at 10 and 19 weeks of age, data corrected for Urine Creatinine. Abbreviations: Sodium (Na), Potassium (K), Chloride (Cl), Inorganic Phosphate (Inorg P). One way ANOVA bonferroni corrected for multiple comparisons. *P<0.05, **P<0.01, ***P<0.001. SEM, Standard Error of the Mean; NS, Not Significant, data shown to four decimal places.

Assay	Units	10 week					19 week				
		Vehicle		Adult KO		P-value	Vehicle		Adult KO		P-value
		Mean	SEM	Mean	SEM		Mean	SEM	Mean	SEM	
Na	mmol/l	0.0397	0.0023	0.0454	0.0021	NS	0.0397	0.0016	0.0544	0.0023	***
K	mmol/l	0.1097	0.0046	0.1098	0.0073	NS	0.1097	0.0036	0.1264	0.0054	NS
Cl	mmol/l	0.0624	0.0043	0.0657	0.0048	NS	0.0624	0.0025	0.0732	0.0034	NS
Urea	mmol/l	0.4336	0.0124	0.4418	0.0202	NS	0.4336	0.0154	0.4899	0.0181	NS
Calcium	mmol/l	0.0004	0.0000	0.0007	0.0000	**	0.0004	0.0000	0.0005	0.0000	NS
Inorg P	mmol/l	0.0151	0.0007	0.0244	0.0012	*	0.0151	0.0011	0.0190	0.0008	**
Glucose	mmol/l	0.0006	0.0000	0.0007	0.0000	NS	0.0006	0.0000	0.0006	0.0000	NS
Urinary protein	µmol/l	0.4718	0.0540	0.2640	0.0330	**	0.4718	0.0257	0.3241	0.0352	**
Uric Acid	µmol/l	0.1973	0.0183	0.1933	0.0201	NS	0.1973	0.0126	0.1464	0.0150	*

Urine was collected from mice over a 24 hour period whilst they were housed in metabolic cages at 10 and 19 weeks of age (**Table 3.5**). Biochemical profiles of the urine reveal that at 10 weeks of age urinary calcium (P=0.0043) and inorganic phosphate (P=0.0107) are higher in the adult KO mice, and urinary protein (P=0.0004) is significantly lower. At 19 weeks of age inorganic phosphate (P=0.0001) and urinary protein (P=0.0001) levels are still significantly altered, as well as lower uric acid (P=0.0088) and higher sodium levels (P=0.0001).

Terminal plasma was collected after a six hour fast (**Table 3.6**). The Adult KO mice have significantly increased levels of urea (P=0.0013), inorganic phosphate (P=0.0363), total protein (P=0.001), albumin (P=0.0219), total cholesterol (P=0.0056), HDL cholesterol (P=0.0013), glucose (P=0.0339), glycerol (P=0.0323), amylase (P=0.0001), and creatinine kinase (P=0.0188).

Table 3.6 Adult KO and Vehicle 20 week Plasma Biochemistry corrected for Plasma Creatine. Abbreviations**:** Alkaline Phosphatase (ALP), Aspartate Aminotransferase (AST), High-Density Lipoprotein (HDL), Low-Density Lipoprotein (LDL), Lactate Dehydrogenase (LDH), Creatinine Kinase (CK). One way ANOVA bonferroni corrected for multiple comparisons. *P<0.05, **P<0.01, ***P<0.001. SEM, Standard Error of the Mean; NS, Not Significant.

Assay	Units	20 week				
		Vehicle		Adult KO		P-value
		Mean	SEM	Mean	SEM	
Sodium	mmol/l	12.5053	1.6578	14.0631	0.4579	NS
Potassium	mmol/l	0.5091	0.0726	0.5770	0.0492	NS
Chloride	mmol/l	9.1993	1.2265	10.1632	0.3930	NS
Urea	mmol/l	0.7974	0.0817	1.1278	0.1532	*
Calcium	mmol/l	0.1530	0.0155	0.2227	0.0239	NS
Inorganic Phosphate	mmol/l	0.1847	0.0166	0.2904	0.0481	*
ALP	U/l	3.5627	0.5286	3.8061	0.1621	NS
AST	U/l	4.3053	0.8006	8.0317	2.5179	NS
Total Protein	g/l	3.9229	0.4263	5.8332	0.6253	**
Albumin	g/l	2.1029	0.3189	2.6568	0.0916	*
Total Cholesterol	mmol/l	0.1734	0.0133	0.2747	0.0307	**
HDL	mmol/l	0.0746	0.0065	0.1296	0.0108	***
LDL	mmol/l	0.0594	0.0086	0.0830	0.0128	NS
Glucose	mmol/l	1.1401	0.1355	1.6483	0.1843	*
Triglycerides	mmol/l	0.1775	0.0395	0.2987	0.0517	NS
Glycerol	µmol/l	81.3602	9.2708	97.1310	3.3754	*
Free Fatty Acids	mmol/l	0.1408	0.0097	0.1926	0.0455	NS
Total Bilirubin	µmol/l	0.1852	0.0455	0.2364	0.0445	NS
LDH	U/l	47.0522	6.6891	72.9749	11.4004	NS
Iron	µmol/l	1.8571	0.2557	2.0543	0.1526	NS
Amylase	U/l	56.9136	6.0050	102.4851	9.6146	***
CK	U/l	0.8768	0.1435	2.4202	0.7824	*
Uric Acid	µmol/l	15.4842	2.1827	23.2980	2.9798	NS
Ketones	mmol/l	0.0203	0.0734	0.0226	0.0037	NS

Adult KO mice have lower urinary protein but they have increased plasma total protein, which suggests their kidneys are retaining more protein than the control mice. Increased urea in their plasma could be due to increased protein breakdown, as dehydration is unlikely due to the mice having ad libitum access to water. As the Adult KO mice have higher plasma inorganic phosphate it is not surprising they also have higher levels in their urine. Plasma phosphate can be generated

by muscle contraction and levels can increase during sustained or rhythmic exercise (Barcroft *et al*., 1971). It has previously been shown that FTO rs9939609A-allele associated with shorter recovery half-times of phosphocreatine and inorganic phosphate after exercise in a primarily type I muscle (Grunnet *et al*., 2009a). Creatine kinase activity in plasma is elevated in all types of muscular dystrophy (Okinaka *et al*., 1961) and I see it increased in Adult KO mice. Finally, increased amylase is normally due to acute pancreatitis or glomerular impairment, which I did not observe in the mice. Raised plasma amylase can be due to amylase binding to high molecular weight protein in the plasma; this is termed macroamylasaemia and is regarded as a benign chemical derangement (Attanasio *et al*., 1987).

3.3.9 Early Adult KO phenotype

As I was not expecting the body composition phenotype that I observed and because I wanted to repeat the study in order to characterise the early phenotype more thoroughly a new cohort of mice was generated.

As previously male mice were treated with vehicle or tamoxifen and put through the phenotyping pipeline outlined in **Figure 3.13**.

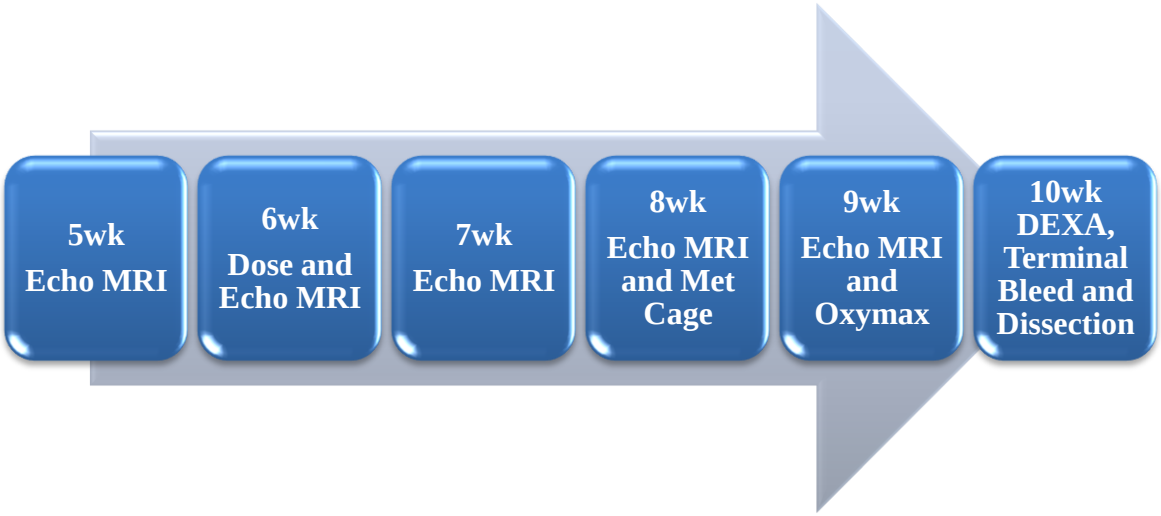

Figure 3.13 Phenotyping pipeline for Adult KO short study cohort. Abbreviations Metabolic cage (Met Cage) Dual-energy X-ray absorptiometry (DEXA).

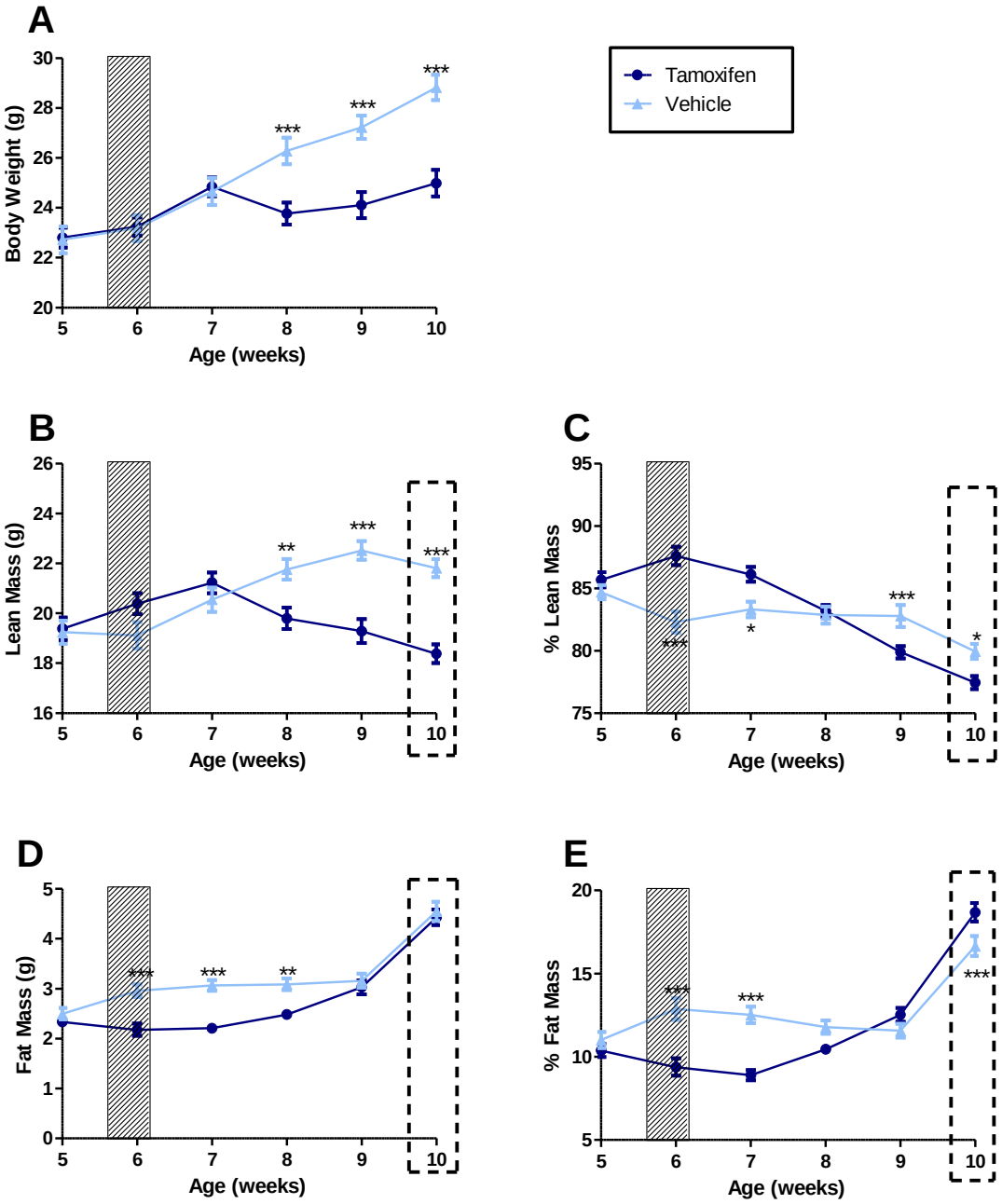

Figure 3.14 Body Weight and Body Composition of Short Study Adult KO cohort. The hatched area at 6 weeks is when mice were treated with tamoxifen or vehicle. The dashed box around the data at 10 weeks old is to draw attention that this data was collected after a 6 hour fast and using DEXA rather than Echo MRI. **A**, Weekly body weight of adult KO mice (n=18 and vehicle-treated control mice (n=18), **B**, Lean mass (g) was reduced in adult KO mice (n=18) compared to controls (n=18) after 8 weeks of age. **C**, Lean mass as a percentage of body weight was initially increased in adult KO mice (n=18) at 6 and 7 weeks old compared to controls (n=18) but then decreases at 9 and 10 weeks, **D**, Fat mass (g) was decreased in the adult KO mice (n=18) at 6-8 weeks of age compared to controls (n=18), **E**, Fat mass as a percentage of body weight was initially decreased in the adult KO mice (n=18) at 6 and 7 weeks compared to controls (n=18) but then is increased at 10 weeks. Time-course data were analysed using the repeated-measures ANOVA with a bonferroni post-test to compare replicate means by time-point. *P<0.05, **P<0.01, ***P<0.001. Data are expressed as mean ± SEM.

As seen previously (**Figure 3.8A**) after Tamoxifen treatment the Adult KO mice weighed significantly less than vehicle treated controls at eight to 10 weeks of age (**Figure 3.14A**). Lean mass in the Adult KO mice was significantly reduced after eight weeks of ages (**Figure 3.14B**), and considering lean mass as a percentage of body weight this is also true at nine and 10 weeks of age although the Adult KO mice have significantly higher percentage of lean mass at six and seven weeks (**Figure 3.14C**). Fat mass was significantly lower in the Adult KO mice following dosing at 6-9 weeks, but this caught up at 10 weeks of age (**Figure 3.14D**). This trend is also seen with percentage fat mass, but the Adult KO have significantly higher levels at 10 weeks of age (**Figure 3.14E**).

At eight weeks of age metabolic caging of Adult KO and control mice showed again that over a 24 hour period there was no significant difference in food or water intake in the Adult KO and control mice (data not shown). There was also no significant difference in food intake at nine weeks of age when the mice were individually housed during calorimetry measurement in the oxymax (data not shown).

Calorimetry data at nine weeks of age (**Figure 3.15A-D**) is altered from the 18 week data (**Figure 3.10A-D**). At nine weeks of age VO_2 consumed (P=0.0308) and VCO_2 produced (P=0.0246) are significantly higher in the light and dark phases of Adult KO mice. There is no significant difference in the RER or energy expenditure between the groups. At 18 weeks of age we observed that the Adult KO mice had significantly lower RER than controls, suggesting they are metabolising more protein and/or fat, whilst at nine weeks of age there is no significant difference. At nine weeks of age the mice are still maturing and their levels of lipogenesis are likely to be higher than in the older Adult KO mice. This can also be observed from the weekly body composition analysis (**Figure 3.14D,E**). This leads to an increase in RER, which may be concealing the altered RER we see in the older mice (Matarese, 1997).

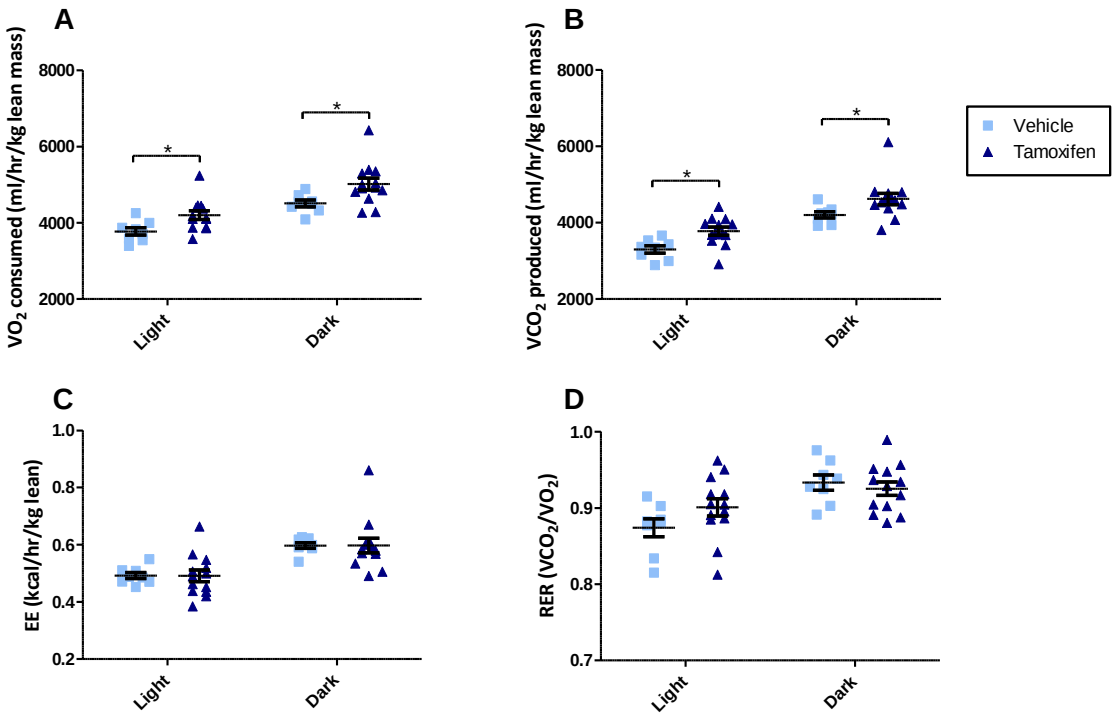

Figure 3.15 Energy expenditure and metabolism of Short Study Adult Onset KO mice at 9 weeks. A, VO_2 consumed, **B**, VCO_2 produced, and **C**, energy expenditure (EE), adjusted for variation in lean mass using multiple linear regression (ANCOVA). **D**, respiratory exchange ratio (RER). Adult onset KO mice (n=13) control mice (n=8). Measurements were made over a 22-hour period during the dark and light phases in 9-week old mice. Data are expressed as mean ± SEM and individual data points are shown. For details of the lean-mass adjustment made in panels **A, B, C**, see Methods, *P<0.05, **P<0.01, ***P<0.001.

Dissection at 10 weeks of age revealed that the Adult KO mice have significantly lower calf muscle weights (P=0.0167) (**Figure 3.16A**) and a trend for increased abdominal WAT which is found between the intestines (P=0.0680) (**Figure 3.16E**). Liver, epigonadal WAT and BAT did not differ significantly (**Figure 3.16B,C,D**). BMD and BMC measured using DEXA were also unchanged in the Adult KO mice (**Figure 3.16F,G**).

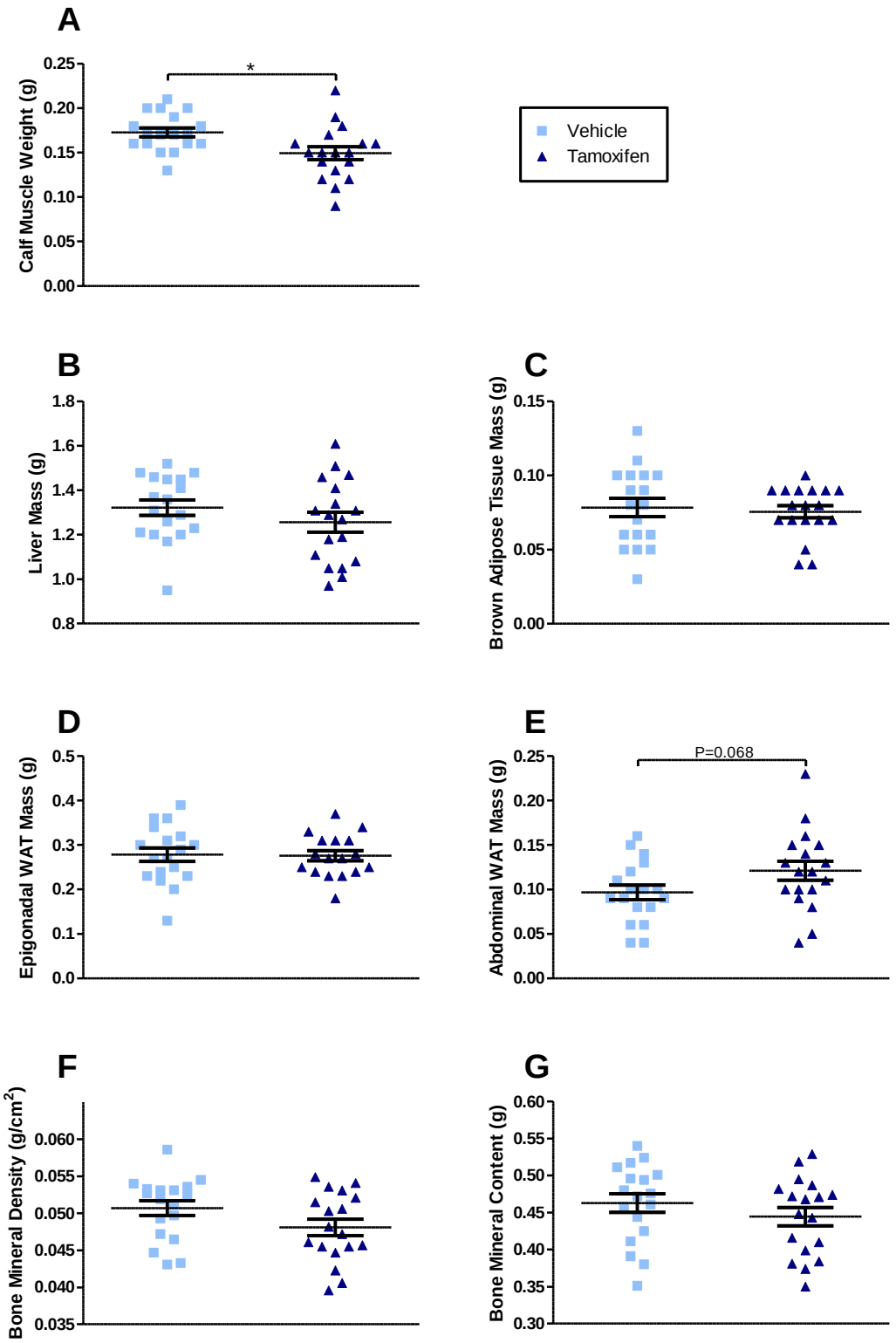

Figure 3.16 Organ Weights and DEXA analysis of Adult KO Short Study Cohort. Adult KO (n=18) and Vehicle treated control mice (n=18) **A**, Calf Muscle mass (g) is decreased in Adult KO mice, **B**, Liver mass (g), **C**, Brown Adipose Tissue mass (g), **D**, Epigonadal WAT mass (g), **E**, Abdominal WAT mass (g) shows a trend for being increased in Adult KO mice, **F**, Bone Mineral Density (g/cm^2) **G**, Bone Mineral Content (g). Data plotted with SEM and analysed by one way ANOVA bonferroni corrected for multiple comparisons. *P<0.05, **P<0.01, ***P<0.001. Data are expressed as mean ± SEM.

Table 3.7 Plasma Amino Acids and Intermediates, and Free Fatty Acid Content in Adult KO Short Study Cohort. Mice were fasted for 6 hours before terminal bleeds, Adult KO (n=17) Vehicle Control (n=13). One way ANOVA bonferroni corrected for multiple comparisons. *P<0.05, **P<0.01, ***P<0.001. SEM, Standard Error of the Mean; NS, Not Significant. Plasma analysis carried out by Dr. Fredrik Jernersen, in the Department of Pharmacology at the University of Oxford.

Assay	Units	10 week				
		Vehicle		Adult KO		P-value
		Mean	SEM	Mean	SEM	
Amino Acids and Intermediates						
Total Cysteine	µM	243.0198	7.8300	267.6206	7.1630	NS
Total Homocysteine	µM	4.8669	0.3178	5.1635	0.2633	NS
Total Methionine	µM	49.9292	2.4355	44.2453	2.7815	NS
Arginine	µM	69.5848	6.5900	85.2235	14.0664	NS
Valine	µM	227.8583	12.0013	204.4670	7.9431	NS
Proline	µM	95.8795	8.1189	74.2674	5.0380	NS
Leucine	µM	165.9899	11.1757	154.9439	5.7199	NS
Isoleucine	µM	92.2536	6.5283	95.8239	4.0101	NS
Phenylalanine	µM	93.7395	5.3166	86.2159	3.0111	NS
Tyrosine	µM	111.1401	5.4274	78.3890	4.2232	***
Tryptophan	µM	67.1999	2.3883	79.1001	2.3918	**
Glutamate	µM	227.2782	12.8507	174.3341	8.9051	*
Serine	µM	159.3600	8.9069	142.5389	4.5439	NS
Glutamine	µM	744.8057	21.1759	736.6318	13.7495	NS
Glutamate + Glutamine	µM	972.0840	28.3536	910.9659	20.0011	NS
Ornithine	µM	102.1678	9.0068	76.5908	5.0573	NS
Cystathione	µM	2.2895	0.1668	1.7358	0.1522	*
Glutathione	µM	72.1174	5.9040	73.7016	5.4463	NS
Free Fatty Acids						
[14:0]	µM	3.6497	0.4901	5.1439	0.6134	NS
[16:0]	µM	417.9152	22.8433	447.7451	21.5687	NS
[16:1]	µM	41.9465	4.8945	55.5068	3.5123	NS
[18:0]	µM	72.4836	4.8938	82.2394	6.2118	NS
[18:1]	µM	160.7253	12.2078	188.9844	10.7193	NS
[18:2]	µM	263.0839	21.2919	268.6470	19.1445	NS
[18:3n-6]	µM	9.3721	1.1711	7.7810	0.4888	NS
[18:3n-3]	µM	16.5859	2.0078	19.1157	1.6225	NS
[20:3]	µM	16.5859	2.0078	19.1157	1.6225	NS
[20:4]	µM	6.5855	0.3123	6.7652	0.3809	NS
SCD-16		0.0993	0.0086	0.1238	0.0056	*
SCD-18		2.2884	0.1967	2.4259	0.1553	NS

There has recently been some literature suggesting FTO is regulated by nutrient levels and may play a role in amino acid sensing (Cheung *et al*., 2013, Gulati *et al*., 2013). Our mice should be

consuming the same amount of nutrients, but if loss of FTO is altering these pathways, this could lead to alterations in plasma amino acid levels and decreased protein synthesis, which could be the cause of the reduced lean mass we observed in the adult KO mice.

Analysis of plasma amino acid and free fatty acids was carried out on plasma samples I collected by Dr. Fredrik Jernersen, in the Department of Pharmacology at the University of Oxford, using Liquid chromatography tandem mass spectrometry (LC-MS/MS). The Adult KO mice have significantly lower plasma tyrosine (P=0.0001), glutamate (P=0.013), and cystathione (P=0.0115), and significantly increased tryptophan (P=0.0042) compared to control mice. There is also a trend for increased total cysteine (P=0.028 by student's t-test not significant with one way ANOVA) and decreased proline and ornithine (P=0.025 and P=0.013 by student's t-test respectively) (**Table 3.7**).

Analysis of plasma free fatty acids revealed that there are no significant differences in their concentration using a one-way ANOVA, however there is a trend for increased plasma Palmitoleic acid [16:1] in the Adult KO mice (P=0.0283 student's t-test). The SCD-16 index is the ratio of 16:1n-7/16:0 and the higher SCD-16 may reflect higher SCD-1 activity, which can predispose to metabolic dysfunction (Cedernaes *et al*., 2013).

3.4 Discussion

3.4.1 Summary

The data indicates that FTO has a role in influencing body composition and metabolic substrate utilisation. They also show that removal of FTO can be as deleterious as increasing its expression, as both adult onset KO mice and mice globally overexpressing *Fto* mice have increased fat mass (Church *et al*., 2010). This suggests that in man the at-risk allele could influence BMI either by decreasing or increasing FTO levels, or by impairment of its proper regulation. Removal of FTO may impact on the amino acid metabolism in the mice resulting in altered plasma levels and body composition that we observe.

3.4.2 Global Adult Conditional *Fto* KO

The phenotype of our mouse carrying a constitutive global KO of *Fto* (McMurray *et al*., 2013) is very similar to the two previously published models (Fischer *et al*., 2009, Gao *et al*., 2010). They showed marked perinatal mortality and a clear divergence of body weight from controls early in the perinatal period (Fischer *et al*., 2009, Gao *et al*., 2010). This may reflect changes that occurred *in utero* and/or a requirement for FTO from birth.

To avoid the high perinatal lethality of germline KO mice, and to address the role of the *Fto* gene in adult mice, we generated an inducible global KO mouse and inactivated the *Fto* gene at six weeks of age. These mice showed much improved viability compared to mice with a germline KO of *Fto*. However, some increased mortality with respect to controls remained. The cause of this remains unclear and prior to their deaths the mice were not reported to have been unwell at daily check. Given the phenotype of children with enzymatic null mutations, one may speculate that the demise of the three mice in question could have been linked to a cardiac phenomenon but this is far from certain (Boissel *et al*., 2009).

3.4.3 Body Composition

Adult onset KO mice showed a reduction in body weight in the weeks immediately following gene deletion, but convergence of body weight towards the last four weeks of the study (17–20 weeks of age). The lower weight is consistent with data from both our own and published germline global KO mice. Interestingly, in a previous study, female germline global *Fto* KO mice also showed convergence of body weight with controls by about 13 weeks of age (Gao *et al*., 2010).

The significantly reduced lean mass at nine and 20 weeks of age in adult onset KO mice (compared to controls) is consistent with data from the germline KO mice. This derives from a lower rate of gain of lean mass rather than lean mass wasting. The most striking observation in the adult onset KO mice was the marked gain in fat mass (both fat weight and fat expressed as a percentage of body weight increased). By 20 weeks of age the fat weight in the adult onset KO was almost double (1.92X) that of controls. This contrasts with all three constitutive KO models, which showed a reduction in fat mass. Given the lower rate of gain of lean mass it would be interesting to look at the effect of *Fto* loss in older animals in which growth had plateaued to examine how the loss of *Fto* affects established body composition. In man the effect of the SNPs in *FTO* are strong in childhood and adolescence, but begin to weaken with age (Jacobsson *et al*., 2009, Hardy *et al*., 2010, Jacobsson *et al*., 2011). It would be interesting to age the adult KO mice to examine the phenotype of these mice later on, as the fat mass may start to plateau or decline compared to wild-types, and their glucose tolerance may begin to alter.

The gain in fat mass in adult onset KO mice was more significant at 20 weeks of age when body weight differences were smaller. Thus, the lower weight of adult onset KO mice appears to be due, at least in part, to a lower lean body mass. Further, due to a redistribution of lean mass and fat mass, combined with an increase in fat mass, body weight was no longer significantly different in adult onset KO and control mice 20 weeks after deletion of *Fto*. At 20 weeks of age, adult onset KO mice weigh, on average, 1.5 g less than controls: around 0.9 g of this difference is not explained by the observed changes in lean and fat mass, and may possibly be attributable to changes in skeletal growth. Our germline knockout male mice showed reduced bone mineral

content and density (unpublished observations). However, at 10 weeks we saw no significant difference in BMD or BMC in the adult onset KO mice.

Looking at the weekly lean and fat mass measurements it is clear that the change in body weight of the Adult onset KO mice is due to the decrease in lean mass at eight weeks of age. It was also interesting to see that the fat mass of adult KO mice was significantly lower during and after treatment (6-8 weeks) and then caught back up to control levels at nine weeks. This is reminiscent of the early adiposity rebound observed in children with the at-risk A allele, whose normal BMI peaks in the first year and then there is decline in adiposity up to about five years of age after which it then increases (Sovio *et al*., 2011, Frayling and Ong, 2011).

The effect of adult onset global deletion of *Fto* on lean mass suggests that it could be interesting to examine *FTO* genotype in conditions of cachexia to see if there is a modifying effect. An initial study in chronic obstructive pulmonary disease (COPD) suggests variation of lung function with FTO genotype and proposes a link with cachexia in a subset of these patients (Wan *et al*., 2011). In the future I would like to characterise the muscle fibre-types to allow us to understand if inactivation of *Fto* effects muscle growth and the proportions of glycolytic or oxidative fibres. This would also allow us to thoroughly examine if there is loss of muscle fibres and regeneration or if muscle mass declines in formation after inactivation of *Fto*.

3.4.4 Energy Expenditure

There has been some discussion about the most appropriate way to correct energy expenditure for differences in body weight and composition in *Fto* KO mice and mouse models in general (Speakman, 2010, Kaiyala and Schwartz, 2011, Butler and Kozak, 2010, Choi *et al*., 2011). Using multiple linear regression to control for variation in lean mass, we found no significant difference in energy expenditure between the KO and littermate controls in both light and dark phases (McMurray *et al*., 2013). This is in contrast to the study by Gao *et al.* who reported an increased energy expenditure tested by ANCOVA (Gao *et al*., 2010). Using the ratio method, in which data were analysed by dividing energy expenditure by lean mass, our results show increased energy

expenditure in line with both previous studies. However, ratio analyses are confounded by the very different lean masses of the knockout and littermate control groups (Fischer *et al*., 2009, Gao *et al*., 2010). ANCOVA analysis, which is more correct, reveals that our germline KO mice show no differences in energy expenditure (McMurray *et al*., 2013). The different result obtained by Gao *et al*., is likely to be explained by differences in body composition in their mouse model. This problem is now widely recognized and it is accepted that regression based adjustment is the most appropriate way to account for differences in body weight or composition, as has been the case in human studies for many years (Kaiyala and Schwartz, 2011, Tschop *et al*., 2012). We conclude that in our global germline knockout there is no detectable difference in energy expenditure rate between knockout and wild-type littermates.

Energy expenditure in 18 week old Adult onset KO, when adjusted for lean mass variation using multiple linear regression, was not significantly different between the two groups. We also did not detect any significant differences in 24 hour food intake measurements. It would be interesting to know if the differences in body weight are due to changes in food intake or expenditure - small differences in these parameters (too small to detect in our experiments) could have a cumulative effect over a long time period. Other possible explanations for the reduced body weight include changes in the efficiency with which energy is extracted from food and changes in metabolism.

We also observed altered carbon dioxide output in adult onset KO mice. This resulted in a large reduction in RER at 18 weeks in the adult onset KO mice. That this occurred with a reduction in lean body mass may be in keeping with increased protein utilisation at the expense of carbohydrate. The observed metabolic switch is consistent with the reduction in lean body mass. How loss of FTO causes this metabolic switch is an important question for future research. Given the effects on lean mass and RER in adult onset KO mice this may be an interesting avenue for future investigation.

3.4.5 Amino Acid Sensing

Recently, it has been shown that FTO expression is regulated *in vitro* by amino acid availability (Cheung *et al*., 2013, Gulati *et al*., 2013). They describe a role for FTO in the coupling of amino acid levels to mTORC1 signalling. These findings suggest that FTO may influence body composition through playing a role in cellular nutrient sensing. Therefore, perhaps in the Adult onset KO mice deletion of FTO affects the proper regulation of this pathway, causing the cells to think they are in an amino acid starved state, leading to the decrease in lean mass that we observe. As the mice are not truly in an amino acid starved state as food intake is not different from control animals perhaps these nutrients end up being stored as fat, causing the increased fat mass we see in the 20 week old Adult KO mice.

The amino acid changes in the plasma in the Adult KO mice are also intriguing. Although only significant in three cases, 12 of the 18 amino acids and intermediates analysed were present at lower levels in the plasma of Adult onset KO mice. During a fasted state, muscle protein serves as the principal reservoir to replace blood amino acid taken up by other tissues. Blood amino acids serve not only as precursors for the synthesis of proteins but also as precursors for hepatic gluconeogenesis (Wolfe, 2006). Consequently, the protein mass of essential tissues and organs, as well as the necessary plasma glucose concentration, can be maintained despite the absence of nutritional intake, provided muscle mass is adequate to supply the required amino acids. In the adult onset KO mice lean mass is significantly decreased, which therefore could affect these important metabolic functions.

Increased plasma cysteine is associated with obesity [Reviewed in (Elshorbagy *et al*., 2012)] whereas plasma tryptophan levels are usually low in the obese, which can cause decreased levels of serotonin and depression (Caballero *et al*., 1988, Breum *et al*., 2003). Although not significant we see a trend for increased plasma total cysteine in the adult KO mice. Cysteine can promote adiposity by inhibiting lipolysis and stimulating lipogenesis via H_2O_2 production, and at 10 weeks of age this is when percentage fat mass of the Adult onset KO mice begins to be significantly increase. The SCD-16 index is the ratio of 16:1n-7/16:0, which is significantly increased in Adult

KO mice. The higher SCD-16 may reflect higher SCD-1 activity, which can predispose to metabolic dysfunction (Cedernaes *et al*., 2013). Thorough investigation of SCD-1 activity and expression in different tissues may aid in explaining the metabolic abnormalities in the Adult KO mice.

Tryptophan uptake occurs via a transport carrier, located at the blood-brain barrier. The carrier is shared between Trp and several other large neutral amino acids (LNAAs) and is competitive (principally leucine, isoleucine, valine, tyrosine, and phenylalanine). Therefore, changes in the blood of tryptophan or any of the other LNAAs can alter this transport (Fernstrom and Fernstrom, 1995). I see a significant decrease in plasma tyrosine and a trend for decreased leucine, valine and phenylalanine, which could lead to an increase in brain tryptophan levels. Tyrosine, which is significantly reduced in the Adult KO mice is an essential precursor to dopamine (Fernstrom, 1990), and so is likely to alter production of this neurotransmitter in the Adult KO mice. Finally many of the amino acids that I see are decreased are important in the ornithine/urea cycle (ornithine, proline, tyrosine and glutamate), which could explain the increased urea we see in the plasma in 20 week old Adult KO mice (**Table 3.6**).

Plasma tyrosine is significantly decreased at 10 weeks of age; however urinary adrenaline, noradrenaline and dopamine at 10 weeks of age in the first cohort were not significantly different from controls. Homozygous FTO^{I367F} showed significantly higher levels of dopamine and noradrenaline at 10 weeks of age, although these mice had an increased lean mass and RER suggesting that they had an increased metabolic rate (Church *et al*., 2009).

3.4.6 Tamoxifen

Tamoxifen is metabolised to its active form, 4-hydroxy-tamoxifen, which mimics the effects of oestradiol and can act on the oestrogen receptor. The tamoxifen inducible-Cre allowed us to delete *Fto* ubiquitously in the adult mouse using the *Cre-Lox* recombination system, but to do so mice must be treated with tamoxifen to activate the *ERT2*-Cre; the *ERT2*-Cre contains a mutated oestrogen receptor which does not respond to endogenous oestrogens. The *ERT2*-Cre has been

developed to be 10 times more sensitive to 4-hydroxy-tamoxifen than the original *ERT*-Cre (Indra *et al*., 1999). The tamoxifen inducible Cre line that we used contained ERT2 allowing us to use much lower doses of tamoxifen to achieve the same effects and reducing some of the potential off-target effects associated with tamoxifen.

Tamoxifen is widely used as a breast cancer drug. Generally tamoxifen is well-tolerated and serious side-effects are rare (Brown, 2002). However tamoxifen can increase endometrial cancer incidence in women and is a potent liver carcinogen in rats. Liver carcinomas have only been observed after prolonged periods of dosing in rats [6-12 months (Williams *et al*., 1993), two years (Greaves *et al*., 1993), 6-11 months (Carthew *et al*., 1995)], and none have been observed in mice (Martin *et al*., 1997, Brown, 2002). Tamoxifen has been shown to cause DNA-adducts, which are formed in a dose-dependent manner and accumulate with repeated administration. In C57BL/6 mice these have been seen to occur after dosing for four days with 120 mg/kg tamoxifen, but there is a rapid loss within three days followed by a slower removal over several weeks (Martin *et al*., 1997). Therefore our mice treated with 200 mg/kg tamoxifen may also have had these adducts present, however as there is no increase in liver tumours in the mouse from tamoxifen dosing (Martin *et al*., 1997, Brown, 2002), and we see no liver phenotype ourselves this is unlikely to be detrimental.

Oestradiol decreases food intake, body weight and fat mass, and tamoxifen treatment has been shown to mimic this effect in rats (Gray *et al*., 1993, Wade and Heller, 1993, Lopez *et al*., 2006). The doses used in these papers are lower than the doses we administered to induce Cre-Lox recombination in our mice, so tamoxifen may be causing these effects in our mice. After tamoxifen treatment our Adult KO mice have gained less weight than the vehicle control group (**Figure 3.8A**), however if we look at our Cre control group that are also dosed with tamoxifen this effect is not seen and their body weight curve is not significantly different from the vehicle control group (**Figure 3.7A**), therefore I do not believe that the decreased weight gain seen in the Adult KO mice after tamoxifen dosing is due to the anorectic effects of tamoxifen and so must be caused by deletion of *Fto* in the mice.

3.4.7 Conclusions

Whether FTO is a good drug target for obesity is still an open question. Despite there being some undesirable effects of knocking it out in the adult mouse, there may be a therapeutic range of inhibition that would be beneficial in man. It also remains to be proven that the catalytic activity of FTO is solely responsible for the effects that have been shown by gene manipulation.

In conclusion, my data demonstrate that FTO loss in adulthood is better tolerated and leads to changes in both lean and fat mass (through alterations in metabolism). Thus our study shows a complex role for FTO in peripheral metabolism and substrate utilisation.

Chapter 4:

In vitro analysis of *Fto* function

4.1 Introduction

FTO has been shown to be expressed throughout the body, and is highly expressed in the brain (Gerken *et al*., 2007). FTO is localised to the cell nucleus (Gerken *et al*., 2007, McTaggart *et al*., 2011), although after sub-cellular fractionation some have reported FTO expression in the cytoplasm (Gulati *et al*., 2013). FTO has been shown to partially co-localise with nuclear speckles (Jia *et al*., 2011). Nuclear speckles contain splicing or splicing-related cofactors such as SC35, SART1 and RNA polymerase II, indicating that FTO may play a role in mRNA processing or spliceosome formation (Jia *et al*., 2011). Jia and colleagues have shown that FTO does not affect spliceosome formation, but they did show that inhibition of transcription using actinomycin D resulted in increased co-localisation of FTO with splicing factors, suggesting that FTO may be linked to processing of recently transcribed mRNA.

If FTO alters processing of mRNA this could also affect translation levels. Gulati and colleagues were able to show that *Fto* knockout MEFs have reduced levels of translation compared to wild-types (Gulati *et al*., 2013). They were also able to show that *Fto* knockout MEFs have a reduced rate of cell growth compared to wild-types.

Aminoacyl-tRNA synthetases (AARSs), attach specific amino acids to their cognate tRNAs, in a process known as 'charging'. During charging several AARSs associate together to form macromolecular assemblies known as the multi-synthetase complexes (MSCs), which increase translation efficiency. Gulati and colleagues found that there was a reduction of MSC components in $Fto^{-/-}$ MEFs, and that this could be rescued by re-expressing *Fto* in these cells, indicating FTO may be involved in regulating MSC protein levels (Gulati *et al*., 2013). They then went on to show

that *Fto*$^{-/-}$ MEFs had decreased activation of the mTORC1 pathway. mTORC1 senses nutrient availability in the cell leading to alterations in protein synthesis. This supports a previous study where FTO expression is regulated by essential amino acid availability (Cheung *et al*., 2013).

The mTORC signalling pathway is crucial for cell growth and metabolism. In zebrafish, Torc1 signalling has been shown to regulate cilia length through translational regulation (Yuan *et al*., 2012). In this model, increased TORC1 increases cilia length, and inhibition with rapamycin decreases cilia length (Yuan *et al*., 2012). It was shown that cilia, which are too long or too short, could not function properly, disrupting the establishment of left-right asymmetry (Yuan *et al*., 2012, Yuan and Sun, 2012). Boehlke and colleagues suggest the reverse, with primary cilia affecting mTORC1 activity and cell size through LKB1 activation when fluid flow causes cilia to bend.

Diseases resulting in the disruption of cilia and/or the basal body complex are called ciliopathies. These diseases can present a range of phenotypes but they often have a strong developmental component and often present during childhood in patients. Characteristics can include obesity, renal disease, hepatic fibrosis, skeletal dysplasias, endocrinopathies, neurodevelopmental defects, CNS anomalies, laterality defects, and congenital heart disease [reviewed in (Cardenas-Rodriguez and Badano, 2009, Ferkol and Leigh, 2012)]. FTO is likely to have a developmental effect as *Fto*$^{-/-}$ mice are growth retarded and have poor survival rates compared to wild-type littermates (Fischer *et al*., 2009, McMurray *et al*., 2013). A mutation in *FTO* (R316Q), identified in a consanguineous family, abolishes the demethylase function of FTO. This causes severe congenital defects when present in patients homozygous for the mutation (Boissel *et al*., 2009). These patients are also growth retarded and do not survive past 30 months of age.

Cilia are directly coupled to the Hedgehog developmental signalling pathway, and there is evidence of cilia involvement in other developmental signalling pathways such as Platelet-Derived Growth Factor Receptor signalling and, Canonical and Non-canonical WNT signalling [reviewed in (Eggenschwiler and Anderson, 2007, Goetz and Anderson, 2010)]. The WNT signalling

pathway has been implicated in embryonic development, adult tissue remodelling as well as cellular metabolism. WNT signalling is linked to cellular mechanisms of fuel sensing such as mTOR, hexosamine biosynthesis pathway and lipid sensing [reviewed in (Sethi and Vidal-Puig, 2010)]. Canonical WNT signalling has also been shown to be involved in mesenchymal stem cell fate, with activation leading to differentiation into myoblasts and osteoblasts lineages by inhibiting the expression of *Pparg* and *Cebpa*. In the absence of WNT signalling *Pparg* and *Cebpa* are expressed leading to adipogenic differentiation (Ross *et al*., 2000, Bennett *et al*., 2002).

The *in vitro* studies suggest that FTO has an important role in the cell regulating metabolism and cellular growth. In the mouse FTO has been shown to affect body weight and composition, but it also appears to have a role in development, which is more striking in humans. In this chapter I aim to confirm some of the current findings that FTO is important for cell growth and translation. I also investigate if FTO plays a role in development, by investigating cilia formation, signalling, and adipogenesis.

4.2 Methods

4.2.1 siRNA used for *Fto* Knockdown

Gene knockdown was achieved using the methods described in Chapter 2 Materials and Methods **Section 2.5.1**. The siRNAs used in this chapter were:

Fto – CCUGCGAUGAUGAAGUGGACCUUAA (Invitrogen, California, U.S.A.)

Stealth RNAi™ siRNA Negative Control Medium GC (Invitrogen, California, U.S.A.)

4.2.2 mRNA Translation Assay

Cells were counted and plated on a 12-well plate at the desired density and left to adhere and grow overnight. Cells were then incubated with growth media containing 1 or 2 μM puromycin for 5-40 minutes before harvesting. Protein was extracted from the cells as described in Chapter 2 **section 2.4.1**. Immunoblots or dot-blots were performed using the mouse monoclonal anti-Puromycin antibody (3RH11, Kerafast, Boston, U.S.A.). This was adapted from the methods by Schmidt and colleagues (Schmidt *et al*., 2009)

4.2.3 MEF Cilia measurements

MEFs were plated and allowed to grow for 24 hours. MEF growth medium was then changed for serum-free MEF growth media and cells were grown for a further 48 hours, to induce cilia formation. Media was then removed and the cells washed with DPBS. Cells were fixed and permeabilised by adding 100 % methanol to the cells and placing at -20 °C. As described in Chapter 2, **Section 2.5.3**, cells were then stained with primary antibodies for mouse monoclonal acetylated-α-tubulin (1 in 250, T6793 Sigma) rabbit polyclonal anti-mouse γ-tubulin (1 in 1000, ab11317 Abcam, Cambridge, UK). Secondary antibodies Alexa Fluor® 488 Goat Anti-mouse IgG (Invitrogen) and Alexa Fluor® 647 Goat Anti-Rabbit IgG (Invitrogen) were then used at a 1 in 200

dilution. Hoechst 33342 was used to stain nuclei. Fields of view were randomly selected and cilia were measured and counted in each image.

4.2.4 Immunoblots

Antibodies used for immunoblotting in this chapter.

Table 4.1 Primary Antibodies used for Immunoblots.

Protein	Supplier	Product Code
FTO	In House	-
ACTIN	Millipore	MAB1501R
PUROMYCIN	Kerafast	EQ0001
P70S6K	Cell Signaling	2708
P70S6K-Phospho (Thr389)	Cell Signaling	9234
S6	Cell Signaling	2317
S6-Phospho (Ser235/236)	Cell Signaling	4858
ACC-Phospho (Ser79)	Cell Signaling	3661
SIRT1	Millipore	04-1557
EIF2α	Cell Signaling	2103
EIF2α-Phospho (Ser51)	Cell Signaling	3398
STAT3-Phospho (Tyr705)	Cell Signaling	9131
mTOR	Cell Signaling	4517

4.2.5 qRT-PCR analysis of Gene Expression in MEFs

RNA was extracted and gene expression in MEFs was analysed using quantitative real-time PCR as described in the materials and methods (**Chapter 2 Section 2.3.3**). Taqman Assay identifications for each Taqman probe are given in **Table 4.2**.

Table 4.2 Taqman Gene Expression Assay, Probe Assay Identification.

Gene	Gene Name	Taqman Assay ID
Acyl-Coenzyme A dehydrogenase, long-chain	*Acadl*	Mm00599660_m1
β-Actin	*Actb*	4352933-1104034
Adiponectin	*Adipoq*	Mm01343606_m1
Adiponectin Receptor 2	*Adipor2*	Mm01184030_m1
Cluster of Differentiation 36 Antigen	*Cd36*	Mm00432403_m1
Chromodomain helicase DNA binding protein 1	*Cdh-1*	Mm00486918_m1
CCAAT/enhancer binding protein α	*Cebpa*	Mm01265914_s1
Carnitine palmitoyltransferase 1a	*Cpt1a*	Mm00550438_m1
Carnitine palmitoyltransferase 1b	*Cpt1b*	Mm00487200_m1
Fat Mass and Obesity Associated	*Fto*	Mm00488755_m1

Glyceraldehyde-3-phosphate dehydrogenase	*Gapdh*	4352932-1211040
Lymphoid enhancer binding factor 1	*Lef1*	Mm00550265_m1
Leptin	*Lep*	Mm00434759_m1
Lipoprotein lipase	*Lpl*	Mm00434770_m1
Matrix metallopeptidase 2	*Mmp2*	Mm00439508_m1
Phosphoenolpyruvate carboxykinase 1	*Pck1*	Mm01247058_m1
Peroxisome proliferator activated receptor γ	*Pparg*	Mm00440945_m1
Stearoyl-Coenzyme A desaturase 1	*Scd1*	Mm00772290_m1
Sterol regulatory element binding transcription factor 1	*Srebf1*	Mm01138344_m1
Vascular endothelial growth factor A	*Vegf*	Mm00437304_m1

4.3 Results

4.3.1 Cellular Localisation of FTO

Most studies so far suggest that FTO is localised to the cell nucleus (Gerken *et al*., 2007, McTaggart *et al*., 2011), although a fractionation experiment has suggested there may be some cytoplasmic expression (Gulati *et al*., 2013). To confirm localisation of FTO in wild-type, knockout and overexpression cells I generated MEFs from the global $Fto^{-/-}$ and $R26^{Fto/Fto}$ mouse lines with littermate controls. Wild-type mice from the $R26^{Fto/Fto}$ mouse line, with only the two endogenous copies of *Fto* will be called FTO-2, and mice which have 2 additional copies of the *Fto* gene are referred to as FTO-4.

Hoechst 33342 was used to visualise the nucleus, and mitotracker red was used to visualise mitochondria as in (Gerken *et al*., 2007). In *Fto* wild-type MEFs, FTO expression appears to be localised to the nucleus, whilst in $Fto^{-/-}$ MEFs, FTO is not detected (**Figure 4.1**). In FTO-2 and FTO-4 cells we also see expression of FTO in the nucleus, however there does appear to be some cytoplasmic expression of FTO (**Figure 4.2**). This is more striking in the FTO-4 cells where we can see increased FTO signal, in the nucleus and the cytoplasm.

There does appear to be some non-specific binding of the primary antibody though, as if the gain of the detector is increased we can see signal in the $Fto^{-/-}$ cells (**Figure 4.3**). When this antibody is used for immunoblots some non-specific bands at other sizes can be seen, therefore the cytoplasmic staining maybe due to off-target antibody binding. Cells were stained and imaged on separate days which may account for differences seen in the wild-type cells ($Fto^{+/+}$ vs. FTO-2).

`

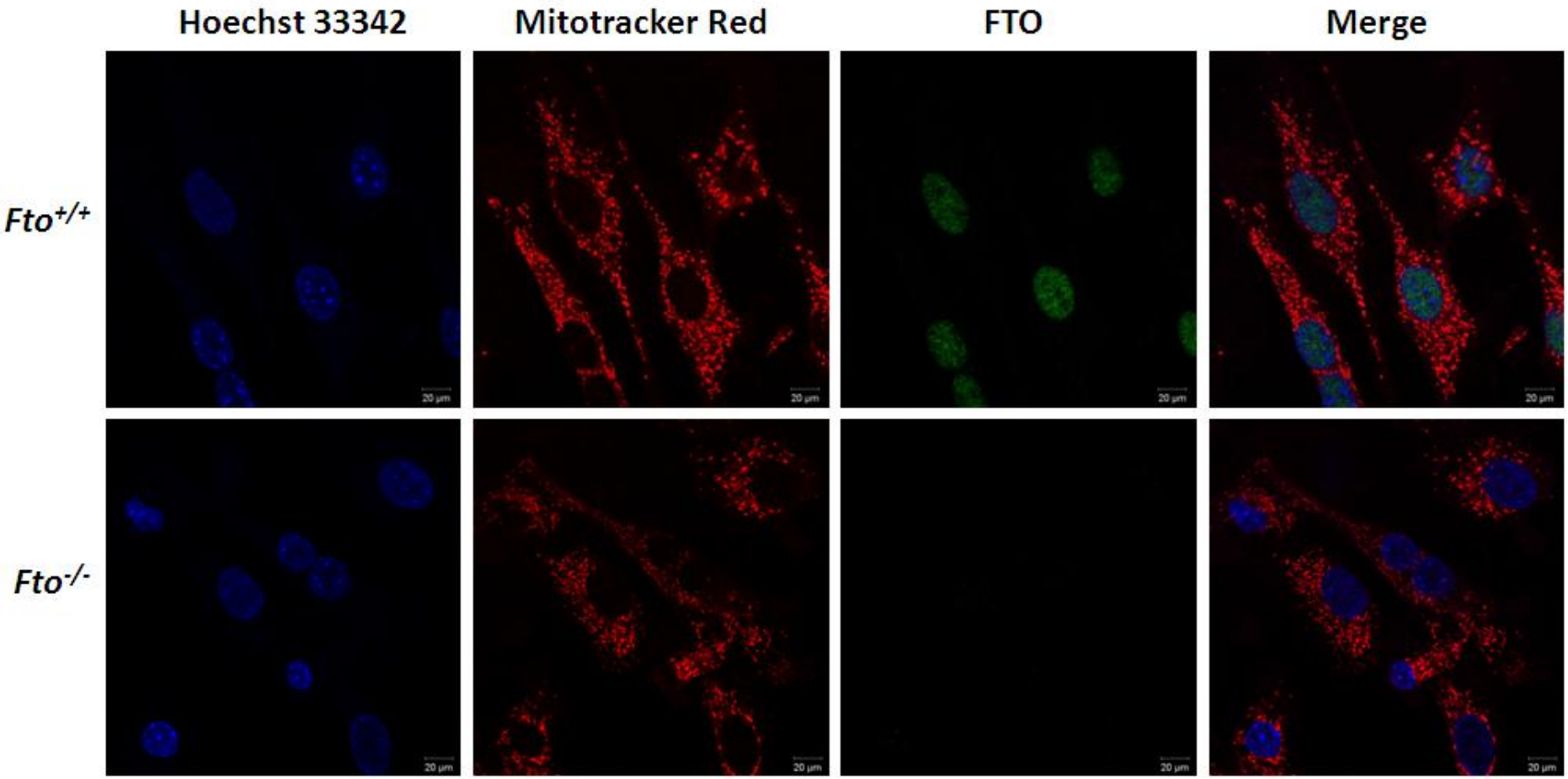

Figure 4.1 Cellular Localisation of FTO in Wild-type and FTO Knockout MEFs. Immunocytochemistry showing localisation of FTO (green) in comparison to nuclei (blue) and mitochondria (red) in *Fto*$^{+/+}$ and *Fto*$^{-/-}$ MEFs, Scale bars: 20 µm.

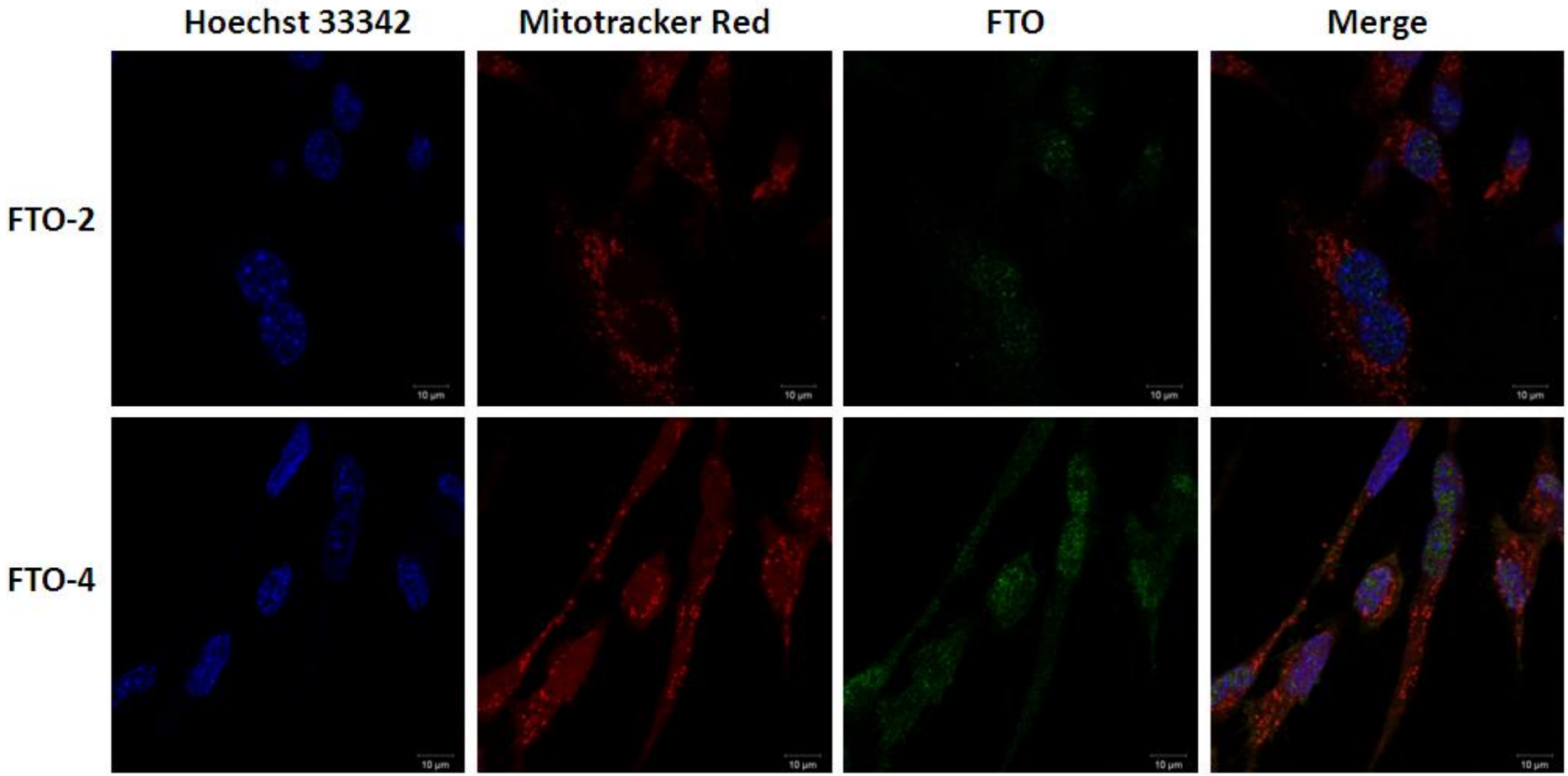

Figure 4.2 Cellular Localisation of FTO in Wild-type and FTO Overexpression MEFs. Immunocytochemistry showing localisation of FTO (green) in comparison to nuclei (blue) and mitochondria (red) in FTO-2 and FTO-4 MEFs, Scale bars: 10 µm.

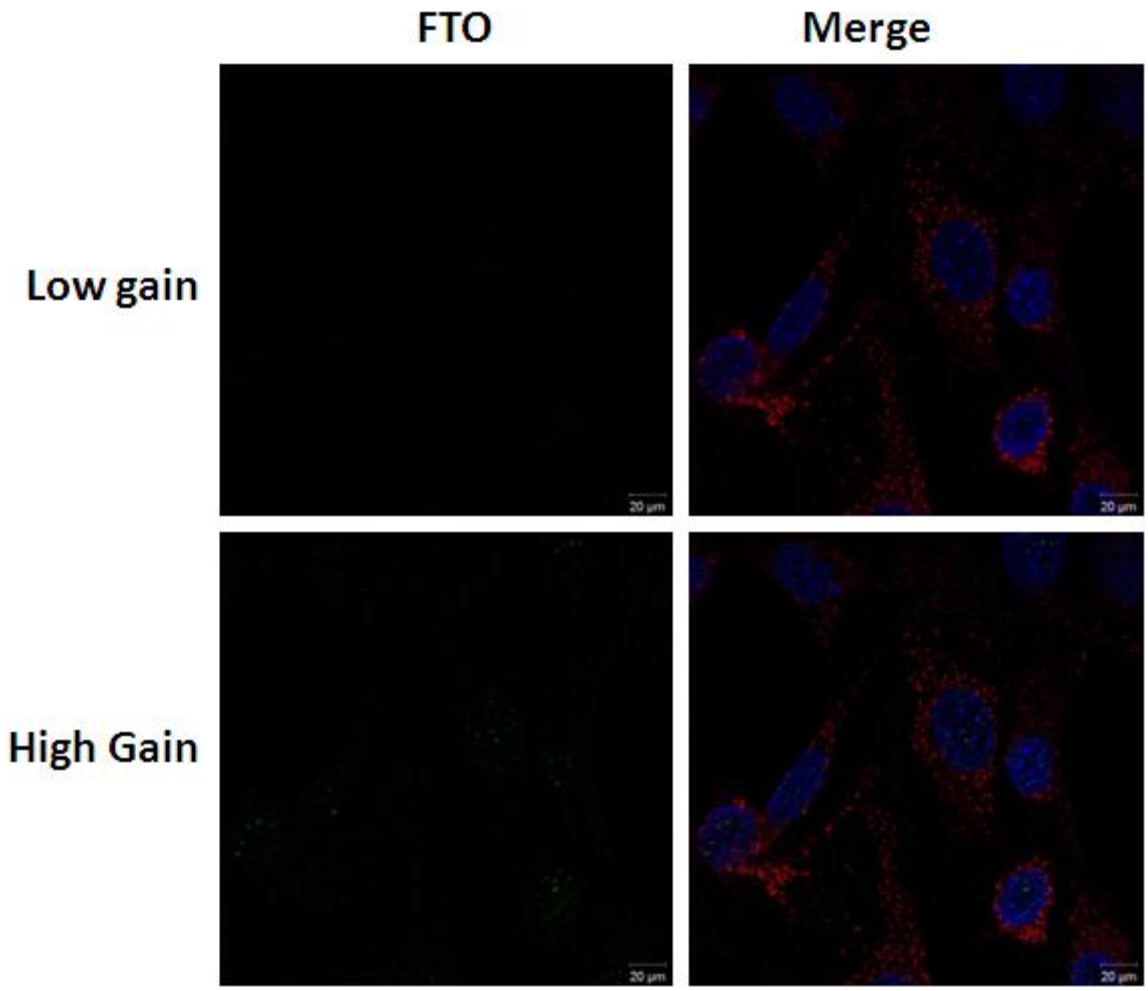

Figure 4.3 FTO Antibody does show some unspecific binding in FTO Knockout MEFs. Fto Knockout MEFs stained with the FTO antibody examined with low gain on the 488 (green) channel, or with high detector gain where some FTO expression can be seen. Scale bars: 20 μm.

4.3.2 FTO affects Cellular Proliferation

Gulati and colleagues showed that *Fto*$^{-/-}$ MEFs have reduced rates of cell growth (Gulati *et al*., 2013). As I saw decreased lean mass in my *Fto* adult knockout mice, I decided to investigate the effect of *Fto* knockdown in C2C12 cells, a mouse myoblast cell line. When FTO is knocked down in C2C12 cells, *Fto* gene expression is 10.13 % relative to cells treated with control siRNA (data not shown), and FTO protein levels are 22.44 %, **Figure 4.9**).

To measure cell viability after *Fto* knockdown separate plates of cells were treated with siRNA and then after 24, 48 and 72 hours calcein (live stain) and ethidium homodimer (dead stain) were used to stain the cells. Knockdown of *Fto* in C2C12 cells caused a reduction in live signal at 48 hours

(**Figure 4.4A**) but no significant differences in the dead staining (**Figure 4.4B**). When this study was repeated, live staining was significantly decreased in *Fto* siRNA treated cells at 48 and 72 hours, and again there was no significant difference in dead staining (**Figure 4.4C,D**). This suggests that there is a reduction in proliferation rather than increased cell death in C2C12 cells treated with *Fto* siRNA.

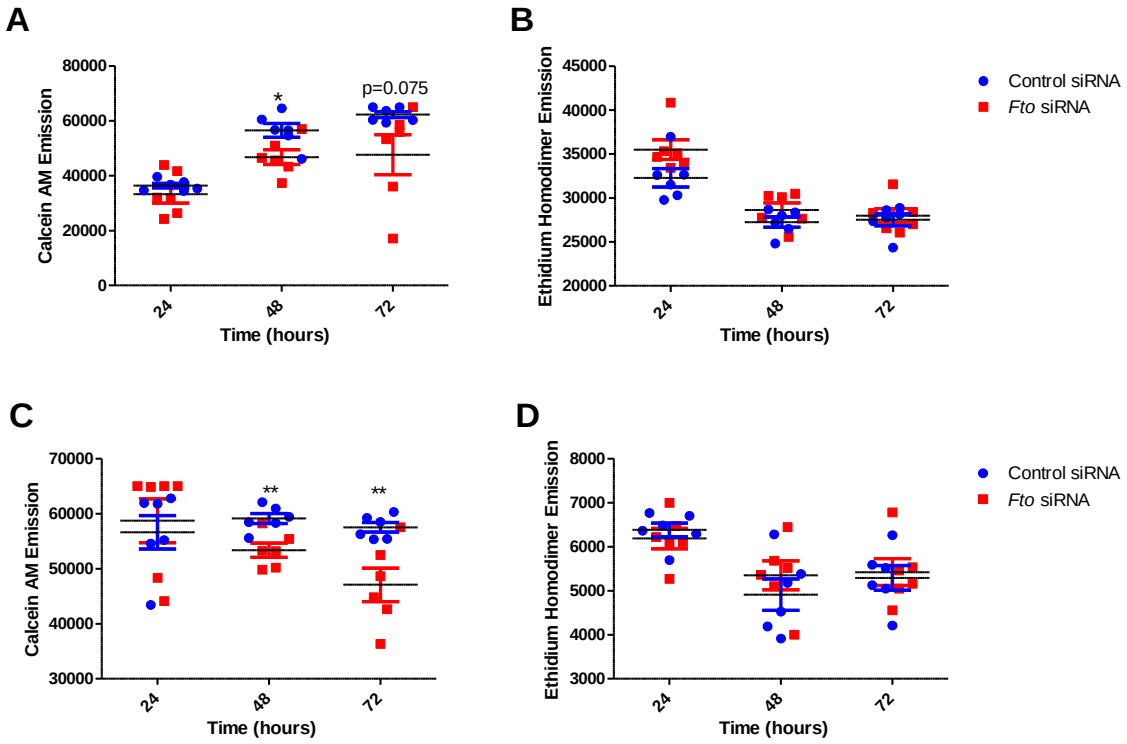

Figure 4.4 Live/Dead Cell Viability Assay of C2C12 treated with scrambled control or *Fto* siRNA. Cells were plated and treated with control scrambled or *Fto* siRNA. After 24 hours, media was changed to normal growth media, and viability was measured using Calcein AM (Tanaka *et al*.), **A,** and Ethdium homodimer (Dead), **B**, fluorescence levels after 24, 48 and 72 hours. **C** and **D** show a repeat of this study. Data analysed by student's t-test *P<0.05, **P<0.01, ***P<0.001. Data shown as mean ± SEM.

This study was then repeated using $Fto^{+/+}$ and $Fto^{-/-}$ MEFs (**Figure 4.5**). Unlike the results of Gulati and colleagues, and our C2C12 results, we could see no significant difference between the live (**Figure 4.5A**) and dead stains (**Figure 4.5B**) in the *Fto* knockout MEFs (Gulati *et al*., 2013).

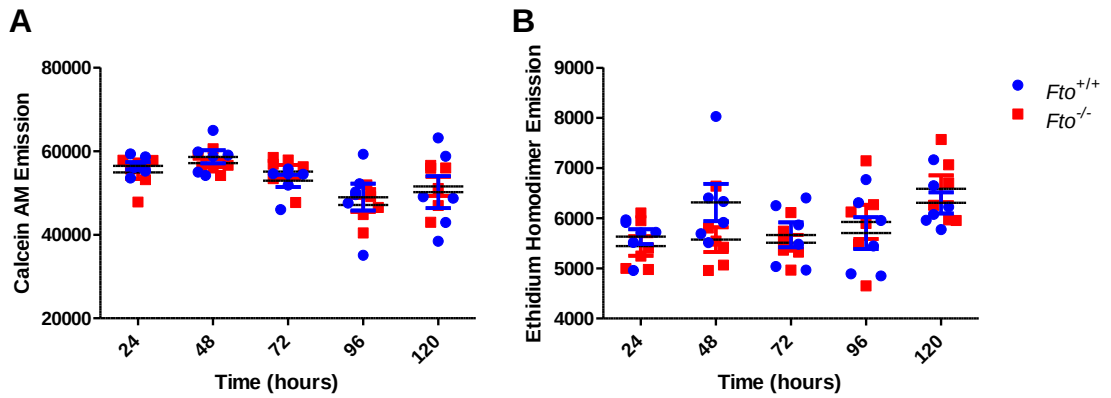

Figure 4.5 Live/Dead Cell Viability Assay of *Fto*$^{+/+}$ and *Fto*$^{-/-}$ MEFs. Cells were plated and after 24, 48, 72, 96 and 120 hours, viability was measured using Calcein AM (Tanaka *et al*.), **A,** and Ethdium homodimer (Dead), **B**, fluorescence levels. Data analysed by student's t-test *P<0.05, **P<0.01, ***P<0.001. Data shown as mean ± SEM.

Gulati and colleagues also showed that mRNA translation rates were decreased in *Fto*$^{-/-}$ MEFs, by using puromycin incorporation into nascent proteins (Gulati *et al*., 2013). I repeated this study initially using 1 μM puromycin, but could not detect such a prominent difference in my wild-type and *Fto*$^{-/-}$ MEFs (**Figure 4.6A**). It did however appear that FTO-4 MEFs had a decreased puromycin incorporation compared to FTO-2 MEFs (**Figure 4.6A**).

I then repeated this using the same conditions and time points as Gulati and colleagues, using 2 μM Puromycin. This concentration of puromycin does appear to show decreased incorporation into *Fto*$^{-/-}$ MEFs (**Figure 4.6B**), with no difference observed in FTO overexpression MEFs, however running the proteins on a gel like this made quantification of the results challenging.

I repeated this experiment a number of times to establish ideal timings to harvest the cells from 5 – 40 minutes (data not shown). I then repeated the experiment using 15 and 40 minute time points in triplicate, and performed a dot-blot of the protein lysate so that quantification of all labelled proteins, regardless of their size would be possible. *Fto*$^{-/-}$ MEFs again appear to show no significant difference when 1 μM puromycin is used, however when 2 μM puromycin is used there does appear to be less incorporation into the nascent proteins (**Figure 4.7A**). This can also be seen if we correct the puromycin signal for ACTIN levels (**Figure 4.7B**). The use of 2 μM puromycin

does not cause a significant difference (P=0.112) however this does replicate the trend observed by Gulati and colleagues, and suggests that *Fto*$^{-/-}$ MEFs are more sensitive to this level of puromycin present in the media than wild-type cells.

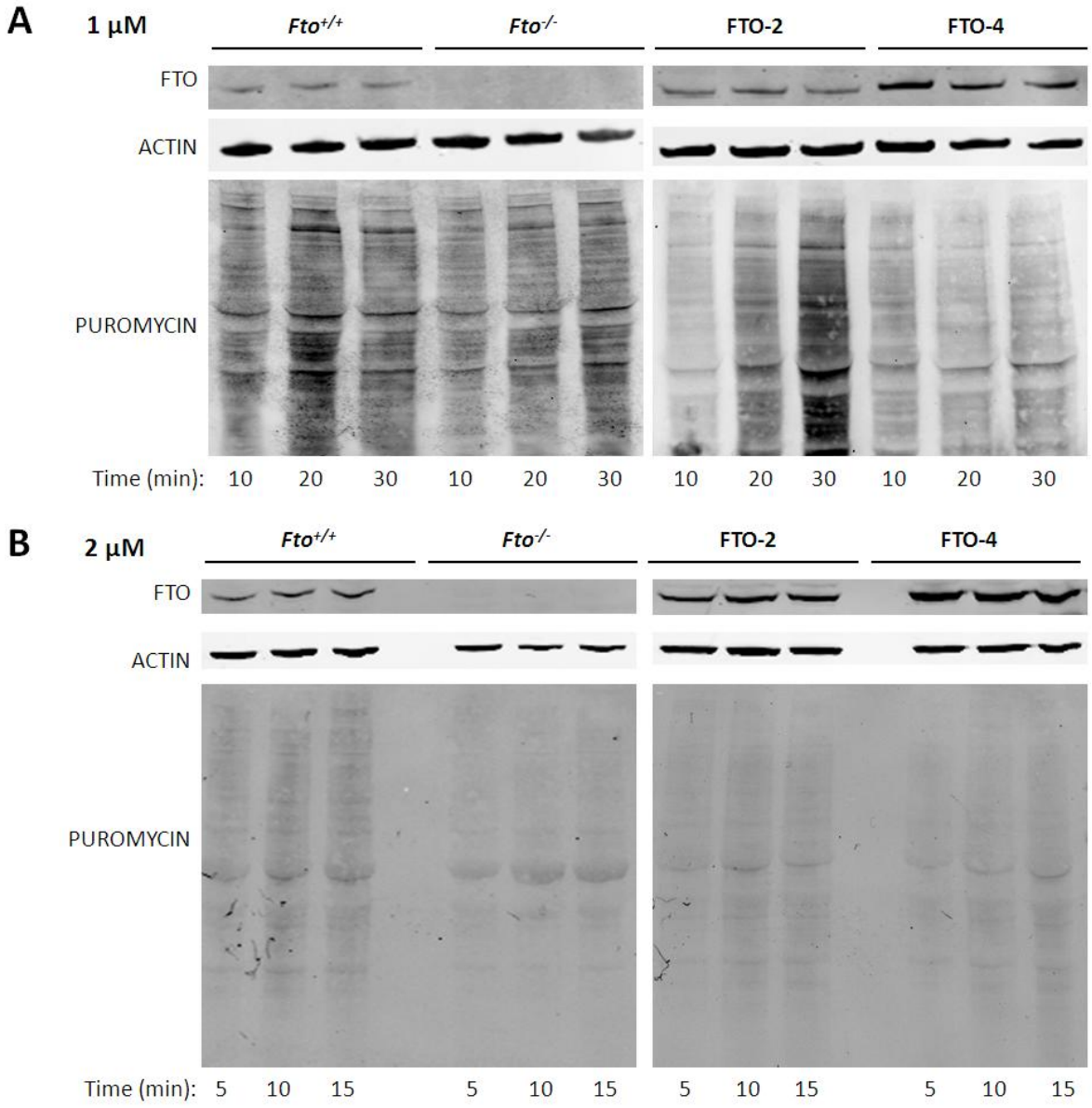

Figure 4.6 mRNA translation Assay in FTO Wild-type, Knockout and Overexpression MEFs. A Immunoblots of FTO, ACTIN, and proteins labelled with puromycin after 10, 20 and 30 minutes incubated with 1 µM puromycin. **B** Immunoblots of FTO, ACTIN, and proteins labelled with puromycin after 5, 10 and 15 minutes incubated with 2 µM puromycin.

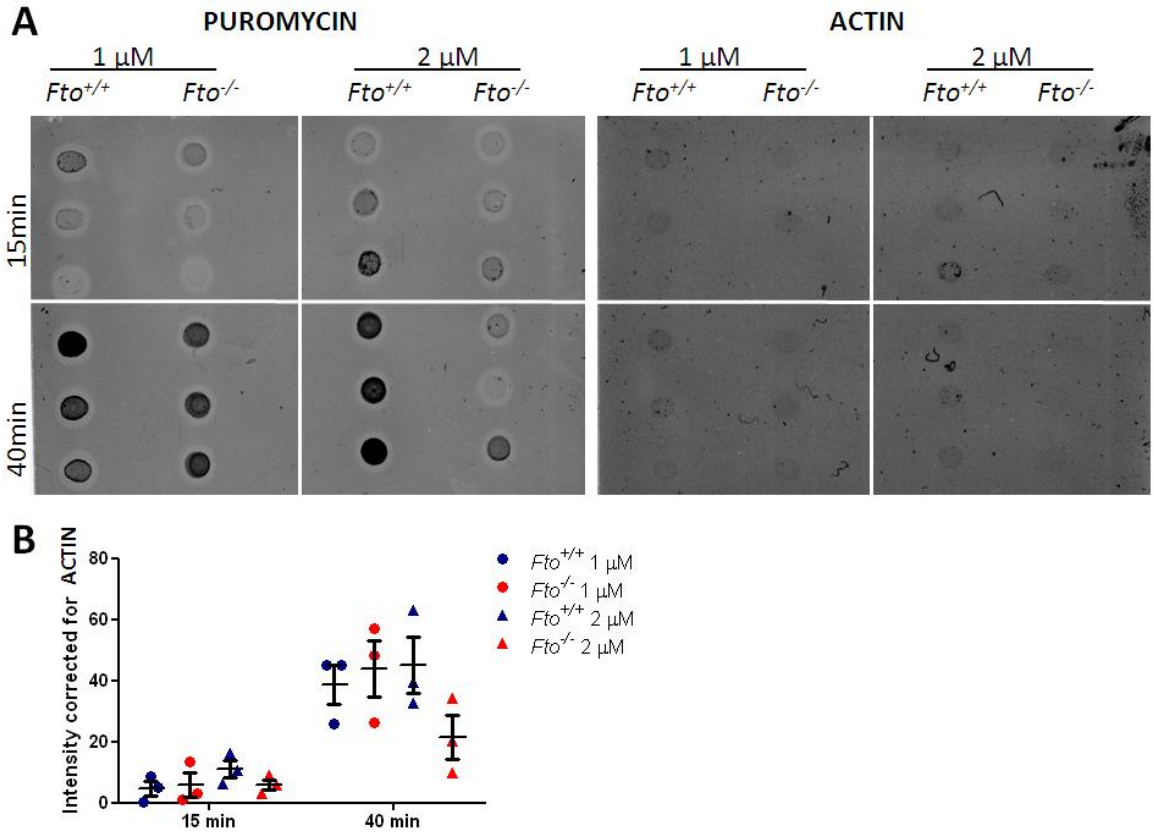

Figure 4.7 mRNA translation Assay in FTO Wild-type and Knockout MEFs. A Dot-blots of proteins labelled with puromycin and ACTIN after incubation with 1 or 2 µM puromycin for 15 and 40 minutes. **B** Puromycin intensity corrected for ACTIN intensity for each individual dot. Data analysed using Odyssey Sa Analysis Software, (LI-COR Biosciences, Cambridge, UK). Data shown as mean ± SEM.

I then examined the effect on FTO-2 and FTO-4 MEFs (**Figure 4.8**). No difference can be observed between the wild-type and FTO overexpression cells when treated with 1 or 2 µM puromycin (**Figure 4.8A**). When the data is corrected for ACTIN levels, there is trend at 15 minutes for increased puromycin incorporation with 1 µM puromycin, which is significant when 2 µM is used (P=0.0216 **Figure 4.8B**). At 40 minutes this trend can still be seen but is not significant between either treatment group, this may be due to them reaching a saturation point at 40 minutes.

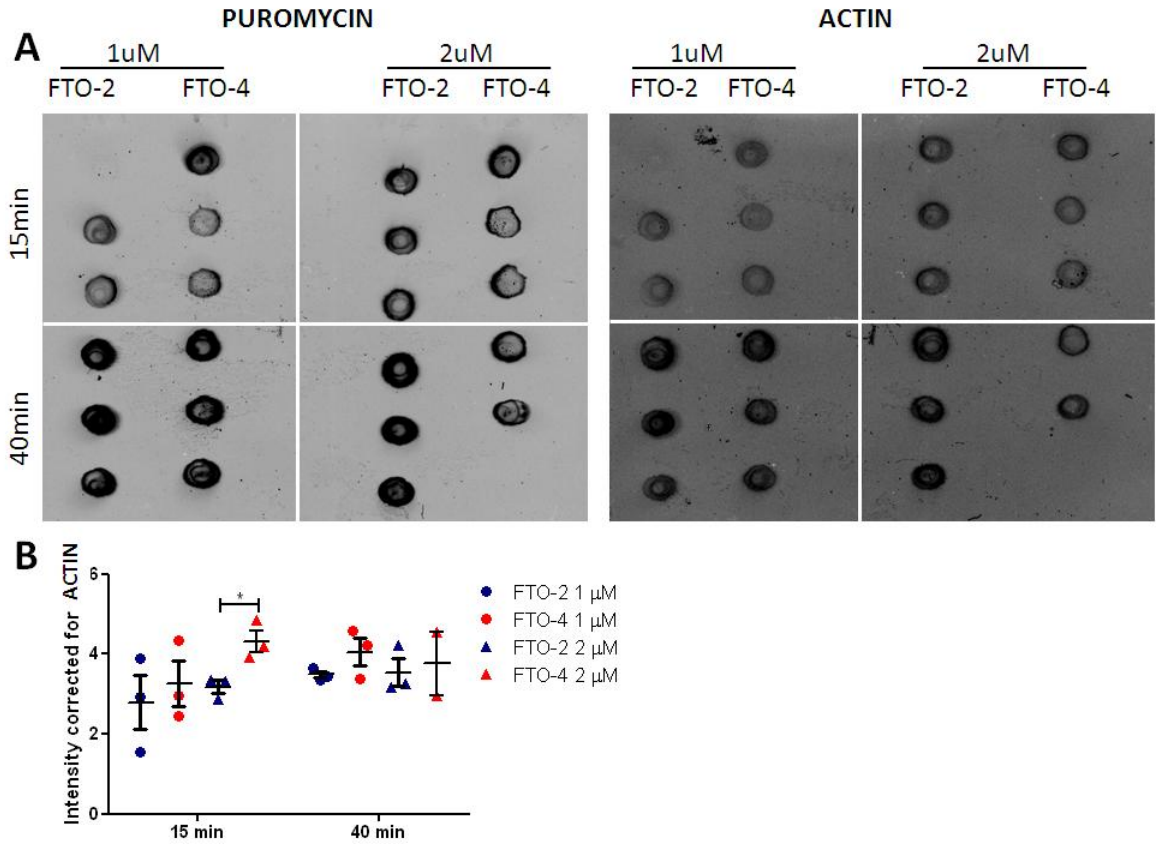

Figure 4.8 mRNA translation Assay in FTO Wild-type and Overexpression MEFs. A Dot-blots of proteins labelled with puromycin and ACTIN after incubation with 1 or 2 μM puromycin for 15 and 40 minutes. **B** Puromycin intensity corrected for ACTIN intensity for each individual dot. Data analysed using Odyssey Sa Analysis Software, (LI-COR Biosciences, Cambridge, UK). Data shown as mean ± SEM.

4.3.3 Protein Expression Differences in *Fto* Knockdown C2C12 cells

The cell proliferation differences we saw in the C2C12 cells lead me to investigate the mechanism behind this. I decided to investigate the protein expression changes in the control and *Fto* knockdown cells. To do this I used stable isotope labelling by amino acids in cell culture (SILAC, as described in Chapter 2 Materials and Methods, **Section 2.5.8**). C2C12 cells were grown in 'heavy' or 'light' media, the cells grown in the 'heavy' media were treated with *Fto* siRNA and the 'light' cells with control, cells were fractionated into nuclear and cytoplasmic compartments, and proteins analysed by mass spectrometry. Fold changes greater than 1.5 were considered valid, and these results were analysed using Interactive Pathway Analysis of Complex 'omics Data (IPA, Ingenuity Systems, California, U.S.A.).

In total there were 1444 differently expressed proteins between the *Fto* knockdown and wild-type C2C12, 730 in the cytoplasmic fraction and 714 in the nuclear fraction. The top 10 networks with changes identified using IPA are shown in **Table 4.3**.

Table 4.3 Top Networks of Proteins Altered Following 24 hours of *Fto* Knockdown in C2C12 Cells. Data analysed by IPA, Ingenuity Software.

Network	Score	Focus Molecules
Gene Expression, Protein Synthesis, Cellular Assembly and Organisation	49	31
DNA Replication, Recombination, and Repair, Cellular Assembly and Organisation, Reproductive System Development and Function	47	30
Molecular Transport, RNA Trafficking, Cell Morphology	42	28
Cell Cycle, Digestive System Development and Function, Endocrine System Development and Function	39	27
Molecular Transport, RNA Trafficking, Hair and Skin Development and Function	40	28
Cell Cycle, Cellular Assembly and Organisation, Cellular Function and Maintenance	35	26
DNA Replication, Recombination, and Repair, Cell Cycle, Cancer	34	25
Cellular Assembly and Organisation, Cellular Function and Maintenance, Cell Cycle	33	24
Cellular Compromise, Cellular Function and Maintenance, Molecular Transport	33	24
Cellular Assembly and Organisation, Cellular Function and Maintenance, Cell-to-Cell Signalling and Interaction	33	24

The top network, 'Gene Expression, Protein Synthesis, Cellular Assembly and Organisation' was particularly interesting to us due to the previously observed differences in amino acid sensing and translation that FTO has been implicated in (Cheung *et al*., 2013, Gulati *et al*., 2013).

The top changes in protein expression are shown in (**Table 4.4**). There are several proteins here that are involved in the cell cycle (NUSAP1, CDK5RAP3, CKS2, NCAPD2) metabolism (GSK3B, MAN2B2, SLC25A3, SLC6A6) RNA processing (PCF11) cell migration and development (GSK3B, TNS3, PLOD1, PLXNB2, EPHB6) and muscle function (TAC1, MYL9). Confirmation of these protein changes by immunoblot is still ongoing.

Table 4.4 Top Protein Fold Changes after 24 hours of *Fto* Knockdown in C2C12 Cells.

Protein	Fold Change after *Fto* knockdown	Fraction	Function
NUSAP1	↑ 15.693	Nuclear	Mitotic Spindle Organisation
GSK3B	↑ 11.971	Cytoplasmic	Energy Metabolism, neuronal cell development, and body pattern formation
GOLT1B	↑ 11.036	Nuclear	May be involved in fusion of ER-derived transport vesicles with the Golgi complex
TNS3	↑ 5.015	Nuclear	May play a role in actin remodelling. Involved in the dissociation of the integrin-tensin-actin complex.
MAN2B2	↑ 4.942	Nuclear	Hydrolyses Mannose
SLC25A3	↑ 4.319	Nuclear	Mitochondrial Membrane Phosphate transporter
PCF11	↑ 3.830	Nuclear	pre-mRNA processing
PLOD1	↑ 3.220	Nuclear	Forms hydroxylysine residues in collagens, which stabilise intermolecular collagen cross-links
VSTM4	↑ 2491	Nuclear	Membrane Protein
PLXNB2	↑ 2.474	Cytoplasmic	Transmembrane receptors that participate in axon guidance and cell migration in response to semaphorins
TAC1	↓ 14.72	Nuclear	Contract (directly or indirectly) many smooth muscles
PSMG2	↓ 12.539	Cytoplasmic	Chaperone protein which promotes assembly of the 20S proteasome
TJP2	↓ 8.814	Nuclear	Tight junction protein
PLCB1	↓ 7.473	Cytoplasmic	Catalyzes the formation of inositol 1,4,5-trisphosphate and diacylglycerol from phosphatidylinositol 4,5-bisphosphate
CDK5RAP3	↓ 6.784	Cytoplasmic	Potential regulator of CDK5 activity. May be involved in cell proliferation
EPHB6	↓ 5.953	Nuclear	Modulates cell adhesion and migration
SLC6A6	↓ 4.671	Cytoplasmic	Required for the uptake of taurine
MYL9	↓ 4.372	Nuclear	Regulation of both smooth muscle and non-muscle cell contractile activity via its phosphorylation.
CKS2	↓ 3.631	Cytoplasmic	Important in cell cycle regulation
NCAPD2	↓ 3.601	Cytoplasmic	Regulatory subunit of the condensin complex, which converts interphase chromatin into mitotic-like condensed chromosomes.

4.3.4 Amino Acid Sensing and Autophagy

FTO has been shown to be regulated by nutrient availability, in particular essential amino acids (Cheung *et al*., 2013). It has also been shown to be involved in mTORC1 signalling in response to amino acid status (Gulati *et al*., 2013). Much of the regulation in this pathway is controlled by protein phosphorylation, and so would not be detected by SILAC. I therefore decided to examine phosphorylation status of several proteins involved in the mTORC1 signalling pathway and nutrient sensing.

In C2C12 cells protein was collected at 24 hours after *Fto* knockdown (**Figure 4.9**). FTO expression levels are significantly lower, 22.44 % in cells treated with *Fto* siRNA compared with control treated cells (P=0.0064). Protein levels of total P70S6K, total S6, ACC-phospho, and SIRT1 were not significantly different in control versus *Fto* siRNA treated cells. Levels of P70S6K-phosphorylation, which indicate mTORC1 activation in the presence of amino acids, were significantly higher compared to ACTIN and total P70S6K (P=0.00058 and P=0.030 respectively). Total EIF2α was increased, although this was not significant (P=0.076) and EIF2α phosphorylation levels are increased relative to ACTIN, although again this was not significant (P=0.054). Phosphorylation of EIF2α occurs in the absence of amino acids, hypoxia, oxidative stress or dsRNA and turns off global translation. Increased phosphorylation in P70S6K and EIF2α suggest dysregulation in the amino acid sensing pathways (**Figure 4.9**).

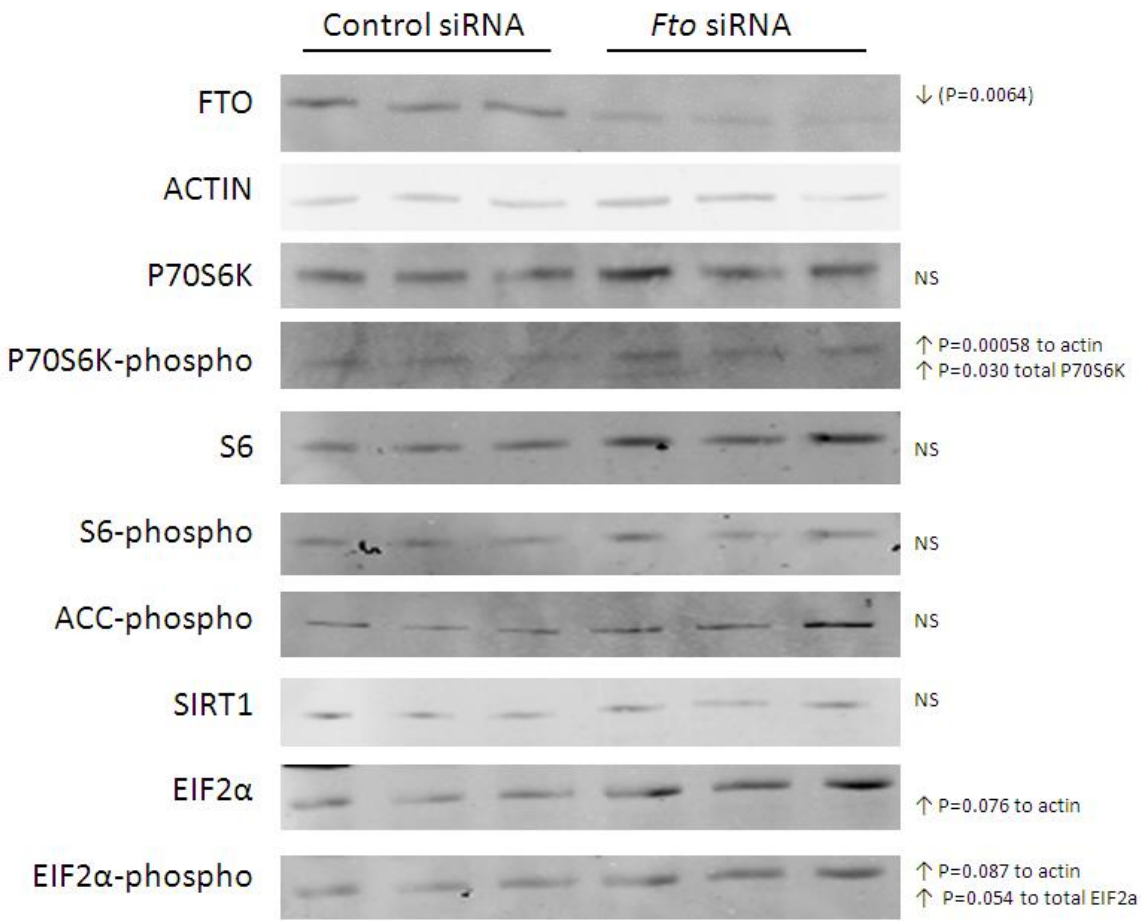

Figure 4.9 Immunoblots of Proteins involved in Amino Acid Regulatory Pathways in control and *Fto* siRNA treated C2C12s. One representative blot for ACTIN and FTO is shown. Band Intensity analysed using Odyssey Sa Analysis Software, (LI-COR Biosciences, Cambridge, UK). Data analysed by student's t-test *P<0.05, **P<0.01, ***P<0.001. NS, not significant. Details of Antibodies used are in **Table 4.1**.

Protein was also extracted for analysis from wild-type and *Fto*$^{-/-}$ MEFs (**Figure 4.10**). FTO protein was not detected in the *Fto*$^{-/-}$ MEFs. No significant difference was detected in levels of total EIF2α, EIF2α-phospho, STAT3-phospho, total S6, total P70S6K, P70S6K-phospho, or total MTOR. Phosphorylation of S6 showed a trend for increased levels relative to total S6 (P=0.0597) but not to ACTIN levels (P=0.941).

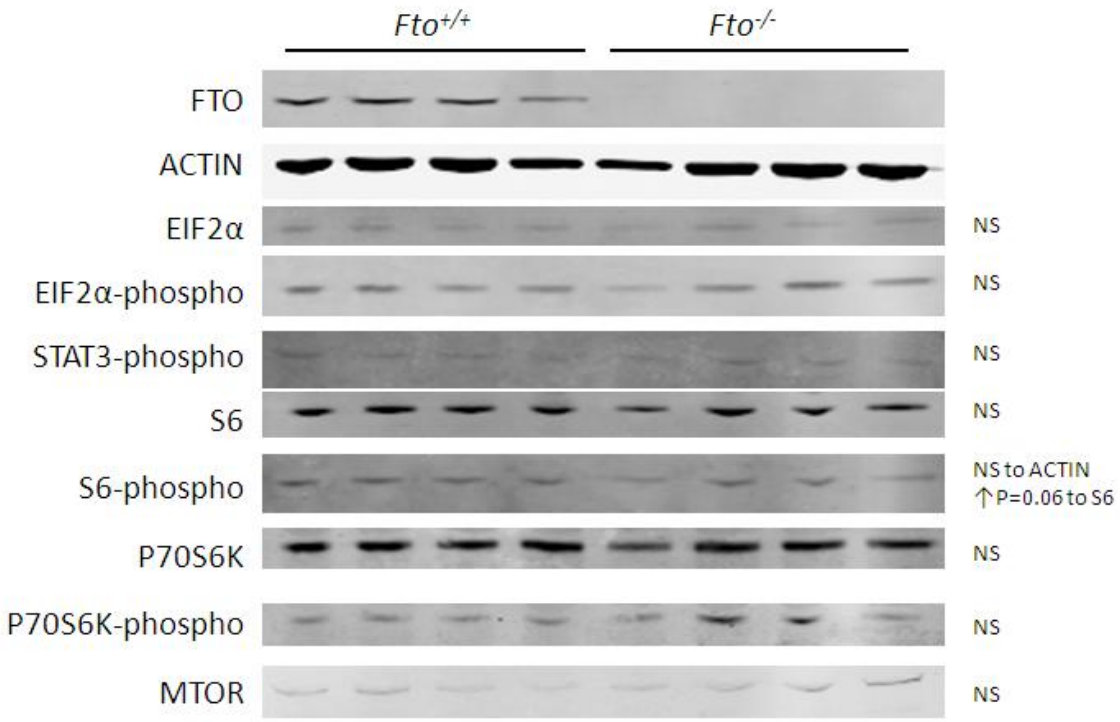

Figure 4.10 Immunoblots of Proteins involved in Amino Acid Regulatory Pathways in control and *Fto*$^{+/+}$ and *Fto*$^{-/-}$ MEFs. One representative blot for ACTIN and FTO is shown. Band Intensity analysed using Odyssey Sa Analysis Software, (LI-COR Biosciences, Cambridge, UK). Data analysed by student's t-test *P<0.05, **P<0.01, ***P<0.001. NS, not significant. Details of Antibodies used are in **Table 4.1**.

4.3.5 FTO KO Pups have Increased Postnatal Lethality

It has been previously noted that *Fto*$^{-/-}$ pups have reduced survival compared to wild-type littermates, despite being born at Mendelian ratios (Fischer *et al*., 2009, Gao *et al*., 2010, McMurray *et al*., 2013). This suggests that the effects of FTO deficiency manifest shortly after birth. I wanted to investigate the early phenotype to try and shed more light on their increased postnatal-death.

Several matings were set up and pups collected when found at P0-P2, pups were weighed and culled and blood plasma was collected for glucose and insulin measurements. Forty-three pups were analysed in the study and the different genotypes were present in a normal distribution (Chi squared equals 1.372 with 2 degrees of freedom, P=0.5036, **Figure 4.11A**). From the 14 *Fto*$^{-/-}$pups analysed four were found dead and an additional pup which was close to death; therefore by P2 we

are seeing 35.7 % lethality of *Fto*$^{-/-}$ pups (5/14). In addition to this one heterozygous pup was found dead (1/20), but no wild-type pups were found dead (0/9).

A

Genotype	Observed	Expected
Fto+/+	9	10.75
Fto+/-	20	21.5
Fto-/-	14	10.75
Total	43	43

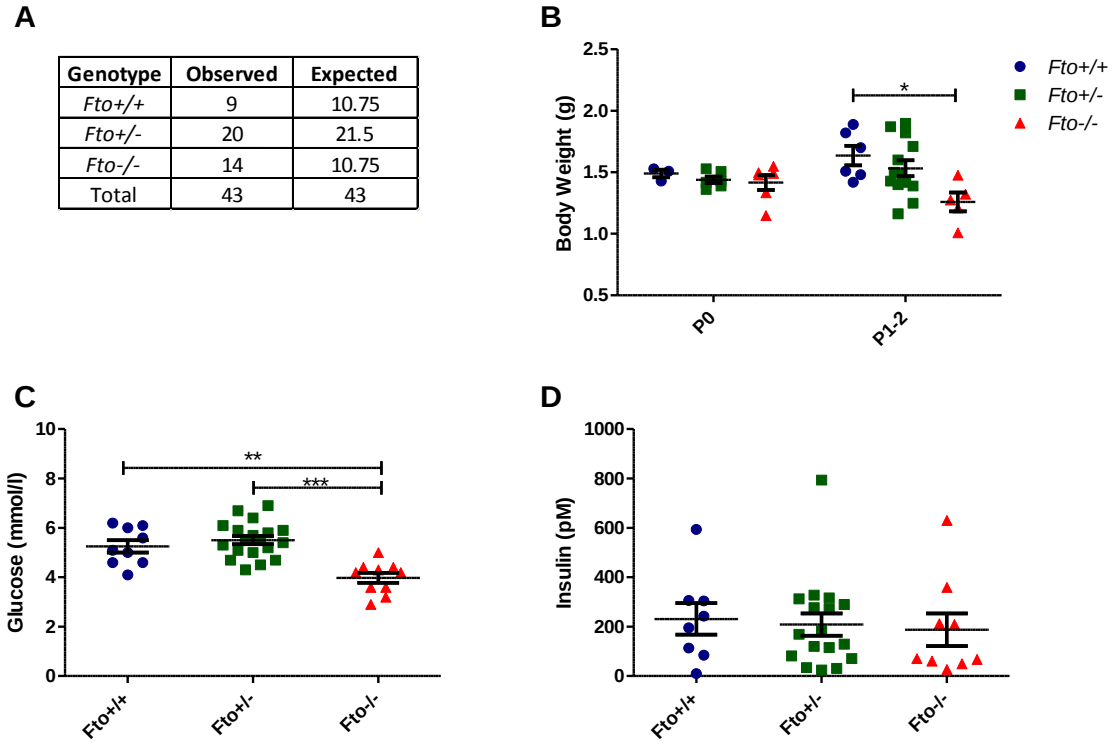

Figure 4.11 *Fto*$^{-/-}$ pups have reduced blood glucose, and reduced body weight after P1. A The number of pups of each genotype observed, and the number expected by Mendelian Ratio. **B** Body weight of pups at P0 and P1-2 when litters were spotted. **C** Blood glucose levels of *Fto*$^{+/+}$ (n=9) *Fto*$^{+/-}$ (n=19) *Fto*$^{-/-}$ (n=10) pups at P0-P2, pups had milk spots. **D** Plasma insulin of *Fto*$^{+/+}$ (n=8) *Fto*$^{+/-}$ (n=17) *Fto*$^{-/-}$ (n=9) pups at P0-P2, pups had milk spots. Data analysed by one-way ANOVA *P<0.05, **P<0.01, ***P<0.001. Data shown as mean ± SEM.

Body weight was measured when pups were culled, at P0 there was no significant difference between the genotypes (**Figure 4.11B**), but at P1-2 *Fto*$^{-/-}$ pups weighed significantly less than wild-type littermates (P=0.0225, **Figure 4.11B**). Pups were grouped in this way as it was difficult to differentiate between P1 or P2, when the dam littering was missed.

Blood glucose and insulin were measured when the pups were culled (**Figure 4.11C,D**). Blood glucose was significantly lower in *Fto*$^{-/-}$ pups than in wild-type or heterozygous littermates, although insulin levels did not differ significantly.

4.3.6 FTO Effects Cilia Formation and WNT signalling

One of the proteins highly upregulated in the *Fto* knockdown C2C12 cells was GSK3β (**Table 4.4**). Inspection of the SILAC data revealed that several proteins were differentially regulated in the WNT-β-CATENIN signalling pathway (**Figure 4.12**). The protein β-CATENIN was identified as a unique hit in the cytoplasmic fraction of *Fto* knockdown C2C12 cells; this suggests that it is present here in high levels, so it may be undergoing proteasome degradation.

This supported work by a collaborator, which suggests that FTO antagonises WNT signalling and leads to developmental defects in zebrafish associated with ciliopathies (Osborn, DPS *et al*, manuscript in preparation). I decided to investigate signs of cilia defects in the $Fto^{-/-}$ mice.

Casual observation of the $Fto^{-/-}$ mice by Chris Church and me during the years working with them would suggest that they do not suffer with *situs inversus* or any obvious malformations other than their short stature; however we have not examined this thoroughly. A wild-type and a $Fto^{-/-}$ female mouse at 24 weeks of age were analysed by the necropsy team at MRC Harwell, however no differences were observed in tissue structure or morphology (data not shown). As 40-50 % of $Fto^{-/-}$ pups do not make it to weaning this may suggest that it is the more severely affected animals which die postnatally. We then investigated the heads, lungs and kidneys of P0 pups (one wild-type and five $Fto^{-/-}$) but found no significant differences (data not shown).

Timed matings were set up to examine the morphology of the $Fto^{-/-}$ pups at E15.5. None of the dissected pups displayed left-right patterning abnormalities. Tissues were collected and cilia examined using immunohistochemistry for acetylated-TUBULIN, gamma-TUBULIN, and IFT88 in collaboration with Sonia Christou-Savina and Daniel Osborn at the Institute of Child Health, UCL. Cells in the Choroid plexus, where cerebrospinal is produced, appear less ciliated and the cilia present are shorter in $Fto^{-/-}$ mice, when examined with the acetylated-TUBULIN and IFT88 (**Figure 4.13A,B**). The psuedostratified cilia in the nasopharynx also appear shorter, and have fewer motile bundles (**Figure 4.13C**). In the cochlea the cilia appear unperturbed (**Figure 4.13D**), however the primary cilia lining the kidney ducts were shorter in $Fto^{-/-}$ mice (**Figure 4.13E**).

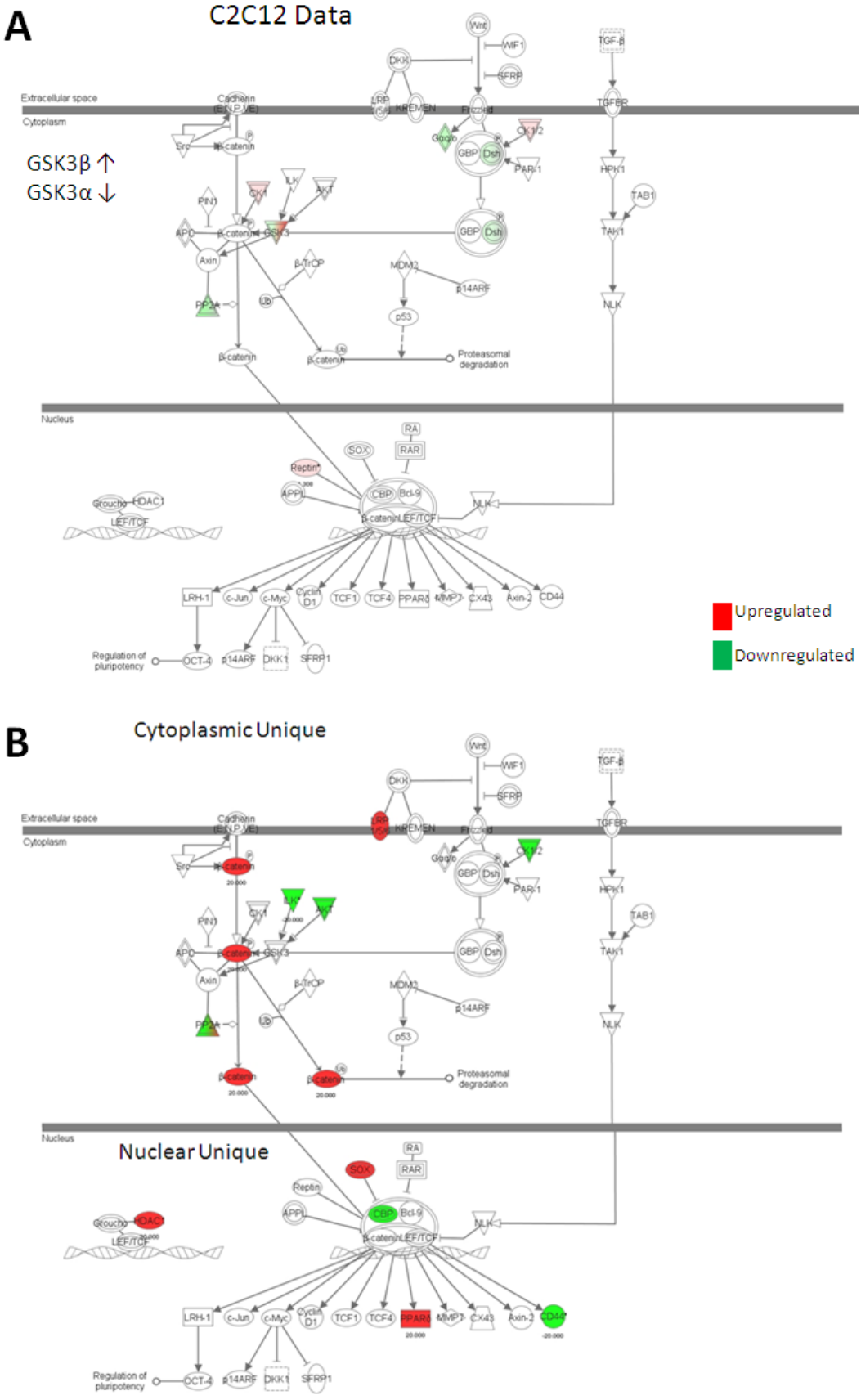

Figure 4.12 Protein changes following 24 hours of *Fto* knockdown in C2C12 cells in WNT and β-CATENIN signalling pathways. Data analysed and pathways drawn by IPA, Ingenuity Software. Red is upregulated and green in downregulated with the intensity of colour reflecting the level of change. **A** Changes in the proteins after 24 hours of *Fto* knockdown. **B** Unique hits in either the control or *Fto* knockdown C2C12 cell in the cytoplasmic and nuclear fractions.

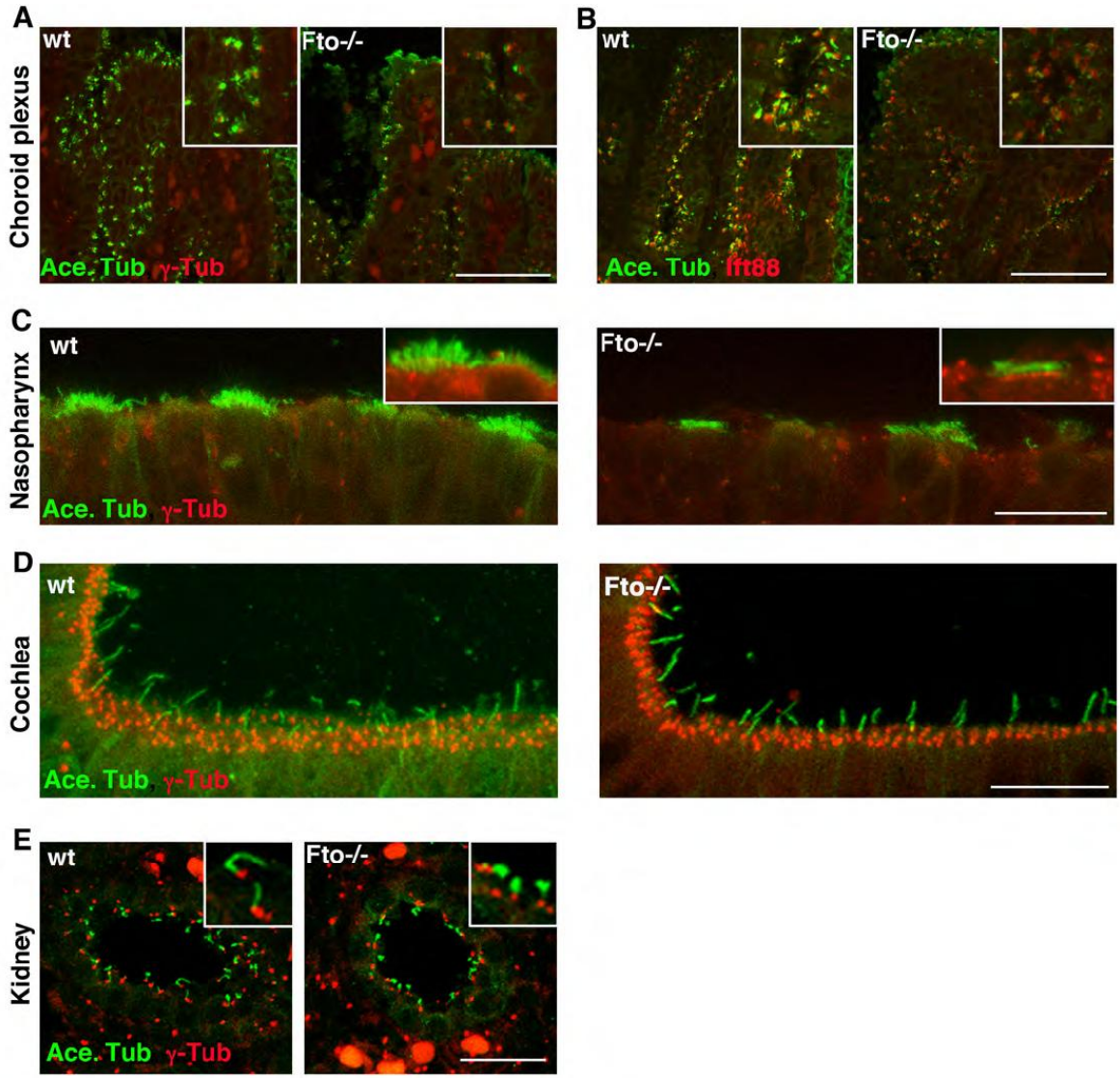

Figure 4.13 E15.5 *Fto*$^{-/-}$ mouse embryos display tissue specific cilia defects. Whole mount sections from wild-type and *Fto*$^{-/-}$ animals showing immunolocalisation of acetylated-α tubulin (green)and γ-tubulin or IFT88 (red) in the choroid plexus (**A**,**B**); nasopharynx (**C**); cochlea (**D**); kidney (**E**). Loss of FTO results in shortened cilia in the choroid plexus, nasopharynx and kidney whilst cilia in the cochlea appear unperturbed. Scale bars: **A**,**B** 50 μm; **C**,**D**,**E** 20 μm. I collected and prepared the tissues, Daniel Osborn and Sonia Christou-Savina, at the UCL Institute of Child Health, performed the immunohistochemistry and imaging.

I then decided to examine the primary cilia on the *Fto*$^{-/-}$ and FTO overexpression MEFs to see if these showed any abnormal morphology. Examination of *Fto*$^{-/-}$ MEFs revealed more cells had no cilium present (P=0.00136) and that more cilia were classified as short compared to the cilia found on *Fto*$^{+/+}$ MEFs (P=0.00.166, **Figure 4.14A,B**). No significant differences were observed between FTO-2 and FTO-4 MEF cilia (**Figure 4.14A,C**).

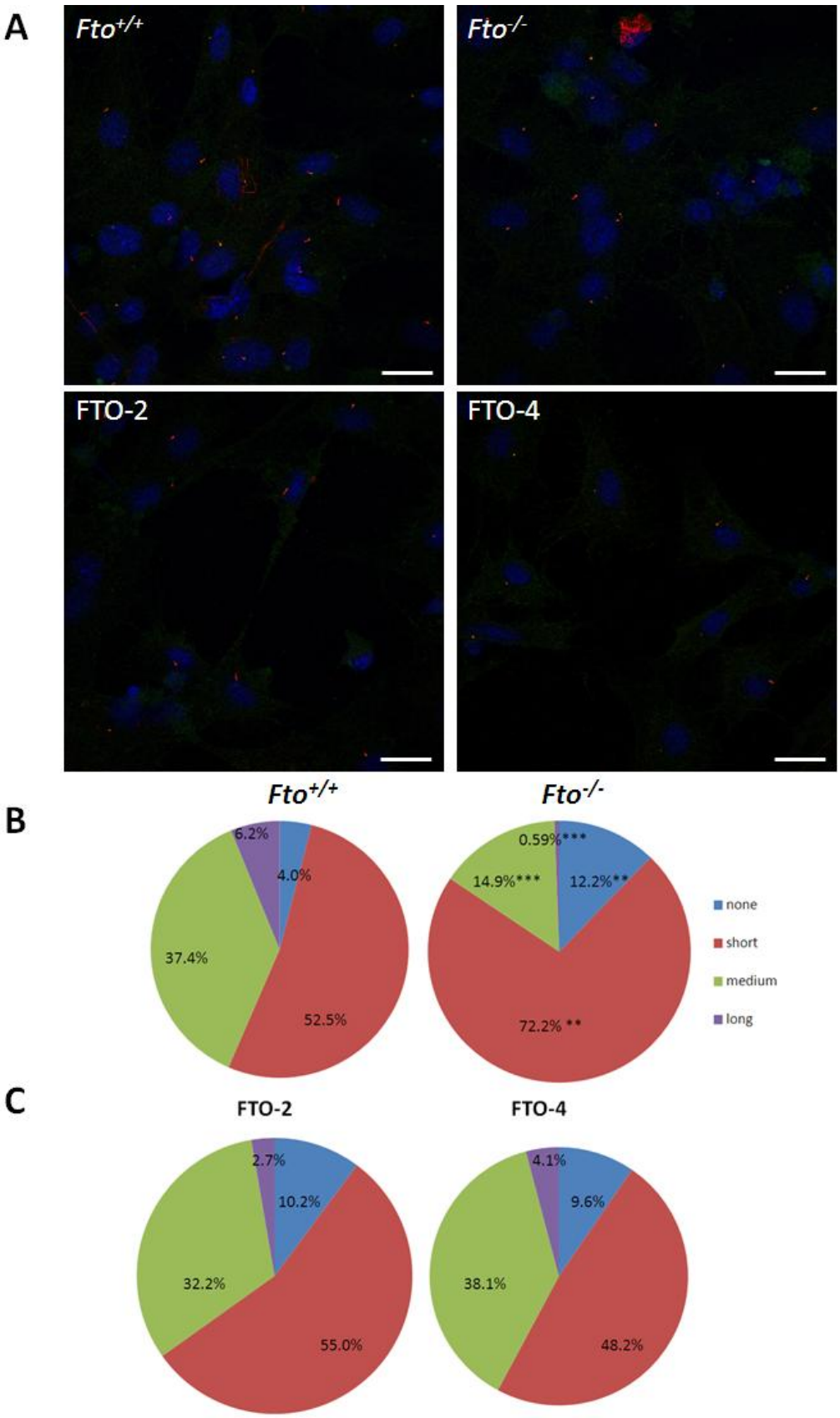

Figure 4.14 Assessment of Cilia Length of FTO$^{+/+}$, FTO$^{-/-}$, FTO-2 and FTO-4 MEFs. A Immunocytochemistry showing immunolocalisation of acetylated-α tubulin (red) and γ-tubulin (green) and nuclei (Hoechst 33342) in FTO$^{+/+}$, FTO$^{-/-}$, FTO-2 and FTO-4 MEFs, Scale bars: 20 μm. **B** Percentage of cilia present at different length from n=10 randomly selected areas of each genotype; none – nuclei present but no cilium stained; short (1-4 μm) medium (4-8 μm) and long (>8 μm). Data analysed by student's t-test *P<0.05, **P<0.01, ***P<0.001.

4.3.7 FTO Alters Adipogenic Differentiation

Global *Fto*$^{-/-}$ mice have reduced body weight, and reduced fat and lean mass compared with wild-type littermates (Fischer *et al*., 2009, McMurray *et al*., 2013). Adipocyte size is also significantly reduced in the *Fto*$^{-/-}$ mice (Fischer *et al*., 2009). Mice which express two additional copies of FTO weigh significantly more than wild-type littermates, and have significantly increased fat mass with increased adipocyte size (Church *et al*., 2010). As WNT signalling and Cilia play important roles in development and differentiation of cells I decided to investigate the adipogenic potential of *Fto*$^{-/-}$ and FTO overexpression MEFs.

Cells of each genotype were grown in triplicate in 6-well plates, when confluent cells were treated with differentiation media as described in Chapter 2 materials and methods, **Section 2.5.2a**. Oil red O staining was used to visualise neutral lipids present in the cells (**Figure 4.15**) and haematoxylin to stain nuclei of cells present. Visual eye assessment and microscopy at x0.71 magnification showed less oil red O staining in *Fto*$^{-/-}$ MEFs and in FTO-4 MEFs compared to their wild-type controls (**Figure 4.15**) and at x10 magnification it was observed that the adipocytes appear morphologically similar between the genotypes and that a large number of undifferentiated cells are also present. Quantification of the areas of differentiated cells (red stained cells) showed that significantly less adipocytes were formed in both *Fto*$^{-/-}$ and FTO-4 MEFs compared to the wild-type MEFs (**Figure 4.16A,B**).

Separate plates run in parallel were used for RNA extraction from the MEF cells before and after differentiation. Gene expression was then analysed using Real-time qPCR, examining a selection of genes involved in adipogenesis, WNT/β-CATENIN signalling and metabolism. In wild-type and *Fto*$^{-/-}$ MEFs before differentiation (**Figure 4.17A**) we found that *Fto* expression was significantly lower in the *Fto*$^{-/-}$ MEFs (P=0.0145). A truncated *Fto* transcript is still expressed in these *Fto*$^{-/-}$ MEFs which we believe to be broken down by nonsense-mediated decay, and is not translated, but is detectable by qPCR.

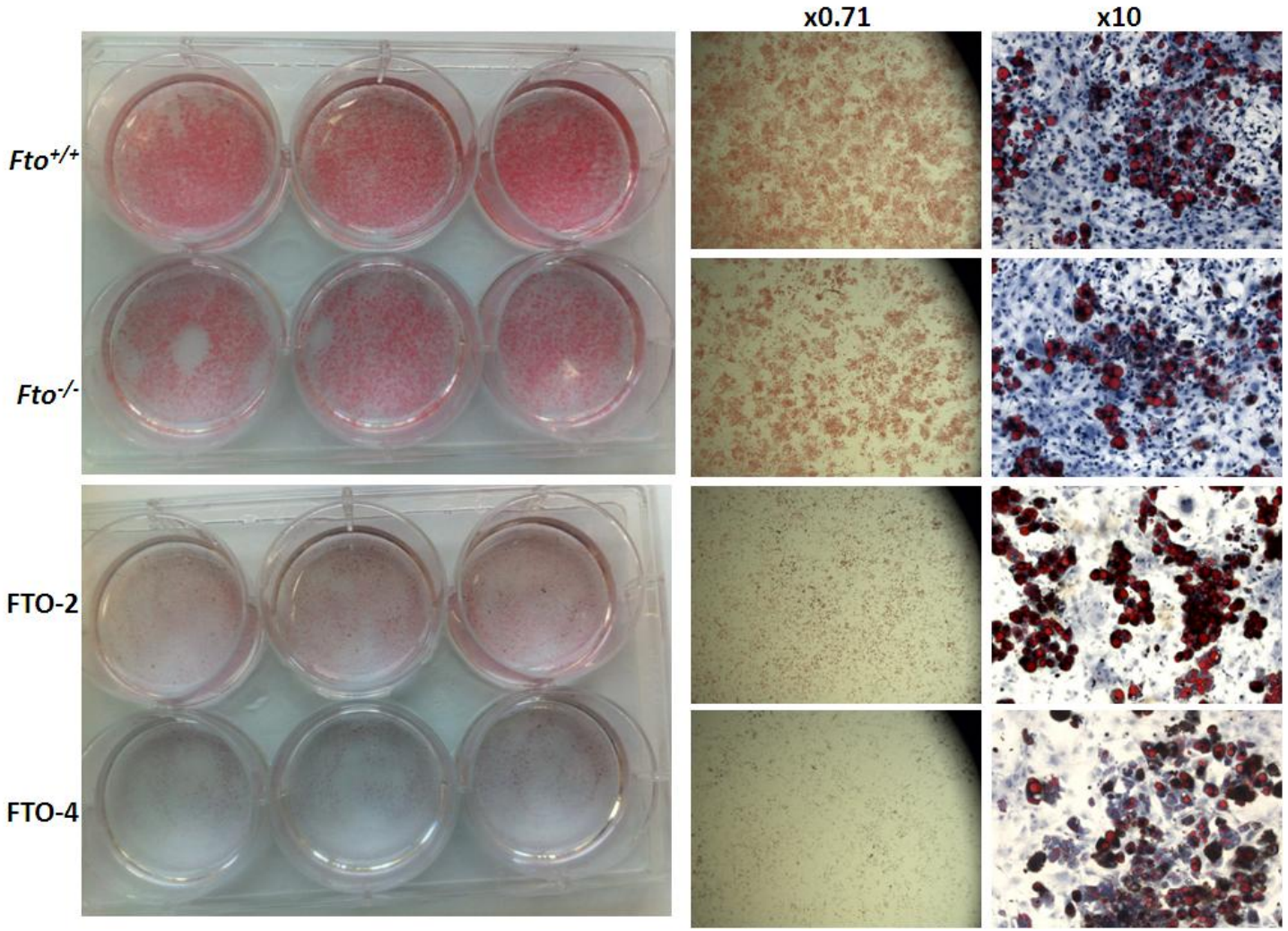

Figure 4.15 Reduced Adipogenic Differentiation of MEFs in FTO knockout and FTO Overexpression MEFs. MEFs of each genotype were allowed to differentiate for ten days. Adipocytes were then stained with Oil Red O (red) to establish the levels of differentiation (imaged in plates and at x0.71). Cells were then stained with haematoxylin to visualise all cells present in the dish (x10).

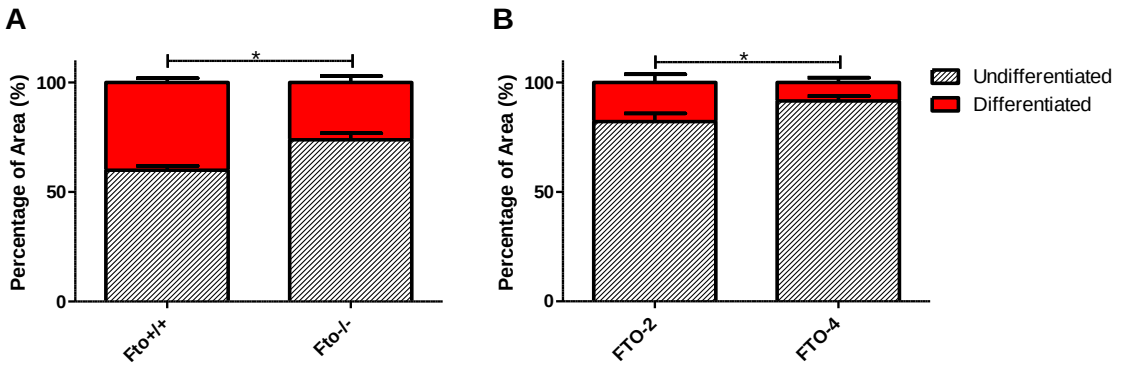

Figure 4.16 Percentage of FTO Knockout and FTO Overexpression MEFs staining with Oil Red O after adipogenic differentiation. Images at x0.71 (n=3 per genotype) were analysed by Volocity Imaging Software (Perkin Elmer, Massachusetts, U.S.A) Data analysed by student's t-test *P<0.05, **P<0.01, ***P<0.001. Data shown as mean ± SEM.

Along with a decrease in *Fto*, *Adipoqr2* and *Srebf1*are expressed at significantly lower levels in *Fto*$^{-/-}$ MEFs (P=0.0312 and P=0.0176 respectively). Expression of *Vegfa* is nearly significantly lower (P=0.0531) and *Mmp2* expression is significantly increased (P=0.00338). *Lep* which is only expressed in adipocytes was undetectable in the undifferentiated MEFs, and *Pck-1* was undetectable in undifferentiated *Fto*$^{-/-}$ MEFs (**Figure 4.17A**).

In differentiated wild-type and *Fto*$^{-/-}$ MEFs (**Figure 4.17B**), *Fto* was expressed at significantly lower levels than wild-type MEFs (P=6.8E-5). None of the other genes investigated were downregulated, however the *Fto*$^{-/-}$ MEFs had significantly higher expression levels of *Acadl*, *Cpt1a*, *Cpt1b*, *Lep*, *Mmp2*, *Pck-1* and *Srebf1*than wild-type littermate control MEFs.

When comparing gene expression levels pre- and post-differentiation (**Figure 4.17C**), *Adipoq*, *Adipoqr2*, *Cd36*, *Cebpa*, *Cpt1b*, *Lpl*, *Pck-1*, *Pparg*, *Scd1*, *Srebf1* and *Vegfa* are upregulated following differentiation for both genotypes. *Cdh1*, *Cpt1a*, and *Fto* are expressed at lower levels following differentiation.

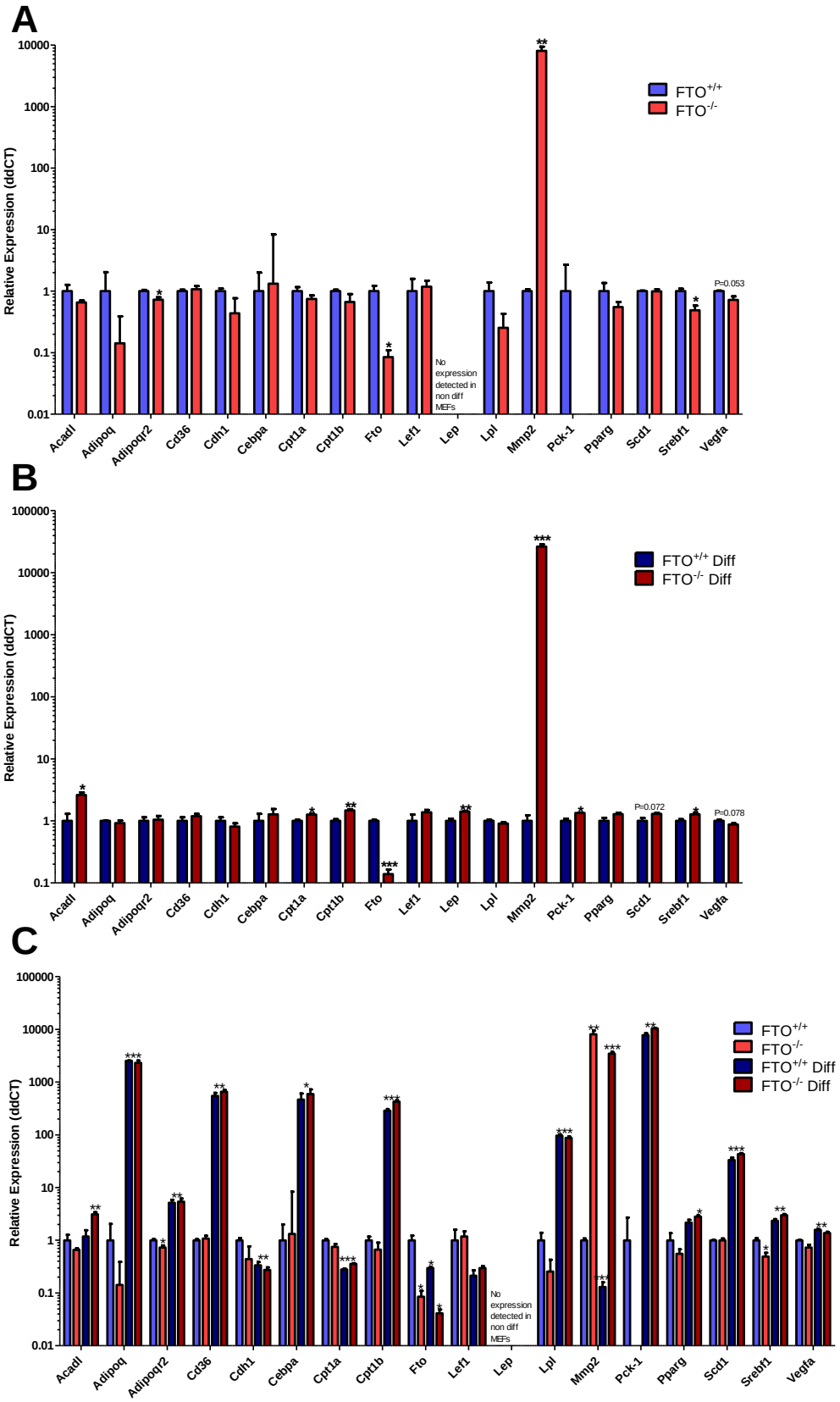

Figure 4.17 Relative gene expression in FTO$^{-/-}$ and FTO$^{+/+}$ differentiated and undifferentiated MEFs. Gene expression in undifferentiated **A**, and differentiated **B** FTO$^{+/+}$ and FTO$^{-/-}$ MEFs, **C** data combined in comparison to FTO$^{+/+}$ undifferentiated (n=3 per group) relative to *Gapdh* (2^ddCT). For abbreviations please see **Table 4.2**. Data analysed by student's t-test *P<0.05, **P<0.01, ***P<0.001. Data expressed as mean ± SEM.

The same genes were also analysed in FTO-2 and FTO-4 MEFs pre- and post-adipogenic differentiation (**Figure 4.18**). Analysis reveals that *Fto* is expressed at 3.6 times the level in FTO-4 compared with FTO-2 MEFs (P=0.000143, **Figure 4.18A**). Significantly higher levels of *Lef1* and *Pck-1* were also seen in FTO-4 MEFs (P=6.02E-5, and P=0.00161 respectively), whilst *Acadl, Adipoq, Adipor2, Cd36, Cdh1, Cebpa, Lpl, Pparg, Scd1* and *Srebf1* were expressed at significantly lower levels. In undifferentiated cells expression of *Lep* was not detected.

Post-differentiation *Fto* levels were significantly higher in FTO-4 MEFs (P=0.000269, **Figure 4.18B**). Expression of *Cd36, Cdh1, Cpt1b, Lef1, Lep, Lpl, Pck-1, Pparg* and *Scd1* was lower in the FTO overexpression MEFs (**Figure 4.18B**).

Similar genes are altered following differentiation in the FTO-2 and FTO-4 MEFs (**Figure 4.18C**). Increased expression of *Adipoq, Adipoqr2, Cd36, Cebpa, Cpt1b, Lpl, Pck-1, Scd1* and *Vegfa* are again seen in both FTO-2 and FTO-4 MEFs post-differentiation, with decreased levels of *Cdh1*, and *Lef1*. However unlike before we see no significant difference in *Cpt1a* expression and there are significantly lower levels of *Pparg* and *Srebf1* being expressed post-differentiation (**Figure 4.17C**, **Figure 4.18C**).

Table 4.5 summarises the significant gene expression changes in the *Fto* knockout and FTO overexpression MEFs compared with their wild-type controls. Genes which are differentially regulated between the $Fto^{-/-}$ and FTO-4 MEFs pre-adipogenesis are *Fto* and *Vegfa*. Pre-adipogenesis *Adipoqr2* and *Srebf1* are both downregulated in $Fto^{-/-}$ and FTO-4 MEFs compared to controls. In differentiated MEFs *Fto, Cpt1b, Lep* and *Pck-1* are differentially regulated in $Fto^{-/-}$ and FTO-4 MEFs.

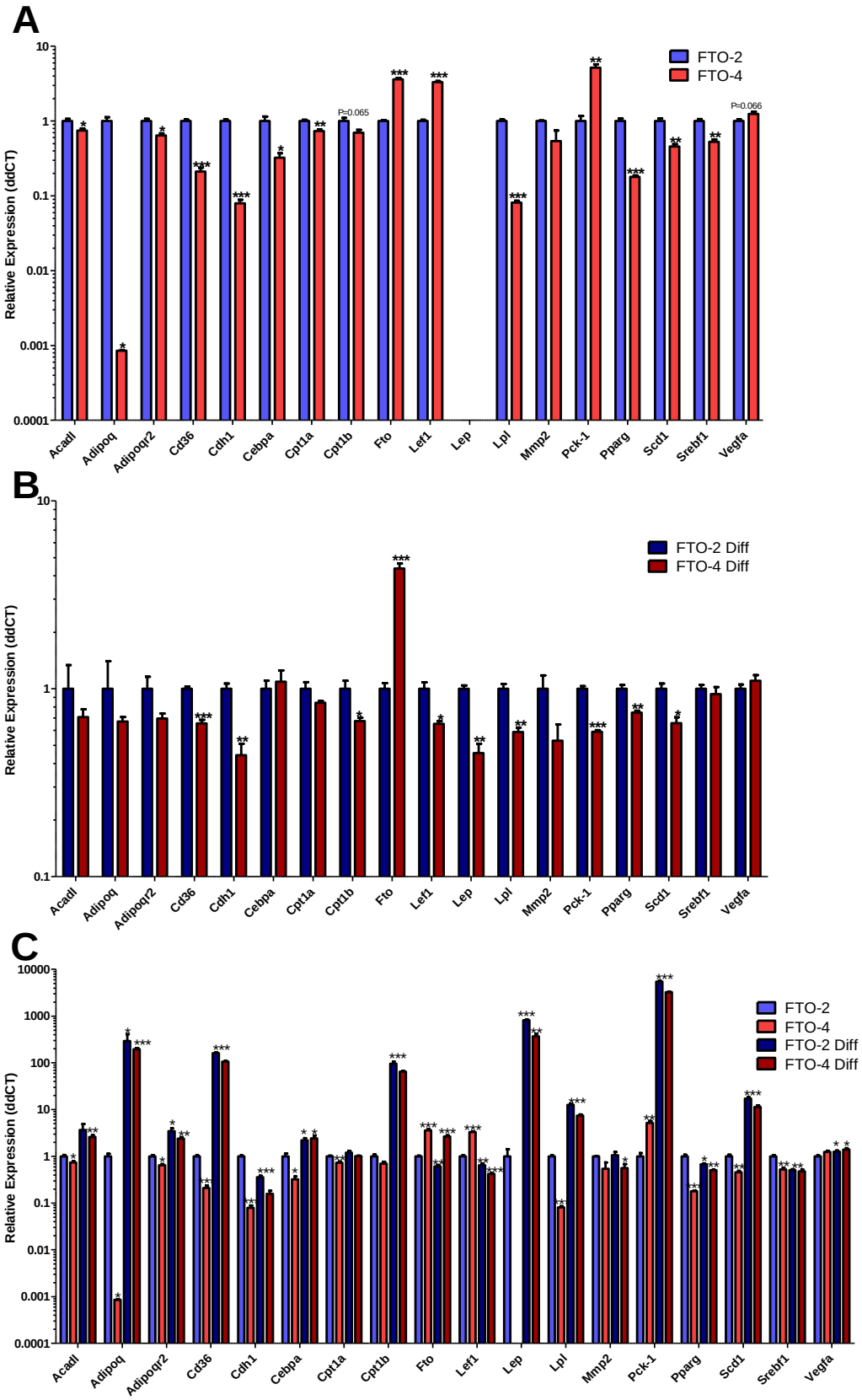

Figure 4.18 Relative gene expression in FTO-2 and FTO-4 differentiated and undifferentiated MEFs. Gene expression in undifferentiated **A**, and differentiated **B** FTO-2 and FTO-4 MEFs, **C** data combined in comparison to FTO-2 undifferentiated (n=3 per group) relative to *Gapdh* (2^ddCT). For abbreviations please see **Table 4.2**. Data analysed by student's t-test *P<0.05, **P<0.01, ***P<0.001. Data expressed as mean ± SEM.

Table 4.5 Summary of Gene Expression Differences in undifferentiated and differentiated FTO Knockout and FTO Overexpression MEFs. NS – not significant. Data analysed by student's t-test *P<0.05, **P<0.01, ***P<0.001.

mRNA	$FTO^{+/+}$ vs. $FTO^{-/-}$	FTO-2 vs. FTO-4	diff $FTO^{+/+}$ vs. diff $FTO^{-/-}$	diff FTO-2 v diff FTO-4
Acadl	NS	↓ (*)	↑ (*)	NS
Adipoq	NS	↓ (*)	NS	NS
Adipoqr2	↓ (*)	↓ (*)	NS	NS
Cd36	NS	↓ (***)	NS	↓ (***)
Cdh1	NS	↓ (***)	NS	↓ (**)
Cebpa	NS	↓ (*)	NS	NS
Cpt1a	NS	↓ (**)	↑ (*)	NS
Cpt1b	NS	↓ (P=0.065)	↑ (**)	↓ (*)
Fto	↓ (*)	↑ (***)	↓ (***)	↑ (***)
Lef1	NS	↑ (***)	NS	↓ (*)
Lep	-	-	↑ (**)	↓ (**)
Lpl	NS	↓ (***)	NS	↓ (**)
Mmp2	↑ (**)	NS	↑ (***)	NS
Pck-1	-	↑ (**)	↑ (*)	↓ (***)
Pparg	NS	↓ (***)	NS	↓ (**)
Scd1	NS	↓ (**)	↑ (P=0.072)	NS
SREBF1	↓ (*)	↓ (**)	↑ (*)	NS
Vegfa	↓ (P=0.053)	↑ (P=0.066)	↓ (P=0.078)	NS

4.4 Discussion

4.4.1 Summary

FTO is expressed in the nucleus, but some expression can be seen in the cytoplasm in cells which overexpress FTO. When *Fto* is knocked down in C2C12 cells proliferation is decreased, however we have not been able to show that proliferation is decreased in *Fto*$^{-/-}$ MEFs. We were able to see decreased mRNA translation in *Fto*$^{-/-}$ MEFs, when 2 μM puromycin was used for labelling, replicating the results of Gulati and colleagues (Gulati *et al*., 2013). Using SILAC I have been able to observe protein expression differences in control and *Fto* knockdown C2C12 cells, most notably in protein synthesis, cell cycle and RNA trafficking pathways.

I have been able to replicate the increased postnatal lethality in the *Fto*$^{-/-}$ mice (Fischer *et al*., 2009, Gao *et al*., 2010, McMurray *et al*., 2013), and I have also observed that the *Fto*$^{-/-}$ mice have significantly decreased plasma glucose compared to wild-type and heterozygous littermates.

Finally *Fto* may play a role in WNT/β-CATENIN signalling. We have observed protein expression differences in this pathway using SILAC. We have also observed aberrant cilia formation in *Fto*$^{-/-}$ mice at E15.5 in the choroid plexus, nasopharynx and kidney. I then went on to show that *Fto*$^{-/-}$ MEFs also have increased short or absent primary cilia compared to wild-type controls. FTO overexpression and *Fto*$^{-/-}$ MEFs form less adipogenic cells when differentiated and have alterations in gene expression pathways involved in WNT/β-CATENIN signalling, adipogenesis and cellular metabolism.

4.4.2 FTO localisation

It has been shown that FTO is ubiquitously expressed and is localised to the cell nucleus, using transfection of a YFP-tagged FTO (Gerken *et al*., 2007), and in tissue using an in house generated antibody (McTaggart *et al*., 2011). Fractionation of cells used for immunoblotting has suggested that there may be some cytoplasmic expression of FTO (Gulati *et al*., 2013) and one study suggests

that FTO is expressed in the cytoplasm in response to fasting (Vujovic *et al*., 2013) although this opposes the study of McTaggart and colleagues.

I did not examine the effect of nutritional status in my MEF experiments, however my results indicate that FTO expression is absent in *Fto*$^{-/-}$ cells and higher protein levels are present in overexpression MEFs (**Figure 4.1**, **Figure 4.2**). The antibody does appear to have some unspecific binding to other targets at low levels (as seen in **Figure 4.3**). I do not believe that this is FTO as immunoblots using the same cells at a later passage did not have FTO protein present (**Figure 4.6** and **Figure 4.10**).

FTO does appear to be expressed in the cytoplasm of FTO-4 MEFs. This could be due to the excessive amount of protein being degraded, or perhaps this has uncovered a role for FTO in the cytoplasm which can be more easily seen when high levels of the protein are present. Gerken and colleagues transfected cells with FTO tagged with YFP and under the control of a T7 and SP6 RNA polymerase promoters, which is not as strong as the CAGGs promoter in the FTO-4 cells [chicken β-actin promoter/enhancer coupled with the cytomegalovirus (CMV) immediate-early enhancer (Church *et al*., 2010)] which maybe why they do not see cytoplasmic FTO.

4.4.3 Amino Acid sensing

Work from the group of Prof. Giles Yeo suggests that FTO expression is controlled by amino acid availability, and that FTO is involved in coupling amino acid sensing to mTORC1 signalling (Cheung *et al*., 2013, Gulati *et al*., 2013).

I do see decreased cell proliferation in C2C12 cells treated with *Fto* siRNA, but I could not replicate the results of Gulati and colleagues using *Fto*$^{-/-}$ MEFs (Gulati *et al*., 2013). The assay I carried out uses calcein. Calcein is transported through the membrane by live cells, once inside intracellular esterases remove the acetomethoxy group, trapping the molecule inside and emitting a strong green fluorescence, dead cells lack active esterases, so only live cells are labelled. To stain dead cells I used ethidium homodimer, which can stain all dead or dying cells, as they have

compromised cell membranes. This is advantageous over TUNEL staining which only stains cells which have undergone programmed cell death. The assay used by Gulati and colleagues measures cellular metabolic activity via NAD(P)H-dependent cellular oxidoreductase enzymes (Gulati *et al*., 2013). Metabolic rate and oxygen consumption have been previously shown to be tightly regulated by mTOR activity (Schieke *et al*., 2006, Cunningham *et al*., 2007). It is therefore surprising that they do not see a significant difference until 120 hours, as they have shown disruption in the mTORC1 signalling pathway in the absence of FTO (Gulati *et al*., 2013).

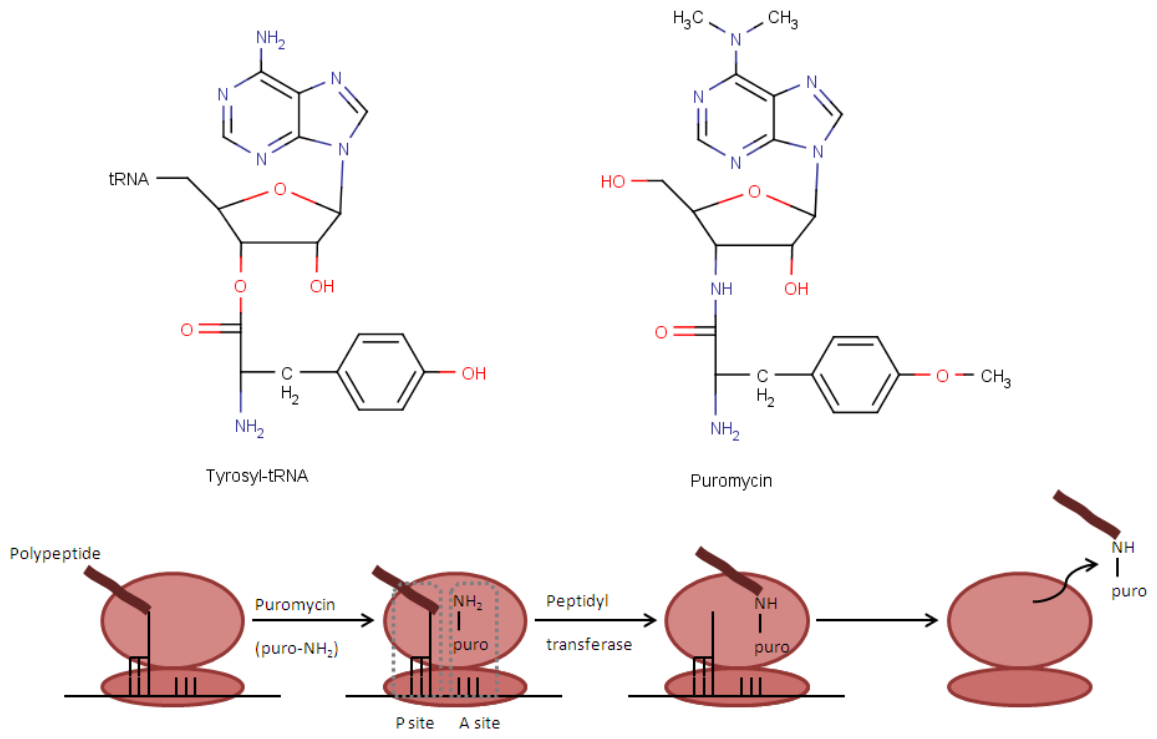

Figure 4.19 Puromycin Incorporation into developing polypeptide chains. Part of the Puromycin molecule resembles the 3' end of the aminoacylated tRNA. It can enter the A site in the ribosome and transfers to the growing polypeptide chain, causing the formation of a puromycylated nascent chain and premature chain release.

Gulati and colleagues also suggest that *Fto*$^{-/-}$ MEFs have reduced levels of mRNA translation using a puromycin incorporation assay, this is outlined in **Figure 4.19**. They examined the effect of 2 μM puromycin for 5, 10 and 15 minutes. I initially repeated their assay using only 1 μM of puromycin and did not observe a clear difference in the *Fto*$^{-/-}$ cells, but there did appear to be lower levels in the FTO overexpression MEFs **Figure 4.6**. When I increased the dose to 2 μM I could still not

observe a clear difference **Figure 4.7**. I proceeded by carrying out the assay in triplicate and then using dot-blots to quantify the amount of protein labelled with puromycin, and correct for protein level using ACTIN. I could not see a significant difference between wild-type and knockout cells at 1 or 2 μM although there was a trend for decreased puromycin incorporation in *Fto*$^{-/-}$ MEFs treated with 2 μM puromycin. It is interesting that a higher dose of puromycin appears to effect the *Fto*$^{-/-}$ MEFs whilst a lower dose does not, suggesting that the *Fto*$^{-/-}$ cells may be more sensitive to the increased levels of puromycin. In *E.coli* several nucleotides of the 23S rRNAs (A2439, G2505, G2553) showed altered chemical reactivities in the presence of puromycin (Rodriguez-Fonseca *et al*., 2000), and some rRNA nucleotides may be potentially modified by methylation [2-meG-1835, 5-meC-1962, 6-meA-2503, and 2-meG at one of positions 2445-2447 (Smith *et al.*, 1992)]. Sites of modification in *E.coli* are not necessarily conserved in yeast or higher eukaryotes, and the process in which these modifications occur is not fully understood (Smith *et al*., 1992). Methylation of bases in rRNA does occur in eukaryotes, the majority are 2′-O-ribose substituents, but human RNA does include a 6-meA in 18S and another in 28S (Maden and Hughes, 1997), how this methylation occurs and what function it plays is unknown, but these are highly conserved in eukaryotes (Maden and Hughes, 1997). Speculatively FTO could be involved with rRNA processing and methylation; this may alter translation levels, that may be more sensitive to high puromycin levels. Puromycin may also be taken up more readily by *Fto*$^{-/-}$ MEFs causing greater sensitivity and toxicity. It has previously been observed that different cells can be more sensitive to puromycin as well as other compounds, and it would be interesting to measure the uptake of different concentrations of puromycin in MEFs of each FTO genotype (Dudani *et al*., 1988).

I was also unsuccessful at replicating the altered amino acid signalling pathway differences. They show significantly decreased Phospho-S6 (Gulati *et al*., 2013). My results in C2C12 cells show a significant increase in Phospho-P70S6K, and the *Fto*$^{-/-}$ MEFs showed a trend for increased phosphorylation in relation to total S6 protein levels (**Figure 4.10**). Upon close inspection of their materials and methods they use the antibody I have used for Phospho-P70S6K, which I see significantly increased in C2C12 cells treated with *Fto* siRNA, which contradicts their results.

Increased levels of EIF2α phosphorylation in *Fto* knockdown C2C12 cells would indicate a decrease in protein synthesis, but suggests that the pathway involved may be ER-stress related (Palam *et al*., 2011). This change was not observed in *Fto*$^{-/-}$ MEFs. Gulati and colleagues deprived their cells of amino acids for 24 hours, which I have not done, and it would be interesting to see if this additional stress would allow me to replicate their results (Gulati *et al*., 2013).

The SILAC data does indicate that protein synthesis and gene expression is one of the highly effected networks when *Fto* is knocked down in C2C12 cells. Out of the 35 genes in this network 24 are downregulated suggesting a decrease in protein synthesis and gene expression in these cells. Many of the proteins involved in protein synthesis as well as other cellular functions are regulated by modifications such as phosphorylation. SILAC cannot provide information on protein modifications, but it can provide a list of differently regulated proteins of which the pathways involved can be investigated. Therefore some of the proteins we expect to play a role in protein synthesis may be aberrantly modified in C2C12 cells treated with *Fto* siRNA however our SILAC results would not include them. However, the SILAC results need to be validated on a protein by protein basis, and I am yet to successfully confirm these results.

4.4.4 FTO and Muscle

Lean mass in Global *Fto*$^{-/-}$ mice is significantly lower than in wild-type controls (Fischer *et al*., 2009, Gao *et al*., 2010, McMurray *et al*., 2013). The *Fto* adult KO mice also have significantly lower amounts of lean mass, although medio-basal hypothalamic deletion of *Fto* using AAV-Cre did not alter body weight or composition (McMurray *et al*., 2013). Skeletal muscle is the largest depot of protein in the body. Gulati and Yeo suggest that the loss of FTO expression may prevent cells from responding appropriately to amino acids, causing a decrease in protein synthesis and an increase in autophagy (Gulati and Yeo, 2013).

We see more of an effect in C2C12 cells which are treated with *Fto* siRNA than *Fto*$^{-/-}$ MEFs in terms of difference in live cell staining and EIF2α phosphorylation. This may be due to C2C12 cells being myoblasts and so may be more sensitive to FTO loss than fibroblasts. I would like to try

differentiating the MEFs into myoblasts to see if lack of FTO has any effect on their proliferation, gene expression and morphology.

4.4.5 Role of FTO in Development

FTO has been previously shown to effect development. Human patients with a catalytically null form of FTO which contains the R316Q mutation exhibit severe postnatal growth retardation, brain malformations, cardiac abnormalities and microcephaly, with lethality before three years of age (Boissel *et al*., 2009). This is more severe than the growth retarded phenotype, and increased postnatal lethality observed in *Fto*$^{-/-}$ mice (Fischer *et al*., 2009, Gao *et al*., 2010, McMurray *et al*., 2013).

In the short study I carried out I saw 35.7 % lethality in *Fto*$^{-/-}$ pups by P2, whereas this was only 5 % in *Fto*$^{+/-}$ mice, and no recorded deaths in the wild-type littermates. These *Fto*$^{-/-}$ mice were hypoglycaemic compared to littermates. This suggests that these mice have an underlying metabolic defect, but not hyperinsulinaemia as the *Fto*$^{-/-}$ mice do not have significantly increased insulin levels. It could be caused by a number of conditions such as fatty acid oxidation disorders, defects in ketone body utilisation/synthesis, carnitine deficiency, gluconeogenic disorders, glycogen storage disorders or defects in the transport of glucose (Arya *et al*., 2013). It would be interesting to investigate this observation further and identify the underlying cause, as this could be the cause of increased postnatal death in these animals.

Cilia defects are normally associated with developmental abnormalities, neurological problems and sometimes with obesity and hyperphagia as seen in patients with Bardet-Biedel Syndrome (BBS) and Alström Syndrome (Davenport *et al*., 2007, Mukhopadhyay and Jackson, 2013, Bisgrove and Yost, 2006). The *Fto*$^{-/-}$ mice have reduced body weight, lean mass and fat mass. When this data is adjusted for their reduced body weight they eat significantly more per gram of lean mass than littermate controls (Fischer *et al*., 2009) and it has previously been observed that *Fto*$^{-/-}$ mice are prone to diet induced obesity (Gao *et al*., 2010) although we have not observed this ourselves (in

house data unpublished). The adult *Fto*$^{-/-}$ mice also gain significantly more fat mass than controls; however we have not examined the cilia in these mice to see if they are abnormal.

In the E15.5 *Fto*$^{-/-}$ mice we found a variety of cilia morphology alterations in different tissues. In the MEFs the primary cilia were also disrupted. Examining tissues in newborn pups did not reveal any classical alterations associated with cilia defects such as cystic kidneys, disrupted airways, or unusual left-right patterning. A wild-type and a *Fto*$^{-/-}$ mouse were also fully examined by necropsy but no significant differences in tissue morphology were identified. The mice that reach adulthood may not be as severely affected as the pups that die before weaning, and I think it is important to continue to examine the mice after birth to identify what is causing the decreased mortality in *Fto*$^{-/-}$ mice.

Our data also suggests that WNT/β-CATENIN signalling may be disrupted in C2C12 cells treated with *Fto* siRNA, which could explain the cilia abnormalities in the *Fto*$^{-/-}$ MEFs and E15.5 mice. This could also explain why adipogenic differentiation is altered in *Fto*$^{-/-}$ MEFs. Cilia have been implicated in the WNT signalling pathway, and may act as a switch between canonical and non-canonical WNT signalling (Simons *et al*., 2005, Bisgrove and Yost, 2006). Investigating the gene and protein expression in response to WNT ligands such as WNT3a or WNT5a may reveal significant differences between wild-type and *Fto*$^{-/-}$ and FTO overexpression mice, and allow us to see what role this signalling pathway plays in the phenotype of the mice.

4.4.6 Adipocyte Differentiation

In the *Fto*$^{-/-}$ and overexpression MEFs we observed significantly less adipogenic differentiation than in MEFs from wild-type littermates. Recently Simpson-Golabi-Behmel Syndrome (SGBS) pre-adipocytes which have been treated with *Fto* shRNA showed no difference in adipogenesis compared to control treated cells (Tews *et al*., 2013). The differences between our results may be due to their incomplete knockout of FTO or that these are a human cell line generated from subcutaneous WAT of an infant which has SGBS (Fischer-Posovszky *et al*., 2008). These cells are therefore already partially on their way to becoming full adipocytes, whereas the MEFs that I used

are further removed. Primary MEFs are known to differentiate with variable efficiency [usually 10-70 % (Rosen and MacDougald, 2006)] which may explain why the percentage of cells that differentiate are much lower in my experiment.

The recent data of Tews and colleagues suggests that FTO plays a role in *de novo* lipogenesis, rather than adipogenic differentiation. They also showed an upregulation of *UCP-1* in FTO deficient adipocytes which led to a brown adipocyte phenotype (Tews *et al*., 2013). I have not investigated the expression of *Ucp-1* in *Fto*$^{-/-}$ mice or MEFs, but it would be interesting to investigate these results in our mice, as we do not see a difference in energy expenditure in our *Fto*$^{-/-}$ mice (McMurray *et al*., 2013). I would also like to expand these studies by differentiating the different genotypes of MEFs into brown adipocytes by using BMP-7, and investigating the differences in fat oxidation and lipogenesis in these cells.

In the differentiated knockout and overexpression MEFs I investigated the expression of a selection of genes involved in differentiation, WNT signalling and metabolism. One striking observation is the upregulation of *Mmp2* in *Fto*$^{-/-}$ MEFs, both before and after differentiation. MMP2 may be able to activate GSK3β by cleaving off the N-terminal domain, preventing it from being inactivated (Kandasamy and Schulz, 2009). Although most matrix metalloproteinases are secreted and activated extracellularly, recently an intracellular isoform of MMP2 has been identified (Lovett *et al*., 2012). This could lead to increased β-CATENIN phosphorylation and breakdown in the cytoplasm, which we believe may be occurring in our *Fto* deficient C2C12 cells. MMP2 expression has also been shown to be induced by WNT signalling in T-cells, and increases their migration (Wu *et al*., 2007a). *Mmp2* is located just outside of the region deleted in the *Fused toe* mouse (Peters *et al*., 2002), meaning it is only 1.24 Mb away from *Fto* (**Figure 4.20**). We therefore cannot be certain if inactivation of *Fto* is resulting in this altered expression or if it is due to an alteration in the genetic landscape, confirmation that MMP2 expression is increased at the protein level is still under investigation. We have previously examined expression of *Rpgrip1l* which is not altered in the *Fto*$^{-/-}$ or FTO overexpression mice (in house data, unpublished) but thorough investigation of the remaining genes in the region is required to ensure their transcription

is unaffected. Expression of *Lef1* is also effected by WNT signalling, in FTO-4 cells *Lef1* expression is significantly increased before differentiation, and decreased after differentiation, in *Fto*$^{-/-}$ MEFs *Lef1* expression is not significantly different. WNT signalling induces expression of *Lef1*, which could suggest that activation of this pathway, which aids in adipogenesis, is impaired in the FTO-4 MEFs (Bowers and Lane, 2008).

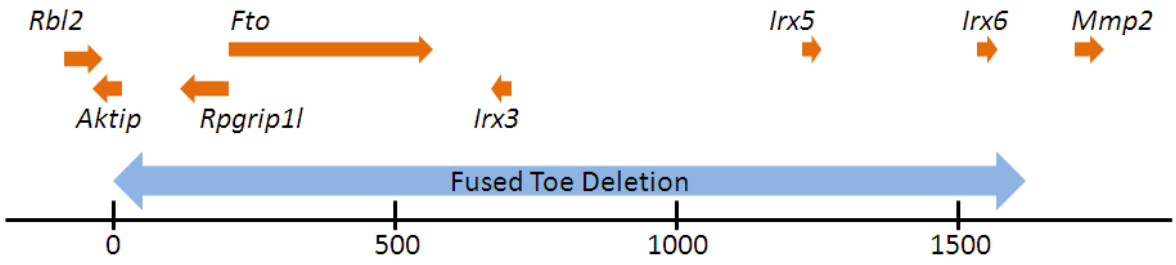

Figure 4.20 Physical and transcriptional map of the *Fused toe* locus on mouse Chromosome 8. A blue arrow indicates the genomic region of 1.6Mb that is deleted in the *Fused toe* mice.

A number of genes are differentially regulated between the FTO overexpression and *Fto*$^{-/-}$ MEFs. Expression of *Lep* is increased in differentiated *Fto*$^{-/-}$ MEFs but decreased in FTO-4 MEFs. In FTO-4 mice plasma leptin levels are significantly reduced compared to wild-type littermates when corrected for their increased body weight (Church *et al.*, 2010). In *Fto*$^{-/-}$ mice leptin levels are reduced (Fischer *et al.*, 2009), and our in house data (unpublished) show that leptin is not significantly different from wild-type mice which when corrected for the reduced fat mass suggests leptin levels are increased compared to wild-type mice. Our results in MEFs appear to reflect these observations in mice.

The other differentially regulated genes are *Cpt1b* and *Pck-1* in differentiated MEFs. Both are expressed at higher levels in the *Fto*$^{-/-}$ MEFs and decreased levels in the FTO-4 MEFs. CPT1b is involved in β-oxidation of long chain fatty acids, and PCK-1 is an enzyme involved in gluconeogenesis, converting oxaloacetate into phosphoenolpyruvate and carbon dioxide (Chakravarty *et al.*, 2005). This may indicate that in the differentiated *Fto*$^{-/-}$ MEFs there is an

increase in gluconeogenesis and β-oxidation, whereas the reverse is true in the FTO-4 MEFs. Further investigation is needed to substantiate this hypothesis.

In the various FTO mouse models, there are clear effects on fat mass. In the global *Fto*$^{-/-}$ mice fat mass is reduced in grams and in percentage of body weight, and adipocytes are significantly smaller (Fischer *et al*., 2009, McMurray *et al*., 2013). Gao and colleagues observed increased fat mass in their female global *Fto*$^{-/-}$ mice, and this trend was observed in both sexes in their neuronal *Fto*$^{-/-}$ mice (Gao *et al*., 2010). Fat mass is also significantly reduced in mice which are homozygous for the FTO^{I367F} mutation (Church *et al*., 2009). In mice which overexpress FTO, fat mass and adipocyte size are significantly increased (Church *et al*., 2010), and in adult *Fto*$^{-/-}$ mice fat mass is also significantly increased at 20 weeks of age (McMurray *et al*., 2013). The results in mice indicate that adipogenesis and fat storage is affected by FTO. My results indicate that FTO can also affect adipogenesis in MEFs; therefore the effects on fat mass in the *Fto* mutant mice may not be secondary to alterations in metabolism.

Chapter 5:

Inhibiting FTO Function

5.1 Introduction

When FTO was first associated with an increased BMI its function was unknown. Sequence analysis revealed that it had a double-stranded beta-helix fold homologous to those of Fe (II) and 2OG oxygenases, such as AlkB (Gerken *et al*., 2007). Gerken and colleagues showed that FTO is capable of demethylating 1-meA, 3-meC and was shown to have a strong preference for 3-meT on single stranded DNA and RNA. FTO has since been shown to also act on 3-meU (Jia *et al*., 2008) and 6-meA (Jia *et al*., 2011).

2OG oxygenases have a wide range of functions, which include: DNA repair, posttranslational modifications, and fatty acid metabolism [reviewed in (Clifton *et al*., 2006)]. These enzymes require non-haem iron [Fe(II)] as a cofactor, use oxygen and, almost always, 2OG as co-substrates, and produce succinate and carbon dioxide as by-products.

FTO localises to the nucleus (Gerken *et al*., 2007) and has been shown to partially localise with splicing and splicing-related speckle factors (nuclear speckles) such as SART1, SC35, and Pol II-S2P but not with telomere marker TRF1, the replication site PCNA, the Cajal body marker Coilin, the cleavage body marker CstF64 or the P-body marker DCP1A (Jia *et al*., 2011). When Pol II-S2P transcription is inhibited, FTO levels decrease in the nucleoplasm and concentrate around SC35 and Pol II-S2P suggesting a dynamic interaction of FTO with the nuclear speckles. Perhaps FTO functions in processing pre-mRNA or other nuclear RNAs (Jia *et al*., 2011).

The N-terminal of FTO contains the catalytic core vital for its demethylase activity, whilst the activity of the C-terminal domain is still not fully understood, but may be important for stabilising

the N-terminal domain (Han *et al*., 2010). Inside the N-terminal are several highly conserved histidine and carboxylate residues His 228/231, Asp 230/233, His 304/307 Arg 313/316 and Arg 319/322 which bind the substrates (Gerken *et al*., 2007, Sanchez-Pulido and Andrade-Navarro, 2007, Han *et al*., 2010). Mutation of His-304 reduces 2OG turnover and mutation of Arg-313 ablates activity (Gerken *et al*., 2007).

In 2009 a consanguineous Israeli-Arab family was described in which nine siblings were homozygous for the R316Q mutation in *FTO*, which generates a catalytically inactive protein (Boissel *et al*., 2009). All individuals which were homozygous carriers were severely growth retarded, had multiple congenital malformations, and died in infancy. The heterozygous parents of these children had no obvious metabolic phenotype, and adiposity was not measured in heterozygous or wild-type relatives. Another study associated loss of function mutations in *FTO* with both lean and obese individuals (Meyre *et al*., 2010). Although the SNPs in intron one are associated with obesity in multiple populations and murine studies strongly suggest that FTO has a role in energy balance, it appears that loss of one functional copy of *FTO* in humans can be compatible with being lean or obese.

There are many questions still unanswered. How can the DNA/RNA demethylation function of FTO be linked to obesity? Why does a catalytically inactive form of FTO present a severe developmental and lethal phenotype in humans and a knockout in the mouse produces growth retarded mice with increased mortality? Perhaps, the methylation reversed by human FTO is a signal for gene regulation rather than merely for DNA/RNA damage? In this chapter I aimed to identify or generate a mouse carrying a mutation in the catalytic core of FTO. To do this I screened the ENU archive at MRC Harwell and created a targeting construct to create a mouse which would be able to conditionally overexpress a catalytically inactive form of FTO, FTO^{R313A}. I also used pharmacological intervention to inhibit FTO function *in vivo* as a first step in evaluating the therapeutic potential of FTO as a target.

5.2 Methods

5.2.1 Harwell *Fto* ENU Archive Screen

The Harwell ENU DNA archive (Quwailid *et al*., 2004) (http://www.har.mrc.ac.uk/services/dna_archive/) was screened using the LightScanner (R) System (Idaho Technology Inc., Salt Lake City, Utah, U.S.A.). DNA was screened from pools of four individuals and confirmed with individual DNA samples. Primers used to screen *Fto* exon five sequences from the Harwell ENU-induced mutagenesis archive were:

FTOex5F 5'-GATAGCATGTACTGACTAATAAACG-3'

FTOex5R 5'-CCACATTCAGTTAAGCATGAATC-3'

Hotshot MasterMix and LCGreen dye (Idaho Technology Inc., Utah, U.S.A.) using PCR programme LS58H (95 ^{o}C 2 min; 44 cycles of: 95 ^{o}C for 30 s, 58 ^{o}C for 30 s, 72 ^{o}C for 30 s; 95^{o}C for 30 s; 25 ^{o}C for 30 s; 15 ^{o}C for 30 s). Amplified samples were then run on the light scanner to assess melt curves. Any interesting samples were identified and repeated.

5.2.2 Creating a Conditional FTO^{R313A} Overexpression Mouse

General cloning methods are included in chapter 2. The specific cloning steps and sequences are provided in this chapter. In order to overexpress the mutagenised *Fto* cDNA from an independent locus we utilised a targeting construct containing recombinogenic arms of homology, a promoter sequence interrupted by a *LoxP* (Cre recombinase recognition site) flanked transcriptional stop cassette and *PGK-Neo*, a unique restriction endonuclease site necessary for transgene insertion and an *FRT* (Flp recombinase recognition site) flanked IRES-EFGP (Internal Ribosome Entry Sequence-Enhanced green-fluorescent protein) reporter cassette. The *ROSA26* targeting vector was a gift of Professor Jens Brüning (University of Cologne), and the shuttle vector containing *Fto* cDNA a gift from Dr. Chris Church (MRC Harwell):

pCAGGs-STOP-EGFP-ROSA-TV

This vector contains the strong CAGGs promoter (chicken β-actin promoter/enhancer coupled with the cytomegalovirus (CMV) immediate-early enhancer). The promoter is followed by a *LoxP* flanked (floxed; flox) transcriptional stop signal. Downstream of the 3' *LoxP* site is a unique *Asc*I site for transgene insertion and then a *FRT* flanked IRES-EGFP cassette.

pR26AscIFto

This is a shuttle vector containing *Fto* cDNA under an optimised Kozac (GCC)GCCA/GCCAUGG) consensus sequence (Kozak, 1987a, Kozak, 1987b). This sequence was flanked by *Asc*I sites to allow excision and transfer to the *ROSA26* targeting vector.

5.2.2.1 Site Directed mutagenesis of pR26AscIFto

The Quikchange site-directed mutagenesis kit (Agilent Technologies, USA) was used according to manufacturer's instructions to produce the R313A mutation in the *Fto* cDNA present in the pR26AscIFto vector, with the following primers:

FTOex5R313Af

5'-GTGTTTTGGCTGGCTCACAGCCTGCGTTTAGTTCCACTCACCGTGGG-3'

FTOex5R313AR

5'-CCACACGGTGAGTGGAACTAAACGCAGGCTGTGAGCCAGCCAAAACAC-3'

Samples were sequenced to confirm mutation presence using primers:

FTO_ex6_For	5'-AATCCTTTGATCCTGCAGTT-3'
cDNA2R	5'-TCTTCTTCCACAGCCCCTCC-3'
FTOcDNAKOF	5'-AACGAGAAGCGGGAAGCTAA-3'
FTOcDNAKOR	5'-GGAAACCACGTCTGTTGAGGT-3'

5.2.2.2 *ROSA26* Final Targeting Vectors

The pCAGGs-STOP-EGFP-ROSA-TV was linearised with *Asc*I (NEB) and the phosphate groups removed using rAPid alkaline phosphatase (Roche). The *Fto* cDNA was excised from p*R26AscIFto* by *AscI* (NEB) and purified using a QiaQuick Gel extraction kit (Qiagen). Subsequently the *Fto* cDNA fragment was inserted by T4 DNA ligation into the *Asc*I site of the *ROSA26* targeting vector to generate pCAGGs-STOP-*Fto*^{R313A}cDNA-EGFP-ROSA-TV. The plasmid was confirmed by restriction digest analysis and DNA sequencing.

5.2.2.3 *ROSA26* Gene Targeting

Fifty micrograms of pCAGGs-STOP-*Fto*^{R313A}cDNA-EGFP-ROSA-TV was linearised with *Asi*SI (NEB). Digest completion was checked on a 0.5 % agarose gel. Linearised DNA was triple phenol:chloroform extracted followed by ethanol precipitation with sodium acetate. The DNA pellet was washed twice in 70 % ethanol before being air dried and resuspended in tissue culture grade PBS (Sigma-Aldrich). The concentration was determined by a NanoDrop ND-1000 Spectrophotometer. Twenty micrograms of the linearised targeting vector was electroporated into semi-confluent R1 129 ES cells (Nagy *et al*., 1993). ES cell transfection, antibiotic selection, hand picking and freezing of ES cell clones was performed by the Transgenesis and Gene Targeting Facility, Mary Lyon Centre Harwell, MRC Harwell (Sara Tull, Denise Lynch, and Dr. Lydia Teboul).

5.2.2.4 Screening ES Cell Clones

The pCAGGs-STOP-*Fto*^{R313A}cDNA-EGFP-ROSA-TV cell clones were selected by G418 (Geneticin; Sigma, resistance conferred by *Neo*) treatment. Surviving ES cell clones were screened by Southern blot analysis using approximately 10 μg of ES cell genomic DNA digested with *Eco*RI (NEB) and a 5' external probe: a 5' DNA fragment was generated by PCR and amplified using primers:

ROSA5'F AAGGATACTGGGGCATACG

ROSA5'R CTTCTCAGCTACCTTTACACACC

Product size 448 bp, annealing temperature 63 °C.

These primers reside immediately 5' to the region of vector homology from the R1 ES cell genomic DNA as previously described (Hitz *et al*., 2007). The 5' DNA fragment was subsequently labelled with αP32-dCTP (see **Chapter 2.2.16**).

5.2.2.5 Targeted ES Cell Clones

The pCAGGs-STOP-*Fto*^{R313A}cDNA-EGFP-ROSA-TV construct generated 1 (out of 96) correctly targeted ES cell clones. This ES cell clone was expanded and confirmed by DNA sequencing and Southern blot analysis. All *LoxP* and *FRT* sites were confirmed in ES cells by DNA sequencing (**Table 5.1**). Targeted ROSACAGGs-*Fto* ES cells were injected into C57BL/6J blastocysts to generate chimeras.

Table 5.1 *ROSA26* Sequencing Primers.

Primer Name	Primer Sequence (5' to 3')	Purpose
Loxp5r26F	TTGTTTCTTTTCTGTGGCTGCGTG	5'*LoxP* site
Loxp5r26R	TCCTCGTGCTTTACGGTATCGC	5'*LoxP* site and CAGGs Promoter
Loxp3r26F	AAACCTCCCACACCTCCCCCTGAA	3'*LoxP* site and *Fto* cDNA
Loxp3r26R	GCCAAGTGTCTTCAAGCTCCT	3'*LoxP* site, *Fto* cDNA, and *Neo* Stop
X3NeoF	ATGGATCCTCAGAAGATGCCCTAC	*Fto* cDNA and 5' *FRT*
X3NeoR	GCTACTTCCATTTGTCACGTCC	DT-A
R26FTOBlntF	CATGAAGCGCGTCCAGACCG	*Fto cDNA*
R26FTOBtStopR	CTAGGATCTTGCTTCCAGCAGCTGG	*Fto cDNA*
FTOpAF	TGGAACAAAGGAGTGAGATTCTGTC	5' FRT and IRES EGFP
FTOpAR	GCTTCGGCCAGTAACGTTAGGG	*Fto* cDNA and 5' *FRT*
R26LxPFTOR	GCTGCCACTGCTGATAGAACTCA	3'*LoxP* site, *Fto* cDNA, and *Neo* Stop
NeoF	TGAATGAACTGCAGGACGAGGCA	PGK *Neo*Stop
NeoR	GCCGCCAAGCTCTTCAGCAATAT	PGK *Neo*Stop

5.2.3 Pharmacological Inhibition of FTO with FG2216 *in vitro*

FG2216 [(1-Chloro-4-hydroxy-isoquinoline-3-carbonyl)-amino]-acetic acid was a kind gift from Prof. Chris Schofield, Department of Chemistry, University of Oxford.

Cells were plated and left to adhere for at least 1 hour before treating overnight with vehicle control (0.5 % DMSO) or 1 μM FG2216.

5.2.3.1 Phenotyping pipeline

Forty C57BL/6J mice (six weeks old) were weighed and then ranked and randomised by cage to evenly distribute mice of different weights to each dosing group. Mice were treated by oral gavage once every other day for 40 days with 10 mg/ml volume of either 2 % methylcellulose (Sigma-Aldrich) 5 % DMSO (vehicle control), or 10mg/ml of FG2216 in 2 % methylcellulose 5 % DMSO pH 7 (60 mg/kg/2 days).

Mice were weighed each week during the trial, and characterised using a standardised metabolic phenotyping pipeline (**Figure 5.1**). Phenotyping tests were performed according to EMPReSS (European Phenotyping Resource for Standardised Screens from EUMORPHIA) standardised protocols as described at http://empress.har.mrc.ac.uk.

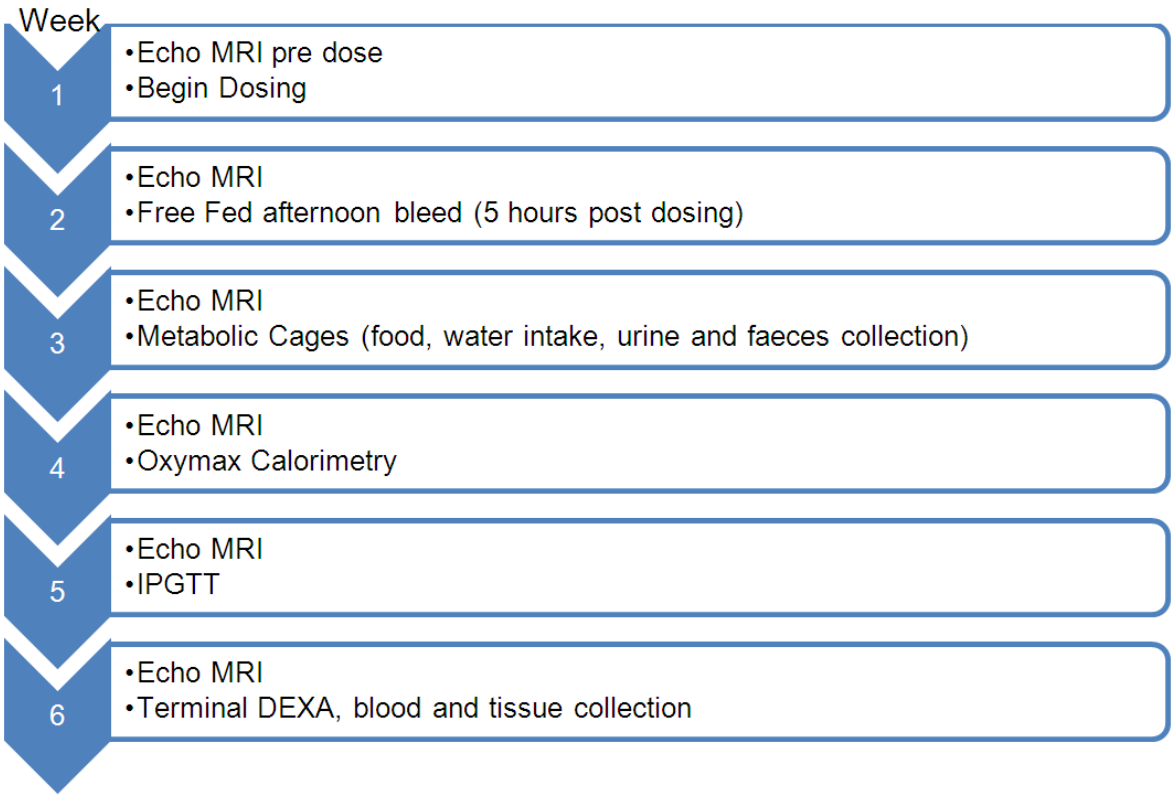

Figure 5.1 Metabolic Phenotype Pipeline. Abbreviations: IPGTT, Intraperitoneal glucose tolerance test**.**

5.3 Results

5.3.1 Generating a Mouse with Catalytically Inactive FTO

The ENU archive at MRC Harwell was screened for mutations in exon 5 of FTO. Plates 1-65 were screened for mutations in exon 5 by Chris Church before he went on to identify FTO I367F (Church *et al*., 2009). I screened plates 66-109 for mutations in FTO exon 5, which together contain approximately 10,400 ENU mutagenised mice. Unfortunately, no mutations in exon 5 were discovered in this screen. Exon 5 is 80 bases long, and ENU mutagenesis at MRC Harwell is expected to generate mutations every 1.01 Mbp (Quwailid *et al*., 2004), therefore the chance of finding a mutation in one of the 10,400 mice was 82.4 %, if the mutagenesis rate occurs equally in all genomic regions.

As the archive screen was not fruitful I went about generating a mouse which could conditionally overexpress FTO^{R313A} from the *Rosa26* locus (**Figure 5.2**). Arginine 313 in the mouse is the equivalent residue to arginine 316 in human FTO, and Gerken and colleagues have previously shown that this mutant protein *in vitro* can no longer demethylate 3-meT (Gerken *et al*., 2007). I believed that this would be a useful tool as I would be able to see if FTO's catalytic function is important for causing the phenotype seen in the *Fto* overexpression mouse model generated by Chris Church (Church *et al*., 2010), and it could be crossed with the conditional *Fto* knockout to investigate the phenotype of mice which only express FTO^{R313A}.

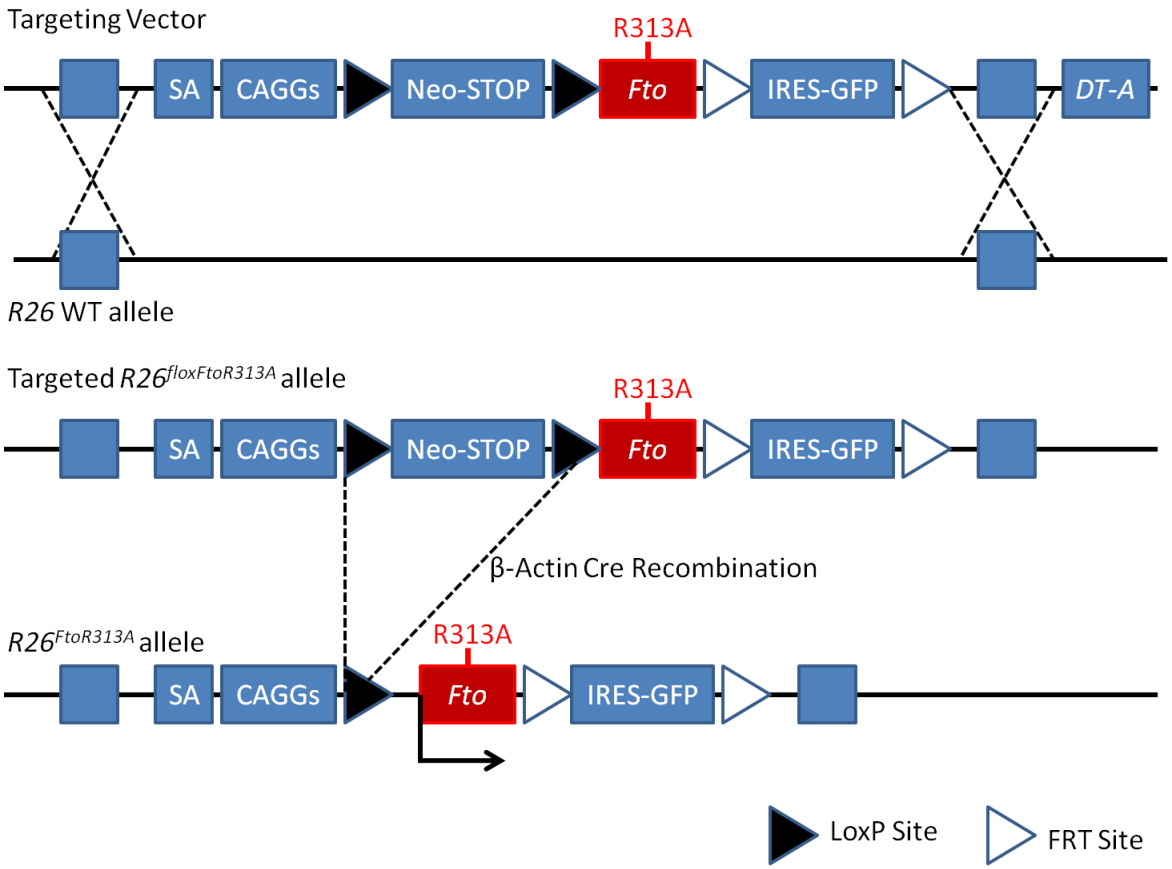

Figure 5.2 Strategy for generating a conditional *FtoR313A* over-expression allele. The targeted ROSA26 allele contains the *Fto*^{R313A} cDNA under the control of CAGGs promoter. A *Lox*P flanked transcriptional stop signal interrupts the expression of the *Fto* cDNA. Cre recombination excises the transcriptional stop cassette activating expression of *Fto* and an IRES eGFP reporter. Mice carrying the floxed allele will be crossed to a Cre recombinase line under the control of the beta-actin promoter for global and germline excision of the STOP cassette and expression of *Fto* from the CAGGs promoter. PGK-Neo, neomycin resistance gene; Stop, transcriptional stop signal; IRES, Internal Ribosome Entry Site; DT-A, diphtheria toxin A; pA, polyadenylation signal.

Unfortunately despite producing nine chimeras (6 male, 3 female), we have not had successful germline transmission from these mice. The generation of the *Rosa26*$^{Fto\text{-}R313A}$ mice has so far been unsuccessful, but work is still being carried out to generate this line.

5.3.2 Pharmacological Inhibition of FTO

Our collaborators in Prof. Chris Schofield's group in the Department of Chemistry at the University of Oxford employed a differential scanning fluorimetry based assay to screen >150 2OG analogues and metal-chelators comprised of 10 structural series. Where this assay was not suitable due to compound fluorescence (e.g. 8-hydroxyquinolines) they assayed FTO inhibition

using liquid chromatography (LC) to measure percentage conversion of 3-meT to thymidine, and to determine IC_{50} values for hits as detailed in (Aik *et al*., 2013).

One compound, FG-2216/IOX3 [(Yan *et al*., 2010) **Figure 5.3A**] gave the lowest IC_{50} value against FTO (2.76 ± 0.9 μM). This is a known inhibitor of the HIF-prolyl hydroxylases (PHD1-3) that is active in cells and animals (Rose *et al*., 2011).

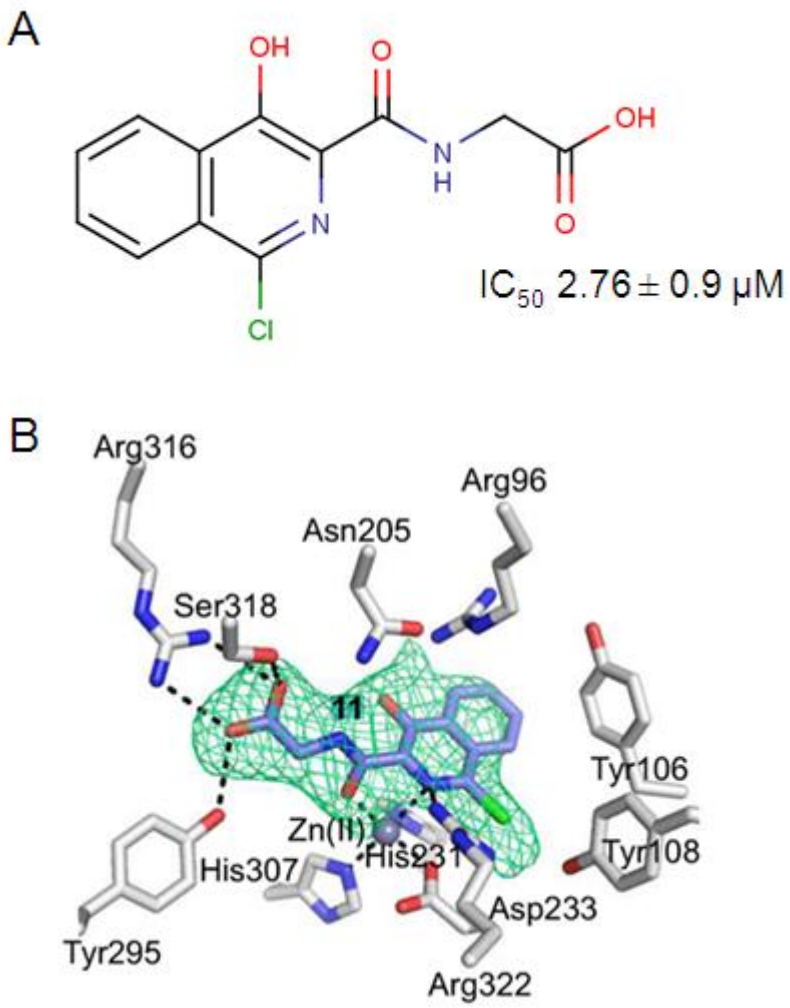

Figure 5.3 FG2216 Chemical Structure and FTO Crystal Structure in complex with FG2216. A, The chemical structure of FG2216, drawn using MarvinSketch v6.0.2 with CPK colouring. **B**, Wall-eyed stereo views from crystal structures of FTO in complex with FG2216 (blue). Residue side chain C (white); O (red); N (blue); Ni (green ball); Zn (grey ball); hydrogen bonds are indicated as black dashes. mFo-DFc ligand omit maps (contour level, σ = 3.0) are indicated as lime green mesh. Image B is courtesy of Wei Shen Aik, Department of Chemisty, University of Oxford.

Wei Shen Aik generated a crystal structure of FTO in complex with FG2216 (2.50 Å resolution) (**Figure 5.3B**) (PDB ID: 4IE6). FG2216 binds into the substrate binding site and the chlorine of

FG2216 sits in the nucleic acid substrate binding site, this predicts that the compound will compete with 2OG and 3-meT for access to the binding site, preventing FTOs normal catalytic activity.

Prolyl hydroxylase inhibitors (PHIs) lead to the activation of the HIF-1 alpha pathway, which causes induction of angiogenesis, erythropoiesis, proliferation, cell survival, inflammation, and energy metabolism (Bao *et al*., 2010). FG2216 has been shown to inhibit HIF-prolyl 4-hydroxylase and induce expression of HIF and VEGF, and to have a cardio-protective effect in a rat model of myocardial infarction (Philipp *et al*., 2006). It has also been shown to induce EPO production in Swiss Webster mice and rhesus macaques, where chronic administration was well tolerated (Hsieh *et al*., 2007). It is currently in clinical trials as a prolyl-hydroxylase inhibitor to treat anaemia in end stage renal disease (ESRD) (Bernhardt *et al*., 2010).

5.3.3 Pharmacological Inhibition of FTO *in vitro*

Tan and colleagues have previously seen that FG2216 can significantly reduce oxygen consumption after 24 hours of treatment in cardiosphere-derived cells, with no impact on cell proliferation (Tan *et al*., 2011). I wanted to replicate these findings and investigate the effects of FG2216 on cell viability and oxygen consumption in my hands, and ensure efficacy of the compound. To do this I used the Seahorse XF24 to measure OCR and ECAR in vehicle and FG2216 treated C2C12 muscle myoblast cells (**Figure 5.4**).

Data collected for OCR and ECAR (**Figure 5.4A,B**) were normalised to the live cell stain values in **Figure 5.4C** to ensure that any variability when plating the cells was eliminated. Basal OCR was significantly reduced in FG2216 treated cells (**Figure 5.4A**), and basal ECAR, although not significant, was increased (**Figure 5.4B**), which together suggests an increase in glycolytic metabolism. Addition of oligomycin, which inhibits the ATP synthase, reduced OCR from baseline in both vehicle and FG2216 treated cells, and increased ECAR, although this increase from baseline was greater in vehicle treated cells. On addition of FCCP, which is a protophore and an uncoupler of oxidative phosphorylation, OCR levels increased significantly less in FG2216 treated cells, than the vehicle group. This indicates that FG2216 treated cells have a reduced maximal

respiration and spare respiratory capacity. The ECAR after addition of FCCP was significantly higher in the vehicle treated cells, which suggests that glycolysis rates were increased further in the vehicle cells but not in FG2216 treated cells. After addition of rotenone and Antimycin A, which inhibit complex I and complex III respectively, OCR levels drop in both groups and there is no significant difference in the remaining non-mitochondrial respiration levels. The effect of these inhibitors on ECAR is not significantly different between the groups. After OCR and ECAR measurements cells were stained with live/dead stain, and live stain levels were significantly lower in FG2216 treated cells (**Figure 5.4C**). However the number of dead cells stained was not significantly different (**Figure 5.4D**), indicating that perhaps cell proliferation is decreased in the FG2216 treated cells.

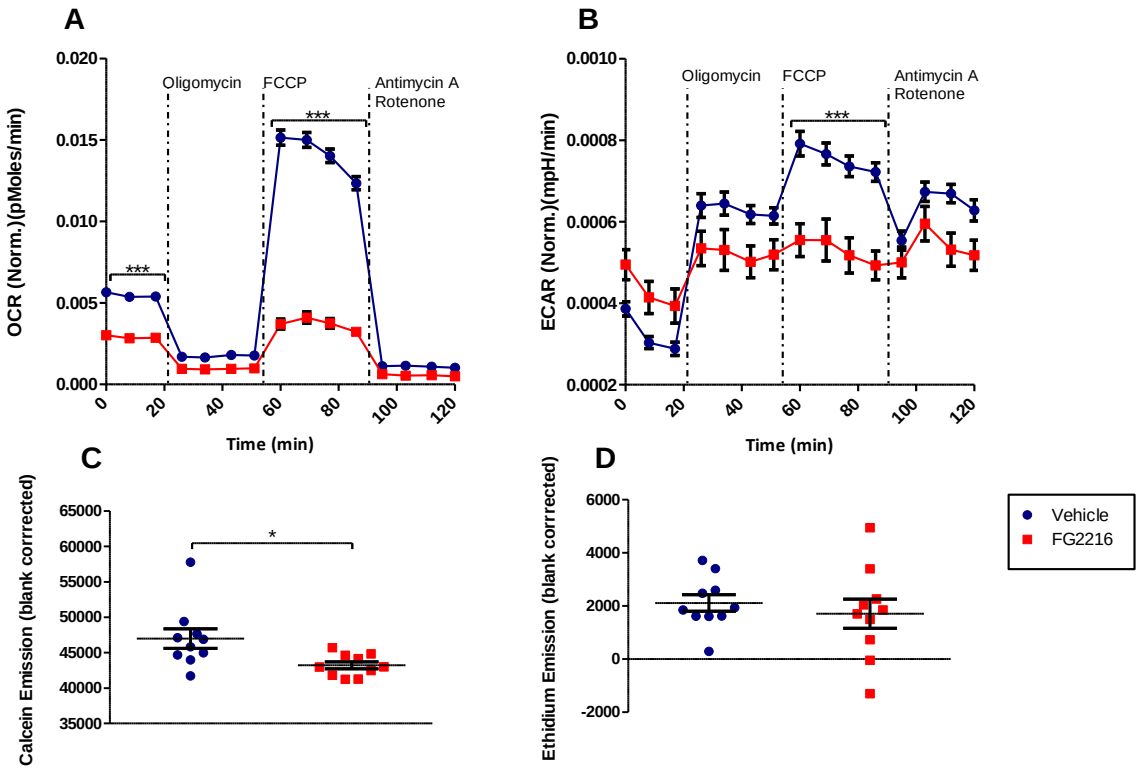

Figure 5.4 Oxygen Consumption Rate (OCR), Extracellular Acidification Rate (ECAR) and Viability of C2C12 treated with 1 µM FG2216 or an equivalent amount of vehicle control for 16 hours. A, OCR and, **B**, ECAR measured in cells treated with vehicle (n=10) and 1 µM FG2216 (n=10) at baseline and after Oligomycin, FCCP and Rotenone treatment, data normalised to live stain (**C**). **C**, Live stain (Calcein) and, **D**, Dead Stain (Ethidium) on cells after OCR and ECAR measurements. The Time-course data were analysed using a 2 way ANOVA with bonferroni post-test (**A,B**). The other comparison p-values (**C,D**), correspond to a student's *t*-test *P<0.05, **P<0.01, ***P<0.001. Data are expressed as mean ± SEM.

FG2216 will not specifically inhibit FTO and has been shown to act on other Prolyl hydroxylases. Therefore, in order to assess what proportion of the differences shown in **Figure 5.5** are due to FTO rather than off-target effects I treated wild-type and *Fto*$^{-/-}$ MEFs with vehicle or FG2216 overnight for 16 hours and measured OCR and ECAR. There was no significant difference in basal OCR between vehicle and FG2216 treated wild-type or *Fto*$^{-/-}$ MEFs (**Figure 5.5A**) as well as after oligomycin and antimycin A and rotenone treatment. Treatment with FCCP reveals a decreased rise in OCR in *Fto*$^{-/-}$ vehicle treated MEFs compared to wild-type vehicle treated MEFs ($P<0.05$ at 60, 69 and 86 minutes). Treatment of wild-type and *Fto*$^{-/-}$ MEFs with 1 μM FG2216 saw a further decreased rise in OCR after FCCP treatment, this was significantly different from wild-type vehicle treated MEFs ($P<0.001$ at 60, 69, 77 and 86 minutes). This was not significantly different from *Fto*$^{-/-}$ vehicle treated MEFs but there is a trend for decreased OCR, suggesting that FG2216 is causing this additional decreased OCR through inhibition of prolyl hydroxylases other than FTO (**Figure 5.5A**). ECAR levels were not significantly different between any of the groups, although as in **Figure 5.5B** there is a trend for increased basal ECAR in FG2216 treated wild-type and *Fto*$^{-/-}$ MEFs (**Figure 5.5B**). Oligomycin, FCCP and rotenone did not reveal any significant differences between the groups, although as before it would appear the FG2216 treatment stopped the increase in ECAR after FCCP, which is seen in vehicle treated wild-type and *Fto*$^{-/-}$ MEFs (**Figure 5.5B**). Live staining was significantly lower in *Fto*$^{-/-}$ MEFs treated with FG2216 than wild-type vehicle and FG2216 treated MEFs (**Figure 5.5C**). There was no significant difference in wild-type FG2216 treated MEFs compared to vehicle treated wild-types (**Figure 5.5C**). Dead stain showed no differences between any of the groups (**Figure 5.5D**).

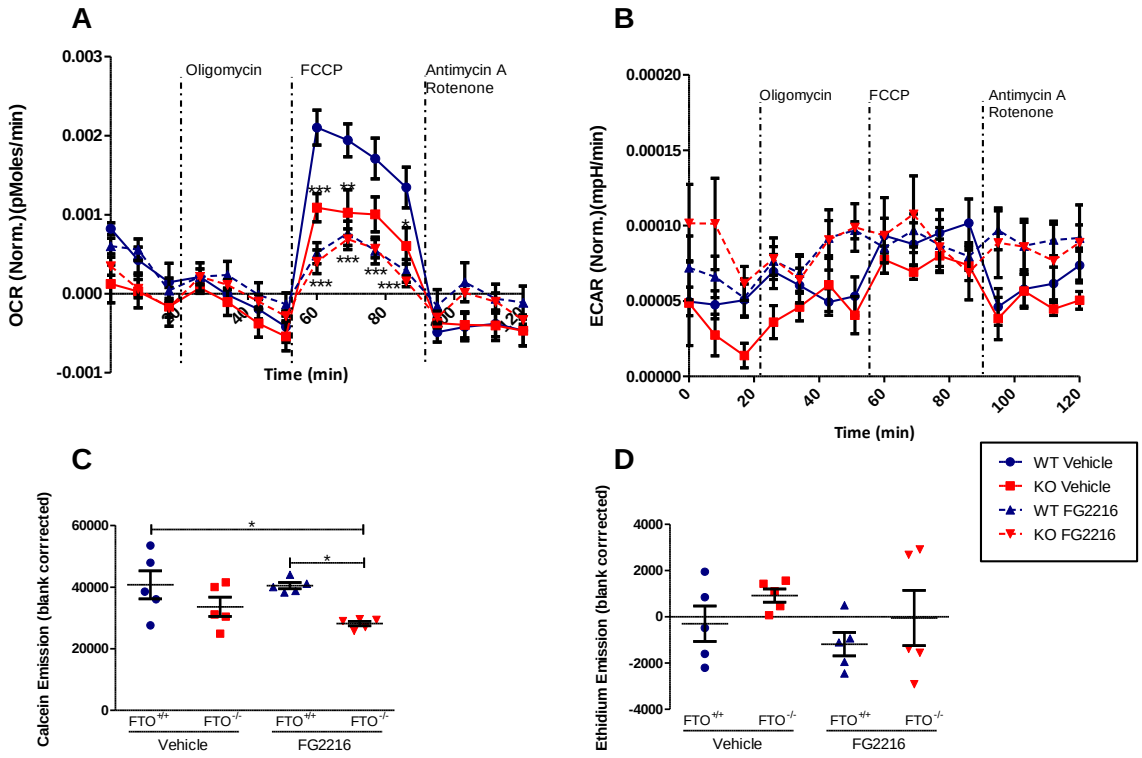

Figure 5.5 Oxygen Consumption Rate (OCR), Extracellular Acidification Rate (ECAR) and Viability of *Fto*$^{+/+}$ and *Fto*$^{-/-}$ MEFs treated with 1 µM FG2216 or an equivalent amount of vehicle control for 16 hours. A, OCR and, **B**, ECAR measured in *Fto*$^{+/+}$ and *Fto*$^{-/-}$ MEFs cells treated with vehicle and 1 µM FG2216 (n=5 per group) at baseline and after Oligomycin, FCCP and Rotenone treatment, data normalised to live stain (**C**). **C**, Live stain (Calcein) and, **D**, Dead Stain (Ethidium) on cells after OCR and ECAR measurements. The Time-course data were analysed using a 2 way ANOVA with bonferroni post-test (**A,B**). The other comparison p-values (**C,D**), correspond to one-way ANOVA with bonferroni correction *P<0.05, **P<0.01, ***P<0.001 compared to wild-type vehicle treated cells. Data are expressed as mean ± SEM.

5.3.4 Pharmacological Inhibition of FTO *in vivo*

FG2216 has previously been shown to increase plasma EPO levels in mice and Rhesus macaques (Hsieh *et al*., 2007) and it has been used in clinical trials to treat anaemia and end stage renal disease (Bernhardt *et al*., 2010), but the effect of FG2216 on body weight or composition have not been reported. We were interested to see if treatment with FG2216, an inhibitor of FTO, in wild-type adult mice might produce an effect similar to adult deletion of *Fto*, where body weight gain is decreased and lean mass is decreased and fat mass increased (McMurray *et al*., 2013).

Short toxicity trials of n=1-2 mice dosed with vehicle or FG2216 at 40 mg/kg and then a separate trial using 60 mg/kg were carried out to ensure that oral gavage of the drug in our hands was safe before large cohorts of mice were tested. These doses were used based on the work of Hsieh and

colleagues, who dosed Rhesus macaques for six to eight weeks with 40 and 60 mg/kg (Hsieh *et al*., 2007). The drug was well tolerated over a 24 hour period with no change in body weight or phenotype of the mice and no differences were noticeable during dissection (data not shown).

As the dose was well tolerated we decided to test the effect of FG2216 60 mg/kg on a cohort of mice. We decided to dose the animals on alternate days as Hsieh and colleagues had treated Rhesus macaques twice weekly with either 40 or 60 mg/kg FG2216 and were able to observe increases in plasma EPO. Mice were grouped and treated as in the methods **5.2.3.1** and **Figure 5.1**. There were no observed side-effects of the drug and all mice completed the trial, vehicle dosed (n=20) and 60 mg/kg FG2216 dosed (n=20).

To test the efficacy of the drug in our hands *in vivo* we looked at levels of erythropoietin (Bao *et al*.), a glycoprotein hormone that controls erythropoiesis, using an ELISA [(R&D Systems, Minneapolis, U.S.A.) **Figure 5.6**]. EPO has been previously shown to increase after dosing with FG2216 and other inhibitors of HIF-prolyl 4-hydroxylases, as these lead to stabilisation of HIF which induces transcription of genes that ameliorate the effects of hypoxia, including EPO and its receptor (Hsieh *et al*., 2007). We saw that mice treated with 60 mg/kg FG2216 had significantly increased levels of EPO at one week after dosing (P=7.2E-16 **Figure 5.6A**) and 40 days after dosing (P=4.70E-17 **Figure 5.6B**) compared with vehicle treated mice, and that the levels were not higher at the end of the study than at 1 week after dosing, suggesting levels increase and then plateau (**Figure 5.6C**).

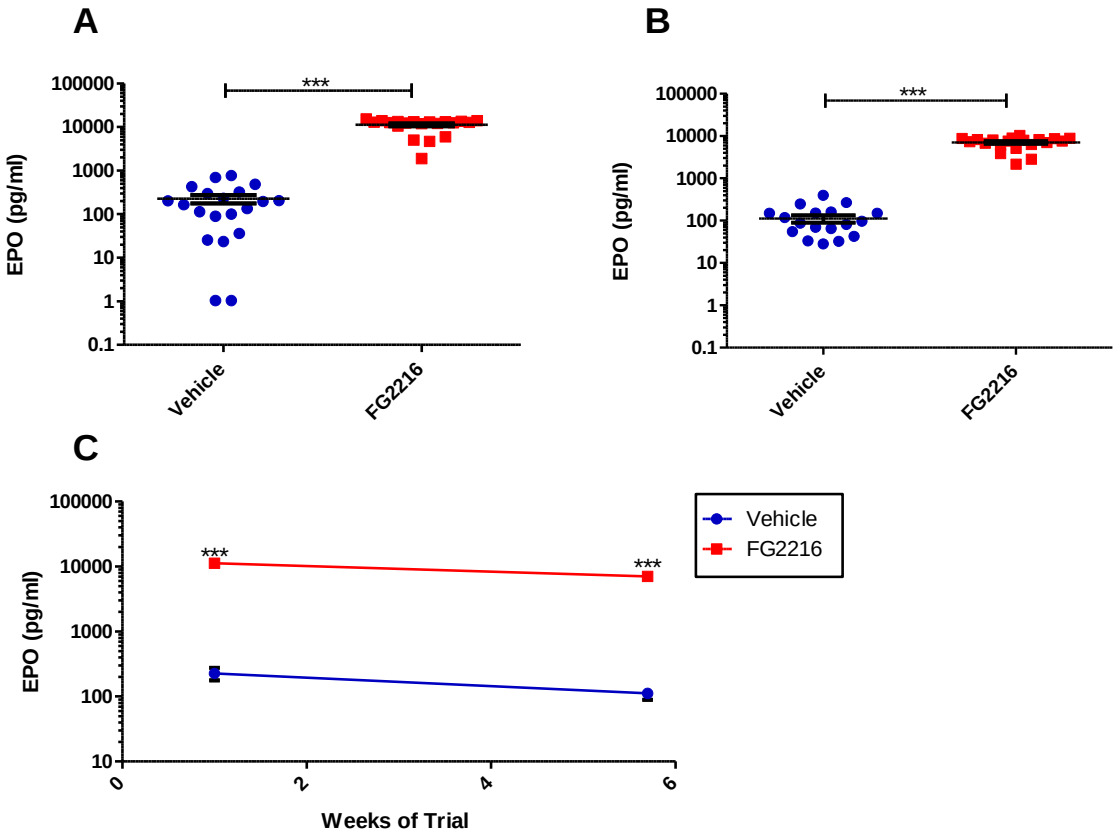

Figure 5.6 Plasma EPO levels in vehicle and 60mg/kg FG2216 treated mice. A, Plasma EPO levels after one week of dosing in vehicle (n=20) and 60mg/kg FG2216 (n=20) treated mice. **B**, Terminal plasma EPO levels at 40 days after beginning of the trial, vehicle (n=20) and 60mg/kg FG2216 (n=20) treated mice. **C**, Data from **A** and **B** plotted to show that FG2216 treated animals had consistently higher levels of plasma EPO. Data analysed by student's t-test *P<0.05, **P<0.01, ***P<0.001. Data are expressed as mean ± SEM.

EPO is predominately produced in the liver and kidney, so we also confirmed the increased plasma EPO by looking at EPO expression in liver after 40 days of dosing (**Figure 5.7**). If we quantify the EPO expression with ACTIN expression we see that EPO is expressed at significantly higher levels in mice treated with 60 mg/kg FG2216 (P=3.34E-4 **Figure 5.7A,B**).

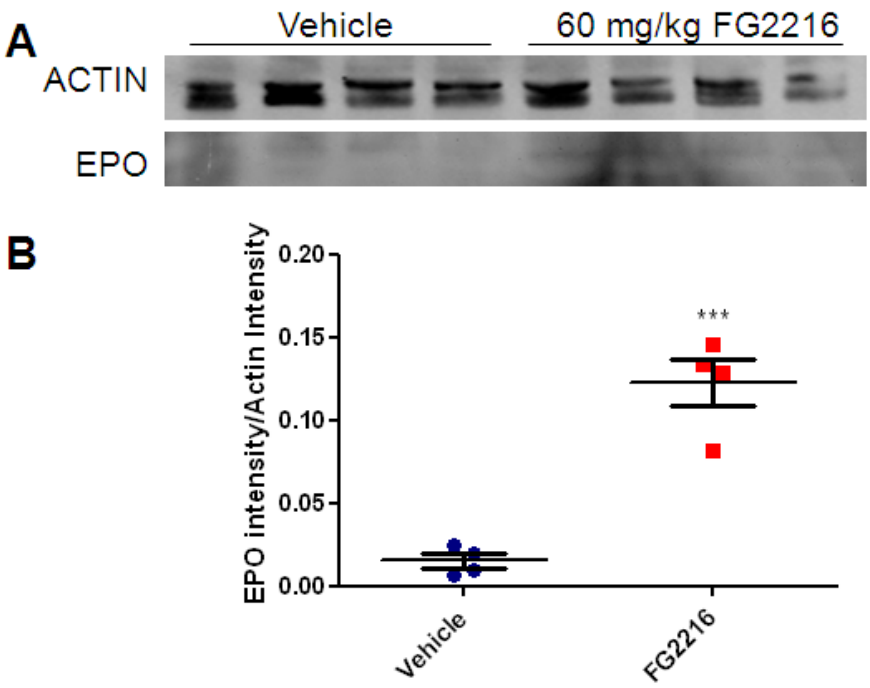

Figure 5.7 Liver EPO protein expression in vehicle and 60 mg/kg FG2216 treated mice. A, ACTIN and EPO immunoblots of vehicle (n=4) and 60 mg/kg treated (n=4) mice. B, Quantification of Blots in A. Actin: mouse monoclonal antibody, Millipore (MAB1501R); EPO: Rabbit Polyclonal antibody, Abcam (ab129452). Data analysed by student's t-test *P<0.05, **P<0.01, ***P<0.001. Data are expressed as mean ± SEM.

To see if inhibition of FTO would also affect its expression at the protein level we also looked at FTO levels in whole liver, brain and calf muscle (**Figure 5.8**). Levels of FTO in these tissues were unaffected by FG2216 dosing.

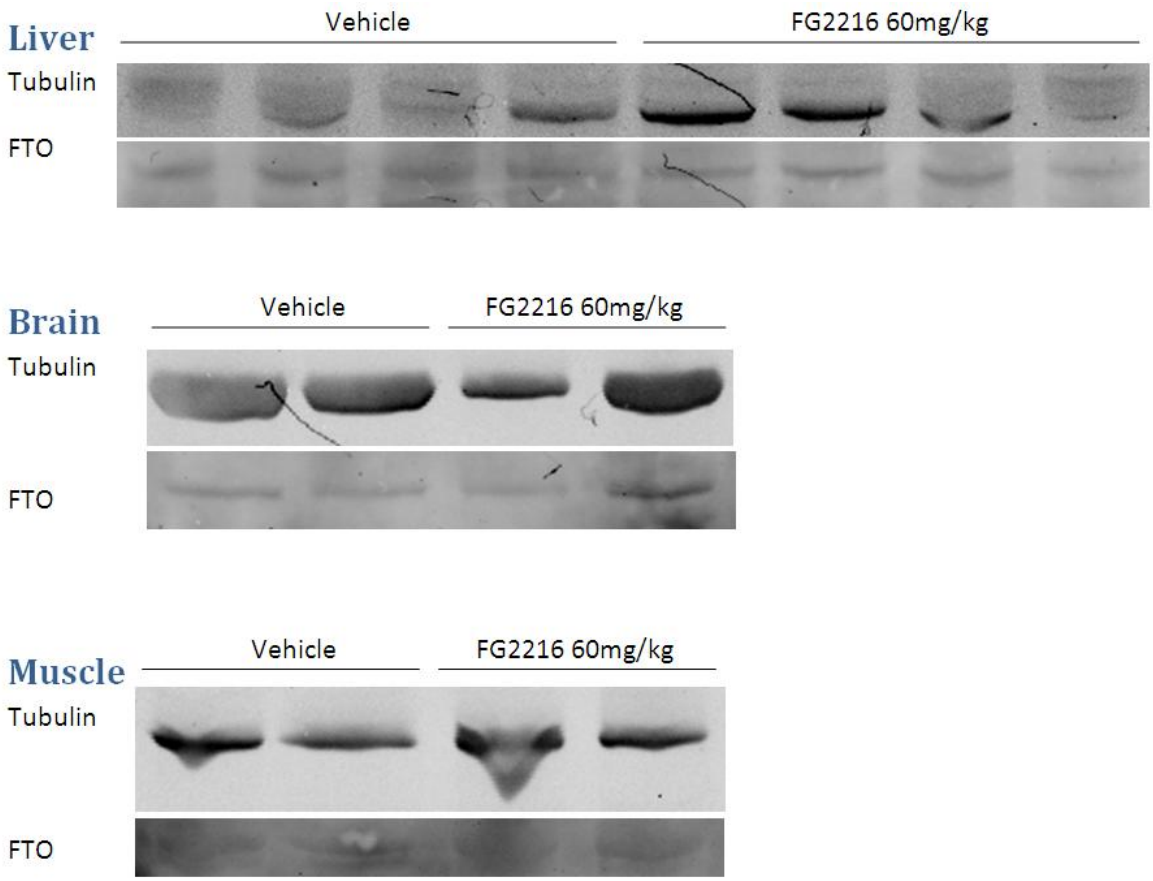

Figure 5.8 FTO Protein expression in whole liver, brain and gastrocnemius muscle in Vehicle and 60 mg/kg FG2216 treated mice after the 40 day dosing trial. FTO: Custom made rabbit anti recombinant mFTO antibody; Tubulin: 12G10 anti alpha-tubulin antibody from the Developmental Studies Hybridoma Bank, University of Iowa.

Body weight, fat mass and lean mass were measured prior to dosing, and then weekly until the end of the trial (**Figure 5.9**). There was no significant difference in body weight between vehicle and 60 mg/kg FG2216 treated animals during the trial (**Figure 5.9A**). There was also no significant difference in fat mass (**Figure 5.9B**), fat mass as a percentage of body weight (**Figure 5.9C**), lean mass (**Figure 5.9D**) or lean mass as a percentage of body weight (**Figure 5.9E**) at any point before or during the trial, suggesting that this dose of FG2216 has no effect on body weight or composition.

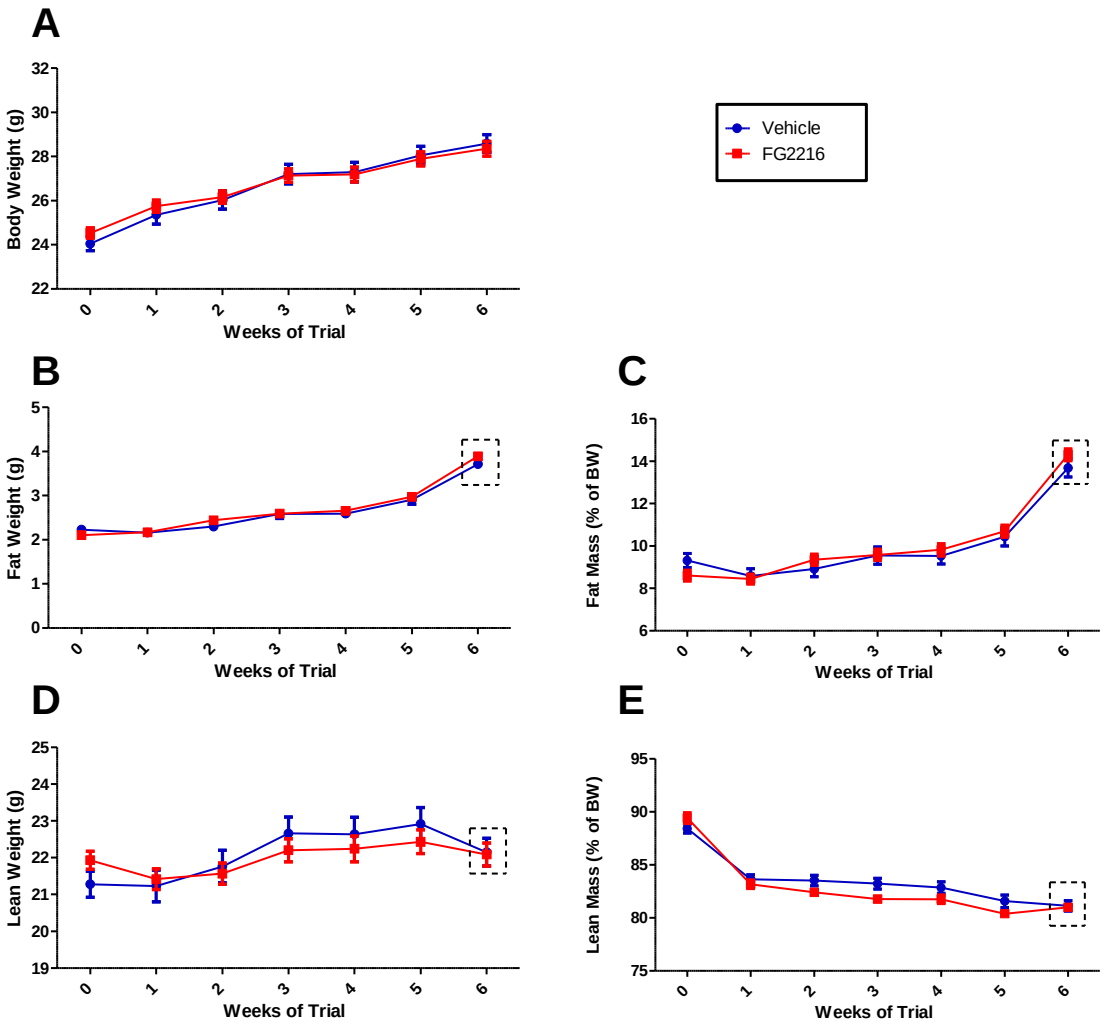

Figure 5.9 Body weight and composition of vehicle and FG2216 60mg/kg treated mice. A, Weekly body weight, **B** Fat weight, **C**, Fat weight as a percentage of body weight, **D**, Lean weight, **E**, Lean weight as a percentage of body weight of Vehicle (n=20) and 60 mg/kg FG2216 (n=20). Fat and lean mass data collected using Echo MRI and dashed boxes indicate data was collected using DEXA. Data were analysed using a 2 way ANOVA with bonferroni post-test *P<0.05, **P<0.01, ***P<0.001. Data are expressed as mean ± SEM.

Three weeks into the trial the mice were placed into metabolic cages for 24 hours. Water and food intake as well as urine and faeces output were measured in this time (**Figure 5.10**). There was no significant difference in water intake (**Figure 5.10A**) food intake (**Figure 5.10B**) or in urine or faeces production in the 24 hour period (**Figure 5.10C,D**). Biochemical profiles of the collected urine (**Table 5.2**) reveal that there are some differences between vehicle and 60 mg/kg FG2216 dosed mice. FG2216 dosed mice have significantly lower calcium (P=6.4E-4) glucose (P=0.00485) and uric acid (P=0.00539) in their urine than controls. Urinary sodium, potassium, chlorine, urea, inorganic phosphate and urinary protein were not significantly altered.

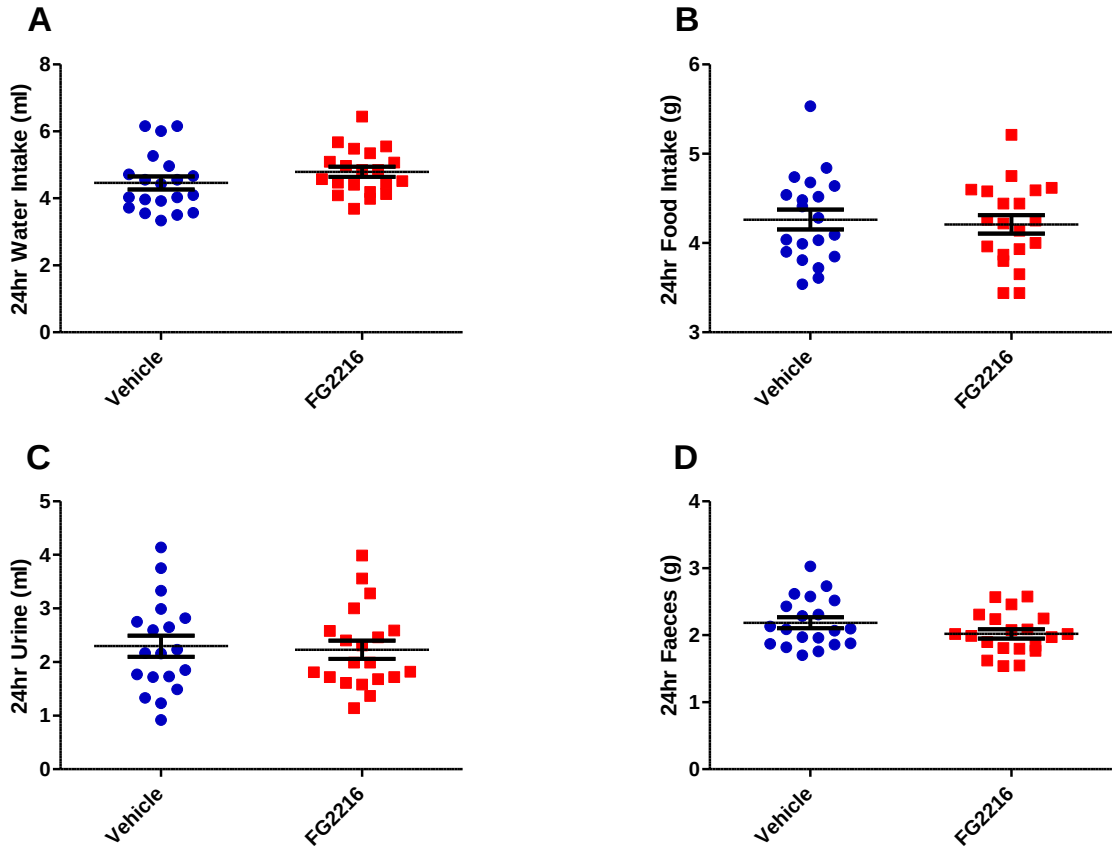

Figure 5.10 Vehicle and 60 mg/kg FG2216 treated mice in Metabolic cages for 24 hours. A, Water intake, **B**, Food Intake, **C**, Urine produced, **D**, Faeces produced in a 24 hour period from vehicle (n=20) and 60 mg/kg FG2216 (n=20) treated mice in metabolic cages. Data analysed by student's t-test *P<0.05, **P<0.01, ***P<0.001. Data are expressed as mean ± SEM and individual data points are shown.

Table 5.2 Urine Biochemistry corrected for Urine Creatinine. Vehicle (n=19) and 60 mg/kg FG2216 (n=20) treated mice. Abbreviations: Sodium (Na), Potassium (K), Chloride (Cl), Inorganic Phosphate (Inorg P). One way ANOVA bonferroni corrected for multiple comparisons. *P<0.05, **P<0.01, ***P<0.001. SEM, Standard Error of the Mean; NS, Not Significant, data shown to four decimal places.

Assay	Units	Vehicle		FG2216 60 mg/kg		P-value
		Mean	SEM	Mean	SEM	
Na	mmol/l	0.0846	0.0019	0.0833	0.0032	NS
K	mmol/l	0.1692	0.0040	0.1644	0.0040	NS
Cl	mmol/l	0.1268	0.0030	0.1231	0.0040	NS
Urea	mmol/l	0.6279	0.0157	0.6033	0.0128	NS
Calcium	mmol/l	0.0008	0.0001	0.0005	0.0000	***
Inorganic Phosphate	mmol/l	0.0132	0.0014	0.0141	0.0011	NS
Glucose	mmol/l	0.0014	0.0002	0.0009	0.0000	**
Urinary protein	µmol/l	0.3782	0.0523	0.4411	0.0326	NS
Uric Acid	µmol/l	0.4450	0.0809	0.1819	0.0403	**

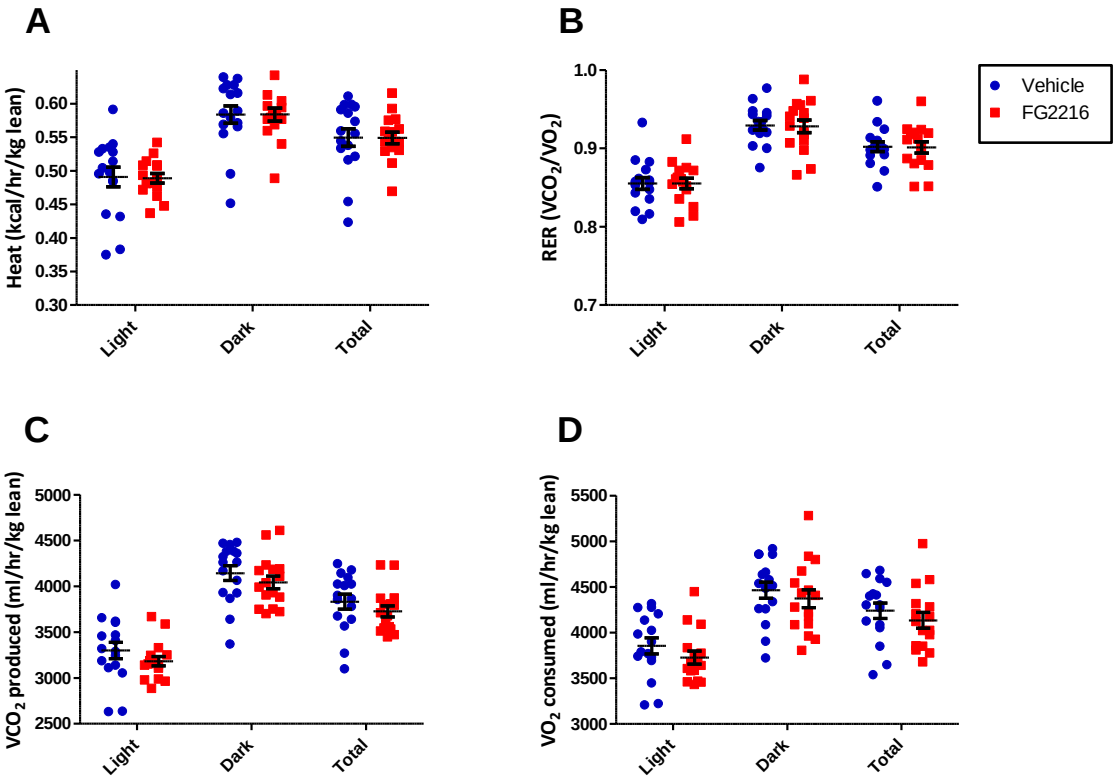

Figure 5.11 Indirect Calorimetry from vehicle and 60 mg/kg FG2216 treated mice. A, Heat, **B**, RER, **C**, Volume of CO_2 produced and, **D**, Volume of O_2 consumed from vehicle treated (n=16) and 60 mg/kg FG2216 (n=16) treated mice, measured by oxymax. Data are expressed as mean ± SEM and individual data points are shown. For details of the lean-mass adjustment made in panels **A, B, C**, see Materials and Methods, *P<0.05, **P<0.01, ***P<0.001. Data are expressed as mean ± SEM and individual data points are shown.

Four weeks into the trial mice were placed into the oxymax to measure indirect calorimetry over a 21 hour period (**Figure 5.11**). Data were corrected for the amount of lean mass of the animals [which was not significantly different (**Figure 5.9D,E**)], and presented as an average during the light phase, dark phase and total time period. Heat and RER were calculated and there was no significant difference between vehicle and drug-treated groups (**Figure 5.11A,B**). There was also no difference in the volume of CO_2 produced or oxygen consumed (**Figure 5.11C,D**). Additionally there was no significant difference in food eaten whilst mice were housed in the oxymax cages (data not shown).

During the fifth week of the trial mice were fasted overnight before undergoing an IPGTT. Individual plots are shown in **Figure 5.12A**, and the average of these can be seen in **Figure 5.12B**.

There was no significant difference at T0, T60 or T120 between vehicle and FG2216 treated mice. If we calculate the AUC for each individual mouse (**Figure 5.12C**) there is no significant difference seen between the groups.

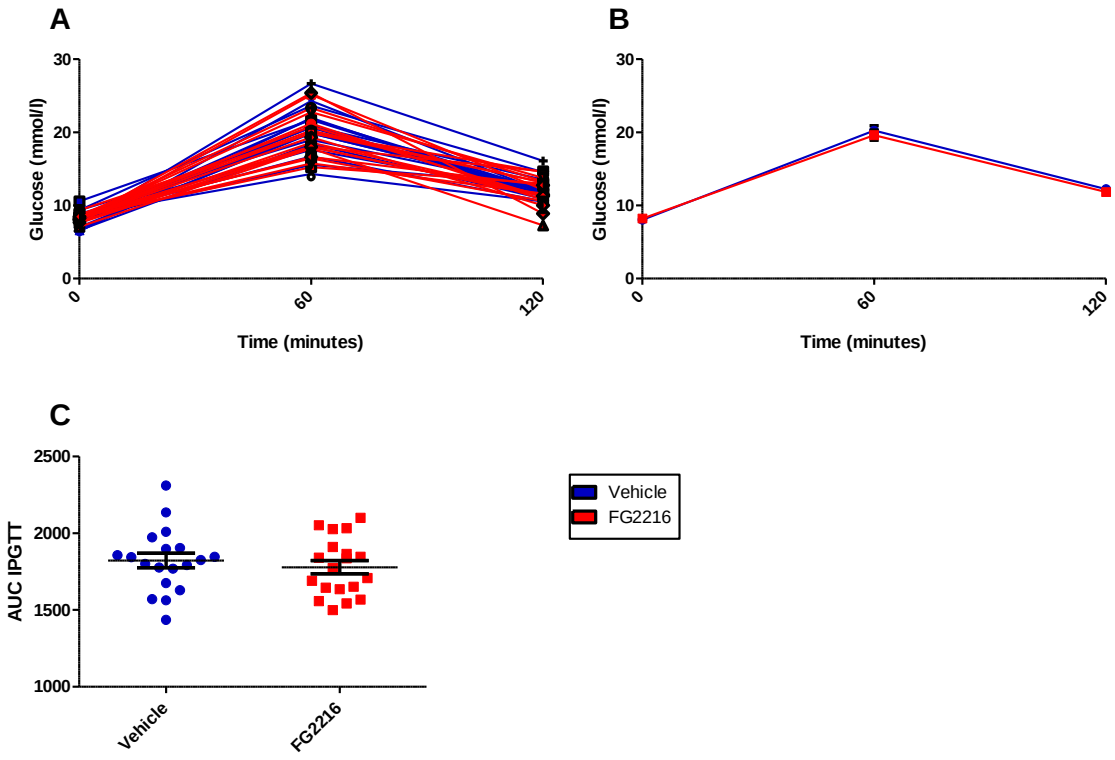

Figure 5.12 Intraperitoneal glucose tolerance test (IPGTT) of vehicle and 60 mg/kg FG2216 treated mice. A, Individual blood glucose curves, **B**, Average blood glucose curves, **C**, Area under the curve (AUC) for vehicle (n=20) and 60 mg/kg FG2216 (n=20) treated mice. Data analysed by student's t-test *P<0.05, **P<0.01, ***P<0.001. Data are expressed as mean ± SEM and individual data points are shown.

At the end of the trial mice were fasted for six hours before being terminally anaesthetised and put into the DEXA. A retro-orbital bleed and dissection were then performed. BMD and BMC were significantly lower in the FG2216 treated mice (P=3.46E-4 and P=1.15E-3 respectively **Figure 5.13A,B**). Liver mass was significantly heavier (P=0.0276) in FG2216 treated mice. A non-linear semi-quantitative examination (Shackelford *et al.*, 2002) of sections of the liver from vehicle and 60 mg/kg FG2216 treated mice by our on-site veterinary pathologist Dr. Cheryl Scudamore, revealed there were no altered pathology in these mice (data not shown). As liver is one of the tissues which produce EPO perhaps this is due to the increased demand of EPO production.

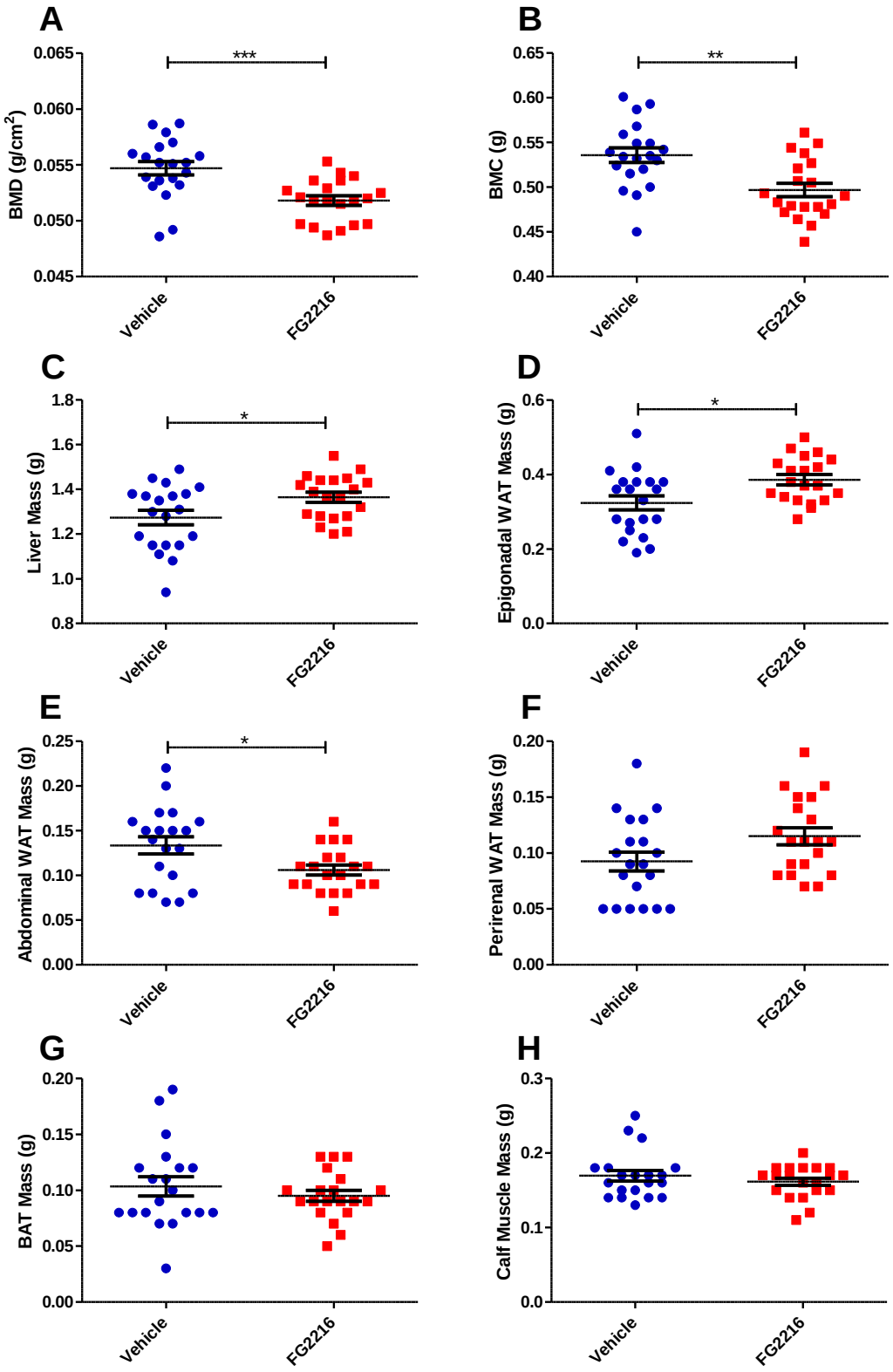

Figure 5.13 DEXA and organ weights of vehicle and 60 mg/kg FG2216 treated mice. A, Bone mineral density (BMD), **B**, Bone Mineral Content (BMC), **C**, Liver mass, **D**, Epigonadal white adipose tissue (WAT), **E**, Abdominal WAT, **F**, Peri-renal WAT, **G**, Brown adipose tissue (BAT), **H**, Calf muscle weight of vehicle (n=20) and 60 mg/kg FG2216 (n=20) treated mice. Data analysed by student's t-test *P<0.05, **P<0.01, ***P<0.001. Data are expressed as mean ± SEM and individual data points are shown.

FG2216 treated mice had significantly increased epigonadal fat pad weights compared to vehicle dosed controls (P=0.0105), but significantly lower abdominal WAT weight (P=0.0186 **Figure 5.13D,E**), which indicates that FG2216 treated mice have an altered preference for location of fat storage. Peri-renal WAT, BAT and calf muscle weights were not significantly different between treatment groups (**Figure 5.13F,G,H**).

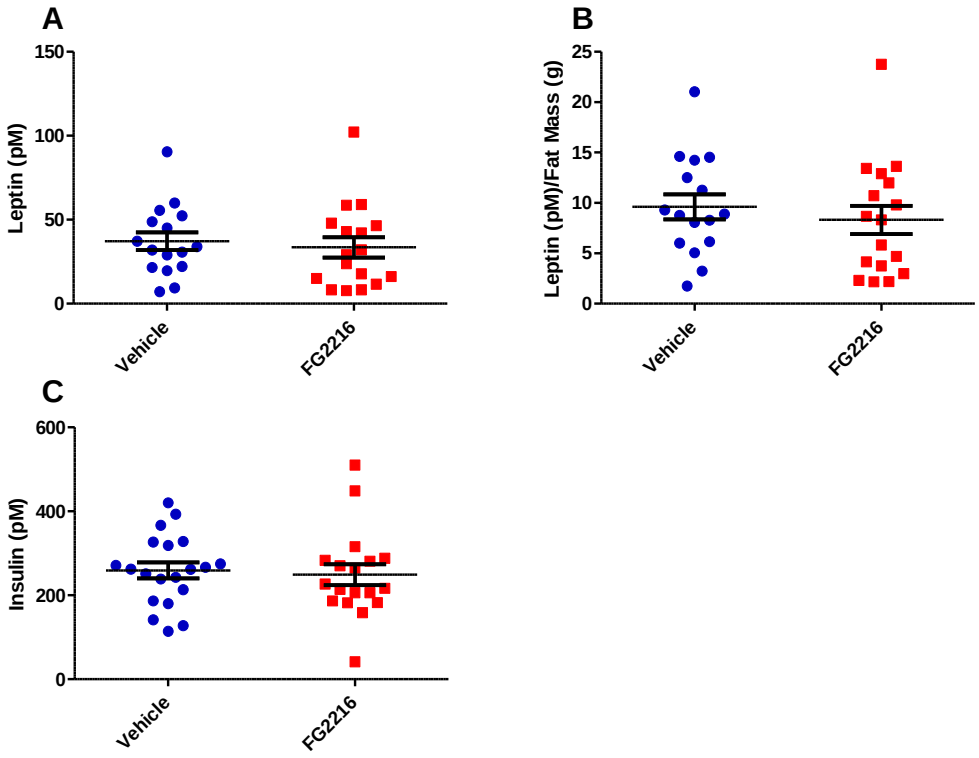

Figure 5.14 Terminal Plasma Leptin and Insulin of vehicle and 60 mg/kg FG2216 treated mice. A, Plasma leptin, **B**, Plasma leptin levels corrected for body fat mass, **C**, Plasma insulin levels from vehicle (n=20) and 60 mg/kg FG2216 (n=20) treated mice. Data analysed by student's t-test *P<0.05, **P<0.01, ***P<0.001. Data are expressed as mean ± SEM and individual data points are shown.

Leptin and insulin were measured in the terminal plasma. There was no significant difference in leptin levels or in leptin levels adjusted for fat mass of the mice (**Figure 5.14A,B**). There was also no significant difference in plasma insulin levels in the FG2216 treated mice (**Figure 5.14C**).

The biochemical profile of the terminal plasma reveals some differences between the vehicle and FG2216 treated animals (**Table 5.3**). FG2216 dosed mice have significantly higher plasma urea (P=2.73E-8), creatinine (P=1.77E-6), ALP (P=4.36E-7) and iron (P=9.83E-5), and significantly decreased levels of chloride (P=1.77E-6), calcium (P=0.0372), inorganic phosphate (P=0.0140), creatinine kinase (P=0.0371) and uric acid (P=0.00172). The levels of total protein show a trend to be decreased (P=0.0526) and total cholesterol shows a trend to be increased (P=0.0587) in FG2216 treated mice.

Table 5.3 Plasma Biochemistry vehicle (n=20) and 60 mg/kg FG2216 (n=20) treated mice. Abbreviations**:** Alkaline Phosphatase (ALP), Alanine Transaminase (ALT), Aspartate Aminotransferase (AST), High-Density Lipoprotein (HDL), Low-Density Lipoprotein (LDL), Lactate Dehydrogenase (LDH), Creatinine Kinase (CK). One way ANOVA bonferroni corrected for multiple comparisons. *P<0.05, **P<0.01, ***P<0.001. SEM, Standard Error of the Mean; NS, Not Significant.

Assay	Units	Vehicle		FG2216 60 mg/kg		P-value
		Mean	SEM	Mean	SEM	
Sodium	mmol/l	143.950	0.407	143.167	0.326	NS
Potassium	mmol/l	6.488	0.456	5.738	0.245	NS
Chloride	mmol/l	106.050	0.285	103.556	0.336	***
Urea	mmol/l	8.522	0.162	10.716	0.274	***
Creatinine	µmol/l	11.960	0.381	17.760	1.040	***
Calcium	mmol/l	1.816	0.056	1.660	0.045	*
Inorganic Phosphate	mmol/l	2.752	0.157	2.280	0.071	*
ALP	U/l	79.675	2.083	99.055	2.410	***
ALT	U/l	30.035	5.485	33.930	5.448	NS
AST	U/l	70.155	6.646	75.030	9.250	NS
Total Protein	g/l	45.440	0.456	42.885	1.418	P=0.0526
Albumin	g/l	23.370	0.317	22.640	0.390	NS
Total Cholesterol	mmol/l	2.150	0.076	2.348	0.068	P=0.0587
HDL	mmol/l	1.310	0.048	1.420	0.045	NS
LDL	mmol/l	0.421	0.017	0.456	0.012	NS
Glucose	mmol/l	17.516	1.521	15.551	1.005	NS
Triglycerides	mmol/l	0.760	0.096	0.682	0.063	NS
Glycerol	µmol/l	319.525	46.491	200.440	11.845	NS
Free Fatty Acids	mmol/l	0.666	0.043	0.689	0.020	NS
Total Billirubin	µmol/l	4.115	0.360	4.038	0.284	NS
LDH	U/l	717.905	69.157	555.617	74.673	NS
Iron	µmol/l	21.450	0.783	28.165	1.330	***
Amylase	U/l	577.435	17.058	563.675	28.378	NS
CK	U/l	159.760	35.694	48.240	2.625	*
Uric Acid	µmol/l	186.260	26.578	92.889	4.401	**
Fructosamine	µmol/l	189.895	2.931	186.625	5.897	NS

5.4 Discussion

5.4.1 Summary

I have so far been unsuccessful at generating a mouse which will express catalytically inactive FTO. We have however identified an inhibitor of FTO, at least *in vitro*, FG2216. This compound is also an inhibitor of HIF-prolyl hydroxylases, and is currently in clinical trials for haemoglobin correction in anaemic non-dialysis patients with chronic kidney disease, and EPO induction in dialysis patients from Fibrogen (Bernhardt *et al*., 2010). It has also been patented for 'fat regulation' and 'treatment of diabetes' by Fibrogen (U.S. Patent numbers: 7618940, 8202834, 8124582). We do not observe a significant impact on body weight and metabolism at the dose we have evaluated.

5.4.2 FTO R316Q Catalytically inactive FTO in man

An R316Q mutation is responsible for an autosomal-recessive lethal syndrome in a large Palestinian Arab consanguineous multiplex family (Boissel *et al*., 2009). Boissel and colleagues showed that this mutation inactivates the enzymatic activity of FTO, preventing conversion of the co-substrate 2OG to succinate and that it was unable to demethylate 3-meT in DNA, which has also been seen with the equivalent mutation in mouse R313A *in vitro* (Gerken *et al*., 2007). They predicted that this is most likely due to the inability of the mutant protein to interact with the co-substrate 2OG.

It is unknown exactly how FTO^{R316Q} causes the debilitating malformations and early lethality seen in these patients. Boissel and colleagues showed that FTO is ubiquitously expressed in fetal as well as adult tissues, with notably high levels in the CNS and liver. This wide spatio-temporal pattern of *FTO* expression is consistent with the broad spectrum of clinical manifestations present in this family. FTO is ubiquitously expressed in the mouse with high levels in the brain, in particular the hypothalamus (Gerken *et al*., 2007, Stratigopoulos *et al*., 2008). FTO is also found to be

ubiquitously expressed, with high levels in the brain when looking at tissues from pigs (Madsen *et al*., 2010), sheep (Sebert *et al*., 2010), and chickens (Wang *et al*., 2012), suggesting that this global expression is evolutionarily conserved.

Skin fibroblasts cultured from one FTO^{R316Q} patient showed an altered cell morphology, decreased proliferation and increased expression of the senescence-associated β-galactosidase (Boissel *et al*., 2009). This is similar to observations by Gulati and colleagues that saw decreased proliferation in $Fto^{-/-}$ MEFs compared to wild-type controls (Gulati *et al*., 2013). In the FG2216 treated C2C12 cells I also see decreased live cells but no difference in dead cells after 16 hours of treatment, which suggests that these cells also have reduced proliferation (**Figure 5.4C,D**). The wild-type and $Fto^{-/-}$ MEFs do not show a significant difference in live/dead staining in my hands (**Chapter 4**), but in **Figure 5.5C,D** the FG2216 treated $Fto^{-/-}$ showed significantly less live staining than wild-type vehicle and FG2216 treated MEFs, but there was no significant difference in vehicle and FG2216 treated wild-type MEFs. Perhaps this suggests that the $Fto^{-/-}$ MEFs and the C2C12s are more sensitive to FG2216 treatment than wild-type MEFs or another cell type, as Tan and colleagues also did not see an effect of FG2216 on proliferation in cardiosphere-derived cells (Tan *et al*., 2011).

It is intriguing that although we see increased early lethality in the $Fto^{-/-}$ mice we have not observed any obvious developmental malformations in the embryos or pups. They appear normal during gestation (E8.5-20 dissected) and following birth, although these have only been gross observations and subtle issues have not been examined. The $Fto^{-/-}$ mice do however show a failure to thrive after P1 and in adulthood are growth retarded compared to wild-type littermates, like the homozygous FTO R313A patients (Boissel *et al*., 2009). This could suggest that FTO has a stronger role in human development or it is possible that the presence of the catalytically inactive FTO might have other biochemical consequences, generating a toxic 'gain-of-function' effect. It is also still a possibility that there could be an undetected mutation in the critical region in these patients, as only the coding regions and splice junctions of the known and putative genes in the 6.5 Mb linked region were sequenced (Boissel *et al*., 2009).

Measurements of heterozygous unaffected family members were not obtained from the study, so conclusions linking the R316Q polymorphisms with body weight and composition cannot be drawn, but it was noted that none of the parents were clinically obese (Boissel *et al*., 2009). Given the results in mice so far perhaps the relatives carrying the mutation would be resistant to becoming obese in a similar way to the FTO deficient mouse models (Fischer *et al*., 2009, Church *et al*., 2009, Gao *et al*., 2010).

5.4.3 FG2216 Trial Limitations

Unfortunately we did not see a significant effect of FG2216 treatment on body weight or composition. We did see increased EPO expression in plasma and liver (**Figure 5.6** and **Figure 5.7**). As FG2216 can inhibit HIF prolyl-hydroxylase, which causes stabilisation of HIF and increases signalling in the HIF pathway, we had anticipated some off-target effects *in vivo*, such as increases in plasma EPO, which we observed. This suggests that the compound is being successfully delivered to the animals, but it may not be a high enough dose or via the correct route to see an effect on FTO.

We do not know the half-life of the drug in the mouse, so the dosing regimen may not have kept levels in the plasma high enough to see an effect on FTO, we could therefore increase the dosing to daily and/or increase the dose of the drug administered. Hsieh and colleagues dosed mice with 60 mg/kg intravenously into the tail vein and saw an increase in EPO levels of 100-fold four hours after treatment with FG2216 (Hsieh *et al*., 2007), which is similar to the fold increase we saw after 1 week and after 40 days (**Figure 5.6**). This suggests that there is not an increased effect with intravenous administration, which is beneficial to us as multiple dosing by oral gavage is a less stressful method to administer our drug than multiple intravenous injections. Hsiesh and colleagues also dosed rhesus macaques 60 mg/kg twice weekly over a period of 6-8 weeks and saw no side-effects, which indicated to us that it may be sufficient to dose mice on alternate days.

FTO is highly expressed in the brain and CNS, and although we have shown that adult *AAV*-Cre deletion in the hypothalamus is not sufficient to induce body composition and weight differences,

we cannot rule out that the adult onset knockout phenotype is not due to FTO deletion in a region of the brain and/or in combination with peripheral tissues (McMurray *et al*., 2013). Gao and colleagues used a *Nestin*-Cre line to induce *Fto* knockout in the nervous system and were able to replicate the phenotype in the whole body $Fto^{-/-}$ although they did not use a *Nestin*-Cre control group in their study (Gao *et al*., 2010). The *Nestin*-Cre alone has a body weight and growth retarded phenotype, which does confound analysis of these results [reviewed in (Harno *et al*., 2013)]. Recently it has been shown that $Fto^{-/-}$ mice have a diminished response to cocaine dosing, suggesting a role for FTO in D2R and mediated signalling (Hess *et al*., 2013). Dopaminergic signalling is important to locomotor function, reward, and cognition, so perhaps an altered reward response could lead to increased/decreased weight gain.

We do not know if FG2216 can penetrate the BBB. Only a small class of drugs can actually cross the BBB, they are small molecules with a high lipid solubility and a low molecular mass (Mr) of < 400–500 Da (Pardridge, 2003). If molecules do not meet these criteria then the hydrogen-bonding potential, charge, and conformation of the molecule come into play, and for any given molecule, one of these factors may dominate others (Ajay *et al*., 1999). FG2216 has a molecular weight of 280.66 g/mol or 280.66 Da so is small enough but due to the charged side chains may not be lipid soluble (**Figure 5.3A**).

There are also active mechanisms, which generally depend upon some specificity of molecular recognition and solute concentration at the transporter. Therefore BBB permeability is affected by other factors that determine solute concentration at the brain capillary surface, including plasma protein binding, blood flow through and partitioning into capillary membranes, and distribution into brain parenchyma. These and other parameters such as absorption, first-pass metabolism, distribution into other tissues and elimination pathways are in turn complex functions of physicochemical, biochemical, and physiological determinants, not all of which are directly related to the chemical structure of the drug (Burton *et al*., 2002, Goodwin and Clark, 2005).

In the next trial it would be beneficial to collect blood, brain, cerebrospinal fluid and analyse this by LC-MS/MS to estimate brain exposure to FG2216 (Friden *et al*., 2010). An alternative is to bypass the BBB and deliver FG2216 directly to the brain using an intracranial cannula to allow prolonged dosing.

On a final note, the patients described by Boissel and colleagues had multiple congenital abnormalities so careful assessment would need to be taken when screening FG2216 and other FTO inhibitors for teratogenicity and other toxic effects.

5.4.4 Effects of Prolyl-Hydroxylases Inhibitors

Inhibition of HIF prolyl-hydroxylases stabilises HIF, leading to activation of the HIF pathway which is normally stimulated during hypoxic conditions. It has also been shown that stabilisation of HIF-1a mediates adaptation to hypoxia by downregulating mitochondrial oxygen consumption thereby shunting glucose to glycolysis to maintain ATP production (Kim *et al*., 2006, Papandreou *et al*., 2006). Previous studies have shown that *in vitro* use of other prolyl-hydroxylases inhibitors such as dimethyloxalylglycine (DMOG) also decrease oxygen consumption rate and increase extracellular acidification rate, suggesting that these drugs downregulate mitochondrial oxidative phosphorylation and increase levels of glycolysis (Sridharan *et al*., 2007). FG2216 has also previously been shown to decrease oxygen consumption in this way (Tan *et al*., 2011) and we were able to replicate this effect in C2C12 myoblast cells. We also treated wild-type and *Fto*$^{-/-}$ MEFs to see how much of this was due to inhibition of FTO and what were off-target effects such as inhibition of the PHD proteins. When stimulated with FCCP to identify the maximal respiratory capacity of the cells the FG2216 treated wild-type and *Fto*$^{-/-}$ MEFs had a significantly lower OCR than wild-type vehicle treated cells. The vehicle treated *Fto*$^{-/-}$ MEFs had an intermediate phenotype, with higher OCR than the FG2216 treated cells but lower than the vehicle treated wild-type MEFs, this suggests that a proportion (approximately 22 %) of the maximal respiratory capacity of the cells is affected by FTO inhibition or deletion in MEFs.

PHDs which degrade HIF-1a are not the only prolyl-hydroxylases; there are many enzymes which share this motif [a list of assigned or proposed genes is reviewed in (Rose *et al*., 2011)]. For example, collagen prolyl-hydroxylase, which needs vitamin C to function and leads to scurvy when vitamin C is deficient, and Prolyl 3-hydroxylase 1 which when knocked out causes osteogenesis imperfecta, or brittle bone disease (Marini *et al*., 2007).

The FG2216 treated mice had lower BMD and BMC than vehicle treated controls. Administration of EPO has previously been shown to increase bone formation *in vivo* via the Jak-Stat signalling pathway (Shiozawa *et al*., 2010). However, this was looking at mice dosed with EPO rather than a PHI and other experiments suggest that PHIs can act to reduce osteoclast differentation (Leger *et al*., 2010). Osteoclasts are important for bone resorption, and we do see significantly lower calcium and inorganic phosphate in the plasma of the FG2216 treated mice, which could suggest a decrease in bone resorption but this still does not explain the phenotype we saw. BMD and BMC are significantly lower in the global *Fto*$^{-/-}$ mice (unpublished in house data) but we did not see a BMD or BMC effect when *Fto* was knocked out in the adult mouse (**Chapter 3**), which would indicate adult knockdown or inhibition would not cause this phenotype. There are many types of prolyl-hydroxylase, some of which are important in collagen and bone formation, and if FG2216 can also inhibit for example prolyl 3-hydroxylase, this could cause brittle bone disease in our mice (Marini *et al*., 2007). If we repeat this study it would be important to investigate this phenotype in greater detail.

We also observed low uric acid in the urine and plasma of FG2216 treated mice. In FTO adult knockout mice a decrease in uric acid was only seen in the urine at 19 weeks of age. This could indicate that FG2216 may also inhibit xanthine oxidase, an enzyme which metabolises xanthine to produce uric acid and superoxide. Xanthine has a purine ring structure and so is similar to adenosine and guanosine, so FG2216 may also bind to this enzyme, and inhibit its function. Inhibitors to this enzyme are currently used to treat gout, and interestingly they are also suspected of having teratogenic effects (Fujii and Nishimura, 1972, Kozenko *et al*., 2011). This could indicate that inhibition of xanthine oxidase or an off-target enzyme, such as FTO or another prolyl-

hydroxylase could cause malformations in offspring. The child in this study had some similar phenotypes such as cleft palate and urogenital anomalies as the family described by Boissel and colleagues but also presented with other malformations such as microtia, micrognathia, hypertelorism and lung defects.

Other changes we see in the FG2216 treated mice, which are not seen in the FTO adult knockout mice, could be related to stabilisation of HIF and increases in EPO. For example low plasma chloride levels. These are indicative of a lack of oxygen, and are likely caused by increased chloride being bound to deoxygenated haemoglobin, and the FG2216 treated mice have an increased number of available erythrocytes (Weber, 2007). They also have increased iron, which is also probably due to the increase in erythrocyte numbers.

Having a higher EPO level has often been seen as a positive thing. Living at a high altitude has been shown to be inversely correlated with obesity prevalence in the USA (Voss *et al*., 2013), and with BMI, waist circumferences, and WHR in Tibetans (Sherpa *et al*., 2010). A study looking at EPO overexpression in HFD fed mice, showed improved glucose tolerance, reduced weight gain and fat mass (Hojman *et al*., 2009). There is also another study where dosing with EPO also improved glucose tolerance and weight gain on mice fed a HFD (Hojman *et al*., 2009, Meng *et al*., 2013). It has also been observed that EPO can improve insulin resistance in 3T3 cells (Pan *et al*., 2013). Despite these results several studies looking at normal subjects dosed with EPO did not show an improvement in metabolic function or body composition [reviewed in (Lundby and Olsen, 2011)]. There have also been several studies investigating if EPO improves exercise capacity, but there is no evidence indicating that EPO should increase exercise performance by mechanisms other than increasing oxygen transport capacity (Lundby and Olsen, 2011).

5.4.5 Future Plans

The results of these experiments show that dosing mice with FG2216 at 60 mg/kg on alternate days does not affect body weight, body composition or RER. We shall continue to generate mice which will overexpress Fto^{R313A} as it will be interesting to see if they are protected from the weight gain

we see in our *Fto* overexpression mice, and see if the demethylase function is critical for the phenotype we see (Church *et al*., 2010). When crossed with the $Fto^{-/-}$ mice they will also be useful to investigate the developmental effects of FTO, as perhaps expressing this mutated form will result in the severe development issues observed in humans homozygous for FTO^{R316Q} (Boissel *et al*., 2009).

In the future it would be ideal to follow up this experiment with an increased dose in mice, to see if we can see an effect *in vivo*. To ensure levels of FG2216 are more constant we could dose mice daily and we could increase the dose of FG2216, if toxicity trials reveal no side-effects. I think that it would also be interesting to see the effect of treating a second cohort which have been fed a HFD from weaning, as FG2216 may show a stronger effect when a stress such as HFD is used. When Hojman and colleagues overexpressed EPO the effect was more apparent on mice being fed a HFD than a standard chow (Hojman *et al*., 2009). It would also be intriguing to treat mice with FG2216 by intracranial cannula, to ensure exposure of the brain to the drug.

Screening some of the other FTO inhibitors identified by Chris Schofield's group would allow us to see if we generate similar results. It would also be interesting to screen some of the PHIs that do not inhibit FTO. This would allow us to identify some of the off-target effects in the mice, and may also allow us to identify which structures are likely to have unwanted side-effects, such as decreasing BMC and BMD. It would also be worth investigating methylation levels after pharmacological treatment to see if we can replicate any of the potential targets of FTO (Hess *et al*., 2013, Karra *et al*., 2013) or show general differences in methylation levels *in vitro* and *in vivo*.

Chapter 6:

Gut Hormone Analysis of *Fto* Overexpression Mice

6.1 Introduction

There are many examples of SNPs in and around *FTO* that are associated with increased BMI (Frayling *et al*., 2007, Thorleifsson *et al*., 2009), increased percentage body fat (Kilpelainen *et al*., 2011b), and increased WHR and waist size (Lindgren *et al*., 2009). These effects have been observed across different ages and populations (Adeyemo *et al*., 2010, Lauria *et al*., 2012). One question from these studies is why do these individuals have increased measures of obesity? Do they have an altered metabolism and are predisposed to storing more fat, or is this due to increased food intake and increased intake of calorie rich foods?

Satiety and hunger are controlled by complex neuronal mechanisms and multiple hormones, including those secreted from the gastrointestinal tract. These gut hormones are differentially affected by food intake. Ghrelin is orexigenic and so its levels are high before meals and are suppressed in response to food intake. Others such as PYY and the incretins, GLP-1 and GIP, are anorexigenic, and are released in response to food intake to increase satiety. The hormone leptin which is released from adipose tissue is also anorexigenic. Leptin has been famously reported to control food intake and body weight by studying leptin deficient (*ob/ob*) (Ingalls *et al*., 1950) and leptin receptor deficient (*db/db*) mice (Bahary *et al*., 1990) mice. Both of these mice are obese and hyperphagic due to disrupted leptin signalling.

FTO is ubiquitously expressed and in rodents has been shown to be expressed throughout the brain (Gerken *et al*., 2007, McTaggart *et al*., 2011). There is some evidence that FTO is nutritionally regulated in the brain by fasting, although upregulation (Fredriksson *et al*., 2008, Olszewski *et al*., 2009), downregulation (Gerken *et al*., 2007, Wang *et al*., 2011b) and no significant differences (McTaggart *et al*., 2011, Olszewski *et al*., 2011b) have been reported. Levels of FTO have been shown to be downregulated *in vitro* by removal of glucose or total amino acid levels from the tissue culture media, and that when replaced FTO expression levels are restored (Cheung *et al*., 2013). Gulati and colleagues have also shown that FTO may play a role in nutrient sensing and have described a role for FTO in the coupling of amino acid levels mTORC1 signalling (Gulati *et al*., 2013). One study has found an inverse relationship between FTO and satiety, and that *Fto* levels in the hypothalamus were reduced *in vitro* after the addition of leucine, which *in vivo* reduces feeding and activates anorexigenic neurons synthesizing POMC (Olszewski *et al*., 2009).

Studies in man so far have associated SNPs in *FTO* with increased energy intake. Adults and children homozygous for the risk A allele rs9939609 have been shown to not only have an increased food intake but also a preference for food with a higher energy and fat content (Cecil *et al*., 2008, Speakman *et al*., 2008, Timpson *et al*., 2008, Tanofsky-Kraff *et al*., 2009, Wardle *et al*., 2009, Sonestedt *et al*., 2009). Children and adults with the risk allele have also been shown to have diminished satiety responses compared with this with the T allele (Wardle *et al*., 2008, den Hoed *et al*., 2009). Recently Karra and colleagues have also observed attenuated post-prandial responses in AA carriers in terms of hunger and circulating acyl-ghrelin levels. Subjects also underwent fMRI scans, which revealed that *FTO* genotype modifies responses to food images in homeostatic and reward regions in the brain, such as the hypothalamus and ventral tegmental area (Karra *et al*., 2013). They also demonstrated that $Fto^{-/-}$ mice have higher levels of total ghrelin after a 16 hour fast and in the fed state, with no significant difference in acyl-ghrelin levels (Karra *et al*., 2013). *Fto* has also been reported to affect reward pathways by impairing dopamine receptor 2 and 3 dependent control of neuronal activity and behaviour (Hess *et al*., 2013).

Mice which ubiquitously overexpress *Fto* gain significantly more weight and are hyperphagic compared to wild-type littermates (Church *et al*., 2010). The increased FTO levels lead to a dose-dependent increase in body and fat mass, irrespective of whether they are fed standard or a high-fat diet, however the food intake was more markedly increased when fed a HFD (Church *et al*., 2010). These results mirror the increased food intake seen in human subjects with the A-risk allele having increased food intake, and a preference for high energy foods. These subjects also have a diminished satiety responses and I wanted to investigate the mechanisms involved in the phenotype of these mice and see if dysregulated gut hormones could play a role. Wild-type mice with the two endogenous copies of *Fto* are called FTO-2, and mice which have 2 additional copies of the *Fto* gene are referred to as FTO-4.

6.2 Methods

6.2.1 Gut Hormone Assessment

Ten FTO-2 and ten FTO-4 mice of each sex were phenotyped for food intake and gut hormone levels. Animals receive HFD (D12451, Research Diets, New Brunswick, NJ, U.S.A.) containing 45 kcal % fat, 20 kcal% protein and 35 kcal% carbohydrate (4.7 kcal/g) once weaned to enhance the phenotype as in (Church *et al*., 2010). A summary of the phenotyping protocol is shown in **Figure 6.1**.

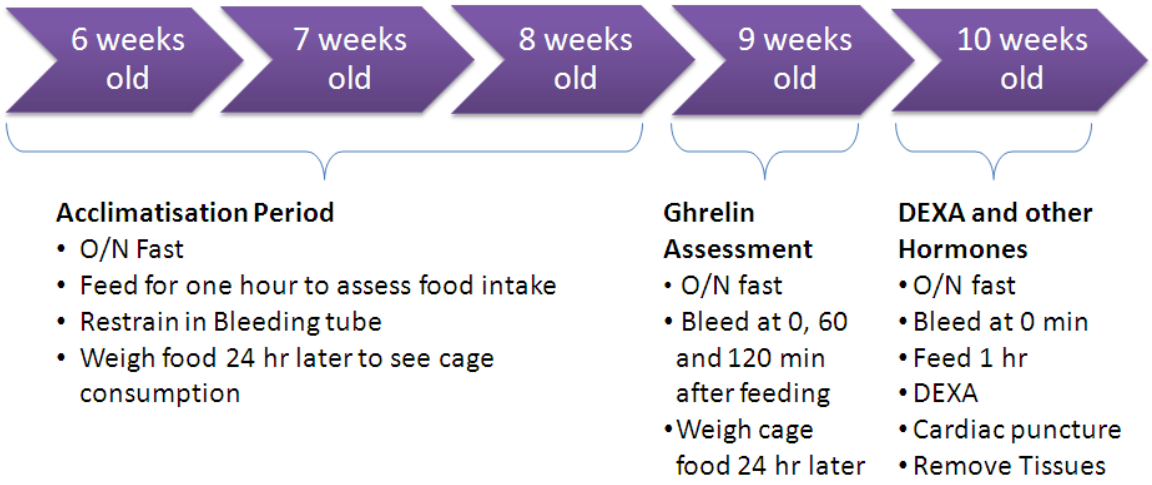

Figure 6.1 Phenotyping pipeline for mice undergoing gut hormone assessment.

Acclimatisation period – 6-8 weeks old

Animals were weighed and fasted overnight for 16 hours. Animals were then reweighed and placed into individual cages and given a weighed food sample of approximately four pellets. After one hour food intake was assessed by reweighing food pellets. Mice were restrained in a bleeding tube for 30 seconds to acclimatise them to the procedure and returned to their home cage.

Ghrelin & Leptin Assessment – 9 weeks old

Animals were weighed and fasted overnight for 16 hours. The mice were then reweighed and a local anaesthetic (EMLA cream, Eutectic Mixture of Local Anaesthetics, Lidocaine/Prilocaine, AstraZeneca, U.K.) was applied to their tails. A blood sample at baseline (T0) was then taken and 2 ul 4-(2-Aminoethyl) benzenesulfonyl fluoride hydrochloride (AEBSF) (Sigma-Aldrich, Dorset, U.K.) was immediately added to prevent degradation of ghrelin and the sample placed on ice. Animals were placed into individual cages and given a weighed food sample of approximately four pellets. After one and two hours food intake was assessed by reweighing food pellets, and blood samples collected as described previously (**Chapter 2 Section 2.7.4**). Animals were then returned to their home cage when phenotyping was complete.

Plasma was collected as described in the general methods and 1 ul 1 M HCl/10 ul was added to acidify sample for ghrelin measurement. Samples were stored at -20 °C.

DEXA and Gut Hormone Panel Assessment - 10 weeks old

Mice were weighed and fasted overnight for 16 hours. The mice were then reweighed and a local anaesthetic (EMLA cream, Eutectic Mixture of Local Anaesthetics, Lidocaine/Prilocaine, AstraZeneca, U.K.) was applied to their tails. A blood sample at baseline (T0) was then taken and 2 ul AEBSF and 2 µl serine protease inhibitor cocktail (Sigma-Aldrich, Dorset, U.K.) were immediately added to prevent degradation of gut hormones and the samples were stored on ice. Animals were placed into individual cages and given a weighed food sample of approximately four pellets. After one hour food intake was assessed by reweighing food pellets, and mice were given a lethal dose of anaesthetic (Euthatal 200mg/ml solution at a dose of approximately 150mg/kg) administered by IP injection. Unconscious mice were analysed by DEXA and blood was collected by cardiac puncture using a syringe which contained approximately 2 ul dipeptidyl peptidase IV inhibitor (Sigma-Aldrich, Dorset, U.K.). Once collected 2 ul AEBSF and 2 µl serine protease inhibitor cocktail were immediately added to prevent degradation of gut hormones and the sample

stored on ice. The hypothalamus of each mouse was grossly dissected and snap-frozen using liquid nitrogen.

Assessment of gut hormone levels was achieved using the Milliplex mouse Gut hormone panel (Millipore, Massachusetts, U.S.A), and analysis performed on the Bioplex suspension array system (Biorad, Munich, Germany). Nine week plasma samples were analysed for the active form of ghrelin (acyl-ghrelin) and leptin, whilst ten week samples were analysed for: amylin (active), ghrelin (active), GIP (total), GLP-1 (active) and PYY (total).

6.2.2 qRT-PCR analysis of Gene Expression in Hypothalami

RNA was extracted and gene expression in the whole hypothalamus was analysed using quantitative real-time PCR as described in the materials and methods (**Chapter 2 Section 2.3.3**). Taqman Assay identifications for each Taqman probe are given in **Table 6.1**.

Table 6.1 Taqman Gene Expression Assay, Probe Assay Identification.

Gene Name	Taqman Assay ID
Gapdh	4352932-1211040
Pomc	Mm00435874_m1
Npy	Mm00445771_m1
Agrp	Mm00475829_g1
Ghsr	Mm00616415_m1
Npy2r	Mm00435350_m1
Lepr	Mm00440181_m1
Cnr1	Mm01212171_s1
Cartpt	Mm00489086_m1
Pmch	Mm01242886_g1
Fto	Mm00488755_m1

6.3 Results

6.3.1 Body Weight and Food Intake

At four weeks of age mice were weaned on to a HFD. To effectively measure gut hormones and food intake it was important to look at the changes before the mice began to diverge in body weight. Based on the results of Chris Church we decided to look at food intake between six and ten weeks of age (Church *et al*., 2010). This allowed the mice to adapt to being weaned on to the HFD and then we could acclimatise them to the stress involved in the fasting and refeeding experiments. Stress in rodents has been shown to reduce food intake, making it difficult for anorexigenic agents to further suppress appetite (De Souza *et al*., 2000, Halatchev *et al*., 2004), therefore we repeated the procedure 3 times before carrying out blood sampling at nine and ten weeks of age.

Body weight was measured weekly prior to fasting the animals overnight for 16 hours (**Figure 6.2**). The female FTO-4 mice did not weigh significantly more than the FTO-2 mice during the five week trial. The male FTO-4 mice did show a trend for increased body weight compared to FTO-2 mice, but this was only significantly different at 7 weeks of age. This effect may be caused by the weekly fasting regime that these mice experienced, however this was beneficial to our study as we did not want a significant difference in body weight affecting the gut hormone trial.

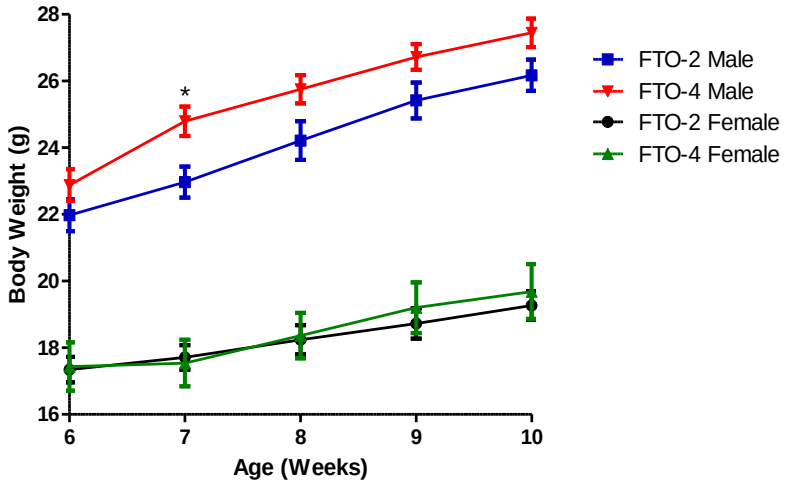

Figure 6.2 Weekly Body Weight of Male and Female FTO-2 and FTO-4 Mice. Weekly body weight of FTO-2 and FTO-4 female (n=10 and n=12 respectively) and male (n=11 and n=10 respectively). The Time-course data were analysed using a 2 way ANOVA with bonferroni post-test *P<0.05, **P<0.01, ***P<0.001. Data expressed as mean ± SEM.

Mice were fasted overnight for 16 hours and reweighed and percentage change in body weight was calculated (**Figure 6.3A,B**) (data unavailable for weight after 16 hours in male FTO-4 mice at six weeks of age). At six and seven weeks of age in the females (P=0.019 and P=0.00013 respectively **Figure 6.3A**) and at seven weeks of age in the males (P=5E-07 **Figure 6.3B**) the FTO-4 mice lost significantly more weight than wild-type littermates, although there were no significant differences at eight, nine or ten weeks of age. The female FTO-4 mice have previously been shown to have an anxiety phenotype in the open field phenotyping test (Church *et al*., 2010). Therefore this loss of a significant difference is likely due to the mice becoming acclimatised to the procedure.

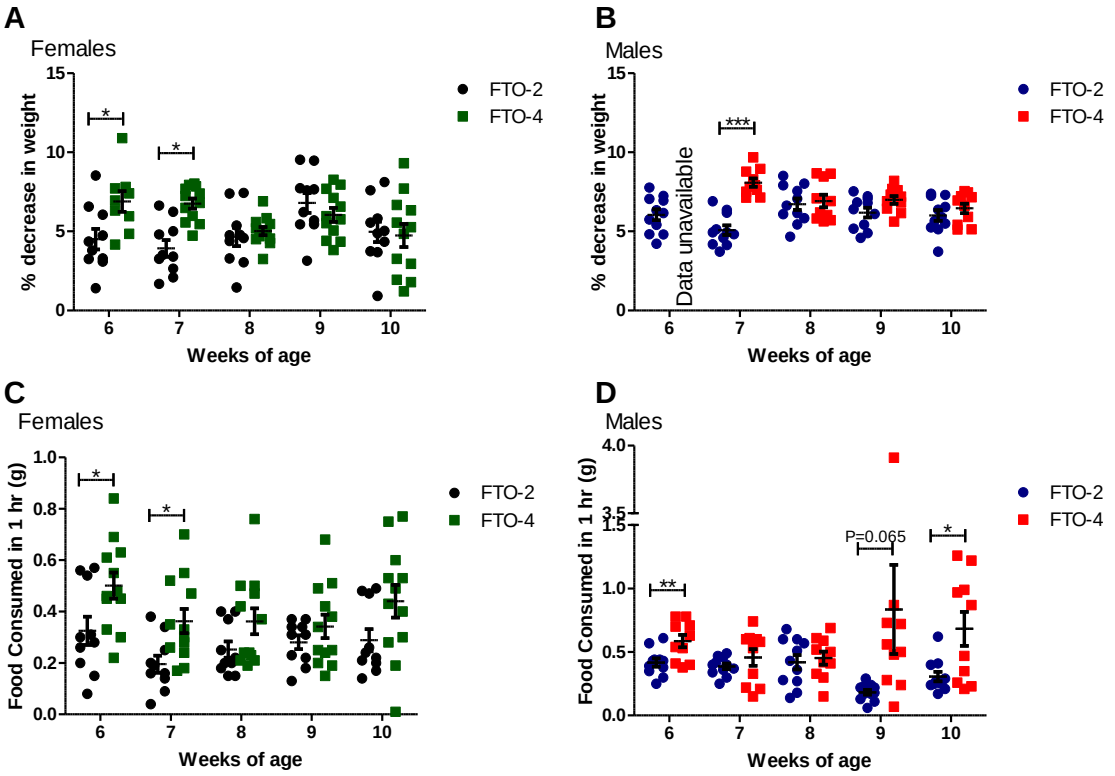

Figure 6.3 Weekly Decrease in Body Weight after 16 hour Fast and Food Consumed in one hour Following Fast in Male and Eemale FTO-2 and FTO-4 Mice. Weekly percentage decrease in body weight following an overnight 16 hour fast in female **A**, and male **B** FTO-2 and FTO-4 mice. Weekly food consumed in one hour following a 16 hour fast in female **C** and male **D** FTO-2 and FTO-4 mice. Female FTO-2 n=10 and FTO-4 n=12, male FTO-2 n=11 and FTO-4 n=10. Data analysed at each time point by student's t-test *P<0.05, **P<0.01, ***P<0.001. Data expressed as mean ± SEM.

Food intake was measured for one hour following the overnight 16 hour fast. Female FTO-4 mice had higher food intake levels throughout the study, but this was only significant at six and seven weeks of age (P=0.029 and P=0.011 respectively, **Figure 6.3C**). Male FTO-4 mice also showed a trend for increased food intake and consumed significantly more than FTO-2 mice at six and ten weeks of age (P=0.009 and P=0.011 respectively, **Figure 6.3D**).

At nine weeks of age food intake was measured for an additional hour, and blood samples were collected at T0, 60 and 120 minutes. Food intake for female mice was not significantly different during one or two hours following the overnight fast (**Figure 6.4A**). Food intake for male FTO-4 mice during this trial was increased, after 1 hour FTO-4 mice ate 0.84 ± 0.35 g compared to 0.18 ± 0.02 g eaten by FTO-2 male mice (**Figure 6.4B**). This was not significantly different after one hour

(P=0.065), although it was after two hours (P=0.035). This result was affected by one outlier, who was calculated to have consumed 3.91 g after 1 hour and 4.08 g after 2 hours (1 hour data can be seen in **Figure 6.3D**), although I believe that this must be an error when the food pellets were initially weighed. If the data from this mouse is removed it can be observed that the FTO-4 male mice have significantly increased food intake after one and two hours **Figure 6.4C**.

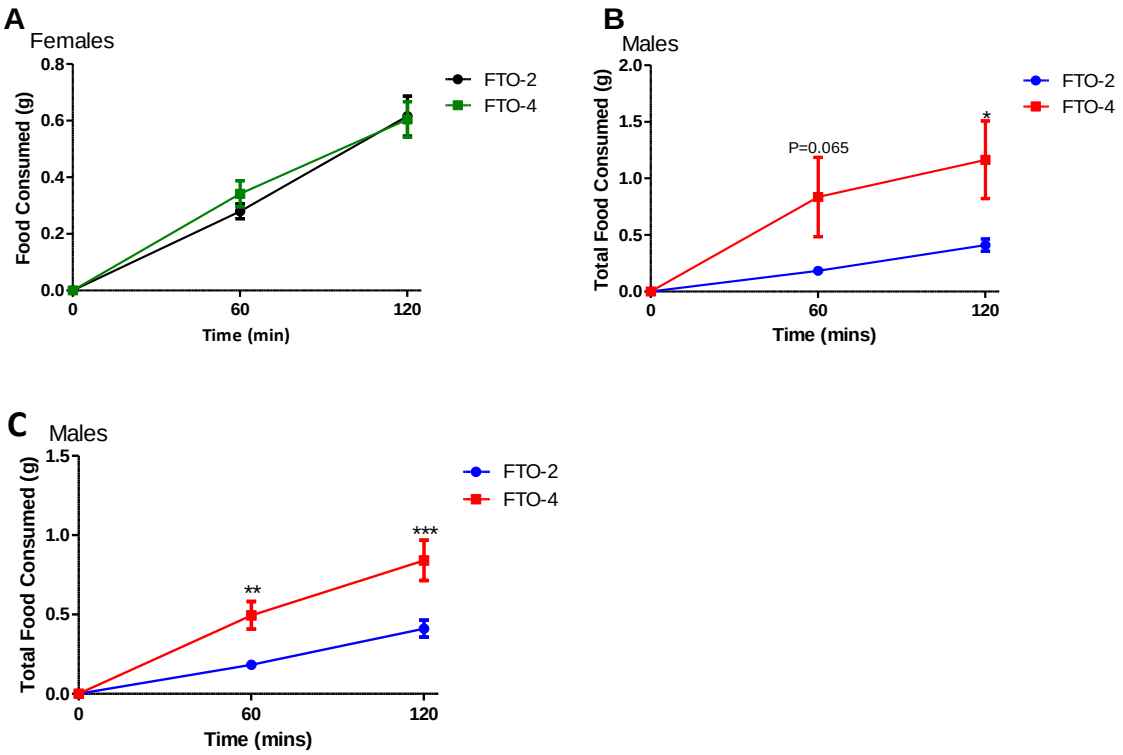

Figure 6.4 Two hour Food Intake Following a 16 hours Fast in Nine week old Male and Female FTO-2 and FTO-4 Mice. Food consumed during a two hour period following a 16 hour fast is female **A**, and male **B** FTO-2 and FTO-4 mice. Data in **C** is the same as **B**, but with the data from one outlier (visible in **Figure 6.3D**) removed. Female FTO-2 n=10 and FTO-4 n=12, male FTO-2 n=11 and FTO-4 n=10, except in **C** where FTO-4 males n=9. Data analysed by 2-way ANOVA with bonferroni correction *P<0.05, **P<0.01, ***P<0.001. Data expressed as mean ± SEM.

6.3.2 Body Composition and Bone Analysis

On the final day of the study, following an overnight fast and one hour of feeding mice were culled and body composition was examined using DEXA analysis (**Figure 6.5**). At ten weeks of age male and female FTO-4 mice do not weigh significantly more than their FTO-2 counterparts (**Figure 6.2**). Lean mass is not significantly altered in female FTO-4 compared to FTO-2 mice (**Figure 6.5A**), but male FTO-4 mice do have significantly more lean mass than wild-type males (19.86 ±

0.487 g compared to 18.35 ± 0.418 g, P=0.0293 **Figure 6.5B**). Female and male FTO-4 mice did not have significantly more fat mass than wild-types (**Figure 6.5C,D**).

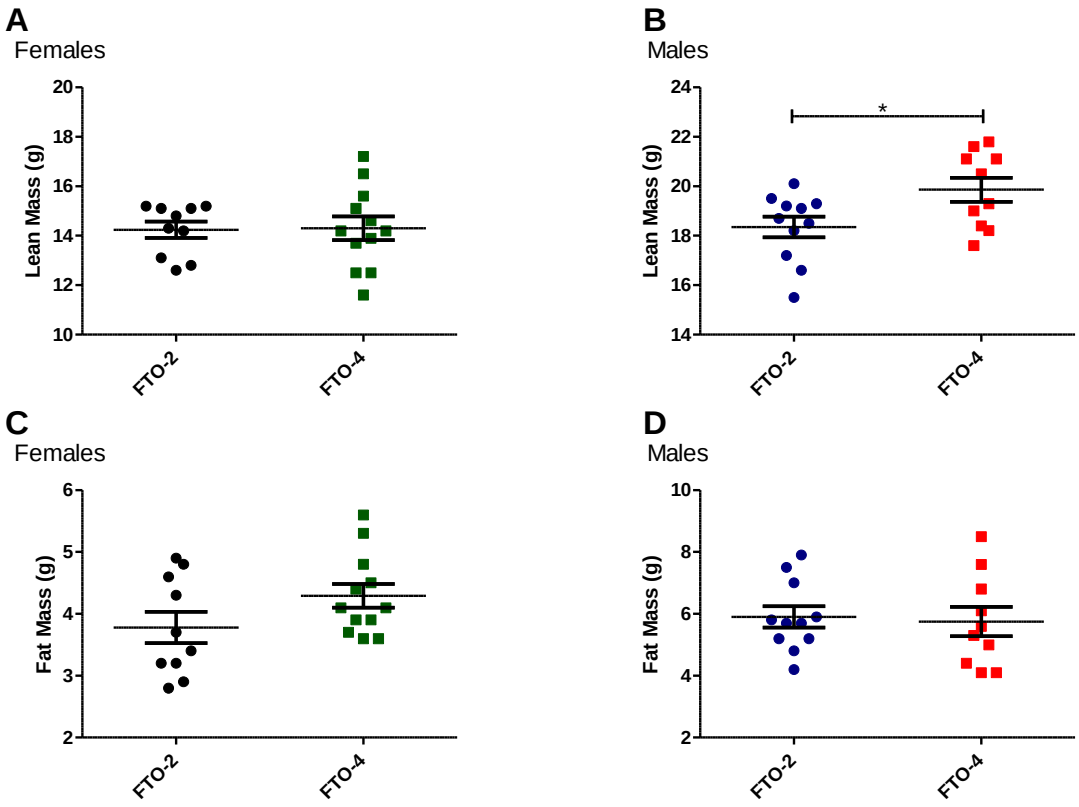

Figure 6.5 DEXA Analysis of Lean and Fat Mass from Male and Female FTO-2 and FTO-4 Mice at 10 weeks of age. Lean mass measured by DEXA at 10 weeks of age in female **A** and male **B** FTO-2 and FTO-4 mice at 10 weeks old. Fat mass measured by DEXA at 10 weeks of age in female **C** and male **D** FTO-2 and FTO-4 mice at 10 weeks old. Female FTO-2 n=10 and FTO-4 n=12, male FTO-2 n=11 and FTO-4 n=10. Data analysed by student's t-test *P<0.05, **P<0.01, ***P<0.001. Data expressed as mean ± SEM.

DEXA analysis also measures BMD and BMC (**Figure 6.6**). Female BMD is not significantly altered, but male FTO-4 mice have significantly increased BMD compared to wild-types (0.0535 ± 0.00096 g/cm^2 compared to 0.0507 ± 0.00047 g/cm^2, P=0.0185). This is also true of the BMC, with no significant difference in the females, but male mice have significantly increased BMC (0.467 ± 0.0105 g compared to 0.434 ± 0.00 g, P=0.00658). We have found previously that male and female FTO-4 mice at 20 weeks old had significantly higher BMC, and that their BMD was increased although not significantly (unpublished data).

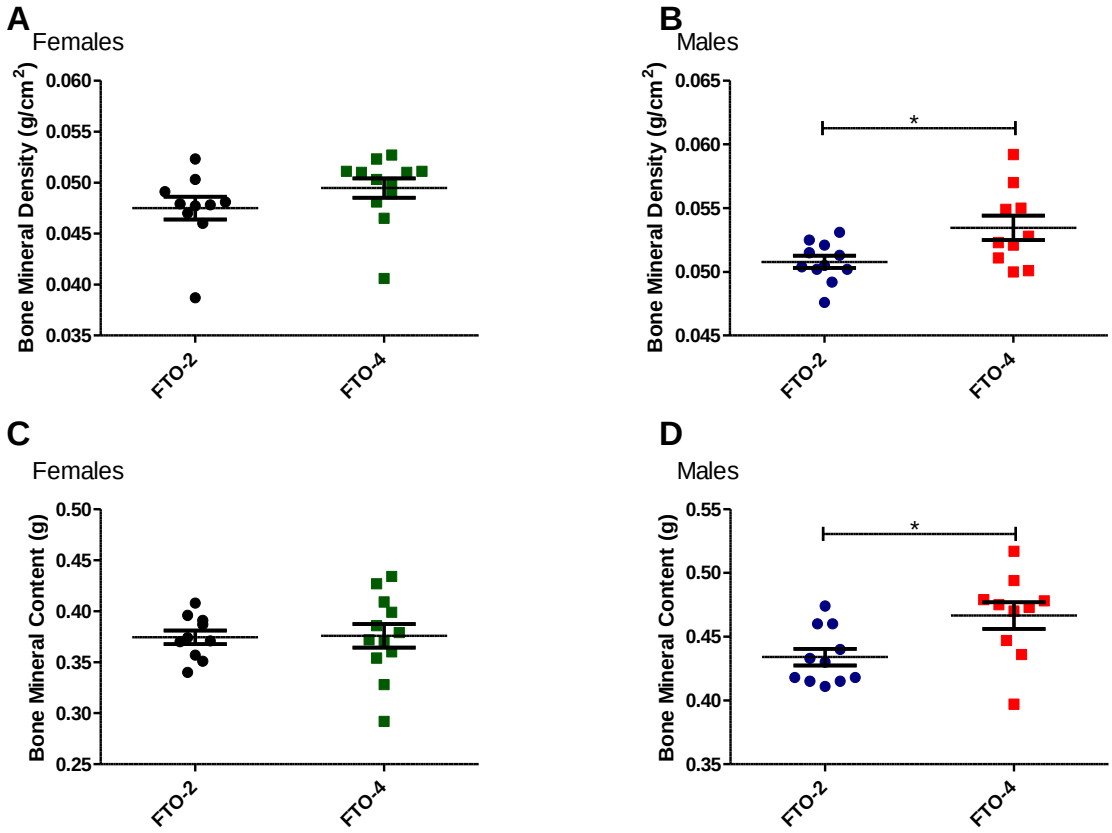

Figure 6.6 DEXA Analysis of BMD and BMC in Male and Female FTO-2 and FTO-4 mice at 10 weeks of age. Bone mineral density (BMD) measured by DEXA at 10 weeks of age in female **A** and male **B** FTO-2 and FTO-4 mice at 10 weeks old. Bone mineral content (BMC) measured by DEXA at 10 weeks of age in female **C** and male **D** FTO-2 and FTO-4 mice at 10 weeks old. Female FTO-2 n=10 and FTO-4 n=12, male FTO-2 n=11 and FTO-4 n=10. Data analysed by student's t-test *P<0.05, **P<0.01, ***P<0.001. Data expressed as mean ± SEM.

Plasma was collected from mice at 10 weeks of age following the overnight fast and one hour refeed by cardiac puncture. The plasma biochemistry measured from this is shown in **Table 6.2**. Female FTO-4 had significantly increased circulating plasma levels of glycerol (P=0.0425) but other parameters measured were unchanged. Levels of HDL cholesterol (P=0.0259), LDL cholesterol (P=0.00039) and glycerol (P=0.00985) were all significantly increased in the plasma of FTO-4 male mice compared to FTO-2 mice. These mice also showed a trend for increased plasma total cholesterol and glucose, although this was not significant.

Table 6.2 Terminal Plasma Biochemistry taken in female and male FTO-2 and FTO-4 mice at 10 weeks of age. Abbreviations: High-Density Lipoprotein (HDL), Low-Density Lipoprotein (LDL) Creatinine Kinase (CK). Female FTO-2 n=10 and FTO-4 n=11, male FTO-2 n=11 and FTO-4 n=9.Data analysed by student's t-test *P<0.05, **P<0.01, ***P<0.001. SEM, Standard Error of the Mean; NS, Not Significant.

Assay	Units	FTO-2		FTO-4		P-value
		Mean	SEM	Mean	SEM	
Females						
Total Cholesterol	mmol/l	1.444	0.260	1.952	0.278	NS
HDL	mmol/l	0.686	0.151	0.883	0.172	NS
LDL	mmol/l	0.246	0.040	0.338	0.052	NS
Glucose	mmol/l	7.293	1.311	10.195	1.101	NS
Triglycerides	mmol/l	0.579	0.063	0.743	0.135	NS
Glycerol	µmol/l	277.625	30.428	394.273	39.418	*
Free Fatty Acids	mmol/l	0.543	0.060	0.456	0.062	NS
CK	U/l	116.900	39.603	96.900	19.312	NS
Males						
Total Cholesterol	(mmol/l)	2.088	0.276	2.724	0.139	P=0.0558
HDL	(mmol/l)	0.970	0.203	1.570	0.113	*
LDL	(mmol/l)	0.328	0.048	0.614	0.042	***
Glucose	(mmol/l)	9.112	1.729	13.469	0.905	P=0.0513
Triglycerides	(mmol/l)	0.979	0.201	1.456	0.219	NS
Glycerol	(µmol/l)	311.182	43.017	471.222	31.302	**
Free Fatty Acids	(mmol/l)	0.660	0.032	0.697	0.118	NS
CK	(U/l)	118.545	37.696	64.333	13.513	NS

6.3.3 Gut Hormone Assessment

Various hormones are important for the regulation of hunger and satiety. At nine and ten weeks of age, female FTO-4 mice did not eat significantly more than FTO-2 mice, but male FTO-4 did (**Figure 6.3C,D** and **Figure 6.4**). Various hormones were measured from plasma collected during the nine and ten week feeding regimes.

Leptin is not a gut hormone, but it does play an important role in anorexigenic signalling. Leptin is produced in adipose tissue, and the greater the adipocyte size and number the greater the levels of leptin in the plasma. Levels of leptin in female mice increase after feeding (**Figure 6.7A**). This

increase is significant after two hours (P=0.0082) in FTO-2 mice, this also increases after two hours in FTO-4 female mice but does not reach significance (P=0.0661). Male FTO-2 mice show decreased circulating plasma leptin after one and two hours refeeding (P=0.0049 and P=0.0138 respectively **Figure 6.7B**). This decrease was not seen in male FTO-4 mice after refeeding and their levels are more constant, this results in the FTO-4 mice having significantly higher plasma leptin after two hours refeeding than FTO-2 male mice (P=0.0060). As leptin is produced in adipose tissue I corrected the data for the amount of fat mass that these mice have, this was measured one week later by DEXA analysis (**Figure 6.5**). This did not dramatically alter the results, however the female FTO-4 mice now have a significant increase in leptin after two hours as is also observed in female FTO-2 mice (P=0.0465 and P=0.0032 respectively **Figure 6.7C**). This fat mass correction had little effect on the male data and FTO-2 mice still have significantly lower leptin levels than FTO-4 male mice after two hours refeeding (P=0.0067 **Figure 6.7D**).

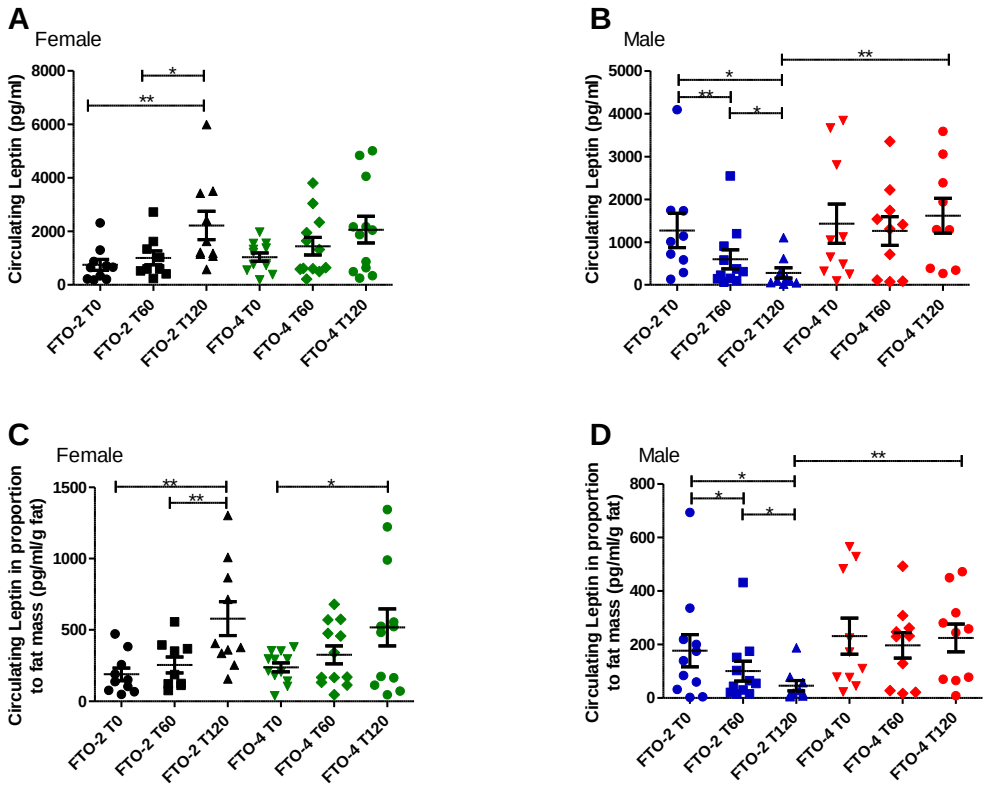

Figure 6.7 Leptin Measurements During a two hour Food Intake Study in Female and Male FTO-2 and FTO-4 Mice at nine weeks of age. Leptin measurements after a 16 hour fast at baseline, and 60 minutes and 120 minutes after reinitiating feeding in female **A**, and male **B**, FTO-2 and FTO-4 mice. Leptin measurements corrected for Fat mass measured at 10 weeks of age by DEXA in female **C**, and male **D**, FTO-2 and FTO-4 mice. Female FTO-2 n=10 and FTO-4 n=12, male FTO-2 n=11 and FTO-4 n=10. Data analysed at each time point by student's t-test *P<0.05, **P<0.01, ***P<0.001. Data expressed as mean ± SEM.

This data is also shown as a time-course in **Figure 6.8**. This clearly illustrates that during the refeeding there is no significant difference in circulating leptin levels in FTO-2 and FTO-4 females (**Figure 6.8A**). In males refeeding leads to a decrease in FTO-2 circulating leptin, but this is not observed in male FTO-4 mice, causing significantly elevated plasma leptin levels in FTO-4 mice (**Figure 6.8B**).

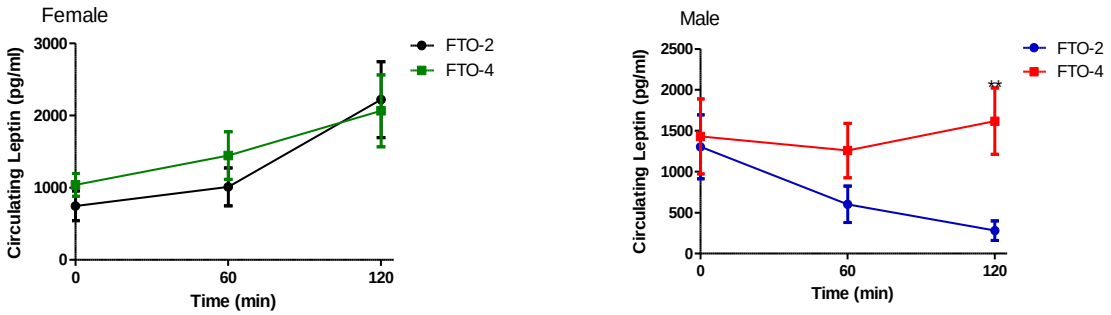

Figure 6.8 Time-course of Leptin Measurements During a two hour Food Intake Study in Female and Male FTO-2 and FTO-4 Mice at nine weeks of age. Leptin measurements after a 16 hour fast at baseline, and 60 minutes and 120 minutes after reinitiating feeding in female A, and male **B**, FTO-2 and FTO-4 mice. Female FTO-2 n=10 and FTO-4 n=12, male FTO-2 n=11 and FTO-4 n=10. Data analysed at each time point by student's t-test *P<0.05, **P<0.01, ***P<0.001. Data expressed as mean ± SEM.

Circulating acyl-ghrelin was also measured at nine weeks of age in male and female FTO-2 and FTO-4 mice. Ghrelin is an orexigenic hormone and acts to increase hunger and food seeking behaviour. Female FTO-4 mice had significantly higher acyl-ghrelin levels at T0 than FTO-2 mice (P=0.0363 **Figure 6.9A**). During the two hour feeding trial baseline ghrelin levels significantly decreased in female FTO-4 mice (P=0.0190), this significant decrease was not observed in the FTO-2 female mice. The male FTO-2 and FTO-4 mice both saw their levels of circulating levels of acyl-ghrelin decrease during the two hour refeeding trial (P=0.0178 and P=0.0027 respectively **Figure 6.9B**). The levels in FTO-2 mice decreased to such a degree that it was undetectable at T120, so the data plotted is the minimal sensitivity of the ELISA. Comparing FTO-2 and FTO-4 mice their levels of acyl-ghrelin are significantly higher than FTO-2 male mice at T60 and T120 (P=1.25E-05 and P=6.098E-06 respectively).

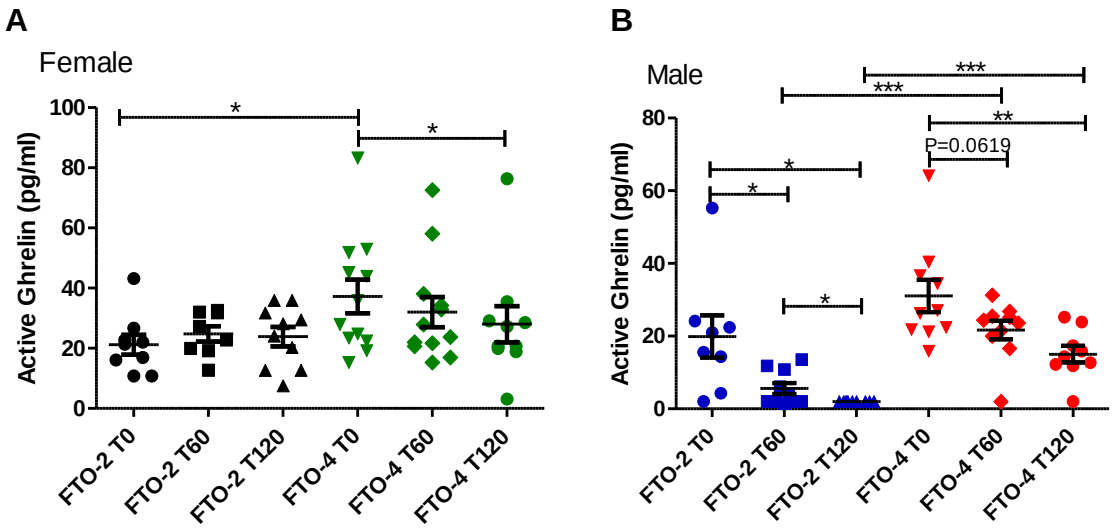

Figure 6.9 Acyl-Ghrelin Measurements During a two hour Food Intake Study in Female and Male FTO-2 and FTO-4 mice at nine weeks of age. Acyl-Ghrelin measurements after a 16 hour fast at baseline, and 60 minutes and 120 minutes after reinitiating feeding in female **A**, and male **B**, FTO-2 and FTO-4 mice. Female FTO-2 n=10 and FTO-4 n=12, male FTO-2 n=11 and FTO-4 n=10. Data analysed at each time point by student's t-test *P<0.05, **P<0.01, ***P<0.001. Data expressed as mean ± SEM.

At nine weeks of age FTO-4 male mice eat significantly more than FTO-2 male mice during the two hour feeding trial, whereas there is no significant difference in the food intake between the female mice (**Figure 6.4**). If I plot the acyl-ghrelin and food intake together you can see in females clearly that despite there being significantly elevated acyl-ghrelin in the FTO-4 mice at T0 this does not appear to impact the food intake during the two hour trial, and ghrelin levels drop to within the same range as the FTO-2 mice (**Figure 6.10A**). For the male mice, those with two additional copies of FTO had a trend for increased acyl-ghrelin levels following the overnight fast (**Figure 6.10B**). These FTO-4 males then ate significantly more during the two hour trial and their acyl-ghrelin levels do not decrease as much as wild-type littermates, suggesting that downregulation of acyl-ghrelin once feeding initiates is failing in these mice (**Figure 6.10B**).

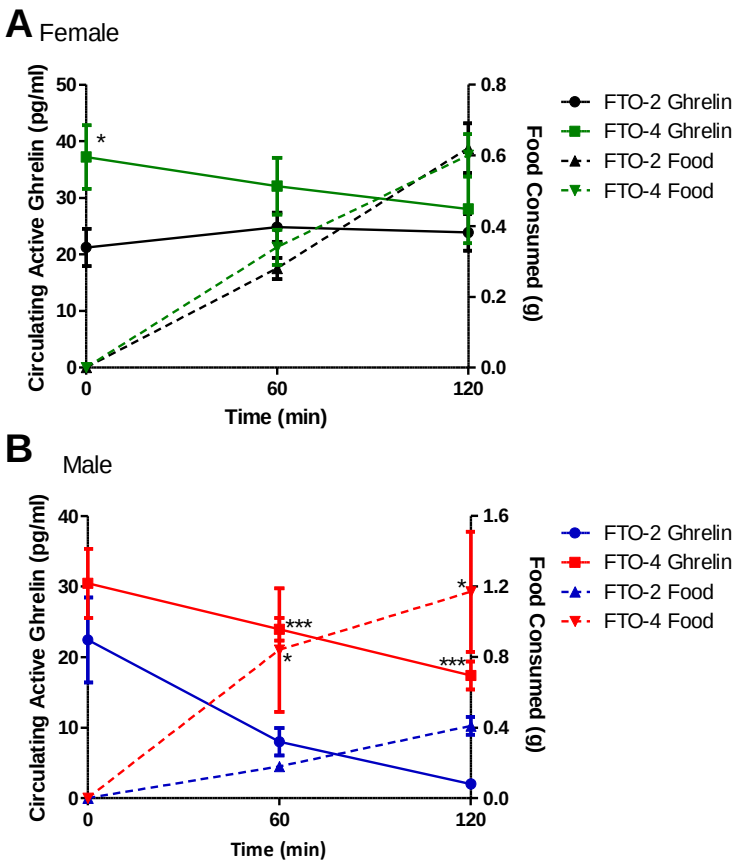

Figure 6.10 Time-course of Acyl-Ghrelin and Cumulative Food Intake Measurements During a two hour Food Intake Study in Female and Male FTO-2 and FTO-4 Mice at nine weeks of age. Acyl-ghrelin and cumulative food intake measurements after a 16 hour fast at baseline, and 60 minutes and 120 minutes after reinitiating feeding in female A, and male **B**, FTO-2 and FTO-4 mice. Female FTO-2 n=10 and FTO-4 n=12, male FTO-2 n=11 and FTO-4 n=10. Data analysed at each time point by student's t-test *P<0.05, **P<0.01, ***P<0.001. Data expressed as mean ± SEM.

At ten weeks of age acyl-ghrelin levels are not significantly altered at T0 or T60 in female FTO-4 mice (**Figure 6.11A**). Male FTO-4 mice have significantly lower levels of acyl-ghrelin at T0 at 10 weeks of age (**Figure 6.11B**). This is the opposite of the acyl-ghrelin result at nine weeks of age in these animals, where levels were higher at T0 and T60 (**Figure 6.9B**). Total GIP levels in FTO-2 and FTO-4 mice rose after feeding for one hour, and no significant differences was observed in the female or male mice (**Figure 6.11C,D**). Levels of total PYY at T0 were not significantly different in female FTO-2 and FTO-4 mice, but after feeding for one hour levels had significantly increased in FTO-4 females compared to FTO-2 mice (P=0.0307 **Figure 6.11E**). The total PYY result observed in males were similar, however the increased levels at T60 were not significant (**Figure 6.11F**).

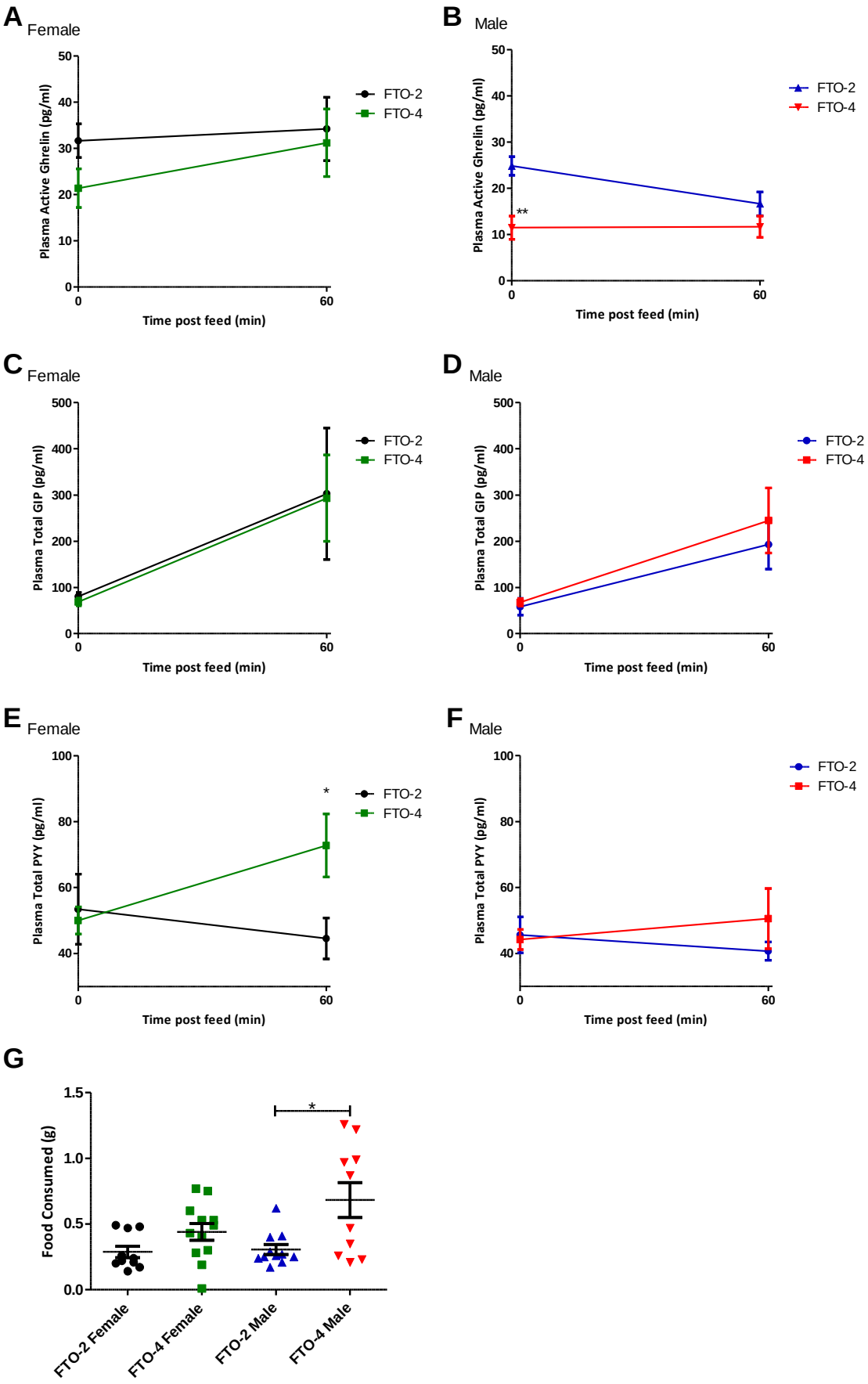
A
Female
Plasma Active Ghrelin (pg/ml)
Time post feed (min)
FTO-2
FTO-4
B
Male
**
C
Female
Plasma Total GIP (pg/ml)
D
Male
E
Female
Plasma Total PYY (pg/ml)
*
F
Male
G
Food Consumed (g)
FTO-2 Female
FTO-4 Female
FTO-2 Male
FTO-4 Male

Figure 6.11 Gut Hormone Measurements During a one hour Food Intake Study in Female and Male FTO-2 and FTO-4 Mice at ten weeks of age. Acyl-Ghrelin measurements after a 16 hour fast at baseline, and 60 minutes after reinitiating feeding in female **A**, and male **B**, FTO-2 and FTO-4 mice. Total GIP measurements after a 16 hour fast at baseline, and 60 minutes after reinitiating feeding in female **C**, and male **D**, FTO-2 and FTO-4 mice. Total PYY measurements after a 16 hour fast at baseline, and 60 minutes after reinitiating feeding in female **E**, and male **F**, FTO-2 and FTO-4 mice. Food intake during one hour feeding trial at 10 weeks of age G. Female FTO-2 n=10 and FTO-4 n=12, male FTO-2 n=11 and FTO-4 n=10. Data analysed at each time point by student's t-test *P<0.05, **P<0.01, ***P<0.001. Data expressed as mean ± SEM.

Active amylin and active GLP-1 were also measured at ten weeks of age at T0 and T60, however the data is not presented as levels were undetectable in some mice at all time points so I do not feel I can interpret the results. The amount of food consumed during the ten week feeding trial was higher but not significantly different in female FTO-2 and FTO-4 mice, however male FTO-4 mice did consume significantly more during this hour (**Figure 6.11G**). This suggests that ghrelin signalling is disrupted at least in male FTO-4 mice, as even when ghrelin levels are significantly lower at T0 they still ate significantly more than wild-type controls.

6.3.4 RNA analysis

Gene expression in the whole hypothalamus of mice at ten weeks of age following an overnight fast and food intake *ad libitum* for one hour was analysed by quantitative real-time PCR. Genes important for food intake regulation and satiety signalling such as *Pomc*, *Agrp*, *Ghsr*, *Npy2r* and *Lepr* were significantly upregulated in female FTO-4 mice (**Figure 6.12A**). Female FTO-4 mice also showed significantly increased levels of *Cartpt* suggesting that these mice may have altered reward pathways. *Fto* expression was also significantly increased in FTO-4 female mice (**Figure 6.12A**). Male FTO-4 also had significantly increased *Ghsr*, *Npy2r*, *Lepr*, and *Fto* (**Figure 6.12B**). However male FTO-4 mice had significantly increased levels of *Npy*, and *Cnr1*, whilst expression of *Pomc*, *Agrp*, and *Cartpt* were not significantly increased (**Figure 6.12B**). This suggests that FTO-4 male mice do have alterations in the gene expression of their satiety and reward signalling pathways in their hypothalami. It would also appear that although both male and female mice have altered expression in their satiety and reward gene expression there are sex differences in the expression of these genes in the hypothalami of the FTO-4 mice.

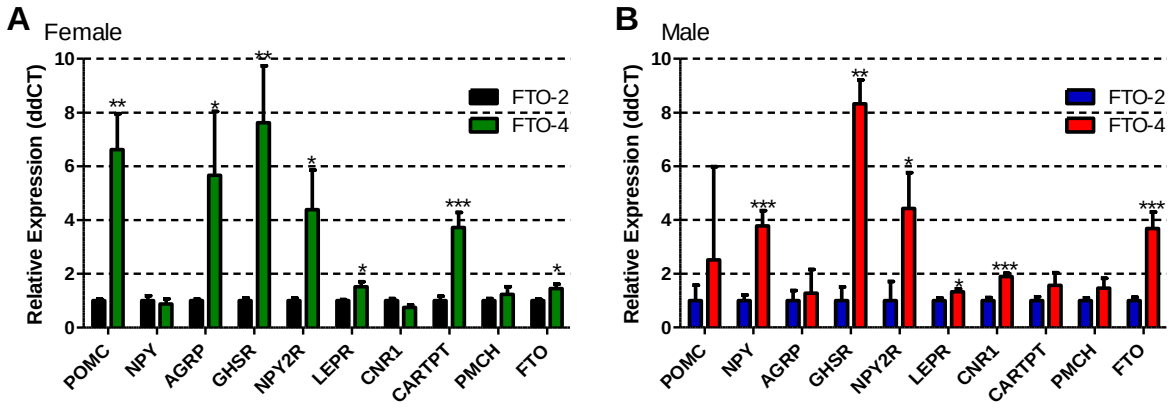

Figure 6.12 Relative Gene Expression in the Hypothalamus of 10 week old Female and Male FTO-2 and FTO-4 Mice. Abbreviations Pro-opiomelanocortin (POMC), Neuropeptide Y (NPY), Agouti related peptide (AGRP), Growth hormone secretagogue receptor (GHSR), Neuropeptide Y2 receptor (NPY2R), Leptin receptor (LEPR), Cannabinoid recptor 1 (CNR1), Cocaine- And Amphetamine-Regulated Transcript Protein (CARTPT), Pro-melanin-concentrating hormone (PMCH). Gene expression in female **A**, and male **B** FTO-2 and FTO-4 mouse hypothalami (n=8 per group) relative to *Gapdh* (2^ddCT). Data analysed by student's t-test *P<0.05, **P<0.01, ***P<0.001. Data expressed as mean ± SEM.

6.4 Discussion

6.4.1 Summary

Male and female mice which ubiquitously overexpress *Fto* weigh significantly more and are hyperphagic compared to wild-type littermates (Church *et al*., 2010). The increased FTO levels lead to a dose-dependent increase in body and fat mass, irrespective of whether they are fed standard or a high-fat diet, however their food intake was more markedly increased when fed a HFD (Church *et al*., 2010).

I studied the hormonal responses to the hyperphagic behaviour of FTO-4 mice. I wanted to see if I could replicate the hyperphagia previously seen, and see if this could be the main cause of the increased body weight and fat mass in these animals. I was not able to replicate the increased body weight of the FTO-4 mice, which I predict is due to the weekly fasting of the mice. The FTO-4 mice were fed a HFD and were hyperphagic at some time points, and when this was not significant they showed a trend for increased food intake. The data I generated indicate that the hyperphagia seen in the FTO-4 mice could be the main cause of the obesity phenotype. I hypothesise that this hyperphagia could be mediated by dysregulation of acyl-ghrelin. Other hormones such as PYY and leptin are increased to try and counteract this effect, and resistance to these anorexigenic hormones may be occurring. *Fto* expression was increased in the hypothalami of the mice, and the FTO-4 mice had altered expression of genes involved in satiety and reward signalling pathways.

6.4.2 *Fto* Overexpression

Acclimatisation of the animals to this study was crucial as stress can affect levels of gut hormones, most notably PYY (le Roux *et al*., 2006). By looking at the percentage decrease in body weight during the fast we can assess if there was a difference in acclimatisation level between our groups. Female FTO-4 mice have an anxiety phenotype (Church *et al*., 2010), as assessed by the open field paradigm. Initially the female and the male FTO-4 mice lost more weight than wild-types, but by

eight weeks this significant difference was abolished, indicating that the animals had been acclimatised to the fasting, and individual feeding.

It was important to carry out this analysis before a divergence in body weight so that it could be assessed if the hormones were a cause or result of the phenotype observed. Female mice did not diverge in body weight, and males only diverged briefly at seven weeks of age, when gut hormone levels were not measured. The divergence in body weight previously observed occurred at approximately six weeks in both genders on HFD (Church *et al*., 2010), this was not observed. Repeatedly fasting the animals is likely to have stopped body weight diverging as during the fasts decreases of 4-8 % body weight were observed in all groups, and FTO-4 mice lost significantly more during the acclimatisation period.

Release of PYY is exaggerated in the FTO-4 mice. PYY is an anorexigenic hormone which acts on neuropeptide Y neurons in the arcuate nucleus, causing postprandial satiety. GIP appears to be functioning normally with increased levels after feeding which should stimulate insulin release.

At nine weeks acyl-ghrelin is upregulated in FTO-4 females post-fast, but this is not the case in males. At ten weeks acyl-ghrelin is significantly lower in male FTO-4 mice than wild-types, and it is lower but not significantly in females. Levels for males then decrease after feeding, as expected (Karra and Batterham, 2009), but neither group of females show significant decreases post-feed. These results are conflicting, but it appears that there may be a dysregulation of ghrelin secretion or response. This is especially true at nine weeks in males, where levels of acyl-ghrelin decrease much slower after feeding, despite eating 35 % more food than wild-type controls.

Fto, Ghsr, Npy2r and *Lepr* were all upregulated in the hypothalami in male and female FTO-4 mice. *Ghsr* have previously been shown to be upregulated, at least in the arcuate nucleus, in response to fasting, and decreased in response to leptin in the rat (Kim *et al*., 2003, Nogueiras *et al*., 2004) and in the Siberian hamster (Tups *et al*., 2004). The *Ghsr* is upregulated approximately 8-fold in both males and females, and so perhaps it is not responding to the refeeding as quickly as it is in the FTO-2 controls, or there is a disruption in leptin signalling in the mice. This would lead

to increased orexigenic signalling in the hypothalamus in these mice, and we do see that the males are consuming significantly more. *Npy2r* binds PYY and *Lepr* binds leptin to downregulate food intake and increase satiety. Upregulation of these genes may be due to the hour of refeeding, but the response is exaggerated in the FTO-4 mice. Although the FTO-4 mice have consumed more food this may be due to them trying to counteract the effects of increased *Ghsr* and so it appears that there is a general dysregulation of the signalling pathway in these mice. *Cnr1* in male FTO-4 mice and *Cartpt* in female FTO-4 mice are upregulated. *Cnr1* knockout mice are lean and have reduced food intake (Ravinet Trillou *et al*., 2004) whereas activation of this receptor with its endogenous ligands leads to increased food intake (Jamshidi and Taylor, 2001, Kirkham *et al*., 2002), therefore upregulation of this gene may stimulate food intake in the males. *Cartpt* is expressed with *Pomc* in the arcuate neurons, where it inhibits food intake in response to leptin (Elias *et al*., 1998), therefore this may cause the increased *Pomc* expression in the females. Finally the male FTO-4 mice have increased levels of *Npy* and the females *Agrp*, these are both orexigenic neuropeptides and stimulate food intake (Schwartz *et al*., 2000).

Previously hypothalamic expression of *Agrp* was elevated in fasting 20 week old FTO-4 male mice, and *Npy* and *Pomc* were unaffected in these mice (Church *et al*., 2010). Fischer and colleagues showed that *Npy*, and *Pomc* were downregulated after fasting in the $Fto^{-/-}$, and no difference is seen in *Agrp*, although they do not report the sex of the mice in this study (Fischer *et al*., 2009). It would be interesting to examine *Fto* overexpression and knockout hypothalami from mice at T0 and at T60 to examine the effect of food intake on the expression of these genes in the wild-type and mutant mice.

6.4.3 Sex Differences

Despite the dysregulation we have seen in both male and female FTO-4 mice there do seem to be some clear sex differences, with males being more hyperphagic. The male FTO-4 mice also show significant increases in their lean mass and BMC and BMD, which are not apparent in the FTO-4 females. Plasma biochemistry reveals more significant changes in the male FTO-4 males, such as

significantly higher levels of HDL, LDL and increased plasma glucose, which were not seen in the females. Previously fasted male FTO-4 mice showed no significant differences in plasma biochemistry (Church *et al*., 2010). Therefore perhaps food intake for one hour has uncovered their impaired glucose homeostasis and high cholesterol levels due to their hyperphagia. Church and colleagues did observe differences in the fasted plasma biochemistry in the female FTO-4 mice at 20 weeks of age, whereas my ten week olds are yet to develop the increased FFAs, triglycerides, and HDL they observed.

Levels of *Fto* expression in male FTO-4 mice are 3.682 ± 0.616 fold higher than male FTO-2 mice, however in female FTO-4 mice they are only upregulated 1.453 ± 0.165 fold. This could account for some of the sex differences we observe in the mice. The male FTO-4 mice have eaten significantly more in the hour prior to this measurement than their FTO-2 controls, whereas the female FTO-4 mice did not eat significantly more than their controls (**Figure 6.3C,D**). It has been previously shown that nutrient levels *in vitro* can regulate FTO gene and protein expression (Cheung *et al*., 2013), so the greater levels of *Fto* expression in the FTO-4 males may be due to their increased food intake, and therefore greater levels of plasma amino acid and glucose. Expression of *Fto* has only been analysed at one hour after refeeding, and it would be beneficial to analyse this expression before and after fasting as well as after refeeding to fully understand the expression of *Fto* as well as the other neuropeptides.

Gender differences have previously been reported in gut hormone secretion. In rats the time to peak PYY concentration was similar in male and females, however females reached significantly higher levels, and the total PYY AUC remained higher in females (Kim *et al*., 2005). Our FTO-4 females reach a higher level of PYY secretion at T60 than the FTO-2 males. Gender has also been shown to effect ghrelin secretion in humans, with females having significantly higher fasting and fed levels than men (Greenman *et al*., 2004). Leptin has also been shown to be at higher levels in females, independent of fat mass (Sinha and Caro, 1998, Casabiell *et al*., 2001). These leptin and ghrelin gender differences were observed in this study, although were not significant.

6.4.4 *FTO* and Leptin

Leptin is produced in adipose tissue and acts in the brain as a potent regulator of food intake. Levels of leptin decrease during periods of fasting, but not in proportion to body fat (Saladin *et al*., 1995, Sinha and Caro, 1998). This decrease in leptin acts to stimulate feeding before stores are negatively affected. Once feeding begins again levels of leptin return to basal levels, this response has been shown to be higher after a carbohydrate based meal than after an isoenergetic fat based meal (Romon *et al*., 1999). An increase, in proportion to fat mass, can be seen in the female mice after feeding for 120 min. In FTO-2 males there is a significant decrease after feeding, and no change was observed in FTO-4 mice. Independent of adiposity females have more circulating leptin than males (Sinha and Caro, 1998), and leptin is regulated in a diurnal pattern (Schoeller *et al*., 1997), with the zenith during the dark cycle and the nadir during the light. The results for the females agree with the return of leptin levels to those pre-fast, and in the males we see a decrease or no change in levels, which might indicate a greater effect of the diurnal regulation. In females there is no significant difference between the groups, whereas in males there is significantly more leptin in proportion to fat mass at 120 min for FTO-4 mice. Leptin is anorexigenic so perhaps this counteracts the higher levels of acyl-ghrelin seen earlier, or the mice are leptin resistant and secrete more to overcome its weaker affect, this may also be why we see upregulation of the *Lepr* in FTO-4 mice.

When leptin was measured previously in the FTO-4 mice at eight weeks of age circulating levels and levels corrected for body weight were significantly lower in FTO-4 than FTO-2 mice, however at 20 weeks of age the leptin levels correlated well with fat mass (Church *et al*., 2010). In this study plasma was collected later in the light period, without entrainment to fasting, and with a shorter six hour fast, which therefore could cause the differences observed between these studies.

Leptin levels in $Fto^{-/-}$ mice were significantly lower (Fischer *et al*., 2009), whilst in $Fto^{I367F/I367F}$ mice, circulating leptin after a six hour fast was not significantly difference (Church *et al*., 2009). Both these mouse models have reduced amounts of fat mass, so when correcting for levels of adipose tissue these mice secrete high levels of leptin in proportion to their fat mass. The 20 week

old overexpression FTO-4 mice have significantly lower leptin levels, and high amounts of adipose tissue so when corrected for fat mass of the mouse, their leptin levels are significantly lower (Church *et al*., 2010). In our hands *Fto*$^{-/-}$ mice did not have significantly different leptin levels at eight weeks of age, however this would still indicate an increased leptin secretion in relation to fat mass (data unpublished). The adult *Fto* knockout mice had higher circulating levels of leptin compared to controls, but this was not significantly different when corrected for fat mass. The available data in the mouse therefore suggests that low levels of functional FTO see increased leptin levels, and high FTO expression causes a reduction in leptin expression, although only when *Fto* expression is altered during development.

Wang and colleagues showed that energy restriction (60 % of *ad libitum* food) in rats caused decreased *Fto* levels in the hypothalamus and brainstem (Wang *et al*., 2011b). They then used *db/db* mice, which have dysfunctional LEPR, and fed them an energy restricted diet. Energy restriction in these mice showed no effect on FTO expression in the brain, and they went on to show that *Fto* expression can be influenced by the LEPRB-STAT3 signalling pathway (Wang *et al*., 2011b).

FTO and *LEP* have both been shown to be involved in regulation of body weight and composition. In adults and adolescents the *FTO* risk SNPs are associated with increased plasma leptin levels (Do *et al*., 2008, Zabena *et al*., 2009, Labayen *et al*., 2011, Qi *et al*., 2008, Andreasen *et al*., 2008). These studies suggest that the *FTO* SNPs are associated with leptin-resistance, which may explain the increase food intake seen in test subjects. Therefore leptin could be a possible intermediary contributing to the association between the FTO polymorphisms and adiposity.

6.4.5 *FTO/Fto* and Food Intake

We were able to observe hyperphagic behaviour in the FTO-4 mice when food intake was measured for one or two hours following a 16 hour fast. This effect was only significant in our male mice. It would be interesting to examine the food intake of these mice for longer periods of

time following the fast, as perhaps we would see an increased food intake in the females during a 24 hour period as observed previously (Church *et al*., 2010).

This hyperphagic behaviour and preference for energy rich foods has been observed in humans with the 'risk' allele (Tanofsky-Kraff *et al*., 2009, Cecil *et al*., 2008). Karra and colleagues have observed attenuated post-prandial responses in AA carriers in terms of hunger and circulating acyl-ghrelin levels (Karra *et al*., 2013). fMRI scans of the subjects revealed that *FTO* genotype modifies responses to food images in homeostatic and reward regions in the brain, such as the hypothalamus and ventral tegmental area (Karra *et al*., 2013). They also demonstrated that $Fto^{-/-}$ mice have higher levels of total ghrelin after a 16 hour fast and in the fed state, with no significant difference in acyl-ghrelin levels (Karra *et al*., 2013). $Fto^{-/-}$ are hyperphagic in relation to their body weight, and perhaps these increased levels of ghrelin are the cause. We see alterations of gene expression related to satiety and reward pathways in the whole hypothalamus of the male and female FTO-4 mice; it would be fascinating to explore gene expression changes in the human hypothalamus. Karra and colleagues have observed that there may be a perturbed epitranscriptomic regulation of ghrelin mRNA, I believe that our FTO-4 mouse model would be key in following up some of these observations, and may help us understand the altered gut hormone regulation I have observed in these mice.

FTO has been shown to co-localise with the satiety mediator oxytocin in the paraventricular nucleus and supraoptic nucleus. FTO has also been shown to upregulate oxytocin expression *in vitro*; however oxytocin levels do not affect FTO expression. This was not one of the genes I examined, but it would be interesting to examine hypothalamic oxytocin expression in relation to FTO.

6.4.6 Reward Pathways controlling Food Intake

In this study I used a HFD, as previously FTO-4 mice have been shown to have a higher food intake when fed this diet over a standard chow (Church *et al*., 2010). This may be due to altered reward pathways in these mice, as suggested by Hess and colleagues (Hess *et al*., 2013). They have

recently shown that *Fto*$^{-/-}$ mice have impaired dopamine receptor 2 and 3 dependent control of neuronal activity and behaviour. Their results indicate that FTO is essential for the dopaminergic effects of cocaine, with *Fto*$^{-/-}$ mice having reduced *Fos* induction and cocaine associated locomotion (Hess *et al*., 2013). They also showed that FTO affects 6-meA methylation levels of a selective subset of mRNA involved in neuronal function, which may influence their translation, although the mechanism behind this is still unclear.

Another study has not found evidence linking hypothalamic FTO with feeding reward in C57BL/6 mice (Olszewski *et al*., 2009). Ingestion of palatable sugar or fat did not affect *Fto* expression in this study, which suggests there is no interaction between FTO and a particular palatable macronutrient.

In my study I do see increased *Cnr1* in male FTO-4 mice, and increased *Cartpt* in female FTO-4 mice. I have only looked at a small selection of changes in the hypothalamus and exploring other brain regions might uncover a clearer role for FTO in reward pathways such as the dopaminergic signalling system in the midbrain. It would be intriguing to repeat the study using a SD to see if the calorific HFD has a stronger influence on these satiety and reward pathways.

6.4.7 Future Plans

Although my data revealed that FTO-4 mice are hyperphagic and a dysregulation of gut hormones and hypothalamic gene expression may be the cause, the underlying mechanisms are still unclear. I would like to repeat this study and examine more parameters in order to understand the differences between the FTO-2 and FTO-4 mice.

In a repeat study I would like to always examine food intake during a two hour window, rather than normally looking for just one hour. This will hopefully uncover more differences and will properly acclimatise the mice for the two hour study at nine weeks of age. Measuring food intake more frequently than once per hour may disturb the animals, so I would keep this consistent. However I would measure food intake again 24 hours after the fast, as this may reveal a

significantly higher food intake in the female FTO-4 as seen previously (Church *et al*., 2010). An automated food weighing system would be ideal for this, and would allow us to fully investigate meal size and frequency to have an idea of disturbed meal initiation or satiety.

I would also like to measure more parameters with the plasma I collect such as insulin, glucagon, amylin, GLP-1, PP and leptin at 10 weeks of age. I did attempt to measure GLP-1 and amylin but despite immediate addition of protease inhibitors to blood samples this was unsuccessful. Peptides such as GLP-1 have a half-life of 30 seconds which may be why measurements were unattainable. I would also like to run a full microarray on the hypothalami of fasted and fed mice to understand the effects of FTO overexpression on regulation of gene expression here, and how nutritional status affects this. Levels of 6-meA methylation have also been examined by some groups researching FTO. Uncovering the effect of FTO overexpression and relating methylation status to gene expression could reveal a mechanism for FTO in the hypothalamus. It would also be beneficial to measure levels of FTO in the stomach, and different regions of the intestine to understand its regulation in response to food intake, and examine gastric emptying time as this has not yet been investigated.

Repeating this experiment using a less rewarding SD may reveal differences in gut hormone levels and food consumption compared to using a HFD. Finally a paired feeding experiment would allow us to examine if the hyperphagia in the FTO-4 mice is solely responsible for their increased body weight and fat mass. In my study repeatedly fasting the animals stopped their body weight diverging, as during the fasts decreases of 4-8 % body weight were observed in all groups, and FTO-4 mice lost significantly more during the acclimatisation period. This suggests that this intervention prevented the significant increases in body weight, and perhaps this is purely due to hyperphagia and not energy expenditure.

Chapter 7:

General Discussion

7.1 Achievement of the Aims and Objectives

The aim of this thesis was to extend the current knowledge of *FTO*, a gene whose exact function is still unclear. My objectives were to determine the role of FTO in the adult mouse, if the demethylase function of FTO is important for its role in energy metabolism and body composition, to investigate the FTO overexpression mice to understand why they are hyperphagic and to analyse the role FTO plays in nutrient and developmental signalling pathways.

Adult inactivation of *Fto* demonstrated that removal of *Fto* may be as deleterious as overexpression, with the adult knockout mice having increased fat mass and decreased lean mass (McMurray *et al*., 2013). It also supported the role FTO plays in development as adult inactivation of *Fto* did not increase mortality rates as seen in the global $Fto^{-/-}$ pups. This study also revealed the importance of effective energy expenditure analysis in the mouse.

I have shown that *Fto* knockdown decreases C2C12 cell proliferation repeating the results of Gulati and colleagues in MEFs (Gulati *et al*., 2013). I also saw decreased mRNA translation in *Fto* knockout MEFs, when 2 μM puromycin was used for labelling, replicating the results of Gulati and colleagues (Gulati *et al*., 2013). I have also been able to show a link between FTO and development, with $Fto^{-/-}$ impacting cilia formation in MEFs and in specific tissues in $Fto^{-/-}$ embryos. Levels of FTO also appear to affect adipogenic differentiation, which could be due to altered WNT/β-CATENIN signalling.

I was unsuccessful at identifying an ENU induced mutation in exon 5 of *Fto* which would impair FTO's demethylase function, and work is still ongoing to generate a mouse which overexpresses a

catalytically null form of FTO. Pharmacological inhibition of FTO was a success *in vitro* and a compound screen identified FG2216, which could be used *in vivo* to inhibit FTO (Aik *et al*., 2013). The *in vivo* effects of FG2216 at 1 mg/kg/2days were not enough to effect body weight or composition. Increasing the dose and looking for biomarkers to investigate the inhibition of FTO are still ongoing.

Finally my research suggests that there is dysregulation of gut hormones and neuronal signalling pathways in the FTO overexpression mice, which could cause the hyperphagia and increased body weight observed in these animals (Church *et al*., 2010).

7.2 Does FTO affect Obesity?

GWAS is a non-hypothesis-driven technique, and can be used to uncover new insight into the biology of a phenotype. *FTO* was "a gene of unknown function in an unknown pathway" (Frayling *et al*., 2007) when the SNPs in intron 1 were first identified. The actual gene(s) or region(s) having an impact on body weight might be in the immediate area or even in LD somewhere else in the region.

FTO and *RPGRIP1L* transcription start sites are in close proximity to each other, and both could be affected by altered enhancers in intron 1 or 2 of *FTO* (Stratigopoulos *et al*., 2008). Research looking at *RPGRIP1L* function has not shown a strong role for this gene in the regulation of body weight. Mouse models show that *Rpgrip1l* has a role in cilia morphology and developmental phenotypes (Vierkotten *et al*., 2007). Patients with ciliopathies are rare, but they correlate well with obesity, with 70 % of BBS ciliopathy patients being overweight and displaying hyperphagia (Sen Gupta *et al*., 2009). Several studies have failed to show an association of *FTO* or *RPGRIP1L* expression with obesity associated SNPs in adipose tissue or skeletal muscle (Kloting *et al*., 2008, Wahlen *et al*., 2008, Grunnet *et al*., 2009b). One study have shown that the 'risk' SNPs in *FTO* can increase its transcription without affecting *RPGRIP1L* in hnRNA or derived fibroblasts (Berulava and Horsthemke, 2010) while a separate study has shown increased FTO mRNA in peripheral blood cells of patients homozygous for the 'risk' allele (Karra *et al*., 2013). Karra and colleagues

were also able to demonstrate that subjects homozygous for the risk allele have dysregulated levels of ghrelin, attenuated post-prandial appetite reduction and altered neural responses in homeostatic and reward brain regions to food images.

Insights from functional genomics studies examining *Fto* knockout, mutation and overexpression in mice suggest a strong role for FTO in the control of body weight, composition (**Table 7.1**) and metabolism (Fischer *et al*., 2009, Church *et al*., 2009, Church *et al*., 2010, Gao *et al*., 2010, McMurray *et al*., 2013). This may be due to the effect of FTO in neurons, and may be due to FTO regulation of reward and/or food-intake pathways in the brain (Gao *et al*., 2010, Hess *et al*., 2013, Karra *et al*., 2013). Examining FTO expression in human brain regions, where it is expressed most highly, could prove interesting however this is not viable for the human population.

I believe that the data has been able to show that FTO expression can clearly affect body composition and is therefore likely to account for a part of or possibly the entire association signal.

7.3 Energy Expenditure and FTO

Originally it was believed that FTO levels could alter energy expenditure, as Fischer and colleagues observed that the *Fto*$^{-/-}$ mice had significantly higher VO_2 consumption, VCO_2 production, and heat generation than wild-type littermates, when normalised to lean body mass (Fischer *et al*., 2009). John Speakman suggests that simply dividing by lean mass "can generate a spurious elevation of metabolic rate if the intercept of the relationship between metabolism and lean body mass is not zero" (Arch *et al*., 2006, Speakman, 2010), and that to correctly normalise data ANCOVA should be used. Gao and colleagues have since reported an increased energy expenditure in their *Fto*$^{-/-}$ mice tested by ANCOVA normalised for lean body mass (Gao *et al*., 2010).

In the field there has been some discussion about the most appropriate way to correct energy expenditure for differences in body weight and composition in both *Fto*$^{-/-}$ mice and mouse models in general (Butler and Kozak, 2010, Speakman, 2010, Kaiyala and Schwartz, 2011, Choi *et al*.,

2011). Using multiple linear regression to control for variation in lean mass, we found no significant difference in energy expenditure between the *Fto*$^{-/-}$ and littermate controls in both light and dark phases. Using the ratio method, in which data were analysed by dividing energy expenditure by lean mass, our results show increased energy expenditure in line with both previous studies. However, ratio analyses are confounded by the very different lean masses of the knockout and littermate control groups (Fischer *et al*., 2009, Gao *et al*., 2010). Using appropriate normalisation methodology reveals that our germline *Fto*$^{-/-}$ mice show no differences in energy expenditure. The different result obtained by Gao and colleagues (Gao *et al*., 2010), is likely to be explained by differences in body composition in their mouse model.

Whilst FTO is required for energy metabolism, FTO loss has no significant effect on energy expenditure when the appropriate statistical method is applied. We hope that this method of analysing energy expenditure will be adopted by other groups when analysing their mouse data, to ensure results are comparable between studies.

7.4 FTOs Involvement in Nutrient and Amino Acid Sensing

Research from the group of Prof Giles Yeo suggests that FTO expression is controlled by nutrient availability, in particular essential amino acid availability, and that FTO is involved in coupling amino acid sensing to mTORC1 signalling (Cheung *et al*., 2013, Gulati *et al*., 2013). Their results suggest that AARSs, which catalyze the production of aminoacyl-tRNAs for protein synthesis (amino acid charging), are markedly reduced in *Fto*$^{-/-}$ MEFs. Their model suggests that FTO is upstream of this process linking availability of amino acids to amino acid charging, which then reduces mTORC1 signalling and leads to reduced cell growth and translation (Gulati *et al*., 2013).

AARSs can be found in the cytoplasm, nucleus and have been shown to be secreted into the extracellular space. They play a key role in translation but have also been shown to be involved in cardiovascular development and the immune response, IFN-γ and p53 signalling as well as mTOR signalling [reviewed in (Guo and Schimmel, 2013)]. If FTO is upstream of AARSs and is involved in amino acid sensing this could implicate FTO in a variety of pathways and could account for its

separate association with melanoma (Iles *et al*., 2013). Recently the role of AARSs in activation of mTORC1 has generated a number of papers. Leucyl-tRNA synthetase (LRS) plays a critical role in amino acid-induced mTORC1 activation by sensing intracellular leucine concentration and initiating molecular events leading to mTORC1 activation (Bonfils *et al*., 2012, Han *et al*., 2012). Gulati and colleagues were also able to show decreased protein levels of LRS in *Fto*$^{-/-}$ MEFs, further supporting its role in mTORC1 signalling. One point to consider is that they observe a reduction in FTO expression three to six hours after nutrient deprivation (Cheung *et al*., 2013, Gulati *et al*., 2013). It is generally recognized that short-term amino acid deprivation can regulate mTOR activity, for example after one hour of amino acid depletion differences in S6K1 phosphorylation can be detected (Hara *et al*., 1998, Kim *et al*., 2002). A role for FTO upstream of mTOR in amino acid sensing is in general questionable because of this.

My results do support FTOs involvement in nutrient sensing, although this may be upstream or downstream of mTOR. The significantly decreased lean mass seen in my adult FTO knockout mice (McMurray *et al*., 2013) could be due to an alteration in this pathway. Skeletal muscle is the largest depot of protein in the body, and so it may be particularly sensitive to amino acid levels. Sudden loss of FTO could deprive the ability of the cells to respond appropriately to amino acid levels, increasing autophagy and decreasing cell proliferation, resulting in a failure of the FTO adult knockout mice to increase their lean body mass. Although I did not see a difference in cellular proliferation in the wild-type and *Fto*$^{-/-}$ MEFs, siRNA knockdown of *Fto* did reduce proliferation in a myoblast cell line (C2C12 cells) in my hands, indicating that some cell types may be more sensitive to loss of *Fto* than others.

The 6-meA modification occurs in rRNA, tRNA and snRNA [reviewed in (Niu *et al*., 2013)]. My result for the puromycin translation assay suggests that the *Fto*$^{-/-}$ MEFs are more sensitive to high levels of puromycin. In *E.coli* several nucleotides of the rRNAs have shown altered chemical reactivities in the presence of puromycin (Rodriguez-Fonseca *et al*., 2000), and some may be potentially modified by methylation (Smith *et al*., 1992). Methylation of bases in rRNA does occur in eukaryotes, and human RNA does include a m6A in 18S and one found in 28S (Maden and

Hughes, 1997), how this methylation occurs and what function it plays is unknown, but they are highly conserved in eukaryotes (Maden and Hughes, 1997). Speculatively FTO could be involved with rRNA processing and methylation; this may alter translation levels, that may be more sensitive to high puromycin levels

Issues in nutrient sensing may also play a role in the dysregulation of satiety signalling. I have observed the FTO overexpression mice, which leads to hyperphagia and increased body weight in these animals. This also supports the dysregulation and impaired response to ghrelin observed in human subjects homozygous for the risk allele (Karra *et al*., 2013). Their findings suggest FTO is involved in the regulation of ghrelin, and the neuronal responses to food. Extending our findings in the overexpression mice will hopefully lead to a more detailed mechanistic role for FTO in satiety signalling, and greater understanding of the phenotype in these animals.

7.5 FTO in development

FTO plays a role in mouse development, which can be seen from the increased mortality and growth retarded phenotype of the global *Fto*$^{-/-}$ mice (Fischer *et al*., 2009, Gao *et al*., 2010, McMurray *et al*., 2013). FTO appears to have a strong role in development processes in man as individuals homozygous for a loss-of-function R316Q mutation in FTO display an array of developmental abnormalities such as growth retardation, microcephaly, psychomotor delay, facial dysmorphism and cardiac abnormalities (Boissel *et al*., 2009). These individuals were part of a consanguineous family and did not survive beyond three years of age.

The cause of the increased mortality in the *Fto*$^{-/-}$ mice is unknown. I have shown that the *Fto*$^{-/-}$ pups are hypoglycaemic compared to littermate controls. This suggests that these mice have an underlying metabolic defect which could be responsible for the increased perinatal lethality although we are yet to identify the exact cause. Analysis of the primary cilia in MEFs reveals that they are shorter and fewer are present in MEFs from *Fto*$^{-/-}$ mice. Cilia in the *Fto*$^{-/-}$ E15.5 embryos also reveal tissue specific abnormalities. Cilia are associated with a range of development processes and diseases involving cilia can result in a range of developmental abnormalities,

neurological problems and sometimes with obesity and hyperphagia. I have not observed any gross malformations or left-right patterning abnormalities in the *Fto*$^{-/-}$ mice other than their growth retarded phenotype.

The mTORC signalling pathway is crucial for cell growth and metabolism. In zebrafish Torc1 signalling has been shown to regulate cilia length through translational regulation (Yuan *et al*., 2012). In this model increased TORC1 increases cilia length, whilst inhibition with rapamycin decreases cilia length (Yuan *et al*., 2012). It was shown that cilia which are too long or too short could not function properly, disrupting the establishment of left-right asymmetry (Yuan *et al*., 2012, Yuan and Sun, 2012). Boehlke and colleagues suggest the reverse, with primary cilia affecting mTORC1 activity and cell size through LKB1 activation when fluid flow causes cilia to bend. This suggests a link between FTOs involvement in mTORC1 signalling and its developmental effects.

Although my data is preliminary we might be observing differences in the canonical WNT signalling pathway in C2C12 cells treated with *Fto* siRNA. Canonical WNT signalling prevents β-CATENIN degradation allowing it to translocate to the nucleus, increasing transcription of WNT target genes. WNT signalling has been implicated in a number of biological processes such as development, energy metabolism and adipogenesis; pathways which may be affected in the FTO mutant mice (Christodoulides *et al*., 2009). WNT signalling may also play a role in formation and function of cilia (Gerdes *et al*., 2007, Corbit *et al*., 2008, Caron *et al*., 2012), although others have found that primary cilia are not needed for normal WNT signalling in the mouse embryo (Huang and Schier, 2009, Ocbina *et al*., 2009). WNT signalling can inhibit adipogenesis as has been demonstrated *in vitro* and *in vivo* in mice which express *Wnt10b* under the control of the fatty-acid-binding protein-4 (*Fabp4*) promoter, which decreases total body fat and is protective against obesity in *ob/ob* and agouti mice (Ross *et al*., 2000, Bennett *et al*., 2002, Longo *et al*., 2004, Wright *et al*., 2007).

Increased WNT signalling will cause a decrease in adipogenesis, but it will stimulate myogenesis and osteoblastogenesis [reviewed in (Christodoulides *et al*., 2009, von Maltzahn *et al*., 2012)]. The various FTO mouse models have altered body compositions and often BMD and BMC are affected as summarised in **Table 7.1**. This could suggest alterations in the WNT signalling pathway during development. A decrease in canonical WNT signalling could lead to a decrease in lean mass and BMC in *Fto*$^{-/-}$ mice. The FTO overexpression mice could therefore show the reverse as they show a trend for increased BMC and BMD and increase lean mass in the females, this would cause a decrease in adipocyte differentiation. However these mice have increased adipocyte size (in house data unpublished) which could be due to reduced adipocyte proliferation and so increased lipid storage in the adipocytes that do form. This theory could also support the body composition differences seen in the *Fto* adult knockout mice, who fail to gain lean mass once *Fto* is inactivated and instead gain fat mass, suggesting a potential decrease in WNT signalling.

Table 7.1 Summary of Fat mass, Lean mass, and Bone mineral Content or Density in the FTO Mouse models.

Mouse	Fat Mass	Lean Mass	Bone Mineral Content or Density
Global *Fto*$^{-/-}$ (Fischer *et al*., 2009)	↓	↓	Data not available
Global *Fto*$^{-/-}$ (Gao *et al*., 2010)	↑ in females, No difference in males	↓	↓
Global *Fto*$^{-/-}$ (McMurray *et al*., 2013)	↓	↓	↓
FTO$^{I367F/I367F}$ (Church *et al*., 2009)	↓	No difference	No difference
FTO Overexpression (Church *et al*., 2010)	↑	↑	↑
Nestin *Fto*$^{-/-}$ (Gao *et al*., 2010)	No difference	↓	↓
Adult *Fto*$^{-/-}$ (McMurray *et al*., 2013)	↑	↓	No difference

FTO does appear to play a role in development. Exploring the role of the WNT signalling pathway and cilia formation in the mouse may elucidate why the *Fto*$^{-/-}$ mice show increased postnatal lethality, and why they become growth retarded after birth. It may also explain the development abnormalities observed in the human subjects homozygous for a catalytically inactive form of

FTO, and may add to our understanding of how FTO influences obesity. Further study and clarification of differences in WNT signalling are needed to validate this hypothesis.

7.6 FTO and the brain

FTO is ubiquitously expressed with notably high levels of expression observed in the hypothalamus and cerebellum (Gerken *et al*., 2007). Manipulation of *Fto* expression in the ARC in rats using sterotactic injections of specific AAV vectors has also given some insight into its function (Tung *et al*., 2010). Overexpression of FTO increased expression of *Stat3* and reduced food intake, suggesting that leptin signalling is involved in this process, whilst downregulation of FTO caused an increase in food intake. There is some evidence that FTO is nutritionally regulated in the brain in mice and rats by fasting, although upregulation (Fredriksson *et al*., 2008, Olszewski *et al*., 2009), downregulation (Gerken *et al*., 2007, Wang *et al*., 2011b) and no significant differences (McTaggart *et al*., 2011, Olszewski *et al*., 2011b) have all been reported (summarised in **Table 1.3**).

One study has examined inactivation of FTO in the nervous system by crossing their Fto^{flox} allele with the *Nestin*-Cre line (Gao *et al*., 2010). They found that this line had a similar phenotype to the global $Fto^{-/-}$ line, with decreased body weight, lean mass, body length and BMD in the neural-specific *Fto* knockout animals. Western blots of tissues from the mice reveal that there is a decrease in FTO levels in the brain, although a small band is still present in the hypothalamus, whilst FTO levels are unaffected in WAT, BAT and liver. This study strongly suggests that FTO mainly functions in the nervous system to generate the phenotype of the $Fto^{-/-}$ mice. Previously the *Nestin*-Cre line has had some issues which can affect phenotyping results. Mice which have only the *Nestin*-Cre have a reduced body weight and decreased body length due to a decrease in growth hormone (Galichet *et al*., 2010). As Gao and colleagues did not use a *Nestin*-Cre only control in their study it is difficult to interpret their results appropriately, as the results they observe could be due to the presence of the *Nestin*-Cre alone, or a combination of inactivation of *Fto* and the presence of the *Nestin*-Cre (as will be discussed in **Section 7.7**).

To extend our findings in the *Fto* adult knockout mice we collaborated with Dr. Tony Coll's team at the Metabolic Research Laboratories in Cambridge who carried out AAV-Cre injections into adult mice to temporally inactivate *Fto* in the adult mediobasal hypothalamus. These mice did not present with the same body composition and calorimetry differences that were observed in the global adult knockout mice, although they did show a reduction in weight gain which might be due to a decreased food intake (McMurray *et al*., 2013). This would suggest that mediobasal hypothalamic loss of FTO is not sufficient to produce the phenotype observed in the adult knockout mice, but does not rule out other brain regions as key to FTOs function.

FTO has also been specifically inactivated in dopaminergic neurons using a *Dat*-Cre line (Hess *et al*., 2013). This group was interested in exploring the neuronal activity and behaviour of the $Fto^{-/-}$ mice, which showed attenuated activation of GIRK channel conductance by cocaine and quinpirole, and used the dopaminergic knockout to confirm these results. This suggests that FTO is involved in reward pathway signalling and regulation controlled by dopaminergic neurons, although deletion here is not reported to alter body weight and composition.

Several studies have suggested that the FTO 'risk' in man may be associated with increased food intake or increased preference for energy-rich foods (Cecil *et al*., 2008, Speakman *et al*., 2008, Timpson *et al*., 2008, Tanofsky-Kraff *et al*., 2009, Wardle *et al*., 2009, Sonestedt *et al*., 2009). The underlying mechanism had however not been investigated. Karra and colleagues used fMRI in normal weight individuals who were either homozygous for the protective or risk allele (Karra *et al*., 2013). They found that neural responses to food images in homeostatic and reward regions in the brain were modulated by genotype, as well as neural responses to circulating acyl-ghrelin. This was the first direct evidence that showed that rs9939609 genotype markedly impacts neural responsivity to food cues and circulating acyl-ghrelin (Karra *et al*., 2013). My results in the FTO overexpression mice using a HFD suggest a dysregulation of satiety signalling. These differences between the wild-type and overexpression mice may explain the hyperphagic behaviour and increased body weight observed in these animals. Future studies investigating the effect of a SD,

and other phenotyping tests exploring their reward and/or addiction associated behaviour may be worth exploring in the FTO overexpression mice.

The importance of FTOs function in the brain may be why I do not observe a phenotype in my mice treated with FG2216, as we do not yet know if this compound can cross the BBB. Successful penetration of the BBB needs to be assessed or intracranial administration may be required to allow access of the blood to the CNS. Biomarkers such as 6-meA levels examined by Hess and colleagues could be used to ensure an effective dose is inhibiting FTO function in the brain.

I believe that FTO is likely to play a role in neuronal control of food intake and maintenance of metabolic homeostasis; however I also believe that due to its expression in the periphery it is also likely to mediate effects elsewhere in the body. Further experiments looking at manipulation of FTO expression in peripheral tissues such as skeletal muscle and adipose tissue will be important in understanding its function in these tissues.

7.7 Potential Conditional Cre-line Limitations

Conditional mutagenesis is an extremely valuable tool to explore the role of your gene of interest in a variety of tissues and cell types; however with any technique it does have its limitations.

It had been assumed that Cre recombinase expression did not adversely affect the physiology of the host cell. However, there have been reports on the apparent toxic effects of Cre, such as Cre-catalyzed chromosome rearrangements (Schmidt *et al*., 2000) and reduced growth and DNA damage (Loonstra *et al*., 2001, de Alboran *et al*., 2001, Silver and Livingston, 2001). It is not difficult to test for the independent effect of Cre when performing a conditional knockout experiment. However mice carrying only the Cre transgene are not always used as controls, perhaps due to the widespread impression that the expression of Cre has minimal if any effects on the cell. As mentioned in **Section 7.6** this can make data interpretation difficult if the conditional mutant presents with any of the phenotypes associated with the Cre-line alone.

Cre expression is normally engineered by pronuclear microinjection, and this may not control where the transgene is integrated into the genome (Lee *et al*., 2006, Harno *et al*., 2013). This can disrupt endogenous genes, lead to multiple copies integrating into the genome, or low levels of Cre activity (Harno *et al*., 2013). These can then cause problems with inefficient Cre recombination or a non-uniform/mosaic pattern of recombination (Ryding *et al*., 2001).

Conditional mutagenesis in a specific tissue or cell type is reliant on the specificity of the promoter used to express Cre. The easiest way is to visualise this is using a reporter strain such as the ROSA-LacZ. This enables examination of non-specific or ineffective deletion. Some lines such as the *Nestin*-Cre are known to be expressed in tissues other than those desired. The *Nestin*-Cre is expressed in all somite derived tissue, which includes the kidney, heart, lung, muscle, intestine, pancreas, spleen, testis and thymus (Dubois *et al*., 2006), this could therefore mean that the results of Gao and colleagues who examined *Fto* inactivation using the *Nestin*-Cre may be due to its effect is tissues outside of the nervous system, as they only looked at peripheral FTO protein levels in liver, WAT and BAT, which are not somite-derived tissues (Gao *et al*., 2013).

It is not only the *Nestin*-Cre which has presented with non-specific expression. Many others including the *Rip*-Cre line which is designed for pancreatic expression can also have expression in the hypothalamus, the *Synapsin*-Cre which is predicted to show expression in the CNS also shows expression in the testis, and the *Ap2*-Cre which should be adipose tissue specific also shows expression in the CNS, bladder, eye, heart, intestine, kidney, and lung along with several other tissues (Harno *et al*., 2013).

To ensure the Cre lines used in our studies are appropriate and well controlled, I utilised a reporter line to examine the temporal tamoxifen-inducible ubiquitous Cre. In the *Fto* adult knockout study I compared the data from my adult knockout animals to animals which were genetically identical carrying both Cre and floxed Fto alleles, but were treated with vehicle, and a tamoxifen-treated Cre expressing control. As the Vehicle and Cre control animals did not show significant differences in weight, body length, or body composition throughout the study I then analysed only the vehicle

and adult KO groups. In studies using the *Fto*$^{-/-}$ and FTO overexpression mouse lines when these lines were generated using the *Actin-Cre*, the Cre was subsequently bred out of the lines to ensure this would not affect results.

7.8 FTO mechanism of action

Eukaryotic cells contain several varieties of RNA and more than 100 different modifications have been identified in cellular RNAs including mRNA, rRNA, tRNA, small nuclear RNA (snRNA) and small nucleolar RNA (snoRNA) (Cantara *et al*., 2011, Machnicka *et al*., 2013). *In vitro* studies have identified a number of possible methylated nucleotides which FTO is able to demethylate: 3-meT, 1-meA, 3-meC, 3-meU and 6-meA. Of these FTO is likely to have a preference for 3-meT, 3-meU and 6-meA, although the exact function of FTO is still unknown (Gerken *et al*., 2007, Han *et al*., 2010, Jia *et al*., 2011).

Examination of 6-meA modification reveals it is present at high levels in mRNA, and has a high correlation with stop codons, long internal exons and 3'UTR (Dominissini *et al*., 2012, Meyer *et al*., 2012). This suggests that this modification may be involved in control of translation, splicing or miRNA binding. FTO has been shown to co-localise with nuclear splicing speckles by two separate groups, which would support it acting on 6-meA and influencing splicing (Jia *et al*., 2011, Berulava *et al*., 2013).

If FTO is demethylating RNA, what is methylating it? Do these lesions occur by alkylation damage (Aas *et al*., 2003), or are there proteins involved? The only protein identified so far that methylates 6-meA is METTL3, which like FTO is ubiquitously expressed; however unlike FTO it has notably high expression in the testis (Bokar *et al*., 1997). This may suggest that it has closer relationship with another AlkB family member ALKBH5. This protein can demethylate 6-meA at a comparable level to FTO and is also ubiquitously expressed, but it has high expression in the testis (Zheng *et al*., 2013). ALKBH5 also co-localises with nuclear splicing speckles. *Alkbh5*$^{-/-}$ are viable and have a normal appearance and no body weight phenotype, however they do have a spermatogenic defect which may be explained by its high expression in the testis (Zheng *et al*., 2013). The phenotype of

these mice is very different from *Fto*$^{-/-}$ mice, which suggests that if FTOs main role is demethylating 6-meA, it and ALKBH5 may catalyse different mRNA substrates in a cell/tissue specific manner. The *Alkbh7*$^{-/-}$ mice do have an obesity phenotype (Solberg *et al*., 2013). Although this protein is related to FTO, unlike FTO it is localised to the mitochondria and is thought to play a role directly or indirectly in short chain fatty acid metabolism. ALKBH7 has also not been shown to have oxidative demethylase activity *in vitro* (Lee *et al*., 2005, Fu *et al*., 2013). It is therefore unclear if the function of ALKBH7 can help enlighten us to the function of FTO.

FTO has a two-fold preference for 3-meU in single stranded RNA over 3-meT in single stranded DNA (Jia *et al*., 2008). Little is known about these modifications and how they might impact on gene expression and translation. FTO has been shown to affect a number of modifications *in vivo*, and it may function in this way to regulate RNA processing and stability. Although others have examined levels of methylation with decreased and increased levels of FTO, it would be interesting to examine the RNA and/or DNA binding to FTO. This could be achieved using cross-linking immunoprecipitation sequencing (CLIP-seq) or chromatin-immunoprecipitation sequencing (CHIP-seq). This would allow us to understand FTOs targets *in vivo*, whether they are DNA or RNA and what type of RNA, and allow us to understand its role in control of body weight.

The function of the C' terminal of FTO is still unknown as it does not share homology with any identified protein domains (Han *et al*., 2010). It may be involved in protein binding, regulation or degradation of FTO, but this is very speculative and needs further investigation using immunoprecipitation to indentify binding partners specific to this region of FTO.

It is not fully understood how FTO affects body weight. Studies have implicated FTO in a number of pathways from nutrient sensing, mTOR signalling, and leptin signalling to UCP-1 and reward pathways.

One hypothesis is that nutrient levels or other signalling pathways involved in metabolic homeostasis alter expression of FTO (**Figure 7.1**). FTO then demethylates its substrate, which could be 3-meT, 3-meU, 6-meA or it may be unspecific and could demethylate a combination of

them. I believe that this may be the case as altered 3-meU and 6-meA have been observed when FTO is manipulated (Meyer *et al*., 2012, Berulava *et al*., 2013). If FTO acts on ssDNA it is likely to affect transcription. If FTO acts on RNA this could alter RNA stability, transport, or splicing and translation of the mRNA transcript, which could then alter protein expression. The effected proteins are likely to be involved in control of the cell cycle, cell growth, proliferation and nutrient sensing such as proteins involved in the mTOR and AMPK signalling pathways. This in turn alters cellular metabolism and energy levels, affects signalling at a tissue level, which then impacts on whole body metabolism, which can then feedback leading to normalisation of FTO expression. In the mouse models of FTO this feedback does not occur appropriately, leading to the array of phenotypes we observe.

7.9 Future Perspectives

The precise function of FTO, and how the GWAS identified SNPs cause an increase in body weight is still to be determined. Many questions still exist, and more knowledge is needed to understand FTOs true function *in vivo*.

It is clear that FTO is ubiquitously expressed and that whole body manipulation of FTO has generated some fascinating mouse models. Tissue specific modification of FTO using conditional mutagenesis may identify key tissues for FTOs function. Taking advantage of well characterised Cre lines and using appropriate controls will give us more information about where and when FTO is important in the mouse. AAV-Cre injection into specific tissues or brain regions will also be a useful tool. Manipulation of FTO in adipose tissue and skeletal muscle may reveal if these tissues play an important role or if the brain is key to FTOs function.

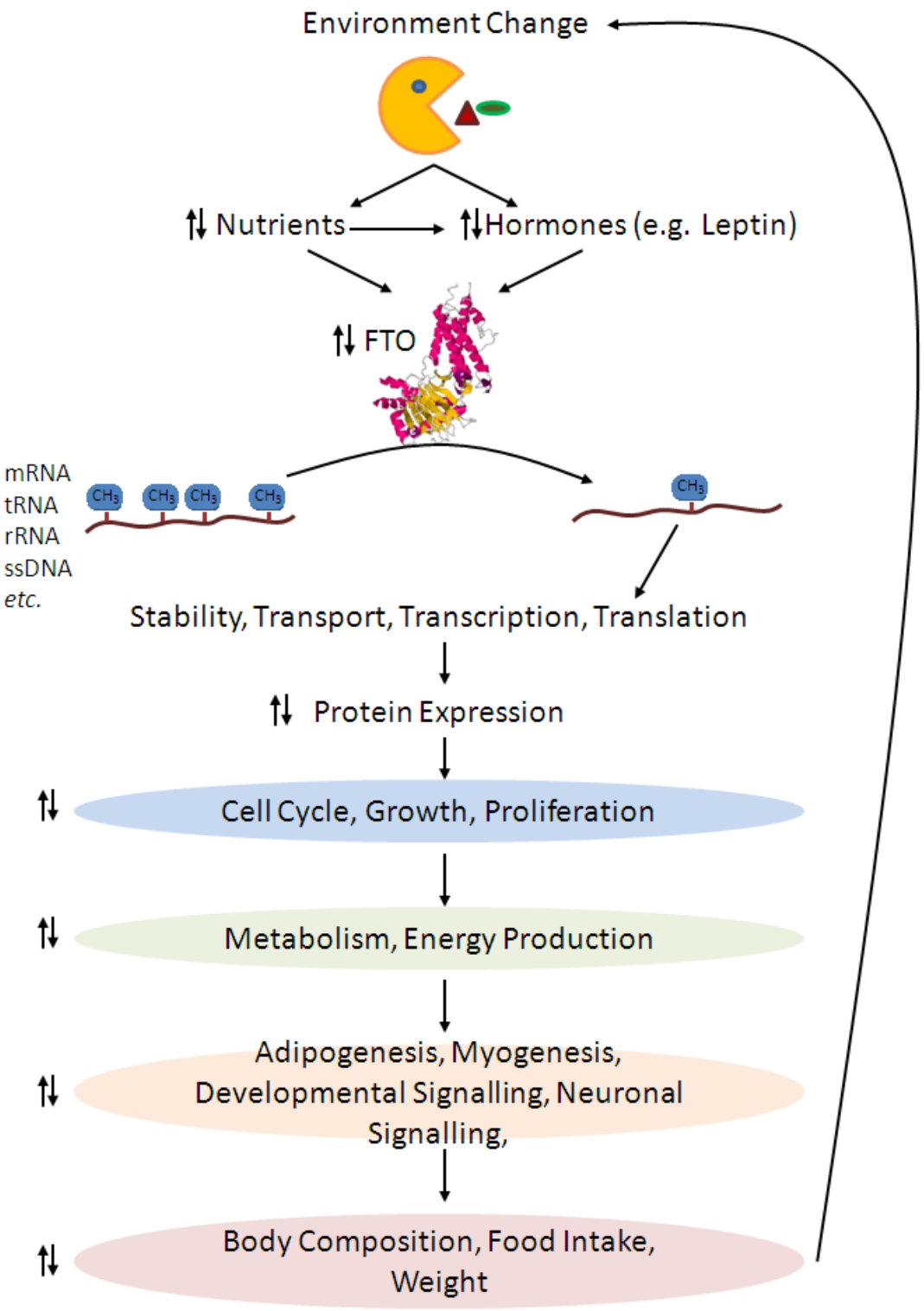

Figure 7.1 Possible Mechanism of Action for FTO. Environmental changes in food intake, availability of nutrients and molecules involved in these signalling pathways alter FTO expression. FTO may demethylate mRNA, tRNA, rRNA or single stranded DNA (ssDNA)*in vivo*. This then alters the stability, transport, transcription and translation of RNA which in turn alters expression of proteins. These proteins are likely involved in nutrient sensing such as MTOR. These is in turn cause alterations which feedback on the pathway.

Although whole body adult knockout of *Fto* bypassed the developmental defects and poor survival of the global germline knockout, it did not protect mice from an abnormal body composition, lowering lean mass and increasing fat mass. Investigating the phenotype of mice expressing a catalytic null form of FTO will prove useful in understanding this function *in vivo*. Future investigations using pharmacological manipulation of FTO, especially if a specific inhibitor can be identified, will prove useful in understanding the mechanisms *in vivo*, and may lead to better therapies for patients. Partial inactivation of the catalytic function of FTO could be a more viable option than complete inactivation, hopefully preventing the unwanted effects. Also ensuring inhibition of FTO in the brain, by screening for compounds which can cross the BBB, may improve results if we are sure that FTO functions in the brain or specific brain regions.

The *Fto* knockout and overexpression lines could also be used to cross with other models of obesity to investigate if FTO can modify their phenotype. Could loss of FTO decrease body weight in models such as *ob/ob* or *db/db* mice? This may uncover in which pathways and brain regions FTO is taking effect. Crossing FTO mutants with mutants of methyl transferases, such as METTL3 may also help us uncover the role of these modifications *in vitro*.

FTO is a fascinating gene, and its role as a demethylase has uncovered an exciting new process which may be involved in body weight regulation. New technology such as TALENs and ZFNs will make genetic manipulation of the mouse a faster process in the future. Utilisation of the mouse to investigate the function of novel genes identified by GWAS could be a gold standard for future studies.

References

AAS, P. A., OTTERLEI, M., FALNES, P. O., VAGBO, C. B., SKORPEN, F., AKBARI, M., SUNDHEIM, O., BJORAS, M., SLUPPHAUG, G., SEEBERG, E. & KROKAN, H. E. 2003. Human and bacterial oxidative demethylases repair alkylation damage in both RNA and DNA. *Nature,* 421**,** 859-63.

ACEVEDO-AROZENA, A., WELLS, S., POTTER, P., KELLY, M., COX, R. D. & BROWN, S. D. 2008. ENU mutagenesis, a way forward to understand gene function. *Annu Rev Genomics Hum Genet,* 9**,** 49-69.

ADEYEMO, A., CHEN, G., ZHOU, J., SHRINER, D., DOUMATEY, A., HUANG, H. & ROTIMI, C. 2010. FTO Genetic Variation and Association with Obesity in West Africans and African-Americans. *Diabetes*.

AHMAD, T., CHASMAN, D. I., MORA, S., PARE, G., COOK, N. R., BURING, J. E., RIDKER, P. M. & LEE, I. M. 2010. The fat-mass and obesity-associated (FTO) gene, physical activity, and risk of incident cardiovascular events in white women. *Am Heart J,* 160**,** 1163-9.

AIK, W., DEMETRIADES, M., HAMDAN, M. K., BAGG, E. A., YEOH, K. K., LEJEUNE, C., ZHANG, Z., MCDONOUGH, M. A. & SCHOFIELD, C. J. 2013. Structural basis for inhibition of the fat mass and obesity associated protein (FTO). *J Med Chem,* 56**,** 3680-8.

AJAY, BEMIS, G. W. & MURCKO, M. A. 1999. Designing libraries with CNS activity. *J Med Chem,* 42**,** 4942-51.

ALMIND, K. & KAHN, C. R. 2004. Genetic determinants of energy expenditure and insulin resistance in diet-induced obesity in mice. *Diabetes,* 53**,** 3274-85.

ALTMULLER, J., PALMER, L. J., FISCHER, G., SCHERB, H. & WJST, M. 2001. Genomewide scans of complex human diseases: true linkage is hard to find. *Am J Hum Genet,* 69**,** 936-50.

ANASTASSIADIS, K., FU, J., PATSCH, C., HU, S., WEIDLICH, S., DUERSCHKE, K., BUCHHOLZ, F., EDENHOFER, F. & STEWART, A. F. 2009. Dre recombinase, like Cre, is a highly efficient site-specific recombinase in E. coli, mammalian cells and mice. *Dis Model Mech,* 2**,** 508-15.

ANDREASEN, C. H., STENDER-PETERSEN, K. L., MOGENSEN, M. S., TOREKOV, S. S., WEGNER, L., ANDERSEN, G., NIELSEN, A. L., ALBRECHTSEN, A., BORCH-JOHNSEN, K., RASMUSSEN, S. S., CLAUSEN, J. O., SANDBAEK, A., LAURITZEN, T., HANSEN, L., JORGENSEN, T., PEDERSEN, O. & HANSEN, T. 2008. Low physical activity accentuates the effect of the FTO rs9939609 polymorphism on body fat accumulation. *Diabetes,* 57**,** 95-101.

ANSELME, I., LACLEF, C., LANAUD, M., RUTHER, U. & SCHNEIDER-MAUNOURY, S. 2007. Defects in brain patterning and head morphogenesis in the mouse mutant Fused toes. *Dev Biol,* 304**,** 208-20.

ARCH, J. R., HISLOP, D., WANG, S. J. & SPEAKMAN, J. R. 2006. Some mathematical and technical issues in the measurement and interpretation of open-circuit indirect calorimetry in small animals. *Int J Obes (Lond),* 30**,** 1322-31.

ARITA, Y., KIHARA, S., OUCHI, N., TAKAHASHI, M., MAEDA, K., MIYAGAWA, J., HOTTA, K., SHIMOMURA, I., NAKAMURA, T., MIYAOKA, K., KURIYAMA, H., NISHIDA, M., YAMASHITA, S., OKUBO, K., MATSUBARA, K., MURAGUCHI, M., OHMOTO, Y., FUNAHASHI, T. & MATSUZAWA, Y. 1999. Paradoxical decrease of an adipose-specific protein, adiponectin, in obesity. *Biochem Biophys Res Commun,* 257**,** 79-83.

ARYA, V. B., SENNIAPPAN, S., GUEMES, M. & HUSSAIN, K. 2013. Neonatal Hypoglycemia. *Indian J Pediatr*.

ATTANASIO, A., CASTELLARO, I., RIZZOTTI, P., MARINI, M. & VIDAL, M. 1987. [Macroamylasemia or pancreatitis? A diagnostic problem]. *Minerva Med,* 78**,** 1347-51.

BAHARY, N., LEIBEL, R. L., JOSEPH, L. & FRIEDMAN, J. M. 1990. Molecular mapping of the mouse db mutation. *Proc Natl Acad Sci U S A,* 87**,** 8642-6.

BAO, W., QIN, P., NEEDLE, S., ERICKSON-MILLER, C. L., DUFFY, K. J., ARIAZI, J. L., ZHAO, S., OLZINSKI, A. R., BEHM, D. J., PIPES, G. C., JUCKER, B. M., HU, E., LEPORE, J. J. & WILLETTE, R. N. 2010. Chronic inhibition of hypoxia-inducible factor prolyl 4-hydroxylase improves ventricular performance, remodeling, and vascularity after myocardial infarction in the rat. *J Cardiovasc Pharmacol,* 56**,** 147-55.

BARBER, T. M., BENNETT, A. J., GROVES, C. J., SOVIO, U., RUOKONEN, A., MARTIKAINEN, H., POUTA, A., HARTIKAINEN, A. L., ELLIOTT, P., LINDGREN, C. M., FREATHY, R. M., KOCH, K., OUWEHAND, W. H., KARPE, F., CONWAY, G. S., WASS, J. A., JARVELIN, M. R., FRANKS, S. & MCCARTHY, M. I. 2008. Association of variants in the fat mass and obesity associated (FTO) gene with polycystic ovary syndrome. *Diabetologia,* 51**,** 1153-8.

BARBER, T. M., MCCARTHY, M. I., WASS, J. A. & FRANKS, S. 2006. Obesity and polycystic ovary syndrome. *Clin Endocrinol (Oxf),* 65**,** 137-45.

BARCROFT, H., FOLEY, T. H. & MCSWINEY, R. R. 1971. Experiments on the liberation of phosphate from the muscles of the human forearm during vigorous exercise and on the action of sodium phosphate on forearm muscle blood vessels. *J Physiol,* 213**,** 411-20.

BECK, J. A., LLOYD, S., HAFEZPARAST, M., LENNON-PIERCE, M., EPPIG, J. T., FESTING, M. F. & FISHER, E. M. 2000. Genealogies of mouse inbred strains. *Nat Genet,* 24**,** 23-5.

BENNETT, C. N., ROSS, S. E., LONGO, K. A., BAJNOK, L., HEMATI, N., JOHNSON, K. W., HARRISON, S. D. & MACDOUGALD, O. A. 2002. Regulation of Wnt signaling during adipogenesis. *J Biol Chem,* 277**,** 30998-1004.

BENNETT, L. B., TAYLOR, K. H., ARTHUR, G. L., RAHMATPANAH, F. B., HOOSHMAND, S. I. & CALDWELL, C. W. 2010. Epigenetic regulation of WNT signaling in chronic lymphocytic leukemia. *Epigenomics,* 2**,** 53-70.

BENZINOU, M., CHEVRE, J. C., WARD, K. J., LECOEUR, C., DINA, C., LOBBENS, S., DURAND, E., DELPLANQUE, J., HORBER, F. F., HEUDE, B., BALKAU, B., BORCH-JOHNSEN, K., JORGENSEN, T., HANSEN, T., PEDERSEN, O., MEYRE, D. & FROGUEL, P. 2008. Endocannabinoid receptor 1 gene variations increase risk for obesity and modulate body mass index in European populations. *Hum Mol Genet,* 17**,** 1916-21.

BERG, A. H., COMBS, T. P., DU, X., BROWNLEE, M. & SCHERER, P. E. 2001. The adipocyte-secreted protein Acrp30 enhances hepatic insulin action. *Nat Med,* 7**,** 947-53.

BERNDT, S. I., GUSTAFSSON, S., MAGI, R., GANNA, A., WHEELER, E., FEITOSA, M. F., JUSTICE, A. E., MONDA, K. L., CROTEAU-CHONKA, D. C., DAY, F. R., ESKO, T., FALL, T., FERREIRA, T., GENTILINI, D., JACKSON, A. U., LUAN, J., RANDALL, J. C., VEDANTAM, S., WILLER, C. J., WINKLER, T. W., WOOD, A. R., WORKALEMAHU, T., HU, Y. J., LEE, S. H., LIANG, L., LIN, D. Y., MIN, J. L., NEALE, B. M., THORLEIFSSON, G., YANG, J., ALBRECHT, E., AMIN, N., BRAGG-GRESHAM, J. L., CADBY, G., DEN HEIJER, M., EKLUND, N., FISCHER, K., GOEL, A., HOTTENGA, J. J., HUFFMAN, J. E., JARICK, I., JOHANSSON, A., JOHNSON, T., KANONI, S., KLEBER, M. E., KONIG, I. R., KRISTIANSSON, K., KUTALIK, Z., LAMINA, C., LECOEUR, C., LI, G., MANGINO, M., MCARDLE, W. L., MEDINA-GOMEZ, C., MULLER-NURASYID, M., NGWA, J. S., NOLTE, I. M., PATERNOSTER, L., PECHLIVANIS, S., PEROLA, M., PETERS, M. J., PREUSS, M., ROSE, L. M., SHI, J., SHUNGIN, D., SMITH, A. V., STRAWBRIDGE, R. J., SURAKKA, I., TEUMER, A., TRIP, M. D., TYRER, J., VAN VLIET-OSTAPTCHOUK, J. V., VANDENPUT, L., WAITE, L. L., ZHAO, J. H., ABSHER, D., ASSELBERGS, F. W., ATALAY, M., ATTWOOD, A. P., BALMFORTH, A. J., BASART, H., BEILBY, J., BONNYCASTLE, L. L., BRAMBILLA, P., BRUINENBERG, M., CAMPBELL, H., CHASMAN, D. I., CHINES, P. S., COLLINS, F. S., CONNELL, J. M., COOKSON, W. O., DE FAIRE, U., DE VEGT, F., DEI, M., DIMITRIOU, M., EDKINS, S., ESTRADA, K., EVANS, D. M., FARRALL, M., FERRARIO, M. M., *et al.* 2013. Genome-wide meta-

analysis identifies 11 new loci for anthropometric traits and provides insights into genetic architecture. *Nat Genet,* 45**,** 501-12.

BERNHARDT, W. M., WIESENER, M. S., SCIGALLA, P., CHOU, J., SCHMIEDER, R. E., GUNZLER, V. & ECKARDT, K. U. 2010. Inhibition of prolyl hydroxylases increases erythropoietin production in ESRD. *J Am Soc Nephrol,* 21**,** 2151-6.

BERTHOUD, H. R. 2013. Medicine. Why does gastric bypass surgery work? *Science,* 341**,** 351-2.

BERULAVA, T. & HORSTHEMKE, B. 2010. The obesity-associated SNPs in intron 1 of the FTO gene affect primary transcript levels. *Eur J Hum Genet*.

BERULAVA, T., ZIEHE, M., KLEIN-HITPASS, L., MLADENOV, E., THOMALE, J., RUTHER, U. & HORSTHEMKE, B. 2013. FTO levels affect RNA modification and the transcriptome. *Eur J Hum Genet,* 21**,** 317-23.

BIDDINGER, S. B., ALMIND, K., MIYAZAKI, M., KOKKOTOU, E., NTAMBI, J. M. & KAHN, C. R. 2005. Effects of diet and genetic background on sterol regulatory element-binding protein-1c, stearoyl-CoA desaturase 1, and the development of the metabolic syndrome. *Diabetes,* 54**,** 1314-23.

BIRNBOIM, H. C. & DOLY, J. 1979. A rapid alkaline extraction procedure for screening recombinant plasmid DNA. *Nucleic Acids Res,* 7**,** 1513-23.

BISGROVE, B. W. & YOST, H. J. 2006. The roles of cilia in developmental disorders and disease. *Development,* 133**,** 4131-43.

BJORNSTAD, L. G., MEZA, T. J., OTTERLEI, M., OLAFSRUD, S. M., MEZA-ZEPEDA, L. A. & FALNES, P. O. 2012. Human ALKBH4 interacts with proteins associated with transcription. *PLoS One,* 7**,** e49045.

BODE, J., SCHLAKE, T., IBER, M., SCHUBELER, D., SEIBLER, J., SNEZHKOV, E. & NIKOLAEV, L. 2000. The transgeneticist's toolbox: novel methods for the targeted modification of eukaryotic genomes. *Biol Chem,* 381**,** 801-13.

BOISSEL, S., REISH, O., PROULX, K., KAWAGOE-TAKAKI, H., SEDGWICK, B., YEO, G. S., MEYRE, D., GOLZIO, C., MOLINARI, F., KADHOM, N., ETCHEVERS, H. C., SAUDEK, V., FAROOQI, I. S., FROGUEL, P., LINDAHL, T., O'RAHILLY, S., MUNNICH, A. & COLLEAUX, L. 2009. Loss-of-function mutation in the dioxygenase-encoding FTO gene causes severe growth retardation and multiple malformations. *Am J Hum Genet,* 85**,** 106-11.

BOKAR, J. A., SHAMBAUGH, M. E., POLAYES, D., MATERA, A. G. & ROTTMAN, F. M. 1997. Purification and cDNA cloning of the AdoMet-binding subunit of the human mRNA (N6-adenosine)-methyltransferase. *RNA,* 3**,** 1233-47.

BOLLEPALLI, S., DOLAN, L. M., DEKA, R. & MARTIN, L. J. 2010. Association of FTO gene variants with adiposity in African-American adolescents. *Obesity (Silver Spring),* 18**,** 1959-63.

BONFILS, G., JAQUENOUD, M., BONTRON, S., OSTROWICZ, C., UNGERMANN, C. & DE VIRGILIO, C. 2012. Leucyl-tRNA synthetase controls TORC1 via the EGO complex. *Mol Cell,* 46**,** 105-10.

BOWERS, R. R. & LANE, M. D. 2008. Wnt signaling and adipocyte lineage commitment. *Cell Cycle,* 7**,** 1191-6.

BRAULT, V., BESSON, V., MAGNOL, L., DUCHON, A. & HERAULT, Y. 2007. Cre/loxP-mediated chromosome engineering of the mouse genome. *Handb Exp Pharmacol***,** 29-48.

BRAVARD, A., LEFAI, E., MEUGNIER, E., PESENTI, S., DISSE, E., VOUILLARMET, J., PERETTI, N., RABASA-LHORET, R., LAVILLE, M., VIDAL, H. & RIEUSSET, J. 2011. FTO is increased in muscle during type 2 diabetes, and its overexpression in myotubes alters insulin signaling, enhances lipogenesis and ROS production, and induces mitochondrial dysfunction. *Diabetes,* 60**,** 258-68.

BRESLAUER, K. J., FRANK, R., BLOCKER, H. & MARKY, L. A. 1986. Predicting DNA duplex stability from the base sequence. *Proc Natl Acad Sci U S A,* 83**,** 3746-50.

BRESSLER, J., FORNAGE, M., DEMERATH, E. W., KNOPMAN, D. S., MONDA, K. L., NORTH, K. E., PENMAN, A., MOSLEY, T. H. & BOERWINKLE, E. 2013. Fat mass and obesity gene and cognitive decline: the Atherosclerosis Risk in Communities Study. *Neurology,* 80**,** 92-9.

BREUM, L., RASMUSSEN, M. H., HILSTED, J. & FERNSTROM, J. D. 2003. Twenty-four-hour plasma tryptophan concentrations and ratios are below normal in obese subjects and are not normalized by substantial weight reduction. *Am J Clin Nutr,* 77**,** 1112-8.

BROWN, K. 2002. Breast cancer chemoprevention: risk-benefit effects of the antioestrogen tamoxifen. *Expert Opin Drug Saf,* 1**,** 253-67.

BROWN, S. D. & MOORE, M. W. 2012. Towards an encyclopaedia of mammalian gene function: the International Mouse Phenotyping Consortium. *Dis Model Mech,* 5**,** 289-92.

BRUNING, J. C., GAUTAM, D., BURKS, D. J., GILLETTE, J., SCHUBERT, M., ORBAN, P. C., KLEIN, R., KRONE, W., MULLER-WIELAND, D. & KAHN, C. R. 2000. Role of brain insulin receptor in control of body weight and reproduction. *Science,* 289**,** 2122-5.

BUCHWALD, H., AVIDOR, Y., BRAUNWALD, E., JENSEN, M. D., PORIES, W., FAHRBACH, K. & SCHOELLES, K. 2004. Bariatric surgery: a systematic review and meta-analysis. *JAMA,* 292**,** 1724-37.

BURTON, P. S., GOODWIN, J. T., VIDMAR, T. J. & AMORE, B. M. 2002. Predicting drug absorption: how nature made it a difficult problem. *J Pharmacol Exp Ther,* 303**,** 889-95.

BUTLER, A. A. & KOZAK, L. P. 2010. A recurring problem with the analysis of energy expenditure in genetic models expressing lean and obese phenotypes. *Diabetes,* 59**,** 323-9.

CABALLERO, B., FINER, N. & WURTMAN, R. J. 1988. Plasma amino acids and insulin levels in obesity: response to carbohydrate intake and tryptophan supplements. *Metabolism,* 37**,** 672-6.

CANTARA, W. A., CRAIN, P. F., ROZENSKI, J., MCCLOSKEY, J. A., HARRIS, K. A., ZHANG, X., VENDEIX, F. A., FABRIS, D. & AGRIS, P. F. 2011. The RNA Modification Database, RNAMDB: 2011 update. *Nucleic Acids Res,* 39**,** D195-201.

CAPECCHI, M. R. 1989. Altering the genome by homologous recombination. *Science,* 244**,** 1288-92.

CARDENAS-RODRIGUEZ, M. & BADANO, J. L. 2009. Ciliary biology: understanding the cellular and genetic basis of human ciliopathies. *Am J Med Genet C Semin Med Genet,* 151C**,** 263-80.

CARON, A., XU, X. & LIN, X. 2012. Wnt/beta-catenin signaling directly regulates Foxj1 expression and ciliogenesis in zebrafish Kupffer's vesicle. *Development,* 139**,** 514-24.

CARTHEW, P., RICH, K. J., MARTIN, E. A., DE MATTEIS, F., LIM, C. K., MANSON, M. M., FESTING, M. F., WHITE, I. N. & SMITH, L. L. 1995. DNA damage as assessed by 32P-postlabelling in three rat strains exposed to dietary tamoxifen: the relationship between cell proliferation and liver tumour formation. *Carcinogenesis,* 16**,** 1299-304.

CASABIELL, X., PINEIRO, V., VEGA, F., DE LA CRUZ, L. F., DIEGUEZ, C. & CASANUEVA, F. F. 2001. Leptin, reproduction and sex steroids. *Pituitary,* 4**,** 93-9.

CECIL, J. E., TAVENDALE, R., WATT, P., HETHERINGTON, M. M. & PALMER, C. N. 2008. An obesity-associated FTO gene variant and increased energy intake in children. *N Engl J Med,* 359**,** 2558-66.

CEDERNAES, J., ALSIO, J., VASTERMARK, A., RISERUS, U. & SCHIOTH, H. B. 2013. Adipose tissue stearoyl-CoA desaturase 1 index is increased and linoleic acid is decreased in obesity-prone rats fed a high-fat diet. *Lipids Health Dis,* 12**,** 2.

CHAKRAVARTY, K., CASSUTO, H., RESHEF, L. & HANSON, R. W. 2005. Factors that control the tissue-specific transcription of the gene for phosphoenolpyruvate carboxykinase-C. *Crit Rev Biochem Mol Biol,* 40**,** 129-54.

CHAMBERS, J. C., ELLIOTT, P., ZABANEH, D., ZHANG, W., LI, Y., FROGUEL, P., BALDING, D., SCOTT, J. & KOONER, J. S. 2008. Common genetic variation near MC4R is associated with waist circumference and insulin resistance. *Nat Genet,* 40**,** 716-8.

CHENG, C. W., CHOW, R. L., LEBEL, M., SAKUMA, R., CHEUNG, H. O., THANABALASINGHAM, V., ZHANG, X., BRUNEAU, B. G., BIRCH, D. G., HUI, C. C., MCINNES, R. R. & CHENG, S. H. 2005. The Iroquois homeobox gene, Irx5, is required for retinal cone bipolar cell development. *Dev Biol,* 287**,** 48-60.

CHEUNG, M. K., GULATI, P., O'RAHILLY, S. & YEO, G. S. 2013. FTO expression is regulated by availability of essential amino acids. *Int J Obes (Lond),* 37**,** 744-7.

CHO, Y. S., GO, M. J., KIM, Y. J., HEO, J. Y., OH, J. H., BAN, H. J., YOON, D., LEE, M. H., KIM, D. J., PARK, M., CHA, S. H., KIM, J. W., HAN, B. G., MIN, H., AHN, Y., PARK, M. S., HAN, H. R., JANG, H. Y., CHO, E. Y., LEE, J. E., CHO, N. H., SHIN, C., PARK, T., PARK, J. W., LEE, J. K., CARDON, L., CLARKE, G., MCCARTHY, M. I., LEE, J. Y., OH, B. & KIM, H. L. 2009. A large-scale genome-wide association study of Asian populations uncovers genetic factors influencing eight quantitative traits. *Nat Genet,* 41**,** 527-34.

CHOI, S. J., YABLONKA-REUVENI, Z., KAIYALA, K. J., OGIMOTO, K., SCHWARTZ, M. W. & WISSE, B. E. 2011. Increased energy expenditure and leptin sensitivity account for low fat mass in myostatin-deficient mice. *Am J Physiol Endocrinol Metab,* 300**,** E1031-7.

CHOUDHRY, Z., SENGUPTA, S. M., GRIZENKO, N., THAKUR, G. A., FORTIER, M. E., SCHMITZ, N. & JOOBER, R. 2013. Association between obesity-related gene FTO and ADHD. *Obesity (Silver Spring)*.

CHRISTIAN, M., CERMAK, T., DOYLE, E. L., SCHMIDT, C., ZHANG, F., HUMMEL, A., BOGDANOVE, A. J. & VOYTAS, D. F. 2010. Targeting DNA double-strand breaks with TAL effector nucleases. *Genetics,* 186**,** 757-61.

CHRISTODOULIDES, C., LAGATHU, C., SETHI, J. K. & VIDAL-PUIG, A. 2009. Adipogenesis and WNT signalling. *Trends Endocrinol Metab,* 20**,** 16-24.

CHURCH, C., LEE, S., BAGG, E. A., MCTAGGART, J. S., DEACON, R., GERKEN, T., LEE, A., MOIR, L., MECINOVIC, J., QUWAILID, M. M., SCHOFIELD, C. J., ASHCROFT, F. M. & COX, R. D. 2009. A mouse model for the metabolic effects of the human fat mass and obesity associated FTO gene. *PLoS Genet,* 5**,** e1000599.

CHURCH, C., MOIR, L., MCMURRAY, F., GIRARD, C., BANKS, G. T., TEBOUL, L., WELLS, S., BRUNING, J. C., NOLAN, P. M., ASHCROFT, F. M. & COX, R. D. 2010. Overexpression of Fto leads to increased food intake and results in obesity. *Nat Genet,* 42**,** 1086-92.

CLEMENT, K., VAISSE, C., LAHLOU, N., CABROL, S., PELLOUX, V., CASSUTO, D., GOURMELEN, M., DINA, C., CHAMBAZ, J., LACORTE, J. M., BASDEVANT, A., BOUGNERES, P., LEBOUC, Y., FROGUEL, P. & GUY-GRAND, B. 1998. A mutation in the human leptin receptor gene causes obesity and pituitary dysfunction. *Nature,* 392**,** 398-401.

CLIFTON, I. J., MCDONOUGH, M. A., EHRISMANN, D., KERSHAW, N. J., GRANATINO, N. & SCHOFIELD, C. J. 2006. Structural studies on 2-oxoglutarate oxygenases and related double-stranded beta-helix fold proteins. *J Inorg Biochem,* 100**,** 644-69.

COGHILL, E. L., HUGILL, A., PARKINSON, N., DAVISON, C., GLENISTER, P., CLEMENTS, S., HUNTER, J., COX, R. D. & BROWN, S. D. 2002. A gene-driven approach to the identification of ENU mutants in the mouse. *Nat Genet,* 30**,** 255-6.

COHEN, H. Y., MILLER, C., BITTERMAN, K. J., WALL, N. R., HEKKING, B., KESSLER, B., HOWITZ, K. T., GOROSPE, M., DE CABO, R. & SINCLAIR, D. A. 2004. Calorie restriction promotes mammalian cell survival by inducing the SIRT1 deacetylase. *Science,* 305**,** 390-2.

COMBS, T. P., WAGNER, J. A., BERGER, J., DOEBBER, T., WANG, W. J., ZHANG, B. B., TANEN, M., BERG, A. H., O'RAHILLY, S., SAVAGE, D. B., CHATTERJEE, K., WEISS, S., LARSON, P. J., GOTTESDIENER, K. M., GERTZ, B. J., CHARRON, M. J., SCHERER, P. E. & MOLLER, D. E. 2002. Induction of adipocyte complement-related protein of 30 kilodaltons by PPARgamma agonists: a potential mechanism of insulin sensitization. *Endocrinology,* 143**,** 998-1007.

CORBIT, K. C., SHYER, A. E., DOWDLE, W. E., GAULDEN, J., SINGLA, V., CHEN, M. H., CHUANG, P. T. & REITER, J. F. 2008. Kif3a constrains beta-catenin-dependent Wnt signalling through dual ciliary and non-ciliary mechanisms. *Nat Cell Biol,* 10**,** 70-6.

CORTESE, S., RAMOS OLAZAGASTI, M. A., KLEIN, R. G., CASTELLANOS, F. X., PROAL, E. & MANNUZZA, S. 2013. Obesity in men with childhood ADHD: a 33-year controlled, prospective, follow-up study. *Pediatrics,* 131**,** e1731-8.

COTSAPAS, C., SPELIOTES, E. K., HATOUM, I. J., GREENAWALT, D. M., DOBRIN, R., LUM, P. Y., SUVER, C., CHUDIN, E., KEMP, D., REITMAN, M., VOIGHT, B. F.,

NEALE, B. M., SCHADT, E. E., HIRSCHHORN, J. N., KAPLAN, L. M. & DALY, M. J. 2009. Common body mass index-associated variants confer risk of extreme obesity. *Hum Mol Genet,* 18**,** 3502-7.

CUNNINGHAM, J. T., RODGERS, J. T., ARLOW, D. H., VAZQUEZ, F., MOOTHA, V. K. & PUIGSERVER, P. 2007. mTOR controls mitochondrial oxidative function through a YY1-PGC-1alpha transcriptional complex. *Nature,* 450**,** 736-40.

DARLINGTON, G. J., BERNHARD, H. P., MILLER, R. A. & RUDDLE, F. H. 1980. Expression of liver phenotypes in cultured mouse hepatoma cells. *J Natl Cancer Inst,* 64**,** 809-19.

DAVENPORT, J. R., WATTS, A. J., ROPER, V. C., CROYLE, M. J., VAN GROEN, T., WYSS, J. M., NAGY, T. R., KESTERSON, R. A. & YODER, B. K. 2007. Disruption of intraflagellar transport in adult mice leads to obesity and slow-onset cystic kidney disease. *Curr Biol,* 17**,** 1586-94.

DE ALBORAN, I. M., O'HAGAN, R. C., GARTNER, F., MALYNN, B., DAVIDSON, L., RICKERT, R., RAJEWSKY, K., DEPINHO, R. A. & ALT, F. W. 2001. Analysis of C-MYC function in normal cells via conditional gene-targeted mutation. *Immunity,* 14**,** 45-55.

DE SOUZA, J., BUTLER, A. A. & CONE, R. D. 2000. Disproportionate inhibition of feeding in A(y) mice by certain stressors: a cautionary note. *Neuroendocrinology,* 72**,** 126-32.

DEEB, S. S., FAJAS, L., NEMOTO, M., PIHLAJAMAKI, J., MYKKANEN, L., KUUSISTO, J., LAAKSO, M., FUJIMOTO, W. & AUWERX, J. 1998. A Pro12Ala substitution in PPARgamma2 associated with decreased receptor activity, lower body mass index and improved insulin sensitivity. *Nat Genet,* 20**,** 284-7.

DEN HOED, M., WESTERTERP-PLANTENGA, M. S., BOUWMAN, F. G., MARIMAN, E. C. & WESTERTERP, K. R. 2009. Postprandial responses in hunger and satiety are associated with the rs9939609 single nucleotide polymorphism in FTO. *Am J Clin Nutr,* 90**,** 1426-32.

DIGGLE, P., HEAGERTY, P., LIANG, K.-Y. & ZEGER, S. L. 2002. *Analysis of Longitudinal Data,* Oxford, Oxford University press.

DINA, C., MEYRE, D., GALLINA, S., DURAND, E., KORNER, A., JACOBSON, P., CARLSSON, L. M., KIESS, W., VATIN, V., LECOEUR, C., DELPLANQUE, J., VAILLANT, E., PATTOU, F., RUIZ, J., WEILL, J., LEVY-MARCHAL, C., HORBER, F., POTOCZNA, N., HERCBERG, S., LE STUNFF, C., BOUGNERES, P., KOVACS, P., MARRE, M., BALKAU, B., CAUCHI, S., CHEVRE, J. C. & FROGUEL, P. 2007. Variation in FTO contributes to childhood obesity and severe adult obesity. *Nat Genet,* 39**,** 724-6.

DO, R., BAILEY, S. D., DESBIENS, K., BELISLE, A., MONTPETIT, A., BOUCHARD, C., PERUSSE, L., VOHL, M. C. & ENGERT, J. C. 2008. Genetic variants of FTO influence adiposity, insulin sensitivity, leptin levels, and resting metabolic rate in the Quebec Family Study. *Diabetes,* 57**,** 1147-50.

DOMINISSINI, D., MOSHITCH-MOSHKOVITZ, S., SCHWARTZ, S., SALMON-DIVON, M., UNGAR, L., OSENBERG, S., CESARKAS, K., JACOB-HIRSCH, J., AMARIGLIO, N., KUPIEC, M., SOREK, R. & RECHAVI, G. 2012. Topology of the human and mouse m6A RNA methylomes revealed by m6A-seq. *Nature,* 485**,** 201-6.

DORAJOO, R., BLAKEMORE, A. I., SIM, X., ONG, R. T., NG, D. P., SEIELSTAD, M., WONG, T. Y., SAW, S. M., FROGUEL, P., LIU, J. & TAI, E. S. 2012. Replication of 13 obesity loci among Singaporean Chinese, Malay and Asian-Indian populations. *Int J Obes (Lond),* 36**,** 159-63.

DUBOIS, N. C., HOFMANN, D., KALOULIS, K., BISHOP, J. M. & TRUMPP, A. 2006. Nestin-Cre transgenic mouse line Nes-Cre1 mediates highly efficient Cre/loxP mediated recombination in the nervous system, kidney, and somite-derived tissues. *Genesis,* 44**,** 355-60.

DUDANI, A. K., GUPTA, R. S. & GUPTA, R. 1988. Species-specific differences in the toxicity of puromycin towards cultured human and Chinese hamster cells. *FEBS Lett,* 234**,** 141-4.

DUNCAN, T., TREWICK, S. C., KOIVISTO, P., BATES, P. A., LINDAHL, T. & SEDGWICK, B. 2002. Reversal of DNA alkylation damage by two human dioxygenases. *Proc Natl Acad Sci U S A,* 99**,** 16660-5.

EGGENSCHWILER, J. T. & ANDERSON, K. V. 2007. Cilia and developmental signaling. *Annu Rev Cell Dev Biol,* 23**,** 345-73.

ELIAS, C. F., LEE, C., KELLY, J., ASCHKENASI, C., AHIMA, R. S., COUCEYRO, P. R., KUHAR, M. J., SAPER, C. B. & ELMQUIST, J. K. 1998. Leptin activates hypothalamic CART neurons projecting to the spinal cord. *Neuron,* 21**,** 1375-85.

ELKS, C. E., PERRY, J. R., SULEM, P., CHASMAN, D. I., FRANCESCHINI, N., HE, C., LUNETTA, K. L., VISSER, J. A., BYRNE, E. M., COUSMINER, D. L., GUDBJARTSSON, D. F., ESKO, T., FEENSTRA, B., HOTTENGA, J. J., KOLLER, D. L., KUTALIK, Z., LIN, P., MANGINO, M., MARONGIU, M., MCARDLE, P. F., SMITH, A. V., STOLK, L., VAN WINGERDEN, S. H., ZHAO, J. H., ALBRECHT, E., CORRE, T., INGELSSON, E., HAYWARD, C., MAGNUSSON, P. K., SMITH, E. N., ULIVI, S., WARRINGTON, N. M., ZGAGA, L., ALAVERE, H., AMIN, N., ASPELUND, T., BANDINELLI, S., BARROSO, I., BERENSON, G. S., BERGMANN, S., BLACKBURN, H., BOERWINKLE, E., BURING, J. E., BUSONERO, F., CAMPBELL, H., CHANOCK, S. J., CHEN, W., CORNELIS, M. C., COUPER, D., COVIELLO, A. D., D'ADAMO, P., DE FAIRE, U., DE GEUS, E. J., DELOUKAS, P., DORING, A., SMITH, G. D., EASTON, D. F., EIRIKSDOTTIR, G., EMILSSON, V., ERIKSSON, J., FERRUCCI, L., FOLSOM, A. R., FOROUD, T., GARCIA, M., GASPARINI, P., GELLER, F., GIEGER, C., CONSORTIUM, T. G., GUDNASON, V., HALL, P., HANKINSON, S. E., FERRELI, L., HEATH, A. C., HERNANDEZ, D. G., HOFMAN, A., HU, F. B., ILLIG, T., JARVELIN, M. R., JOHNSON, A. D., KARASIK, D., KHAW, K. T., KIEL, D. P., KILPELAINEN, T. O., KOLCIC, I., KRAFT, P., LAUNER, L. J., LAVEN, J. S., LI, S., LIU, J., LEVY, D., MARTIN, N. G., MCARDLE, W. L., MELBYE, M., MOOSER, V., MURRAY, J. C., MURRAY, S. S., NALLS, M. A., NAVARRO, P., NELIS, M., NESS, A. R., *et al.* 2010. Thirty new loci for age at menarche identified by a meta-analysis of genome-wide association studies. *Nat Genet*.

ELLIOTT, K. S., CHAPMAN, K., DAY-WILLIAMS, A., PANOUTSOPOULOU, K., SOUTHAM, L., LINDGREN, C. M., ARDEN, N., ASLAM, N., BIRRELL, F., CARLUKE, I., CARR, A., DELOUKAS, P., DOHERTY, M., LOUGHLIN, J., MCCASKIE, A., OLLIER, W. E., RAI, A., RALSTON, S., REED, M. R., SPECTOR, T. D., VALDES, A. M., WALLIS, G. A., WILKINSON, M. & ZEGGINI, E. 2013. Evaluation of the genetic overlap between osteoarthritis with body mass index and height using genome-wide association scan data. *Ann Rheum Dis,* 72**,** 935-41.

ELSHORBAGY, A. K., KOZICH, V., SMITH, A. D. & REFSUM, H. 2012. Cysteine and obesity: consistency of the evidence across epidemiologic, animal and cellular studies. *Curr Opin Clin Nutr Metab Care,* 15**,** 49-57.

ESPOSITO, K., PONTILLO, A., DI PALO, C., GIUGLIANO, G., MASELLA, M., MARFELLA, R. & GIUGLIANO, D. 2003. Effect of weight loss and lifestyle changes on vascular inflammatory markers in obese women: a randomized trial. *JAMA,* 289**,** 1799-804.

EWENS, K. G., JONES, M. R., ANKENER, W., STEWART, D. R., URBANEK, M., DUNAIF, A., LEGRO, R. S., CHUA, A., AZZIZ, R., SPIELMAN, R. S., GOODARZI, M. O. & STRAUSS, J. F., 3RD 2011. FTO and MC4R gene variants are associated with obesity in polycystic ovary syndrome. *PLoS One,* 6**,** e16390.

FALNES, P. O., JOHANSEN, R. F. & SEEBERG, E. 2002. AlkB-mediated oxidative demethylation reverses DNA damage in Escherichia coli. *Nature,* 419**,** 178-82.

FAROOQI, I. S., JEBB, S. A., LANGMACK, G., LAWRENCE, E., CHEETHAM, C. H., PRENTICE, A. M., HUGHES, I. A., MCCAMISH, M. A. & O'RAHILLY, S. 1999. Effects of recombinant leptin therapy in a child with congenital leptin deficiency. *N Engl J Med,* 341**,** 879-84.

FAROOQI, I. S., KEOGH, J. M., YEO, G. S., LANK, E. J., CHEETHAM, T. & O'RAHILLY, S. 2003. Clinical spectrum of obesity and mutations in the melanocortin 4 receptor gene. *N Engl J Med,* 348**,** 1085-95.

FAROOQI, I. S., MATARESE, G., LORD, G. M., KEOGH, J. M., LAWRENCE, E., AGWU, C., SANNA, V., JEBB, S. A., PERNA, F., FONTANA, S., LECHLER, R. I., DEPAOLI, A. M. & O'RAHILLY, S. 2002. Beneficial effects of leptin on obesity, T cell

hyporesponsiveness, and neuroendocrine/metabolic dysfunction of human congenital leptin deficiency. *J Clin Invest,* 110**,** 1093-103.

FAROOQI, I. S. & O'RAHILLY, S. 2005. Monogenic obesity in humans. *Annu Rev Med,* 56**,** 443-58.

FAROOQI, I. S. & O'RAHILLY, S. 2008. Mutations in ligands and receptors of the leptin-melanocortin pathway that lead to obesity. *Nat Clin Pract Endocrinol Metab,* 4**,** 569-77.

FAROOQI, I. S., YEO, G. S., KEOGH, J. M., AMINIAN, S., JEBB, S. A., BUTLER, G., CHEETHAM, T. & O'RAHILLY, S. 2000. Dominant and recessive inheritance of morbid obesity associated with melanocortin 4 receptor deficiency. *J Clin Invest,* 106**,** 271-9.

FAWCETT, K. A. & BARROSO, I. 2010. The genetics of obesity: FTO leads the way. *Trends Genet*.

FEINLEIB, M., GARRISON, R. J., FABSITZ, R., CHRISTIAN, J. C., HRUBEC, Z., BORHANI, N. O., KANNEL, W. B., ROSENMAN, R., SCHWARTZ, J. T. & WAGNER, J. O. 1977. The NHLBI twin study of cardiovascular disease risk factors: methodology and summary of results. *Am J Epidemiol,* 106**,** 284-5.

FENG, Y. Q., SEIBLER, J., ALAMI, R., EISEN, A., WESTERMAN, K. A., LEBOULCH, P., FIERING, S. & BOUHASSIRA, E. E. 1999. Site-specific chromosomal integration in mammalian cells: highly efficient CRE recombinase-mediated cassette exchange. *J Mol Biol,* 292**,** 779-85.

FERKOL, T. W. & LEIGH, M. W. 2012. Ciliopathies: the central role of cilia in a spectrum of pediatric disorders. *J Pediatr,* 160**,** 366-71.

FERNSTROM, J. D. 1990. Aromatic amino acids and monoamine synthesis in the central nervous system: influence of the diet. *J Nutr Biochem,* 1**,** 508-17.

FERNSTROM, M. H. & FERNSTROM, J. D. 1995. Brain tryptophan concentrations and serotonin synthesis remain responsive to food consumption after the ingestion of sequential meals. *Am J Clin Nutr,* 61**,** 312-9.

FISCHER-POSOVSZKY, P., NEWELL, F. S., WABITSCH, M. & TORNQVIST, H. E. 2008. Human SGBS cells - a unique tool for studies of human fat cell biology. *Obes Facts,* 1**,** 184-9.

FISCHER, J., KOCH, L., EMMERLING, C., VIERKOTTEN, J., PETERS, T., BRUNING, J. C. & RUTHER, U. 2009. Inactivation of the Fto gene protects from obesity. *Nature,* 458**,** 894-8.

FOX, C. S., LIU, Y., WHITE, C. C., FEITOSA, M., SMITH, A. V., HEARD-COSTA, N., LOHMAN, K., JOHNSON, A. D., FOSTER, M. C., GREENAWALT, D. M., GRIFFIN, P., DING, J., NEWMAN, A. B., TYLAVSKY, F., MILJKOVIC, I., KRITCHEVSKY, S. B., LAUNER, L., GARCIA, M., EIRIKSDOTTIR, G., CARR, J. J., GUDNASON, V., HARRIS, T. B., CUPPLES, L. A. & BORECKI, I. B. 2012. Genome-wide association for abdominal subcutaneous and visceral adipose reveals a novel locus for visceral fat in women. *PLoS Genet,* 8**,** e1002695.

FRAYLING, T. M. & ONG, K. 2011. Piecing together the FTO jigsaw. *Genome Biol,* 12**,** 104.

FRAYLING, T. M., TIMPSON, N. J., WEEDON, M. N., ZEGGINI, E., FREATHY, R. M., LINDGREN, C. M., PERRY, J. R., ELLIOTT, K. S., LANGO, H., RAYNER, N. W., SHIELDS, B., HARRIES, L. W., BARRETT, J. C., ELLARD, S., GROVES, C. J., KNIGHT, B., PATCH, A. M., NESS, A. R., EBRAHIM, S., LAWLOR, D. A., RING, S. M., BEN-SHLOMO, Y., JARVELIN, M. R., SOVIO, U., BENNETT, A. J., MELZER, D., FERRUCCI, L., LOOS, R. J., BARROSO, I., WAREHAM, N. J., KARPE, F., OWEN, K. R., CARDON, L. R., WALKER, M., HITMAN, G. A., PALMER, C. N., DONEY, A. S., MORRIS, A. D., SMITH, G. D., HATTERSLEY, A. T. & MCCARTHY, M. I. 2007. A common variant in the FTO gene is associated with body mass index and predisposes to childhood and adult obesity. *Science,* 316**,** 889-94.

FREDRIKSSON, R., HAGGLUND, M., OLSZEWSKI, P. K., STEPHANSSON, O., JACOBSSON, J. A., OLSZEWSKA, A. M., LEVINE, A. S., LINDBLOM, J. & SCHIOTH, H. B. 2008. The obesity gene, FTO, is of ancient origin, up-regulated during food deprivation and expressed in neurons of feeding-related nuclei of the brain. *Endocrinology,* 149**,** 2062-71.

FRIDEN, M., LJUNGQVIST, H., MIDDLETON, B., BREDBERG, U. & HAMMARLUND-UDENAES, M. 2010. Improved measurement of drug exposure in the brain using drug-specific correction for residual blood. *J Cereb Blood Flow Metab,* 30**,** 150-61.

FRIED, S. K., BUNKIN, D. A. & GREENBERG, A. S. 1998. Omental and subcutaneous adipose tissues of obese subjects release interleukin-6: depot difference and regulation by glucocorticoid. *J Clin Endocrinol Metab,* 83**,** 847-50.

FRIEDMAN, J. M., LEIBEL, R. L., SIEGEL, D. S., WALSH, J. & BAHARY, N. 1991. Molecular mapping of the mouse ob mutation. *Genomics,* 11**,** 1054-62.

FU, D., BROPHY, J. A., CHAN, C. T., ATMORE, K. A., BEGLEY, U., PAULES, R. S., DEDON, P. C., BEGLEY, T. J. & SAMSON, L. D. 2010a. Human AlkB homolog ABH8 Is a tRNA methyltransferase required for wobble uridine modification and DNA damage survival. *Mol Cell Biol,* 30**,** 2449-59.

FU, D., JORDAN, J. J. & SAMSON, L. D. 2013. Human ALKBH7 is required for alkylation and oxidation-induced programmed necrosis. *Genes Dev,* 27**,** 1089-100.

FU, Y., DAI, Q., ZHANG, W., REN, J., PAN, T. & HE, C. 2010b. The AlkB domain of mammalian ABH8 catalyzes hydroxylation of 5-methoxycarbonylmethyluridine at the wobble position of tRNA. *Angew Chem Int Ed Engl,* 49**,** 8885-8.

FUJII, T. & NISHIMURA, H. 1972. Comparison of teratogenic action of substances related to purine metabolism in mouse embryos. *Jpn J Pharmacol,* 22**,** 201-6.

GALICHET, C., LOVELL-BADGE, R. & RIZZOTI, K. 2010. Nestin-Cre mice are affected by hypopituitarism, which is not due to significant activity of the transgene in the pituitary gland. *PLoS One,* 5**,** e11443.

GAN, X. T., ZHAO, G., HUANG, C. X., ROWE, A. C., PURDHAM, D. M. & KARMAZYN, M. 2013. Identification of Fat Mass and Obesity Associated (FTO) Protein Expression in Cardiomyocytes: Regulation by Leptin and Its Contribution to Leptin-Induced Hypertrophy. *PLoS One,* 8**,** e74235.

GAO, X., SHIN, Y. H., LI, M., WANG, F., TONG, Q. & ZHANG, P. 2010. The Fat Mass and Obesity Associated Gene FTO Functions in the Brain to Regulate Postnatal Growth in Mice. *PLoS One,* 5**,** e14005.

GAO, Y., HUANG, C., ZHAO, K., MA, L., QIU, X., ZHANG, L., XIU, Y., CHEN, L., LU, W., TANG, Y. & XIAO, Q. 2013. Depression as a risk factor for dementia and mild cognitive impairment: a meta-analysis of longitudinal studies. *Int J Geriatr Psychiatry,* 28**,** 441-9.

GARTHWAITE, T. L., MARTINSON, D. R., TSENG, L. F., HAGEN, T. C. & MENAHAN, L. A. 1980. A longitudinal hormonal profile of the genetically obese mouse. *Endocrinology,* 107**,** 671-6.

GATES, H., MALLON, A. M. & BROWN, S. D. 2011. High-throughput mouse phenotyping. *Methods,* 53**,** 394-404.

GAUDET, M. M., YANG, H. P., BOSQUET, J. G., HEALEY, C. S., AHMED, S., DUNNING, A. M., EASTON, D. F., SPURDLE, A. B., FERGUSON, K., O'MARA, T., LAMBRECHTS, D., DESPIERRE, E., VERGOTE, I., AMANT, F., LACEY, J. V., JR., LISSOWSKA, J., PEPLONSKA, B., BRINTON, L. A., CHANOCK, S. & GARCIA-CLOSAS, M. 2010. No association between FTO or HHEX and endometrial cancer risk. *Cancer Epidemiol Biomarkers Prev,* 19**,** 2106-9.

GERDES, J. M., LIU, Y., ZAGHLOUL, N. A., LEITCH, C. C., LAWSON, S. S., KATO, M., BEACHY, P. A., BEALES, P. L., DEMARTINO, G. N., FISHER, S., BADANO, J. L. & KATSANIS, N. 2007. Disruption of the basal body compromises proteasomal function and perturbs intracellular Wnt response. *Nat Genet,* 39**,** 1350-60.

GERKEN, T., GIRARD, C. A., TUNG, Y. C., WEBBY, C. J., SAUDEK, V., HEWITSON, K. S., YEO, G. S., MCDONOUGH, M. A., CUNLIFFE, S., MCNEILL, L. A., GALVANOVSKIS, J., RORSMAN, P., ROBINS, P., PRIEUR, X., COLL, A. P., MA, M., JOVANOVIC, Z., FAROOQI, I. S., SEDGWICK, B., BARROSO, I., LINDAHL, T., PONTING, C. P., ASHCROFT, F. M., O'RAHILLY, S. & SCHOFIELD, C. J. 2007. The obesity-associated FTO gene encodes a 2-oxoglutarate-dependent nucleic acid demethylase. *Science,* 318**,** 1469-72.

GEURTS, A. M., COST, G. J., FREYVERT, Y., ZEITLER, B., MILLER, J. C., CHOI, V. M., JENKINS, S. S., WOOD, A., CUI, X., MENG, X., VINCENT, A., LAM, S., MICHALKIEWICZ, M., SCHILLING, R., FOECKLER, J., KALLOWAY, S., WEILER, H., MENORET, S., ANEGON, I., DAVIS, G. D., ZHANG, L., REBAR, E. J., GREGORY, P. D., URNOV, F. D., JACOB, H. J. & BUELOW, R. 2009. Knockout rats via embryo microinjection of zinc-finger nucleases. *Science,* 325**,** 433.

GOETZ, S. C. & ANDERSON, K. V. 2010. The primary cilium: a signalling centre during vertebrate development. *Nat Rev Genet,* 11**,** 331-44.

GOODWIN, J. T. & CLARK, D. E. 2005. In silico predictions of blood-brain barrier penetration: considerations to "keep in mind". *J Pharmacol Exp Ther,* 315**,** 477-83.

GRAY, J. M., SCHROCK, S. & BISHOP, M. 1993. Estrogens and antiestrogens: actions and interactions with fluphenazine on food intake and body weight in rats. *Am J Physiol,* 264**,** R1214-8.

GREAVES, P., GOONETILLEKE, R., NUNN, G., TOPHAM, J. & ORTON, T. 1993. Two-year carcinogenicity study of tamoxifen in Alderley Park Wistar-derived rats. *Cancer Res,* 53**,** 3919-24.

GREENMAN, Y., GOLANI, N., GILAD, S., YARON, M., LIMOR, R. & STERN, N. 2004. Ghrelin secretion is modulated in a nutrient- and gender-specific manner. *Clin Endocrinol (Oxf),* 60**,** 382-8.

GRUNNET, L. G., BRONS, C., JACOBSEN, S., NILSSON, E., ASTRUP, A., HANSEN, T., PEDERSEN, O., POULSEN, P., QUISTORFF, B. & VAAG, A. 2009a. Increased recovery rates of phosphocreatine and inorganic phosphate after isometric contraction in oxidative muscle fibers and elevated hepatic insulin resistance in homozygous carriers of the A-allele of FTO rs9939609. *J Clin Endocrinol Metab,* 94**,** 596-602.

GRUNNET, L. G., NILSSON, E., LING, C., HANSEN, T., PEDERSEN, O., GROOP, L., VAAG, A. & POULSEN, P. 2009b. Regulation and function of FTO mRNA expression in human skeletal muscle and subcutaneous adipose tissue. *Diabetes,* 58**,** 2402-8.

GULATI, P., CHEUNG, M. K., ANTROBUS, R., CHURCH, C. D., HARDING, H. P., TUNG, Y. C., RIMMINGTON, D., MA, M., RON, D., LEHNER, P. J., ASHCROFT, F. M., COX, R. D., COLL, A. P., O'RAHILLY, S. & YEO, G. S. 2013. Role for the obesity-related FTO gene in the cellular sensing of amino acids. *Proc Natl Acad Sci U S A,* 110**,** 2557-62.

GULATI, P. & YEO, G. S. 2013. The biology of FTO: from nucleic acid demethylase to amino acid sensor. *Diabetologia*.

GUO, M. & SCHIMMEL, P. 2013. Essential nontranslational functions of tRNA synthetases. *Nat Chem Biol,* 9**,** 145-53.

GUO, Y., LIU, H., YANG, T. L., LI, S. M., LI, S. K., TIAN, Q., LIU, Y. J. & DENG, H. W. 2011. The fat mass and obesity associated gene, FTO, is also associated with osteoporosis phenotypes. *PLoS One,* 6**,** e27312.

HABEGGER, K. M., HEPPNER, K. M., GEARY, N., BARTNESS, T. J., DIMARCHI, R. & TSCHOP, M. H. 2010. The metabolic actions of glucagon revisited. *Nat Rev Endocrinol,* 6**,** 689-97.

HAIGIS, M. C., MOSTOSLAVSKY, R., HAIGIS, K. M., FAHIE, K., CHRISTODOULOU, D. C., MURPHY, A. J., VALENZUELA, D. M., YANCOPOULOS, G. D., KAROW, M., BLANDER, G., WOLBERGER, C., PROLLA, T. A., WEINDRUCH, R., ALT, F. W. & GUARENTE, L. 2006. SIRT4 inhibits glutamate dehydrogenase and opposes the effects of calorie restriction in pancreatic beta cells. *Cell,* 126**,** 941-54.

HAINER, V. & HAINEROVA, I. A. 2012. Do we need anti-obesity drugs? *Diabetes Metab Res Rev,* 28 Suppl 2**,** 8-20.

HALATCHEV, I. G., ELLACOTT, K. L., FAN, W. & CONE, R. D. 2004. Peptide YY3-36 inhibits food intake in mice through a melanocortin-4 receptor-independent mechanism. *Endocrinology,* 145**,** 2585-90.

HAN, J. M., JEONG, S. J., PARK, M. C., KIM, G., KWON, N. H., KIM, H. K., HA, S. H., RYU, S. H. & KIM, S. 2012. Leucyl-tRNA synthetase is an intracellular leucine sensor for the mTORC1-signaling pathway. *Cell,* 149**,** 410-24.

HAN, T. S., VAN LEER, E. M., SEIDELL, J. C. & LEAN, M. E. 1995. Waist circumference action levels in the identification of cardiovascular risk factors: prevalence study in a random sample. *BMJ,* 311**,** 1401-5.

HAN, Z., NIU, T., CHANG, J., LEI, X., ZHAO, M., WANG, Q., CHENG, W., WANG, J., FENG, Y. & CHAI, J. 2010. Crystal structure of the FTO protein reveals basis for its substrate specificity. *Nature*.

HARA, K., YONEZAWA, K., WENG, Q. P., KOZLOWSKI, M. T., BELHAM, C. & AVRUCH, J. 1998. Amino acid sufficiency and mTOR regulate p70 S6 kinase and eIF-4E BP1 through a common effector mechanism. *J Biol Chem,* 273**,** 14484-94.

HARDY, R., WILLS, A. K., WONG, A., ELKS, C. E., WAREHAM, N. J., LOOS, R. J., KUH, D. & ONG, K. K. 2010. Life course variations in the associations between FTO and MC4R gene variants and body size. *Hum Mol Genet,* 19**,** 545-52.

HARNO, E., COTTRELL, E. C. & WHITE, A. 2013. Metabolic pitfalls of CNS cre-based technology. *Cell Metab,* 18**,** 21-8.

HASSANEIN, M. T., LYON, H. N., NGUYEN, T. T., AKYLBEKOVA, E. L., WATERS, K., LETTRE, G., TAYO, B., FORRESTER, T., SARPONG, D. F., STRAM, D. O., BUTLER, J. L., WILKS, R., LIU, J., LE MARCHAND, L., KOLONEL, L. N., ZHU, X., HENDERSON, B., COOPER, R., MCKENZIE, C., TAYLOR, H. A., JR., HAIMAN, C. A. & HIRSCHHORN, J. N. 2010. Fine mapping of the association with obesity at the FTO locus in African-derived populations. *Hum Mol Genet,* 19**,** 2907-16.

HAUPT, A., THAMER, C., STAIGER, H., TSCHRITTER, O., KIRCHHOFF, K., MACHICAO, F., HARING, H. U., STEFAN, N. & FRITSCHE, A. 2009. Variation in the FTO gene influences food intake but not energy expenditure. *Exp Clin Endocrinol Diabetes,* 117**,** 194-7.

HEARD-COSTA, N. L., ZILLIKENS, M. C., MONDA, K. L., JOHANSSON, A., HARRIS, T. B., FU, M., HARITUNIANS, T., FEITOSA, M. F., ASPELUND, T., EIRIKSDOTTIR, G., GARCIA, M., LAUNER, L. J., SMITH, A. V., MITCHELL, B. D., MCARDLE, P. F., SHULDINER, A. R., BIELINSKI, S. J., BOERWINKLE, E., BRANCATI, F., DEMERATH, E. W., PANKOW, J. S., ARNOLD, A. M., CHEN, Y. D., GLAZER, N. L., MCKNIGHT, B., PSATY, B. M., ROTTER, J. I., AMIN, N., CAMPBELL, H., GYLLENSTEN, U., PATTARO, C., PRAMSTALLER, P. P., RUDAN, I., STRUCHALIN, M., VITART, V., GAO, X., KRAJA, A., PROVINCE, M. A., ZHANG, Q., ATWOOD, L. D., DUPUIS, J., HIRSCHHORN, J. N., JAQUISH, C. E., O'DONNELL, C. J., VASAN, R. S., WHITE, C. C., AULCHENKO, Y. S., ESTRADA, K., HOFMAN, A., RIVADENEIRA, F., UITTERLINDEN, A. G., WITTEMAN, J. C., OOSTRA, B. A., KAPLAN, R. C., GUDNASON, V., O'CONNELL, J. R., BORECKI, I. B., VAN DUIJN, C. M., CUPPLES, L. A., FOX, C. S. & NORTH, K. E. 2009. NRXN3 is a novel locus for waist circumference: a genome-wide association study from the CHARGE Consortium. *PLoS Genet,* 5**,** e1000539.

HEID, I. M., JACKSON, A. U., RANDALL, J. C., WINKLER, T. W., QI, L., STEINTHORSDOTTIR, V., THORLEIFSSON, G., ZILLIKENS, M. C., SPELIOTES, E. K., MAGI, R., WORKALEMAHU, T., WHITE, C. C., BOUATIA-NAJI, N., HARRIS, T. B., BERNDT, S. I., INGELSSON, E., WILLER, C. J., WEEDON, M. N., LUAN, J., VEDANTAM, S., ESKO, T., KILPELAINEN, T. O., KUTALIK, Z., LI, S., MONDA, K. L., DIXON, A. L., HOLMES, C. C., KAPLAN, L. M., LIANG, L., MIN, J. L., MOFFATT, M. F., MOLONY, C., NICHOLSON, G., SCHADT, E. E., ZONDERVAN, K. T., FEITOSA, M. F., FERREIRA, T., LANGO ALLEN, H., WEYANT, R. J., WHEELER, E., WOOD, A. R., ESTRADA, K., GODDARD, M. E., LETTRE, G., MANGINO, M., NYHOLT, D. R., PURCELL, S., SMITH, A. V., VISSCHER, P. M., YANG, J., MCCARROLL, S. A., NEMESH, J., VOIGHT, B. F., ABSHER, D., AMIN, N., ASPELUND, T., COIN, L., GLAZER, N. L., HAYWARD, C., HEARD-COSTA, N. L., HOTTENGA, J. J., JOHANSSON, A., JOHNSON, T., KAAKINEN, M., KAPUR, K., KETKAR, S., KNOWLES, J. W., KRAFT, P., KRAJA, A. T., LAMINA, C., LEITZMANN, M. F., MCKNIGHT, B., MORRIS, A. P., ONG, K. K., PERRY, J. R., PETERS, M. J., POLASEK, O., PROKOPENKO, I., RAYNER, N. W., RIPATTI, S.,

RIVADENEIRA, F., ROBERTSON, N. R., SANNA, S., SOVIO, U., SURAKKA, I., TEUMER, A., VAN WINGERDEN, S., VITART, V., ZHAO, J. H., CAVALCANTI-PROENCA, C., CHINES, P. S., FISHER, E., KULZER, J. R., LECOEUR, C., NARISU, N., SANDHOLT, C., SCOTT, L. J., SILANDER, K., STARK, K., TAMMESOO, M. L., *et al.* 2010. Meta-analysis identifies 13 new loci associated with waist-hip ratio and reveals sexual dimorphism in the genetic basis of fat distribution. *Nat Genet,* 42**,** 949-60.

HESS, M. E., HESS, S., MEYER, K. D., VERHAGEN, L. A., KOCH, L., BRONNEKE, H. S., DIETRICH, M. O., JORDAN, S. D., SALETORE, Y., ELEMENTO, O., BELGARDT, B. F., FRANZ, T., HORVATH, T. L., RUTHER, U., JAFFREY, S. R., KLOPPENBURG, P. & BRUNING, J. C. 2013. The fat mass and obesity associated gene (Fto) regulates activity of the dopaminergic midbrain circuitry. *Nat Neurosci*.

HILDRETH, K. L., VAN PELT, R. E. & SCHWARTZ, R. S. 2012. Obesity, insulin resistance, and Alzheimer's disease. *Obesity (Silver Spring),* 20**,** 1549-57.

HINDORFF, L. A., SETHUPATHY, P., JUNKINS, H. A., RAMOS, E. M., MEHTA, J. P., COLLINS, F. S. & MANOLIO, T. A. 2009. Potential etiologic and functional implications of genome-wide association loci for human diseases and traits. *Proc Natl Acad Sci U S A,* 106**,** 9362-7.

HINNEY, A. & HEBEBRAND, J. 2008. Polygenic obesity in humans. *Obes Facts,* 1**,** 35-42.

HINNEY, A., NGUYEN, T. T., SCHERAG, A., FRIEDEL, S., BRONNER, G., MULLER, T. D., GRALLERT, H., ILLIG, T., WICHMANN, H. E., RIEF, W., SCHAFER, H. & HEBEBRAND, J. 2007. Genome wide association (GWA) study for early onset extreme obesity supports the role of fat mass and obesity associated gene (FTO) variants. *PLoS One,* 2**,** e1361.

HIRSCHHORN, J. N. & DALY, M. J. 2005. Genome-wide association studies for common diseases and complex traits. *Nat Rev Genet,* 6**,** 95-108.

HITZ, C., WURST, W. & KUHN, R. 2007. Conditional brain-specific knockdown of MAPK using Cre/loxP regulated RNA interference. *Nucleic Acids Res,* 35**,** e90.

HO, A. J., STEIN, J. L., HUA, X., LEE, S., HIBAR, D. P., LEOW, A. D., DINOV, I. D., TOGA, A. W., SAYKIN, A. J., SHEN, L., FOROUD, T., PANKRATZ, N., HUENTELMAN, M. J., CRAIG, D. W., GERBER, J. D., ALLEN, A. N., CORNEVEAUX, J. J., STEPHAN, D. A., DECARLI, C. S., DECHAIRO, B. M., POTKIN, S. G., JACK, C. R., JR., WEINER, M. W., RAJI, C. A., LOPEZ, O. L., BECKER, J. T., CARMICHAEL, O. T. & THOMPSON, P. M. 2010. A commonly carried allele of the obesity-related FTO gene is associated with reduced brain volume in the healthy elderly. *Proc Natl Acad Sci U S A,* 107**,** 8404-9.

HOJMAN, P., BROLIN, C., GISSEL, H., BRANDT, C., ZERAHN, B., PEDERSEN, B. K. & GEHL, J. 2009. Erythropoietin over-expression protects against diet-induced obesity in mice through increased fat oxidation in muscles. *PLoS One,* 4**,** e5894.

HONG, C. J., TSAI, P. J., CHENG, C. Y., CHOU, C. K., JHENG, H. F., CHUANG, Y. C., YANG, C. N., LIN, Y. T., HSU, C. W., CHENG, I. H., CHEN, S. Y., TSAI, S. J., LIOU, Y. J. & TSAI, Y. S. 2010. ENU mutagenesis identifies mice with morbid obesity and severe hyperinsulinemia caused by a novel mutation in leptin. *PLoS One,* 5**,** e15333.

HOTAMISLIGIL, G. S. 2006. Inflammation and metabolic disorders. *Nature,* 444**,** 860-7.

HOTAMISLIGIL, G. S., ARNER, P., CARO, J. F., ATKINSON, R. L. & SPIEGELMAN, B. M. 1995. Increased adipose tissue expression of tumor necrosis factor-alpha in human obesity and insulin resistance. *J Clin Invest,* 95**,** 2409-15.

HOTAMISLIGIL, G. S., SHARGILL, N. S. & SPIEGELMAN, B. M. 1993. Adipose expression of tumor necrosis factor-alpha: direct role in obesity-linked insulin resistance. *Science,* 259**,** 87-91.

HOUGH, T. A., NOLAN, P. M., TSIPOURI, V., TOYE, A. A., GRAY, I. C., GOLDSWORTHY, M., MOIR, L., COX, R. D., CLEMENTS, S., GLENISTER, P. H., WOOD, J., SELLEY, R. L., STRIVENS, M. A., VIZOR, L., MCCORMACK, S. L., PETERS, J., FISHER, E. M., SPURR, N., RASTAN, S., MARTIN, J. E., BROWN, S. D. & HUNTER, A. J. 2002. Novel phenotypes identified by plasma biochemical screening in the mouse. *Mamm Genome,* 13**,** 595-602.

HSIEH, M. M., LINDE, N. S., WYNTER, A., METZGER, M., WONG, C., LANGSETMO, I., LIN, A., SMITH, R., RODGERS, G. P., DONAHUE, R. E., KLAUS, S. J. & TISDALE, J. F. 2007. HIF prolyl hydroxylase inhibition results in endogenous erythropoietin induction, erythrocytosis, and modest fetal hemoglobin expression in rhesus macaques. *Blood,* 110**,** 2140-7.

HUANG, P. & SCHIER, A. F. 2009. Dampened Hedgehog signaling but normal Wnt signaling in zebrafish without cilia. *Development,* 136**,** 3089-98.

HUBACEK, J. A., ADAMKOVA, V., DLOUHA, D., JIRSA, M., SPERL, J., TONJES, A., KOVACS, P., PIKHART, H., PEASEY, A. & BOBAK, M. 2012a. Fat mass and obesity-associated (fto) gene and alcohol intake. *Addiction,* 107**,** 1185-6.

HUBACEK, J. A., DLOUHA, D., LANSKA, V. & ADAMKOVA, V. 2012b. Lack of an association between three tagging SNPs within the FTO gene and smoking behavior. *Nicotine Tob Res,* 14**,** 998-1002.

ILES, M. M., LAW, M. H., STACEY, S. N., HAN, J., FANG, S., PFEIFFER, R., HARLAND, M., MACGREGOR, S., TAYLOR, J. C., ABEN, K. K., AKSLEN, L. A., AVRIL, M. F., AZIZI, E., BAKKER, B., BENEDIKTSDOTTIR, K. R., BERGMAN, W., SCARRA, G. B., BROWN, K. M., CALISTA, D., CHAUDRU, V., FARGNOLI, M. C., CUST, A. E., DEMENAIS, F., DE WAAL, A. C., DEBNIAK, T., ELDER, D. E., FRIEDMAN, E., GALAN, P., GHIORZO, P., GILLANDERS, E. M., GOLDSTEIN, A. M., GRUIS, N. A., HANSSON, J., HELSING, P., HOCEVAR, M., HOIOM, V., HOPPER, J. L., INGVAR, C., JANSSEN, M., JENKINS, M. A., KANETSKY, P. A., KIEMENEY, L. A., LANG, J., LATHROP, G. M., LEACHMAN, S., LEE, J. E., LUBINSKI, J., MACKIE, R. M., MANN, G. J., MARTIN, N. G., MAYORDOMO, J. I., MOLVEN, A., MULDER, S., NAGORE, E., NOVAKOVIC, S., OKAMOTO, I., OLAFSSON, J. H., OLSSON, H., PEHAMBERGER, H., PERIS, K., GRASA, M. P., PLANELLES, D., PUIG, S., PUIG-BUTILLE, J. A., RANDERSON-MOOR, J., REQUENA, C., RIVOLTINI, L., RODOLFO, M., SANTINAMI, M., SIGURGEIRSSON, B., SNOWDEN, H., SONG, F., SULEM, P., THORISDOTTIR, K., TUOMINEN, R., VAN BELLE, P., VAN DER STOEP, N., VAN ROSSUM, M. M., WEI, Q., WENDT, J., ZELENIKA, D., ZHANG, M., LANDI, M. T., THORLEIFSSON, G., BISHOP, D. T., AMOS, C. I., HAYWARD, N. K., STEFANSSON, K., BISHOP, J. A. & BARRETT, J. H. 2013. A variant in FTO shows association with melanoma risk not due to BMI. *Nat Genet,* 45**,** 428-32, 432e1.

INDRA, A. K., WAROT, X., BROCARD, J., BORNERT, J. M., XIAO, J. H., CHAMBON, P. & METZGER, D. 1999. Temporally-controlled site-specific mutagenesis in the basal layer of the epidermis: comparison of the recombinase activity of the tamoxifen-inducible Cre-ER(T) and Cre-ER(T2) recombinases. *Nucleic Acids Res,* 27**,** 4324-7.

INGALLS, A. M., DICKIE, M. M. & SNELL, G. D. 1950. Obese, a new mutation in the house mouse. *J Hered,* 41**,** 317-8.

ISHIMORI, N., LI, R., KELMENSON, P. M., KORSTANJE, R., WALSH, K. A., CHURCHILL, G. A., FORSMAN-SEMB, K. & PAIGEN, B. 2004. Quantitative trait loci that determine plasma lipids and obesity in C57BL/6J and 129S1/SvImJ inbred mice. *J Lipid Res,* 45**,** 1624-32.

JACOBSSON, J. A., ALMEN, M. S., BENEDICT, C., HEDBERG, L. A., MICHAELSSON, K., BROOKS, S., KULLBERG, J., AXELSSON, T., JOHANSSON, L., AHLSTROM, H., FREDRIKSSON, R., LIND, L. & SCHIOTH, H. B. 2011. Detailed analysis of variants in FTO in association with body composition in a cohort of 70-year-olds suggests a weakened effect among elderly. *PLoS One,* 6**,** e20158.

JACOBSSON, J. A., RISERUS, U., AXELSSON, T., LANNFELT, L., SCHIOTH, H. B. & FREDRIKSSON, R. 2009. The common FTO variant rs9939609 is not associated with BMI in a longitudinal study on a cohort of Swedish men born 1920-1924. *BMC Med Genet,* 10**,** 131.

JAMES, W. P. 1996. The epidemiology of obesity. *Ciba Found Symp,* 201**,** 1-11; discussion 11-6, 32-6.

JAMSHIDI, N. & TAYLOR, D. A. 2001. Anandamide administration into the ventromedial hypothalamus stimulates appetite in rats. *Br J Pharmacol,* 134**,** 1151-4.

JIA, G., FU, Y., ZHAO, X., DAI, Q., ZHENG, G., YANG, Y., YI, C., LINDAHL, T., PAN, T., YANG, Y. G. & HE, C. 2011. N6-methyladenosine in nuclear RNA is a major substrate of the obesity-associated FTO. *Nat Chem Biol,* 7**,** 885-7.

JIA, G., YANG, C. G., YANG, S., JIAN, X., YI, C., ZHOU, Z. & HE, C. 2008. Oxidative demethylation of 3-methylthymine and 3-methyluracil in single-stranded DNA and RNA by mouse and human FTO. *FEBS Lett,* 582**,** 3313-9.

JIANG, Y., WILK, J. B., BORECKI, I., WILLIAMSON, S., DESTEFANO, A. L., XU, G., LIU, J., ELLISON, R. C., PROVINCE, M. & MYERS, R. H. 2004. Common variants in the 5' region of the leptin gene are associated with body mass index in men from the National Heart, Lung, and Blood Institute Family Heart Study. *Am J Hum Genet,* 75**,** 220-30.

JONSSON, A., RENSTROM, F., LYSSENKO, V., BRITO, E. C., ISOMAA, B., BERGLUND, G., NILSSON, P. M., GROOP, L. & FRANKS, P. W. 2009. Assessing the effect of interaction between an FTO variant (rs9939609) and physical activity on obesity in 15,925 Swedish and 2,511 Finnish adults. *Diabetologia,* 52**,** 1334-8.

JOWETT, J. B., CURRAN, J. E., JOHNSON, M. P., CARLESS, M. A., GORING, H. H., DYER, T. D., COLE, S. A., COMUZZIE, A. G., MACCLUER, J. W., MOSES, E. K. & BLANGERO, J. 2010. Genetic variation at the FTO locus influences RBL2 gene expression. *Diabetes,* 59**,** 726-32.

JUSTICE, M. J., NOVEROSKE, J. K., WEBER, J. S., ZHENG, B. & BRADLEY, A. 1999. Mouse ENU mutagenesis. *Hum Mol Genet,* 8**,** 1955-63.

KAIYALA, K. J. & SCHWARTZ, M. W. 2011. Toward a more complete (and less controversial) understanding of energy expenditure and its role in obesity pathogenesis. *Diabetes,* 60**,** 17-23.

KAKLAMANI, V., YI, N., SADIM, M., SIZIOPIKOU, K., ZHANG, K., XU, Y., TOFILON, S., AGARWAL, S., PASCHE, B. & MANTZOROS, C. 2011. The role of the fat mass and obesity associated gene (FTO) in breast cancer risk. *BMC Med Genet,* 12**,** 52.

KANDASAMY, A. D. & SCHULZ, R. 2009. Glycogen synthase kinase-3beta is activated by matrix metalloproteinase-2 mediated proteolysis in cardiomyoblasts. *Cardiovasc Res,* 83**,** 698-706.

KARRA, E. & BATTERHAM, R. L. 2009. The role of gut hormones in the regulation of body weight and energy homeostasis. *Mol Cell Endocrinol*.

KARRA, E., O'DALY, O. G., CHOUDHURY, A. I., YOUSSEIF, A., MILLERSHIP, S., NEARY, M. T., SCOTT, W. R., CHANDARANA, K., MANNING, S., HESS, M. E., IWAKURA, H., AKAMIZU, T., MILLET, Q., GELEGEN, C., DREW, M. E., RAHMAN, S., EMMANUEL, J. J., WILLIAMS, S. C., RUTHER, U. U., BRUNING, J. C., WITHERS, D. J., ZELAYA, F. O. & BATTERHAM, R. L. 2013. A link between FTO, ghrelin, and impaired brain food-cue responsivity. *J Clin Invest*.

KELLY, T., YANG, W., CHEN, C. S., REYNOLDS, K. & HE, J. 2008. Global burden of obesity in 2005 and projections to 2030. *Int J Obes (Lond),* 32**,** 1431-7.

KESSING, L. V. 2012. Depression and the risk for dementia. *Curr Opin Psychiatry,* 25**,** 457-61.

KILBY, N. J., SNAITH, M. R. & MURRAY, J. A. 1993. Site-specific recombinases: tools for genome engineering. *Trends Genet,* 9**,** 413-21.

KILPELAINEN, T. O., QI, L., BRAGE, S., SHARP, S. J., SONESTEDT, E., DEMERATH, E., AHMAD, T., MORA, S., KAAKINEN, M., SANDHOLT, C. H., HOLZAPFEL, C., AUTENRIETH, C. S., HYPPONEN, E., CAUCHI, S., HE, M., KUTALIK, Z., KUMARI, M., STANCAKOVA, A., MEIDTNER, K., BALKAU, B., TAN, J. T., MANGINO, M., TIMPSON, N. J., SONG, Y., ZILLIKENS, M. C., JABLONSKI, K. A., GARCIA, M. E., JOHANSSON, S., BRAGG-GRESHAM, J. L., WU, Y., VAN VLIET-OSTAPTCHOUK, J. V., ONLAND-MORET, N. C., ZIMMERMANN, E., RIVERA, N. V., TANAKA, T., STRINGHAM, H. M., SILBERNAGEL, G., KANONI, S., FEITOSA, M. F., SNITKER, S., RUIZ, J. R., METTER, J., LARRAD, M. T., ATALAY, M., HAKANEN, M., AMIN, N., CAVALCANTI-PROENCA, C., GRONTVED, A., HALLMANS, G., JANSSON, J. O., KUUSISTO, J., KAHONEN, M., LUTSEY, P. L., NOLAN, J. J., PALLA, L., PEDERSEN, O., PERUSSE, L., RENSTROM, F., SCOTT, R. A., SHUNGIN, D., SOVIO, U., TAMMELIN, T. H., RONNEMAA, T., LAKKA, T. A., UUSITUPA, M., RIOS, M. S.,

FERRUCCI, L., BOUCHARD, C., MEIRHAEGHE, A., FU, M., WALKER, M., BORECKI, I. B., DEDOUSSIS, G. V., FRITSCHE, A., OHLSSON, C., BOEHNKE, M., BANDINELLI, S., VAN DUIJN, C. M., EBRAHIM, S., LAWLOR, D. A., GUDNASON, V., HARRIS, T. B., SORENSEN, T. I., MOHLKE, K. L., HOFMAN, A., UITTERLINDEN, A. G., TUOMILEHTO, J., LEHTIMAKI, T., RAITAKARI, O., ISOMAA, B., NJOLSTAD, P. R., FLOREZ, J. C., LIU, S., NESS, A., SPECTOR, T. D., TAI, E. S., FROGUEL, P., BOEING, H., LAAKSO, M., MARMOT, M., *et al.* 2011a. Physical activity attenuates the influence of FTO variants on obesity risk: a meta-analysis of 218,166 adults and 19,268 children. *PLoS Med,* 8**,** e1001116.

KILPELAINEN, T. O., ZILLIKENS, M. C., STANCAKOVA, A., FINUCANE, F. M., RIED, J. S., LANGENBERG, C., ZHANG, W., BECKMANN, J. S., LUAN, J., VANDENPUT, L., STYRKARSDOTTIR, U., ZHOU, Y., SMITH, A. V., ZHAO, J. H., AMIN, N., VEDANTAM, S., SHIN, S. Y., HARITUNIANS, T., FU, M., FEITOSA, M. F., KUMARI, M., HALLDORSSON, B. V., TIKKANEN, E., MANGINO, M., HAYWARD, C., SONG, C., ARNOLD, A. M., AULCHENKO, Y. S., OOSTRA, B. A., CAMPBELL, H., CUPPLES, L. A., DAVIS, K. E., DORING, A., EIRIKSDOTTIR, G., ESTRADA, K., FERNANDEZ-REAL, J. M., GARCIA, M., GIEGER, C., GLAZER, N. L., GUIDUCCI, C., HOFMAN, A., HUMPHRIES, S. E., ISOMAA, B., JACOBS, L. C., JULA, A., KARASIK, D., KARLSSON, M. K., KHAW, K. T., KIM, L. J., KIVIMAKI, M., KLOPP, N., KUHNEL, B., KUUSISTO, J., LIU, Y., LJUNGGREN, O., LORENTZON, M., LUBEN, R. N., MCKNIGHT, B., MELLSTROM, D., MITCHELL, B. D., MOOSER, V., MORENO, J. M., MANNISTO, S., O'CONNELL, J. R., PASCOE, L., PELTONEN, L., PERAL, B., PEROLA, M., PSATY, B. M., SALOMAA, V., SAVAGE, D. B., SEMPLE, R. K., SKARIC-JURIC, T., SIGURDSSON, G., SONG, K. S., SPECTOR, T. D., SYVANEN, A. C., TALMUD, P. J., THORLEIFSSON, G., THORSTEINSDOTTIR, U., UITTERLINDEN, A. G., VAN DUIJN, C. M., VIDAL-PUIG, A., WILD, S. H., WRIGHT, A. F., CLEGG, D. J., SCHADT, E., WILSON, J. F., RUDAN, I., RIPATTI, S., BORECKI, I. B., SHULDINER, A. R., INGELSSON, E., JANSSON, J. O., KAPLAN, R. C., GUDNASON, V., HARRIS, T. B., GROOP, L., KIEL, D. P., RIVADENEIRA, F., *et al.* 2011b. Genetic variation near IRS1 associates with reduced adiposity and an impaired metabolic profile. *Nat Genet,* 43**,** 753-60.

KIM, B. J., CARLSON, O. D., JANG, H. J., ELAHI, D., BERRY, C. & EGAN, J. M. 2005. Peptide YY is secreted after oral glucose administration in a gender-specific manner. *J Clin Endocrinol Metab,* 90**,** 6665-71.

KIM, D. H., SARBASSOV, D. D., ALI, S. M., KING, J. E., LATEK, R. R., ERDJUMENT-BROMAGE, H., TEMPST, P. & SABATINI, D. M. 2002. mTOR interacts with raptor to form a nutrient-sensitive complex that signals to the cell growth machinery. *Cell,* 110**,** 163-75.

KIM, J. W., TCHERNYSHYOV, I., SEMENZA, G. L. & DANG, C. V. 2006. HIF-1-mediated expression of pyruvate dehydrogenase kinase: a metabolic switch required for cellular adaptation to hypoxia. *Cell Metab,* 3**,** 177-85.

KIM, M. S., YOON, C. Y., PARK, K. H., SHIN, C. S., PARK, K. S., KIM, S. Y., CHO, B. Y. & LEE, H. K. 2003. Changes in ghrelin and ghrelin receptor expression according to feeding status. *Neuroreport,* 14**,** 1317-20.

KIM, S. J., DESTEFANO, M. A., OH, W. J., WU, C. C., VEGA-COTTO, N. M., FINLAN, M., LIU, D., SU, B. & JACINTO, E. 2012. mTOR complex 2 regulates proper turnover of insulin receptor substrate-1 via the ubiquitin ligase subunit Fbw8. *Mol Cell,* 48**,** 875-87.

KIRKHAM, T. C., WILLIAMS, C. M., FEZZA, F. & DI MARZO, V. 2002. Endocannabinoid levels in rat limbic forebrain and hypothalamus in relation to fasting, feeding and satiation: stimulation of eating by 2-arachidonoyl glycerol. *Br J Pharmacol,* 136**,** 550-7.

KISSLER, H. J. & SETTMACHER, U. 2013. Bariatric surgery to treat obesity. *Semin Nephrol,* 33**,** 75-89.

KITADA, K., ISHISHITA, S., TOSAKA, K., TAKAHASHI, R., UEDA, M., KENG, V. W., HORIE, K. & TAKEDA, J. 2007. Transposon-tagged mutagenesis in the rat. *Nat Methods,* 4**,** 131-3.

KLOTING, N., SCHLEINITZ, D., RUSCHKE, K., BERNDT, J., FASSHAUER, M., TONJES, A., SCHON, M. R., KOVACS, P., STUMVOLL, M. & BLUHER, M. 2008. Inverse relationship between obesity and FTO gene expression in visceral adipose tissue in humans. *Diabetologia,* 51**,** 641-7.

KOEPPEN-SCHOMERUS, G., WARDLE, J. & PLOMIN, R. 2001. A genetic analysis of weight and overweight in 4-year-old twin pairs. *Int J Obes Relat Metab Disord,* 25**,** 838-44.

KOPELMAN, P. 2007. Health risks associated with overweight and obesity. *Obes Rev,* 8 Suppl 1**,** 13-7.

KOS, C. H. 2004. Cre/loxP system for generating tissue-specific knockout mouse models. *Nutr Rev,* 62**,** 243-6.

KOWALSKA, I., MALECKI, M. T., STRACZKOWSKI, M., SKUPIEN, J., KARCZEWSKA-KUPCZEWSKA, M., NIKOLAJUK, A., SZOPA, M., ADAMSKA, A., WAWRUSIEWICZ-KURYLONEK, N., WOLCZYNSKI, S., SIERADZKI, J. & GORSKA, M. 2009. The FTO gene modifies weight, fat mass and insulin sensitivity in women with polycystic ovary syndrome, where its role may be larger than in other phenotypes. *Diabetes Metab,* 35**,** 328-31.

KOZAK, M. 1987a. An analysis of 5'-noncoding sequences from 699 vertebrate messenger RNAs. *Nucleic Acids Res,* 15**,** 8125-48.

KOZAK, M. 1987b. At least six nucleotides preceding the AUG initiator codon enhance translation in mammalian cells. *J Mol Biol,* 196**,** 947-50.

KOZENKO, M., GRYNSPAN, D., OLUYOMI-OBI, T., SITAR, D., ELLIOTT, A. M. & CHODIRKER, B. N. 2011. Potential teratogenic effects of allopurinol: a case report. *Am J Med Genet A,* 155A**,** 2247-52.

KRISTIANSSON, K., PEROLA, M., TIKKANEN, E., KETTUNEN, J., SURAKKA, I., HAVULINNA, A. S., STANCAKOVA, A., BARNES, C., WIDEN, E., KAJANTIE, E., ERIKSSON, J. G., VIIKARI, J., KAHONEN, M., LEHTIMAKI, T., RAITAKARI, O. T., HARTIKAINEN, A. L., RUOKONEN, A., POUTA, A., JULA, A., KANGAS, A. J., SOININEN, P., ALA-KORPELA, M., MANNISTO, S., JOUSILAHTI, P., BONNYCASTLE, L. L., JARVELIN, M. R., KUUSISTO, J., COLLINS, F. S., LAAKSO, M., HURLES, M. E., PALOTIE, A., PELTONEN, L., RIPATTI, S. & SALOMAA, V. 2012. Genome-wide screen for metabolic syndrome susceptibility Loci reveals strong lipid gene contribution but no evidence for common genetic basis for clustering of metabolic syndrome traits. *Circ Cardiovasc Genet,* 5**,** 242-9.

KRUDE, H., BIEBERMANN, H., LUCK, W., HORN, R., BRABANT, G. & GRUTERS, A. 1998. Severe early-onset obesity, adrenal insufficiency and red hair pigmentation caused by POMC mutations in humans. *Nat Genet,* 19**,** 155-7.

KULKARNI, R. N., ALMIND, K., GOREN, H. J., WINNAY, J. N., UEKI, K., OKADA, T. & KAHN, C. R. 2003. Impact of genetic background on development of hyperinsulinemia and diabetes in insulin receptor/insulin receptor substrate-1 double heterozygous mice. *Diabetes,* 52**,** 1528-34.

LABAYEN, I., RUIZ, J. R., ORTEGA, F. B., DALLONGEVILLE, J., JIMENEZ-PAVON, D., CASTILLO, M. J., DE HENAUW, S., GONZALEZ-GROSS, M., BUENO, G., MOLNAR, D., KAFATOS, A., DIAZ, L. E., MEIRHAEGHE, A. & MORENO, L. A. 2011. Association between the FTO rs9939609 polymorphism and leptin in European adolescents: a possible link with energy balance control. The HELENA study. *Int J Obes (Lond),* 35**,** 66-71.

LANCHA, A., FRUHBECK, G. & GOMEZ-AMBROSI, J. 2012. Peripheral signalling involved in energy homeostasis control. *Nutr Res Rev,* 25**,** 223-48.

LAURIA, F., SIANI, A., BAMMANN, K., FORAITA, R., HUYBRECHTS, I., IACOVIELLO, L., KONI, A. C., KOURIDES, Y., MARILD, S., MOLNAR, D., MORENO, L. A., PIGEOT, I., PITSILADIS, Y. P., VEIDEBAUM, T. & RUSSO, P. 2012. Prospective analysis of the association of a common variant of FTO (rs9939609) with adiposity in children: results of the IDEFICS study. *PLoS One,* 7**,** e48876.

LE ROUX, C. W., BATTERHAM, R. L., AYLWIN, S. J., PATTERSON, M., BORG, C. M., WYNNE, K. J., KENT, A., VINCENT, R. P., GARDINER, J., GHATEI, M. A. &

BLOOM, S. R. 2006. Attenuated peptide YY release in obese subjects is associated with reduced satiety. *Endocrinology,* 147**,** 3-8.

LEE, D. H., JIN, S. G., CAI, S., CHEN, Y., PFEIFER, G. P. & O'CONNOR, T. R. 2005. Repair of methylation damage in DNA and RNA by mammalian AlkB homologues. *J Biol Chem,* 280**,** 39448-59.

LEE, J. Y., RISTOW, M., LIN, X., WHITE, M. F., MAGNUSON, M. A. & HENNIGHAUSEN, L. 2006. RIP-Cre revisited, evidence for impairments of pancreatic beta-cell function. *J Biol Chem,* 281**,** 2649-53.

LEGER, A. J., ALTOBELLI, A., MOSQUEA, L. M., BELANGER, A. J., SONG, A., CHENG, S. H., JIANG, C. & YEW, N. S. 2010. Inhibition of osteoclastogenesis by prolyl hydroxylase inhibitor dimethyloxallyl glycine. *J Bone Miner Metab,* 28**,** 510-9.

LI, T., WU, K., YOU, L., XING, X., WANG, P., CUI, L., LIU, H., CUI, Y., BIAN, Y., NING, Y., ZHAO, H., TANG, R. & CHEN, Z. J. 2013. Common Variant rs9939609 in Gene FTO Confers Risk to Polycystic Ovary Syndrome. *PLoS One,* 8**,** e66250.

LI, W. D., REED, D. R., LEE, J. H., XU, W., KILKER, R. L., SODAM, B. R. & PRICE, R. A. 1999. Sequence variants in the 5' flanking region of the leptin gene are associated with obesity in women. *Ann Hum Genet,* 63**,** 227-34.

LICINIO, J., CAGLAYAN, S., OZATA, M., YILDIZ, B. O., DE MIRANDA, P. B., O'KIRWAN, F., WHITBY, R., LIANG, L., COHEN, P., BHASIN, S., KRAUSS, R. M., VELDHUIS, J. D., WAGNER, A. J., DEPAOLI, A. M., MCCANN, S. M. & WONG, M. L. 2004. Phenotypic effects of leptin replacement on morbid obesity, diabetes mellitus, hypogonadism, and behavior in leptin-deficient adults. *Proc Natl Acad Sci U S A,* 101**,** 4531-6.

LINDGREN, C. M., HEID, I. M., RANDALL, J. C., LAMINA, C., STEINTHORSDOTTIR, V., QI, L., SPELIOTES, E. K., THORLEIFSSON, G., WILLER, C. J., HERRERA, B. M., JACKSON, A. U., LIM, N., SCHEET, P., SORANZO, N., AMIN, N., AULCHENKO, Y. S., CHAMBERS, J. C., DRONG, A., LUAN, J., LYON, H. N., RIVADENEIRA, F., SANNA, S., TIMPSON, N. J., ZILLIKENS, M. C., ZHAO, J. H., ALMGREN, P., BANDINELLI, S., BENNETT, A. J., BERGMAN, R. N., BONNYCASTLE, L. L., BUMPSTEAD, S. J., CHANOCK, S. J., CHERKAS, L., CHINES, P., COIN, L., COOPER, C., CRAWFORD, G., DOERING, A., DOMINICZAK, A., DONEY, A. S., EBRAHIM, S., ELLIOTT, P., ERDOS, M. R., ESTRADA, K., FERRUCCI, L., FISCHER, G., FOROUHI, N. G., GIEGER, C., GRALLERT, H., GROVES, C. J., GRUNDY, S., GUIDUCCI, C., HADLEY, D., HAMSTEN, A., HAVULINNA, A. S., HOFMAN, A., HOLLE, R., HOLLOWAY, J. W., ILLIG, T., ISOMAA, B., JACOBS, L. C., JAMESON, K., JOUSILAHTI, P., KARPE, F., KUUSISTO, J., LAITINEN, J., LATHROP, G. M., LAWLOR, D. A., MANGINO, M., MCARDLE, W. L., MEITINGER, T., MORKEN, M. A., MORRIS, A. P., MUNROE, P., NARISU, N., NORDSTROM, A., NORDSTROM, P., OOSTRA, B. A., PALMER, C. N., PAYNE, F., PEDEN, J. F., PROKOPENKO, I., RENSTROM, F., RUOKONEN, A., SALOMAA, V., SANDHU, M. S., SCOTT, L. J., SCUTERI, A., SILANDER, K., SONG, K., YUAN, X., STRINGHAM, H. M., SWIFT, A. J., TUOMI, T., UDA, M., VOLLENWEIDER, P., WAEBER, G., WALLACE, C., WALTERS, G. B., WEEDON, M. N., *et al.* 2009. Genome-wide association scan meta-analysis identifies three Loci influencing adiposity and fat distribution. *PLoS Genet,* 5**,** e1000508.

LIU, C., MOU, S. & PAN, C. 2013. The FTO Gene rs9939609 Polymorphism Predicts Risk of Cardiovascular Disease: A Systematic Review and Meta-Analysis. *PLoS One,* 8**,** e71901.

LONGO, K. A., WRIGHT, W. S., KANG, S., GERIN, I., CHIANG, S. H., LUCAS, P. C., OPP, M. R. & MACDOUGALD, O. A. 2004. Wnt10b inhibits development of white and brown adipose tissues. *J Biol Chem,* 279**,** 35503-9.

LOONSTRA, A., VOOIJS, M., BEVERLOO, H. B., ALLAK, B. A., VAN DRUNEN, E., KANAAR, R., BERNS, A. & JONKERS, J. 2001. Growth inhibition and DNA damage induced by Cre recombinase in mammalian cells. *Proc Natl Acad Sci U S A,* 98**,** 9209-14.

LOOS, R. J. 2012. Genetic determinants of common obesity and their value in prediction. *Best Pract Res Clin Endocrinol Metab,* 26**,** 211-26.

LOOS, R. J., LINDGREN, C. M., LI, S., WHEELER, E., ZHAO, J. H., PROKOPENKO, I., INOUYE, M., FREATHY, R. M., ATTWOOD, A. P., BECKMANN, J. S., BERNDT, S. I., JACOBS, K. B., CHANOCK, S. J., HAYES, R. B., BERGMANN, S., BENNETT, A. J., BINGHAM, S. A., BOCHUD, M., BROWN, M., CAUCHI, S., CONNELL, J. M., COOPER, C., SMITH, G. D., DAY, I., DINA, C., DE, S., DERMITZAKIS, E. T., DONEY, A. S., ELLIOTT, K. S., ELLIOTT, P., EVANS, D. M., SADAF FAROOQI, I., FROGUEL, P., GHORI, J., GROVES, C. J., GWILLIAM, R., HADLEY, D., HALL, A. S., HATTERSLEY, A. T., HEBEBRAND, J., HEID, I. M., LAMINA, C., GIEGER, C., ILLIG, T., MEITINGER, T., WICHMANN, H. E., HERRERA, B., HINNEY, A., HUNT, S. E., JARVELIN, M. R., JOHNSON, T., JOLLEY, J. D., KARPE, F., KENIRY, A., KHAW, K. T., LUBEN, R. N., MANGINO, M., MARCHINI, J., MCARDLE, W. L., MCGINNIS, R., MEYRE, D., MUNROE, P. B., MORRIS, A. D., NESS, A. R., NEVILLE, M. J., NICA, A. C., ONG, K. K., O'RAHILLY, S., OWEN, K. R., PALMER, C. N., PAPADAKIS, K., POTTER, S., POUTA, A., QI, L., RANDALL, J. C., RAYNER, N. W., RING, S. M., SANDHU, M. S., SCHERAG, A., SIMS, M. A., SONG, K., SORANZO, N., SPELIOTES, E. K., SYDDALL, H. E., TEICHMANN, S. A., TIMPSON, N. J., TOBIAS, J. H., UDA, M., VOGEL, C. I., WALLACE, C., WATERWORTH, D. M., WEEDON, M. N., WILLER, C. J., WRAIGHT, YUAN, X., ZEGGINI, E., HIRSCHHORN, J. N., STRACHAN, D. P., OUWEHAND, W. H., CAULFIELD, M. J., *et al.* 2008. Common variants near MC4R are associated with fat mass, weight and risk of obesity. *Nat Genet,* 40**,** 768-75.

LOPEZ, M., LELLIOTT, C. J., TOVAR, S., KIMBER, W., GALLEGO, R., VIRTUE, S., BLOUNT, M., VAZQUEZ, M. J., FINER, N., POWLES, T. J., O'RAHILLY, S., SAHA, A. K., DIEGUEZ, C. & VIDAL-PUIG, A. J. 2006. Tamoxifen-induced anorexia is associated with fatty acid synthase inhibition in the ventromedial nucleus of the hypothalamus and accumulation of malonyl-CoA. *Diabetes,* 55**,** 1327-36.

LOVETT, D. H., MAHIMKAR, R., RAFFAI, R. L., CAPE, L., MAKLASHINA, E., CECCHINI, G. & KARLINER, J. S. 2012. A novel intracellular isoform of matrix metalloproteinase-2 induced by oxidative stress activates innate immunity. *PLoS One,* 7**,** e34177.

LUNDBY, C. & OLSEN, N. V. 2011. Effects of recombinant human erythropoietin in normal humans. *J Physiol,* 589**,** 1265-71.

MACHNICKA, M. A., MILANOWSKA, K., OSMAN OGLOU, O., PURTA, E., KURKOWSKA, M., OLCHOWIK, A., JANUSZEWSKI, W., KALINOWSKI, S., DUNIN-HORKAWICZ, S., ROTHER, K. M., HELM, M., BUJNICKI, J. M. & GROSJEAN, H. 2013. MODOMICS: a database of RNA modification pathways--2013 update. *Nucleic Acids Res,* 41**,** D262-7.

MADEN, B. E. & HUGHES, J. M. 1997. Eukaryotic ribosomal RNA: the recent excitement in the nucleotide modification problem. *Chromosoma,* 105**,** 391-400.

MADSEN, M. B., BIRCK, M. M., FREDHOLM, M. & CIRERA, S. 2010. Expression studies of the obesity candidate gene FTO in pig. *Anim Biotechnol,* 21**,** 51-63.

MAEDA, N., SHIMOMURA, I., KISHIDA, K., NISHIZAWA, H., MATSUDA, M., NAGARETANI, H., FURUYAMA, N., KONDO, H., TAKAHASHI, M., ARITA, Y., KOMURO, R., OUCHI, N., KIHARA, S., TOCHINO, Y., OKUTOMI, K., HORIE, M., TAKEDA, S., AOYAMA, T., FUNAHASHI, T. & MATSUZAWA, Y. 2002. Diet-induced insulin resistance in mice lacking adiponectin/ACRP30. *Nat Med,* 8**,** 731-7.

MAFFEI, M., HALAAS, J., RAVUSSIN, E., PRATLEY, R. E., LEE, G. H., ZHANG, Y., FEI, H., KIM, S., LALLONE, R., RANGANATHAN, S. & *ET AL.* 1995. Leptin levels in human and rodent: measurement of plasma leptin and ob RNA in obese and weight-reduced subjects. *Nat Med,* 1**,** 1155-61.

MARINI, J. C., CABRAL, W. A., BARNES, A. M. & CHANG, W. 2007. Components of the collagen prolyl 3-hydroxylation complex are crucial for normal bone development. *Cell Cycle,* 6**,** 1675-81.

MARTIN, E. A., CARTHEW, P., WHITE, I. N., HEYDON, R. T., GASKELL, M., MAUTHE, R. J., TURTELTAUB, K. W. & SMITH, L. L. 1997. Investigation of the formation and

accumulation of liver DNA adducts in mice chronically exposed to tamoxifen. *Carcinogenesis,* 18**,** 2209-15.

MATARESE, L. E. 1997. Indirect calorimetry: technical aspects. *J Am Diet Assoc,* 97**,** S154-60.

MCMURRAY, F., CHURCH, C. D., LARDER, R., NICHOLSON, G., WELLS, S., TEBOUL, L., TUNG, Y. C., RIMMINGTON, D., BOSCH, F., JIMENEZ, V., YEO, G. S., O'RAHILLY, S., ASHCROFT, F. M., COLL, A. P. & COX, R. D. 2013. Adult onset global loss of the fto gene alters body composition and metabolism in the mouse. *PLoS Genet,* 9**,** e1003166.

MCTAGGART, J. S., LEE, S., IBERL, M., CHURCH, C., COX, R. D. & ASHCROFT, F. M. 2011. FTO is expressed in neurones throughout the brain and its expression is unaltered by fasting. *PLoS One,* 6**,** e27968.

MENG, R., ZHU, D., BI, Y., YANG, D. & WANG, Y. 2013. Erythropoietin inhibits gluconeogenesis and inflammation in the liver and improves glucose intolerance in high-fat diet-fed mice. *PLoS One,* 8**,** e53557.

MEYER, K. D., SALETORE, Y., ZUMBO, P., ELEMENTO, O., MASON, C. E. & JAFFREY, S. R. 2012. Comprehensive analysis of mRNA methylation reveals enrichment in 3' UTRs and near stop codons. *Cell,* 149**,** 1635-46.

MEYRE, D., DELPLANQUE, J., CHEVRE, J. C., LECOEUR, C., LOBBENS, S., GALLINA, S., DURAND, E., VATIN, V., DEGRAEVE, F., PROENCA, C., GAGET, S., KORNER, A., KOVACS, P., KIESS, W., TICHET, J., MARRE, M., HARTIKAINEN, A. L., HORBER, F., POTOCZNA, N., HERCBERG, S., LEVY-MARCHAL, C., PATTOU, F., HEUDE, B., TAUBER, M., MCCARTHY, M. I., BLAKEMORE, A. I., MONTPETIT, A., POLYCHRONAKOS, C., WEILL, J., COIN, L. J., ASHER, J., ELLIOTT, P., JARVELIN, M. R., VISVIKIS-SIEST, S., BALKAU, B., SLADEK, R., BALDING, D., WALLEY, A., DINA, C. & FROGUEL, P. 2009. Genome-wide association study for early-onset and morbid adult obesity identifies three new risk loci in European populations. *Nat Genet,* 41**,** 157-9.

MEYRE, D., PROULX, K., KAWAGOE-TAKAKI, H., VATIN, V., GUTIERREZ-AGUILAR, R., LYON, D., MA, M., CHOQUET, H., HORBER, F., VAN HUL, W., VAN GAAL, L., BALKAU, B., VISVIKIS-SIEST, S., PATTOU, F., FAROOQI, I. S., SAUDEK, V., O'RAHILLY, S., FROGUEL, P., SEDGWICK, B. & YEO, G. S. 2010. Prevalence of loss-of-function FTO mutations in lean and obese individuals. *Diabetes,* 59**,** 311-8.

MICHAN, S. & SINCLAIR, D. 2007. Sirtuins in mammals: insights into their biological function. *Biochem J,* 404**,** 1-13.

MONDA, K. L., CHEN, G. K., TAYLOR, K. C., PALMER, C., EDWARDS, T. L., LANGE, L. A., NG, M. C., ADEYEMO, A. A., ALLISON, M. A., BIELAK, L. F., CHEN, G., GRAFF, M., IRVIN, M. R., RHIE, S. K., LI, G., LIU, Y., LU, Y., NALLS, M. A., SUN, Y. V., WOJCZYNSKI, M. K., YANEK, L. R., ALDRICH, M. C., ADEMOLA, A., AMOS, C. I., BANDERA, E. V., BOCK, C. H., BRITTON, A., BROECKEL, U., CAI, Q., CAPORASO, N. E., CARLSON, C. S., CARPTEN, J., CASEY, G., CHEN, W. M., CHEN, F., CHEN, Y. D., CHIANG, C. W., COETZEE, G. A., DEMERATH, E., DEMING-HALVERSON, S. L., DRIVER, R. W., DUBBERT, P., FEITOSA, M. F., FENG, Y., FREEDMAN, B. I., GILLANDERS, E. M., GOTTESMAN, O., GUO, X., HARITUNIANS, T., HARRIS, T., HARRIS, C. C., HENNIS, A. J., HERNANDEZ, D. G., MCNEILL, L. H., HOWARD, T. D., HOWARD, B. V., HOWARD, V. J., JOHNSON, K. C., KANG, S. J., KEATING, B. J., KOLB, S., KULLER, L. H., KUTLAR, A., LANGEFELD, C. D., LETTRE, G., LOHMAN, K., LOTAY, V., LYON, H., MANSON, J. E., MAIXNER, W., MENG, Y. A., MONROE, K. R., MORHASON-BELLO, I., MURPHY, A. B., MYCHALECKYJ, J. C., NADUKURU, R., NATHANSON, K. L., NAYAK, U., N'DIAYE, A., NEMESURE, B., WU, S. Y., LESKE, M. C., NESLUND-DUDAS, C., NEUHOUSER, M., NYANTE, S., OCHS-BALCOM, H., OGUNNIYI, A., OGUNDIRAN, T. O., OJENGBEDE, O., OLOPADE, O. I., PALMER, J. R., RUIZ-NARVAEZ, E. A., PALMER, N. D., PRESS, M. F., RAMPERSAUD, E., RASMUSSEN-TORVIK, L. J., RODRIGUEZ-GIL, J. L., SALAKO, B., SCHADT, E. E., SCHWARTZ, A. G., *et al.* 2013. A meta-analysis identifies new loci associated with body mass index in individuals of African ancestry. *Nat Genet,* 45**,** 690-6.

MONTAGUE, C. T., FAROOQI, I. S., WHITEHEAD, J. P., SOOS, M. A., RAU, H., WAREHAM, N. J., SEWTER, C. P., DIGBY, J. E., MOHAMMED, S. N., HURST, J. A., CHEETHAM, C. H., EARLEY, A. R., BARNETT, A. H., PRINS, J. B. & O'RAHILLY, S. 1997. Congenital leptin deficiency is associated with severe early-onset obesity in humans. *Nature,* 387**,** 903-8.

MUKHOPADHYAY, S. & JACKSON, P. K. 2013. Cilia, tubby mice, and obesity. *Cilia,* 2**,** 1.

NAGY, A., ROSSANT, J., NAGY, R., ABRAMOW-NEWERLY, W. & RODER, J. C. 1993. Derivation of completely cell culture-derived mice from early-passage embryonic stem cells. *Proc Natl Acad Sci U S A,* 90**,** 8424-8.

NAGY, T. R. & CLAIR, A. L. 2000. Precision and accuracy of dual-energy X-ray absorptiometry for determining in vivo body composition of mice. *Obesity Research,* 8**,** 392-8.

NATIONAL HUMAN GENOME RESEARCH INSTITUTE. 2013. *A Catalog of Published Genome-Wide Association Studies* [Online]. Available: http://www.genome.gov/page.cfm?pageID=26525384&start=1&clearquery=1#result_table [Accessed].

NEEL, J. V. 1962. Diabetes mellitus: a "thrifty" genotype rendered detrimental by "progress"? *Am J Hum Genet,* 14**,** 353-62.

NHS UK 2012. Treating Obesity. *In:* UK, N. (ed.).

NIU, Y., ZHAO, X., WU, Y. S., LI, M. M., WANG, X. J. & YANG, Y. G. 2013. N6-methyl-adenosine (m6A) in RNA: an old modification with a novel epigenetic function. *Genomics Proteomics Bioinformatics,* 11**,** 8-17.

NOGUEIRAS, R., TOVAR, S., MITCHELL, S. E., RAYNER, D. V., ARCHER, Z. A., DIEGUEZ, C. & WILLIAMS, L. M. 2004. Regulation of growth hormone secretagogue receptor gene expression in the arcuate nuclei of the rat by leptin and ghrelin. *Diabetes,* 53**,** 2552-8.

OCBINA, P. J., TUSON, M. & ANDERSON, K. V. 2009. Primary cilia are not required for normal canonical Wnt signaling in the mouse embryo. *PLoS One,* 4**,** e6839.

OKADA, Y., KUBO, M., OHMIYA, H., TAKAHASHI, A., KUMASAKA, N., HOSONO, N., MAEDA, S., WEN, W., DORAJOO, R., GO, M. J., ZHENG, W., KATO, N., WU, J. Y., LU, Q., TSUNODA, T., YAMAMOTO, K., NAKAMURA, Y., KAMATANI, N. & TANAKA, T. 2012. Common variants at CDKAL1 and KLF9 are associated with body mass index in east Asian populations. *Nat Genet,* 44**,** 302-6.

OKINAKA, S., KUMAGAI, H., EBASHI, S., SUGITA, H., MOMOI, H., TOYOKURA, Y. & FUJIE, Y. 1961. Serum creatine phosphokinase. Activity in progressive muscular dystrophy and neuromuscular diseases. *Arch Neurol,* 4**,** 520-5.

OLSZANECKA-GLINIANOWICZ, M., DABROWSKI, P., KOCELAK, P., JANOWSKA, J., SMERTKA, M., JONDERKO, K. & CHUDEK, J. 2013. Long-term inhibition of intestinal lipase by orlistat improves release of gut hormones increasing satiety in obese women. *Pharmacol Rep,* 65**,** 666-71.

OLSZEWSKI, P. K., FREDRIKSSON, R., ERIKSSON, J. D., MITRA, A., RADOMSKA, K. J., GOSNELL, B. A., SOLVANG, M. N., LEVINE, A. S. & SCHIOTH, H. B. 2011a. Fto colocalizes with a satiety mediator oxytocin in the brain and upregulates oxytocin gene expression. *Biochem Biophys Res Commun,* 408**,** 422-6.

OLSZEWSKI, P. K., FREDRIKSSON, R., OLSZEWSKA, A. M., STEPHANSSON, O., ALSIO, J., RADOMSKA, K. J., LEVINE, A. S. & SCHIOTH, H. B. 2009. Hypothalamic FTO is associated with the regulation of energy intake not feeding reward. *BMC Neurosci,* 10**,** 129.

OLSZEWSKI, P. K., RADOMSKA, K. J., GHIMIRE, K., KLOCKARS, A., INGMAN, C., OLSZEWSKA, A. M., FREDRIKSSON, R., LEVINE, A. S. & SCHIOTH, H. B. 2011b. Fto immunoreactivity is widespread in the rodent brain and abundant in feeding-related sites, but the number of Fto-positive cells is not affected by changes in energy balance. *Physiol Behav,* 103**,** 248-53.

OUGLAND, R., LANDO, D., JONSON, I., DAHL, J. A., MOEN, M. N., NORDSTRAND, L. M., ROGNES, T., LEE, J. T., KLUNGLAND, A., KOUZARIDES, T. & LARSEN, E. 2012.

ALKBH1 is a histone H2A dioxygenase involved in neural differentiation. *Stem Cells,* 30**,** 2672-82.

PALAM, L. R., BAIRD, T. D. & WEK, R. C. 2011. Phosphorylation of eIF2 facilitates ribosomal bypass of an inhibitory upstream ORF to enhance CHOP translation. *J Biol Chem,* 286**,** 10939-49.

PAN, Y., SHU, J. L., GU, H. F., ZHOU, D. C., LIU, X. L., QIAO, Q. Y., FU, S. K., GAO, F. H. & JIN, H. M. 2013. Erythropoietin improves insulin resistance via the regulation of its receptor-mediated signaling pathways in 3T3L1 adipocytes. *Mol Cell Endocrinol,* 367**,** 116-23.

PAPANDREOU, I., CAIRNS, R. A., FONTANA, L., LIM, A. L. & DENKO, N. C. 2006. HIF-1 mediates adaptation to hypoxia by actively downregulating mitochondrial oxygen consumption. *Cell Metab,* 3**,** 187-97.

PARDRIDGE, W. M. 2003. Blood-brain barrier drug targeting: the future of brain drug development. *Mol Interv,* 3**,** 90-105, 51.

PERRY, J. R., VOIGHT, B. F., YENGO, L., AMIN, N., DUPUIS, J., GANSER, M., GRALLERT, H., NAVARRO, P., LI, M., QI, L., STEINTHORSDOTTIR, V., SCOTT, R. A., ALMGREN, P., ARKING, D. E., AULCHENKO, Y., BALKAU, B., BENEDIKTSSON, R., BERGMAN, R. N., BOERWINKLE, E., BONNYCASTLE, L., BURTT, N. P., CAMPBELL, H., CHARPENTIER, G., COLLINS, F. S., GIEGER, C., GREEN, T., HADJADJ, S., HATTERSLEY, A. T., HERDER, C., HOFMAN, A., JOHNSON, A. D., KOTTGEN, A., KRAFT, P., LABRUNE, Y., LANGENBERG, C., MANNING, A. K., MOHLKE, K. L., MORRIS, A. P., OOSTRA, B., PANKOW, J., PETERSEN, A. K., PRAMSTALLER, P. P., PROKOPENKO, I., RATHMANN, W., RAYNER, W., RODEN, M., RUDAN, I., RYBIN, D., SCOTT, L. J., SIGURDSSON, G., SLADEK, R., THORLEIFSSON, G., THORSTEINSDOTTIR, U., TUOMILEHTO, J., UITTERLINDEN, A. G., VIVEQUIN, S., WEEDON, M. N., WRIGHT, A. F., HU, F. B., ILLIG, T., KAO, L., MEIGS, J. B., WILSON, J. F., STEFANSSON, K., VAN DUIJN, C., ALTSCHULER, D., MORRIS, A. D., BOEHNKE, M., MCCARTHY, M. I., FROGUEL, P., PALMER, C. N., WAREHAM, N. J., GROOP, L., FRAYLING, T. M. & CAUCHI, S. 2012. Stratifying type 2 diabetes cases by BMI identifies genetic risk variants in LAMA1 and enrichment for risk variants in lean compared to obese cases. *PLoS Genet,* 8**,** e1002741.

PETERS, T., AUSMEIER, K., DILDROP, R. & RUTHER, U. 2002. The mouse Fused toes (Ft) mutation is the result of a 1.6-Mb deletion including the entire Iroquois B gene cluster. *Mamm Genome,* 13**,** 186-8.

PETERS, T., AUSMEIER, K. & RUTHER, U. 1999. Cloning of Fatso (Fto), a novel gene deleted by the Fused toes (Ft) mouse mutation. *Mamm Genome,* 10**,** 983-6.

PEYROT, M., RUBIN, R. R., LAURITZEN, T., SKOVLUND, S. E., SNOEK, F. J., MATTHEWS, D. R., LANDGRAF, R. & KLEINEBREIL, L. 2005. Resistance to insulin therapy among patients and providers: results of the cross-national Diabetes Attitudes, Wishes, and Needs (DAWN) study. *Diabetes Care,* 28**,** 2673-9.

PHILIPP, S., JURGENSEN, J. S., FIELITZ, J., BERNHARDT, W. M., WEIDEMANN, A., SCHICHE, A., PILZ, B., DIETZ, R., REGITZ-ZAGROSEK, V., ECKARDT, K. U. & WILLENBROCK, R. 2006. Stabilization of hypoxia inducible factor rather than modulation of collagen metabolism improves cardiac function after acute myocardial infarction in rats. *Eur J Heart Fail,* 8**,** 347-54.

PINHEIRO, J. C. & BATES, D. M. 2000. *Mixed-Effects Models in S and S-Plus,* New York, Springer Verlag.

POOLEY, E. C., FAIRBURN, C. G., COOPER, Z., SODHI, M. S., COWEN, P. J. & HARRISON, P. J. 2004. A 5-HT2C receptor promoter polymorphism (HTR2C - 759C/T) is associated with obesity in women, and with resistance to weight loss in heterozygotes. *Am J Med Genet B Neuropsychiatr Genet,* 126B**,** 124-7.

PRESCOTT, J., THOMPSON, D. J., KRAFT, P., CHANOCK, S. J., AUDLEY, T., BROWN, J., LEYLAND, J., FOLKERD, E., DOODY, D., HANKINSON, S. E., HUNTER, D. J., JACOBS, K. B., DOWSETT, M., COX, D. G., EASTON, D. F. & DE VIVO, I. 2012.

Genome-wide association study of circulating estradiol, testosterone, and sex hormone-binding globulin in postmenopausal women. *PLoS One,* 7**,** e37815.

PROFENNO, L. A., PORSTEINSSON, A. P. & FARAONE, S. V. 2010. Meta-analysis of Alzheimer's disease risk with obesity, diabetes, and related disorders. *Biol Psychiatry,* 67**,** 505-12.

QI, L., KANG, K., ZHANG, C., VAN DAM, R. M., KRAFT, P., HUNTER, D., LEE, C. H. & HU, F. B. 2008. Fat mass-and obesity-associated (FTO) gene variant is associated with obesity: longitudinal analyses in two cohort studies and functional test. *Diabetes,* 57**,** 3145-51.

QUWAILID, M. M., HUGILL, A., DEAR, N., VIZOR, L., WELLS, S., HORNER, E., FULLER, S., WEEDON, J., MCMATH, H., WOODMAN, P., EDWARDS, D., CAMPBELL, D., RODGER, S., CAREY, J., ROBERTS, A., GLENISTER, P., LALANNE, Z., PARKINSON, N., COGHILL, E. L., MCKEONE, R., COX, S., WILLAN, J., GREENFIELD, A., KEAYS, D., BRADY, S., SPURR, N., GRAY, I., HUNTER, J., BROWN, S. D. & COX, R. D. 2004. A gene-driven ENU-based approach to generating an allelic series in any gene. *Mamm Genome,* 15**,** 585-91.

RAGVIN, A., MORO, E., FREDMAN, D., NAVRATILOVA, P., DRIVENES, O., ENGSTROM, P. G., ALONSO, M. E., DE LA CALLE MUSTIENES, E., GOMEZ SKARMETA, J. L., TAVARES, M. J., CASARES, F., MANZANARES, M., VAN HEYNINGEN, V., MOLVEN, A., NJOLSTAD, P. R., ARGENTON, F., LENHARD, B. & BECKER, T. S. 2010. Long-range gene regulation links genomic type 2 diabetes and obesity risk regions to HHEX, SOX4, and IRX3. *Proc Natl Acad Sci U S A,* 107**,** 775-80.

RAMPERSAUD, E., MITCHELL, B. D., POLLIN, T. I., FU, M., SHEN, H., O'CONNELL, J. R., DUCHARME, J. L., HINES, S., SACK, P., NAGLIERI, R., SHULDINER, A. R. & SNITKER, S. 2008. Physical activity and the association of common FTO gene variants with body mass index and obesity. *Arch Intern Med,* 168**,** 1791-7.

RASK-ANDERSEN, M., OLSZEWSKI, P. K., LEVINE, A. S. & SCHIOTH, H. B. 2010. Molecular mechanisms underlying anorexia nervosa: focus on human gene association studies and systems controlling food intake. *Brain Res Rev,* 62**,** 147-64.

RAVINET TRILLOU, C., DELGORGE, C., MENET, C., ARNONE, M. & SOUBRIE, P. 2004. CB1 cannabinoid receptor knockout in mice leads to leanness, resistance to diet-induced obesity and enhanced leptin sensitivity. *Int J Obes Relat Metab Disord,* 28**,** 640-8.

RAY, M. K., FAGAN, S. P. & BRUNICARDI, F. C. 2000. The Cre-loxP system: a versatile tool for targeting genes in a cell- and stage-specific manner. *Cell Transplant,* 9**,** 805-15.

REED, D. R., LI, X., MCDANIEL, A. H., LU, K., LI, S., TORDOFF, M. G., PRICE, R. A. & BACHMANOV, A. A. 2003. Loci on chromosomes 2, 4, 9, and 16 for body weight, body length, and adiposity identified in a genome scan of an F2 intercross between the 129P3/J and C57BL/6ByJ mouse strains. *Mamm Genome,* 14**,** 302-13.

REITZ, C., TOSTO, G., MAYEUX, R. & LUCHSINGER, J. A. 2012. Genetic variants in the Fat and Obesity Associated (FTO) gene and risk of Alzheimer's disease. *PLoS One,* 7**,** e50354.

RINGVOLL, J., MOEN, M. N., NORDSTRAND, L. M., MEIRA, L. B., PANG, B., BEKKELUND, A., DEDON, P. C., BJELLAND, S., SAMSON, L. D., FALNES, P. O. & KLUNGLAND, A. 2008. AlkB homologue 2-mediated repair of ethenoadenine lesions in mammalian DNA. *Cancer Res,* 68**,** 4142-9.

RINGVOLL, J., NORDSTRAND, L. M., VAGBO, C. B., TALSTAD, V., REITE, K., AAS, P. A., LAURITZEN, K. H., LIABAKK, N. B., BJORK, A., DOUGHTY, R. W., FALNES, P. O., KROKAN, H. E. & KLUNGLAND, A. 2006. Repair deficient mice reveal mABH2 as the primary oxidative demethylase for repairing 1meA and 3meC lesions in DNA. *EMBO J,* 25**,** 2189-98.

RINGWALD, M., IYER, V., MASON, J. C., STONE, K. R., TADEPALLY, H. D., KADIN, J. A., BULT, C. J., EPPIG, J. T., OAKLEY, D. J., BRIOIS, S., STUPKA, E., MASELLI, V., SMEDLEY, D., LIU, S., HANSEN, J., BALDOCK, R., HICKS, G. G. & SKARNES, W. C. 2011. The IKMC web portal: a central point of entry to data and resources from the International Knockout Mouse Consortium. *Nucleic Acids Res,* 39**,** D849-55.

RODRIGUEZ-FONSECA, C., PHAN, H., LONG, K. S., PORSE, B. T., KIRILLOV, S. V., AMILS, R. & GARRETT, R. A. 2000. Puromycin-rRNA interaction sites at the peptidyl transferase center. *RNA,* 6**,** 744-54.

ROLLAND-CACHERA, M. F., DEHEEGER, M., BELLISLE, F., SEMPE, M., GUILLOUD-BATAILLE, M. & PATOIS, E. 1984. Adiposity rebound in children: a simple indicator for predicting obesity. *Am J Clin Nutr,* 39**,** 129-35.

ROMON, M., LEBEL, P., VELLY, C., MARECAUX, N., FRUCHART, J. C. & DALLONGEVILLE, J. 1999. Leptin response to carbohydrate or fat meal and association with subsequent satiety and energy intake. *Am J Physiol,* 277**,** E855-61.

ROSE, N. R., MCDONOUGH, M. A., KING, O. N., KAWAMURA, A. & SCHOFIELD, C. J. 2011. Inhibition of 2-oxoglutarate dependent oxygenases. *Chem Soc Rev,* 40**,** 4364-97.

ROSEN, E. D. & MACDOUGALD, O. A. 2006. Adipocyte differentiation from the inside out. *Nat Rev Mol Cell Biol,* 7**,** 885-96.

ROSS, S. E., HEMATI, N., LONGO, K. A., BENNETT, C. N., LUCAS, P. C., ERICKSON, R. L. & MACDOUGALD, O. A. 2000. Inhibition of adipogenesis by Wnt signaling. *Science,* 289**,** 950-3.

RYDING, A. D., SHARP, M. G. & MULLINS, J. J. 2001. Conditional transgenic technologies. *J Endocrinol,* 171**,** 1-14.

SAIKI, R. K., SCHARF, S., FALOONA, F., MULLIS, K. B., HORN, G. T., ERLICH, H. A. & ARNHEIM, N. 1985. Enzymatic amplification of beta-globin genomic sequences and restriction site analysis for diagnosis of sickle cell anemia. *Science,* 230**,** 1350-4.

SALADIN, R., DE VOS, P., GUERRE-MILLO, M., LETURQUE, A., GIRARD, J., STAELS, B. & AUWERX, J. 1995. Transient increase in obese gene expression after food intake or insulin administration. *Nature,* 377**,** 527-9.

SAMAAN, Z., ANAND, S., ZHANG, X., DESAI, D., RIVERA, M., PARE, G., THABANE, L., XIE, C., GERSTEIN, H., ENGERT, J. C., CRAIG, I., COHEN-WOODS, S., MOHAN, V., DIAZ, R., WANG, X., LIU, L., CORRE, T., PREISIG, M., KUTALIK, Z., BERGMANN, S., VOLLENWEIDER, P., WAEBER, G., YUSUF, S. & MEYRE, D. 2012. The protective effect of the obesity-associated rs9939609 A variant in fat mass- and obesity-associated gene on depression. *Mol Psychiatry*.

SAMAD, F., YAMAMOTO, K., PANDEY, M. & LOSKUTOFF, D. J. 1997. Elevated expression of transforming growth factor-beta in adipose tissue from obese mice. *Mol Med,* 3**,** 37-48.

SAMBROOK, J. F., FRITSCH, E. F. & MANIATIS, T. 1989. *MOLECULAR CLONING A LABORATORY MANUAL,* COLD SPRING HARBOR LABORATORY PRESS.

SANCHEZ-PULIDO, L. & ANDRADE-NAVARRO, M. A. 2007. The FTO (fat mass and obesity associated) gene codes for a novel member of the non-heme dioxygenase superfamily. *BMC Biochem,* 8**,** 23.

SANGER, F., NICKLEN, S. & COULSON, A. R. 1977. DNA sequencing with chain-terminating inhibitors. *Proc Natl Acad Sci U S A,* 74**,** 5463-7.

SAUER, B. 1998. Inducible gene targeting in mice using the Cre/lox system. *Methods,* 14**,** 381-92.

SCHERAG, A., DINA, C., HINNEY, A., VATIN, V., SCHERAG, S., VOGEL, C. I., MULLER, T. D., GRALLERT, H., WICHMANN, H. E., BALKAU, B., HEUDE, B., JARVELIN, M. R., HARTIKAINEN, A. L., LEVY-MARCHAL, C., WEILL, J., DELPLANQUE, J., KORNER, A., KIESS, W., KOVACS, P., RAYNER, N. W., PROKOPENKO, I., MCCARTHY, M. I., SCHAFER, H., JARICK, I., BOEING, H., FISHER, E., REINEHR, T., HEINRICH, J., RZEHAK, P., BERDEL, D., BORTE, M., BIEBERMANN, H., KRUDE, H., ROSSKOPF, D., RIMMBACH, C., RIEF, W., FROMME, T., KLINGENSPOR, M., SCHURMANN, A., SCHULZ, N., NOTHEN, M. M., MUHLEISEN, T. W., ERBEL, R., JOCKEL, K. H., MOEBUS, S., BOES, T., ILLIG, T., FROGUEL, P., HEBEBRAND, J. & MEYRE, D. 2010. Two new Loci for body-weight regulation identified in a joint analysis of genome-wide association studies for early-onset extreme obesity in French and german study groups. *PLoS Genet,* 6**,** e1000916.

SCHIEKE, S. M., PHILLIPS, D., MCCOY, J. P., JR., APONTE, A. M., SHEN, R. F., BALABAN, R. S. & FINKEL, T. 2006. The mammalian target of rapamycin (mTOR) pathway

regulates mitochondrial oxygen consumption and oxidative capacity. *J Biol Chem,* 281**,** 27643-52.

SCHMIDT, E. E., TAYLOR, D. S., PRIGGE, J. R., BARNETT, S. & CAPECCHI, M. R. 2000. Illegitimate Cre-dependent chromosome rearrangements in transgenic mouse spermatids. *Proc Natl Acad Sci U S A,* 97**,** 13702-7.

SCHMIDT, E. K., CLAVARINO, G., CEPPI, M. & PIERRE, P. 2009. SUnSET, a nonradioactive method to monitor protein synthesis. *Nat Methods,* 6**,** 275-7.

SCHOELLER, D. A., CELLA, L. K., SINHA, M. K. & CARO, J. F. 1997. Entrainment of the diurnal rhythm of plasma leptin to meal timing. *J Clin Invest,* 100**,** 1882-7.

SCHWARTZ, M. W. & PORTE, D., JR. 2005. Diabetes, obesity, and the brain. *Science,* 307**,** 375-9.

SCHWARTZ, M. W., WOODS, S. C., PORTE, D., JR., SEELEY, R. J. & BASKIN, D. G. 2000. Central nervous system control of food intake. *Nature,* 404**,** 661-71.

SCOTT, L. J., MOHLKE, K. L., BONNYCASTLE, L. L., WILLER, C. J., LI, Y., DUREN, W. L., ERDOS, M. R., STRINGHAM, H. M., CHINES, P. S., JACKSON, A. U., PROKUNINA-OLSSON, L., DING, C. J., SWIFT, A. J., NARISU, N., HU, T., PRUIM, R., XIAO, R., LI, X. Y., CONNEELY, K. N., RIEBOW, N. L., SPRAU, A. G., TONG, M., WHITE, P. P., HETRICK, K. N., BARNHART, M. W., BARK, C. W., GOLDSTEIN, J. L., WATKINS, L., XIANG, F., SARAMIES, J., BUCHANAN, T. A., WATANABE, R. M., VALLE, T. T., KINNUNEN, L., ABECASIS, G. R., PUGH, E. W., DOHENY, K. F., BERGMAN, R. N., TUOMILEHTO, J., COLLINS, F. S. & BOEHNKE, M. 2007. A genome-wide association study of type 2 diabetes in Finns detects multiple susceptibility variants. *Science,* 316**,** 1341-5.

SCOTT, R. A., BAILEY, M. E., MORAN, C. N., WILSON, R. H., FUKU, N., TANAKA, M., TSIOKANOS, A., JAMURTAS, A. Z., GRAMMATIKAKI, E., MOSCHONIS, G., MANIOS, Y. & PITSILADIS, Y. P. 2010. FTO genotype and adiposity in children: physical activity levels influence the effect of the risk genotype in adolescent males. *Eur J Hum Genet,* 18**,** 1339-43.

SCUTERI, A., SANNA, S., CHEN, W. M., UDA, M., ALBAI, G., STRAIT, J., NAJJAR, S., NAGARAJA, R., ORRU, M., USALA, G., DEI, M., LAI, S., MASCHIO, A., BUSONERO, F., MULAS, A., EHRET, G. B., FINK, A. A., WEDER, A. B., COOPER, R. S., GALAN, P., CHAKRAVARTI, A., SCHLESSINGER, D., CAO, A., LAKATTA, E. & ABECASIS, G. R. 2007. Genome-wide association scan shows genetic variants in the FTO gene are associated with obesity-related traits. *PLoS Genet,* 3**,** e115.

SEBERT, S. P., HYATT, M. A., CHAN, L. L., YIALLOURIDES, M., FAINBERG, H. P., PATEL, N., SHARKEY, D., STEPHENSON, T., RHIND, S. M., BELL, R. C., BUDGE, H., GARDNER, D. S. & SYMONDS, M. E. 2010. Influence of prenatal nutrition and obesity on tissue specific fat mass and obesity-associated (FTO) gene expression. *Reproduction,* 139**,** 265-74.

SEDGWICK, B., BATES, P. A., PAIK, J., JACOBS, S. C. & LINDAHL, T. 2007. Repair of alkylated DNA: recent advances. *DNA Repair (Amst),* 6**,** 429-42.

SEN GUPTA, P., PRODROMOU, N. V. & CHAPPLE, J. P. 2009. Can faulty antennae increase adiposity? The link between cilia proteins and obesity. *J Endocrinol,* 203**,** 327-36.

SETHI, J. K. & VIDAL-PUIG, A. 2010. Wnt signalling and the control of cellular metabolism. *Biochem J,* 427**,** 1-17.

SHACKELFORD, C., LONG, G., WOLF, J., OKERBERG, C. & HERBERT, R. 2002. Qualitative and quantitative analysis of nonneoplastic lesions in toxicology studies. *Toxicologic Pathology,* 30**,** 93-96.

SHERPA, L. Y., DEJI, STIGUM, H., CHONGSUVIVATWONG, V., THELLE, D. S. & BJERTNESS, E. 2010. Obesity in Tibetans aged 30-70 living at different altitudes under the north and south faces of Mt. Everest. *Int J Environ Res Public Health,* 7**,** 1670-80.

SHI, T., WANG, F., STIEREN, E. & TONG, Q. 2005. SIRT3, a mitochondrial sirtuin deacetylase, regulates mitochondrial function and thermogenesis in brown adipocytes. *J Biol Chem,* 280**,** 13560-7.

SHIOZAWA, Y., JUNG, Y., ZIEGLER, A. M., PEDERSEN, E. A., WANG, J., WANG, Z., SONG, J., LEE, C. H., SUD, S., PIENTA, K. J., KREBSBACH, P. H. & TAICHMAN, R. S. 2010. Erythropoietin couples hematopoiesis with bone formation. *PLoS One,* 5**,** e10853.

SILVER, D. P. & LIVINGSTON, D. M. 2001. Self-excising retroviral vectors encoding the Cre recombinase overcome Cre-mediated cellular toxicity. *Mol Cell,* 8**,** 233-43.

SIMONS, M., GLOY, J., GANNER, A., BULLERKOTTE, A., BASHKUROV, M., KRONIG, C., SCHERMER, B., BENZING, T., CABELLO, O. A., JENNY, A., MLODZIK, M., POLOK, B., DRIEVER, W., OBARA, T. & WALZ, G. 2005. Inversin, the gene product mutated in nephronophthisis type II, functions as a molecular switch between Wnt signaling pathways. *Nat Genet,* 37**,** 537-43.

SINHA, M. K. & CARO, J. F. 1998. Clinical aspects of leptin. *Vitam Horm,* 54**,** 1-30.

SJOSTROM, L., PELTONEN, M., JACOBSON, P., SJOSTROM, C. D., KARASON, K., WEDEL, H., AHLIN, S., ANVEDEN, A., BENGTSSON, C., BERGMARK, G., BOUCHARD, C., CARLSSON, B., DAHLGREN, S., KARLSSON, J., LINDROOS, A. K., LONROTH, H., NARBRO, K., NASLUND, I., OLBERS, T., SVENSSON, P. A. & CARLSSON, L. M. 2012. Bariatric surgery and long-term cardiovascular events. *JAMA,* 307**,** 56-65.

SKARNES, W. C., ROSEN, B., WEST, A. P., KOUTSOURAKIS, M., BUSHELL, W., IYER, V., MUJICA, A. O., THOMAS, M., HARROW, J., COX, T., JACKSON, D., SEVERIN, J., BIGGS, P., FU, J., NEFEDOV, M., DE JONG, P. J., STEWART, A. F. & BRADLEY, A. 2011. A conditional knockout resource for the genome-wide study of mouse gene function. *Nature,* 474**,** 337-42.

SMITH, J. E., COOPERMAN, B. S. & MITCHELL, P. 1992. Methylation sites in Escherichia coli ribosomal RNA: localization and identification of four new sites of methylation in 23S rRNA. *Biochemistry,* 31**,** 10825-34.

SMITHIES, O., GREGG, R. G., BOGGS, S. S., KORALEWSKI, M. A. & KUCHERLAPATI, R. S. 1985. Insertion of DNA sequences into the human chromosomal beta-globin locus by homologous recombination. *Nature,* 317**,** 230-4.

SMITHIES, O., KORALEWSKI, M. A., SONG, K. Y. & KUCHERLAPATI, R. S. 1984. Homologous recombination with DNA introduced into mammalian cells. *Cold Spring Harb Symp Quant Biol,* 49**,** 161-70.

SOBCZYK-KOPCIOL, A., BRODA, G., WOJNAR, M., KURJATA, P., JAKUBCZYK, A., KLIMKIEWICZ, A. & PLOSKI, R. 2011. Inverse association of the obesity predisposing FTO rs9939609 genotype with alcohol consumption and risk for alcohol dependence. *Addiction,* 106**,** 739-48.

SOLBERG, A., ROBERTSON, A. B., ARONSEN, J. M., ROGNMO, O., SJAASTAD, I., WISLOFF, U. & KLUNGLAND, A. 2013. Deletion of mouse Alkbh7 leads to obesity. *J Mol Cell Biol,* 5**,** 194-203.

SONESTEDT, E., ROOS, C., GULLBERG, B., ERICSON, U., WIRFALT, E. & ORHO-MELANDER, M. 2009. Fat and carbohydrate intake modify the association between genetic variation in the FTO genotype and obesity. *Am J Clin Nutr,* 90**,** 1418-25.

SONGE-MOLLER, L., VAN DEN BORN, E., LEIHNE, V., VAGBO, C. B., KRISTOFFERSEN, T., KROKAN, H. E., KIRPEKAR, F., FALNES, P. O. & KLUNGLAND, A. 2010. Mammalian ALKBH8 possesses tRNA methyltransferase activity required for the biogenesis of multiple wobble uridine modifications implicated in translational decoding. *Mol Cell Biol,* 30**,** 1814-27.

SOVIO, U., MOOK-KANAMORI, D. O., WARRINGTON, N. M., LAWRENCE, R., BRIOLLAIS, L., PALMER, C. N., CECIL, J., SANDLING, J. K., SYVANEN, A. C., KAAKINEN, M., BEILIN, L. J., MILLWOOD, I. Y., BENNETT, A. J., LAITINEN, J., POUTA, A., MOLITOR, J., DAVEY SMITH, G., BEN-SHLOMO, Y., JADDOE, V. W., PALMER, L. J., PENNELL, C. E., COLE, T. J., MCCARTHY, M. I., JARVELIN, M. R. & TIMPSON, N. J. 2011. Association between common variation at the FTO locus and changes in body mass index from infancy to late childhood: the complex nature of genetic association through growth and development. *PLoS Genet,* 7**,** e1001307.

SPEAKMAN, J. R. 2008. Thrifty genes for obesity, an attractive but flawed idea, and an alternative perspective: the 'drifty gene' hypothesis. *Int J Obes (Lond),* 32**,** 1611-7.

SPEAKMAN, J. R. 2010. FTO effect on energy demand versus food intake. *Nature,* 464**,** E1; discussion E2.

SPEAKMAN, J. R., RANCE, K. A. & JOHNSTONE, A. M. 2008. Polymorphisms of the FTO gene are associated with variation in energy intake, but not energy expenditure. *Obesity (Silver Spring),* 16**,** 1961-5.

SPELIOTES, E. K., WILLER, C. J., BERNDT, S. I., MONDA, K. L., THORLEIFSSON, G., JACKSON, A. U., LANGO ALLEN, H., LINDGREN, C. M., LUAN, J., MAGI, R., RANDALL, J. C., VEDANTAM, S., WINKLER, T. W., QI, L., WORKALEMAHU, T., HEID, I. M., STEINTHORSDOTTIR, V., STRINGHAM, H. M., WEEDON, M. N., WHEELER, E., WOOD, A. R., FERREIRA, T., WEYANT, R. J., SEGRE, A. V., ESTRADA, K., LIANG, L., NEMESH, J., PARK, J. H., GUSTAFSSON, S., KILPELAINEN, T. O., YANG, J., BOUATIA-NAJI, N., ESKO, T., FEITOSA, M. F., KUTALIK, Z., MANGINO, M., RAYCHAUDHURI, S., SCHERAG, A., SMITH, A. V., WELCH, R., ZHAO, J. H., ABEN, K. K., ABSHER, D. M., AMIN, N., DIXON, A. L., FISHER, E., GLAZER, N. L., GODDARD, M. E., HEARD-COSTA, N. L., HOESEL, V., HOTTENGA, J. J., JOHANSSON, A., JOHNSON, T., KETKAR, S., LAMINA, C., LI, S., MOFFATT, M. F., MYERS, R. H., NARISU, N., PERRY, J. R., PETERS, M. J., PREUSS, M., RIPATTI, S., RIVADENEIRA, F., SANDHOLT, C., SCOTT, L. J., TIMPSON, N. J., TYRER, J. P., VAN WINGERDEN, S., WATANABE, R. M., WHITE, C. C., WIKLUND, F., BARLASSINA, C., CHASMAN, D. I., COOPER, M. N., JANSSON, J. O., LAWRENCE, R. W., PELLIKKA, N., PROKOPENKO, I., SHI, J., THIERING, E., ALAVERE, H., ALIBRANDI, M. T., ALMGREN, P., ARNOLD, A. M., ASPELUND, T., ATWOOD, L. D., BALKAU, B., BALMFORTH, A. J., BENNETT, A. J., BEN-SHLOMO, Y., BERGMAN, R. N., BERGMANN, S., BIEBERMANN, H., BLAKEMORE, A. I., BOES, T., BONNYCASTLE, L. L., BORNSTEIN, S. R., BROWN, M. J., BUCHANAN, T. A., *et al.* 2010. Association analyses of 249,796 individuals reveal 18 new loci associated with body mass index. *Nat Genet,* 42**,** 937-48.

SRIDHARAN, V., GUICHARD, J., BAILEY, R. M., KASIGANESAN, H., BEESON, C. & WRIGHT, G. L. 2007. The prolyl hydroxylase oxygen-sensing pathway is cytoprotective and allows maintenance of mitochondrial membrane potential during metabolic inhibition. *Am J Physiol Cell Physiol,* 292**,** C719-28.

STANFORD, W. L., COHN, J. B. & CORDES, S. P. 2001. Gene-trap mutagenesis: past, present and beyond. *Nat Rev Genet,* 2**,** 756-68.

STAR, E. N., ZHU, M., SHI, Z., LIU, H., PASHMFOROUSH, M., SAUVE, Y., BRUNEAU, B. G. & CHOW, R. L. 2012. Regulation of retinal interneuron subtype identity by the Iroquois homeobox gene Irx6. *Development,* 139**,** 4644-55.

STRATIGOPOULOS, G., PADILLA, S. L., LEDUC, C. A., WATSON, E., HATTERSLEY, A. T., MCCARTHY, M. I., ZELTSER, L. M., CHUNG, W. K. & LEIBEL, R. L. 2008. Regulation of Fto/Ftm gene expression in mice and humans. *Am J Physiol Regul Integr Comp Physiol,* 294**,** R1185-96.

STUNKARD, A. J., FOCH, T. T. & HRUBEC, Z. 1986. A twin study of human obesity. *JAMA,* 256**,** 51-4.

SUN, X. J., WANG, L. M., ZHANG, Y., YENUSH, L., MYERS, M. G., JR., GLASHEEN, E., LANE, W. S., PIERCE, J. H. & WHITE, M. F. 1995. Role of IRS-2 in insulin and cytokine signalling. *Nature,* 377**,** 173-7.

SWINBURN, B. A., SACKS, G., HALL, K. D., MCPHERSON, K., FINEGOOD, D. T., MOODIE, M. L. & GORTMAKER, S. L. 2011. The global obesity pandemic: shaped by global drivers and local environments. *Lancet,* 378**,** 804-14.

TABASSUM, R., CHAUHAN, G., DWIVEDI, O. P., MAHAJAN, A., JAISWAL, A., KAUR, I., BANDESH, K., SINGH, T., MATHAI, B. J., PANDEY, Y., CHIDAMBARAM, M., SHARMA, A., CHAVALI, S., SENGUPTA, S., RAMAKRISHNAN, L., VENKATESH, P., AGGARWAL, S. K., GHOSH, S., PRABHAKARAN, D., SRINATH, R. K., SAXENA, M., BANERJEE, M., MATHUR, S., BHANSALI, A., SHAH, V. N., MADHU,

S. V., MARWAHA, R. K., BASU, A., SCARIA, V., MCCARTHY, M. I., VENKATESAN, R., MOHAN, V., TANDON, N. & BHARADWAJ, D. 2013. Genome-wide association study for type 2 diabetes in Indians identifies a new susceptibility locus at 2q21. *Diabetes,* 62**,** 977-86.

TAN, S. C., YEOH, K. K., CARR, C. A., HEATHER, L. C., AMBROSE, L., TAN, J. J., SCHOFIELD, C. & CLARKE, K. 2011. Use of Prolyl Hydroxylase Inhibitors to Induce Hif-Related Metabolic Changes and Increase C-Kit Expression in Cardiosphere-Derived Cells. *Heart,* 97**,** 13-14.

TANAKA, T., NGWA, J. S., VAN ROOIJ, F. J., ZILLIKENS, M. C., WOJCZYNSKI, M. K., FRAZIER-WOOD, A. C., HOUSTON, D. K., KANONI, S., LEMAITRE, R. N., LUAN, J., MIKKILA, V., RENSTROM, F., SONESTEDT, E., ZHAO, J. H., CHU, A. Y., QI, L., CHASMAN, D. I., DE OLIVEIRA OTTO, M. C., DHURANDHAR, E. J., FEITOSA, M. F., JOHANSSON, I., KHAW, K. T., LOHMAN, K. K., MANICHAIKUL, A., MCKEOWN, N. M., MOZAFFARIAN, D., SINGLETON, A., STIRRUPS, K., VIIKARI, J., YE, Z., BANDINELLI, S., BARROSO, I., DELOUKAS, P., FOROUHI, N. G., HOFMAN, A., LIU, Y., LYYTIKAINEN, L. P., NORTH, K. E., DIMITRIOU, M., HALLMANS, G., KAHONEN, M., LANGENBERG, C., ORDOVAS, J. M., UITTERLINDEN, A. G., HU, F. B., KALAFATI, I. P., RAITAKARI, O., FRANCO, O. H., JOHNSON, A., EMILSSON, V., SCHRACK, J. A., SEMBA, R. D., SISCOVICK, D. S., ARNETT, D. K., BORECKI, I. B., FRANKS, P. W., KRITCHEVSKY, S. B., LEHTIMAKI, T., LOOS, R. J., ORHO-MELANDER, M., ROTTER, J. I., WAREHAM, N. J., WITTEMAN, J. C., FERRUCCI, L., DEDOUSSIS, G., CUPPLES, L. A. & NETTLETON, J. A. 2013. Genome-wide meta-analysis of observational studies shows common genetic variants associated with macronutrient intake. *Am J Clin Nutr,* 97**,** 1395-402.

TANOFSKY-KRAFF, M., HAN, J. C., ANANDALINGAM, K., SHOMAKER, L. B., COLUMBO, K. M., WOLKOFF, L. E., KOZLOSKY, M., ELLIOTT, C., RANZENHOFER, L. M., ROZA, C. A., YANOVSKI, S. Z. & YANOVSKI, J. A. 2009. The FTO gene rs9939609 obesity-risk allele and loss of control over eating. *Am J Clin Nutr,* 90**,** 1483-8.

TAYLOR, J. R., DIETRICH, E. & POWELL, J. G. 2013. New and emerging pharmacologic therapies for type 2 diabetes, dyslipidemia, and obesity. *Clin Ther,* 35**,** A3-17.

TEWS, D., FISCHER-POSOVSZKY, P., FROMME, T., KLINGENSPOR, M., FISCHER, J., RUTHER, U., MARIENFELD, R., BARTH, T., MOLLER, P., DEBATIN, K. & WABITSCH, M. 2013. FTO deficiency induces UCP-1 expression and mitochondrial uncoupling in adipocytes. *Endocrinology*.

THE INTERNATIONAL HAPMAP CONSORTIUM 2005. A haplotype map of the human genome. *Nature,* 437**,** 1299-320.

THOMAS, G. N., TOMLINSON, B. & CRITCHLEY, J. A. 2000. Modulation of blood pressure and obesity with the dopamine D2 receptor gene TaqI polymorphism. *Hypertension,* 36**,** 177-82.

THOMAS, K. R., FOLGER, K. R. & CAPECCHI, M. R. 1986. High frequency targeting of genes to specific sites in the mammalian genome. *Cell,* 44**,** 419-28.

THORLEIFSSON, G., WALTERS, G. B., GUDBJARTSSON, D. F., STEINTHORSDOTTIR, V., SULEM, P., HELGADOTTIR, A., STYRKARSDOTTIR, U., GRETARSDOTTIR, S., THORLACIUS, S., JONSDOTTIR, I., JONSDOTTIR, T., OLAFSDOTTIR, E. J., OLAFSDOTTIR, G. H., JONSSON, T., JONSSON, F., BORCH-JOHNSEN, K., HANSEN, T., ANDERSEN, G., JORGENSEN, T., LAURITZEN, T., ABEN, K. K., VERBEEK, A. L., ROELEVELD, N., KAMPMAN, E., YANEK, L. R., BECKER, L. C., TRYGGVADOTTIR, L., RAFNAR, T., BECKER, D. M., GULCHER, J., KIEMENEY, L. A., PEDERSEN, O., KONG, A., THORSTEINSDOTTIR, U. & STEFANSSON, K. 2009. Genome-wide association yields new sequence variants at seven loci that associate with measures of obesity. *Nat Genet,* 41**,** 18-24.

TIMMONS, J. A., WENNMALM, K., LARSSON, O., WALDEN, T. B., LASSMANN, T., PETROVIC, N., HAMILTON, D. L., GIMENO, R. E., WAHLESTEDT, C., BAAR, K.,

NEDERGAARD, J. & CANNON, B. 2007. Myogenic gene expression signature establishes that brown and white adipocytes originate from distinct cell lineages. *Proc Natl Acad Sci U S A,* 104**,** 4401-6.

TIMPSON, N. J., EMMETT, P. M., FRAYLING, T. M., ROGERS, I., HATTERSLEY, A. T., MCCARTHY, M. I. & DAVEY SMITH, G. 2008. The fat mass- and obesity-associated locus and dietary intake in children. *Am J Clin Nutr,* 88**,** 971-8.

TIMPSON, N. J., LINDGREN, C. M., WEEDON, M. N., RANDALL, J., OUWEHAND, W. H., STRACHAN, D. P., RAYNER, N. W., WALKER, M., HITMAN, G. A., DONEY, A. S., PALMER, C. N., MORRIS, A. D., HATTERSLEY, A. T., ZEGGINI, E., FRAYLING, T. M. & MCCARTHY, M. I. 2009. Adiposity-related heterogeneity in patterns of type 2 diabetes susceptibility observed in genome-wide association data. *Diabetes,* 58**,** 505-10.

TONJES, A., ZEGGINI, E., KOVACS, P., BOTTCHER, Y., SCHLEINITZ, D., DIETRICH, K., MORRIS, A. P., ENIGK, B., RAYNER, N. W., KORIATH, M., ESZLINGER, M., KEMPPINEN, A., PROKOPENKO, I., HOFFMANN, K., TEUPSER, D., THIERY, J., KROHN, K., MCCARTHY, M. I. & STUMVOLL, M. 2010. Association of FTO variants with BMI and fat mass in the self-contained population of Sorbs in Germany. *Eur J Hum Genet,* 18**,** 104-10.

TREWICK, S. C., HENSHAW, T. F., HAUSINGER, R. P., LINDAHL, T. & SEDGWICK, B. 2002. Oxidative demethylation by Escherichia coli AlkB directly reverts DNA base damage. *Nature,* 419**,** 174-8.

TSCHOP, M. H., SPEAKMAN, J. R., ARCH, J. R., AUWERX, J., BRUNING, J. C., CHAN, L., ECKEL, R. H., FARESE, R. V., JR., GALGANI, J. E., HAMBLY, C., HERMAN, M. A., HORVATH, T. L., KAHN, B. B., KOZMA, S. C., MARATOS-FLIER, E., MULLER, T. D., MUNZBERG, H., PFLUGER, P. T., PLUM, L., REITMAN, M. L., RAHMOUNI, K., SHULMAN, G. I., THOMAS, G., KAHN, C. R. & RAVUSSIN, E. 2012. A guide to analysis of mouse energy metabolism. *Nat Methods,* 9**,** 57-63.

TUNG, Y. C., AYUSO, E., SHAN, X., BOSCH, F., O'RAHILLY, S., COLL, A. P. & YEO, G. S. 2010. Hypothalamic-specific manipulation of Fto, the ortholog of the human obesity gene FTO, affects food intake in rats. *PLoS One,* 5**,** e8771.

TUPS, A., HELWIG, M., KHOROOSHI, R. M., ARCHER, Z. A., KLINGENSPOR, M. & MERCER, J. G. 2004. Circulating ghrelin levels and central ghrelin receptor expression are elevated in response to food deprivation in a seasonal mammal (Phodopus sungorus). *J Neuroendocrinol,* 16**,** 922-8.

VAN DEN BERG, L., DE WAAL, H. D., HAN, J. C., YLSTRA, B., EIJK, P., NESTEROVA, M., HEUTINK, P. & STRATAKIS, C. A. 2010. Investigation of a patient with a partial trisomy 16q including the fat mass and obesity associated gene (FTO): fine mapping and FTO gene expression study. *Am J Med Genet A,* 152A**,** 630-7.

VAN DER HOEVEN, F., SCHIMMANG, T., VOLKMANN, A., MATTEI, M. G., KYEWSKI, B. & RUTHER, U. 1994. Programmed cell death is affected in the novel mouse mutant Fused toes (Ft). *Development,* 120**,** 2601-7.

VELDERS, F. P., DE WIT, J. E., JANSEN, P. W., JADDOE, V. W., HOFMAN, A., VERHULST, F. C. & TIEMEIER, H. 2012. FTO at rs9939609, food responsiveness, emotional control and symptoms of ADHD in preschool children. *PLoS One,* 7**,** e49131.

VIERKOTTEN, J., DILDROP, R., PETERS, T., WANG, B. & RUTHER, U. 2007. Ftm is a novel basal body protein of cilia involved in Shh signalling. *Development,* 134**,** 2569-77.

VOIGHT, B. F., SCOTT, L. J., STEINTHORSDOTTIR, V., MORRIS, A. P., DINA, C., WELCH, R. P., ZEGGINI, E., HUTH, C., AULCHENKO, Y. S., THORLEIFSSON, G., MCCULLOCH, L. J., FERREIRA, T., GRALLERT, H., AMIN, N., WU, G., WILLER, C. J., RAYCHAUDHURI, S., MCCARROLL, S. A., LANGENBERG, C., HOFMANN, O. M., DUPUIS, J., QI, L., SEGRE, A. V., VAN HOEK, M., NAVARRO, P., ARDLIE, K., BALKAU, B., BENEDIKTSSON, R., BENNETT, A. J., BLAGIEVA, R., BOERWINKLE, E., BONNYCASTLE, L. L., BOSTROM, K. B., BRAVENBOER, B., BUMPSTEAD, S., BURTT, N. P., CHARPENTIER, G., CHINES, P. S., CORNELIS, M., COUPER, D. J., CRAWFORD, G., DONEY, A. S., ELLIOTT, K. S., ELLIOTT, A. L., ERDOS, M. R., FOX, C. S., FRANKLIN, C. S., GANSER, M., GIEGER, C., GRARUP,

N., GREEN, T., GRIFFIN, S., GROVES, C. J., GUIDUCCI, C., HADJADJ, S., HASSANALI, N., HERDER, C., ISOMAA, B., JACKSON, A. U., JOHNSON, P. R., JORGENSEN, T., KAO, W. H., KLOPP, N., KONG, A., KRAFT, P., KUUSISTO, J., LAURITZEN, T., LI, M., LIEVERSE, A., LINDGREN, C. M., LYSSENKO, V., MARRE, M., MEITINGER, T., MIDTHJELL, K., MORKEN, M. A., NARISU, N., NILSSON, P., OWEN, K. R., PAYNE, F., PERRY, J. R., PETERSEN, A. K., PLATOU, C., PROENCA, C., PROKOPENKO, I., RATHMANN, W., RAYNER, N. W., ROBERTSON, N. R., ROCHELEAU, G., RODEN, M., SAMPSON, M. J., SAXENA, R., SHIELDS, B. M., SHRADER, P., SIGURDSSON, G., SPARSO, T., STRASSBURGER, K., STRINGHAM, H. M., SUN, Q., SWIFT, A. J., THORAND, B., *et al.* 2010. Twelve type 2 diabetes susceptibility loci identified through large-scale association analysis. *Nat Genet*.

VON MALTZAHN, J., CHANG, N. C., BENTZINGER, C. F. & RUDNICKI, M. A. 2012. Wnt signaling in myogenesis. *Trends Cell Biol,* 22**,** 602-9.

VOSS, J. D., MASUOKA, P., WEBBER, B. J., SCHER, A. I. & ATKINSON, R. L. 2013. Association of elevation, urbanization and ambient temperature with obesity prevalence in the United States. *Int J Obes (Lond).*

VUJOVIC, P., STAMENKOVIC, S., JASNIC, N., LAKIC, I., DJURASEVIC, S. F., CVIJIC, G. & DJORDJEVIC, J. 2013. Fasting induced cytoplasmic Fto expression in some neurons of rat hypothalamus. *PLoS One,* 8**,** e63694.

WADE, G. N. & HELLER, H. W. 1993. Tamoxifen mimics the effects of estradiol on food intake, body weight, and body composition in rats. *Am J Physiol,* 264**,** R1219-23.

WAHLEN, K., SJOLIN, E. & HOFFSTEDT, J. 2008. The common rs9939609 gene variant of the fat mass- and obesity-associated gene FTO is related to fat cell lipolysis. *J Lipid Res,* 49**,** 607-11.

WAN, E. S., CHO, M. H., BOUTAOUI, N., KLANDERMAN, B. J., SYLVIA, J. S., ZINITI, J. P., WON, S., LANGE, C., PILLAI, S. G., ANDERSON, W. H., KONG, X., LOMAS, D. A., BAKKE, P. S., GULSVIK, A., REGAN, E. A., MURPHY, J. R., MAKE, B. J., CRAPO, J. D., WOUTERS, E. F., CELLI, B. R., SILVERMAN, E. K. & DEMEO, D. L. 2011. Genome-wide association analysis of body mass in chronic obstructive pulmonary disease. *Am J Respir Cell Mol Biol,* 45**,** 304-10.

WANG, K., LI, W. D., ZHANG, C. K., WANG, Z., GLESSNER, J. T., GRANT, S. F., ZHAO, H., HAKONARSON, H. & PRICE, R. A. 2011a. A genome-wide association study on obesity and obesity-related traits. *PLoS One,* 6**,** e18939.

WANG, P., YANG, F. J., DU, H., GUAN, Y. F., XU, T. Y., XU, X. W., SU, D. F. & MIAO, C. Y. 2011b. Involvement of leptin receptor long isoform (LepRb)-STAT3 signaling pathway in brain fat mass- and obesity-associated (FTO) downregulation during energy restriction. *Mol Med,* 17**,** 523-32.

WANG, Y., RAO, K., YUAN, L., EVERAERT, N., BUYSE, J., GROSSMANN, R. & ZHAO, R. 2012. Chicken FTO gene: tissue-specific expression, brain distribution, breed difference and effect of fasting. *Comp Biochem Physiol A Mol Integr Physiol,* 163**,** 246-52.

WARDLE, J., CARNELL, S., HAWORTH, C. M., FAROOQI, I. S., O'RAHILLY, S. & PLOMIN, R. 2008. Obesity associated genetic variation in FTO is associated with diminished satiety. *J Clin Endocrinol Metab,* 93**,** 3640-3.

WARDLE, J., LLEWELLYN, C., SANDERSON, S. & PLOMIN, R. 2009. The FTO gene and measured food intake in children. *Int J Obes (Lond),* 33**,** 42-5.

WEBER, R. E. 2007. High-altitude adaptations in vertebrate hemoglobins. *Respir Physiol Neurobiol,* 158**,** 132-42.

WEHR, E., SCHWEIGHOFER, N., MOLLER, R., GIULIANI, A., PIEBER, T. R. & OBERMAYER-PIETSCH, B. 2010. Association of FTO gene with hyperandrogenemia and metabolic parameters in women with polycystic ovary syndrome. *Metabolism,* 59**,** 575-80.

WELLCOME TRUST CASE CONTROL CONSORTIUM 2007. Genome-wide association study of 14,000 cases of seven common diseases and 3,000 shared controls. *Nature,* 447**,** 661-78.

WESTBYE, M. P., FEYZI, E., AAS, P. A., VAGBO, C. B., TALSTAD, V. A., KAVLI, B., HAGEN, L., SUNDHEIM, O., AKBARI, M., LIABAKK, N. B., SLUPPHAUG, G., OTTERLEI, M. & KROKAN, H. E. 2008. Human AlkB homolog 1 is a mitochondrial protein that demethylates 3-methylcytosine in DNA and RNA. *J Biol Chem,* 283**,** 25046-56.

WHO 2000. Redefining obesity and its treatment: The Asia-Pacific Perspective. February 2000 ed.: Health Communications Australia Pty Limited.

WHO 2008a. Waist Circumference a nd Waist–Hip Ratio: Report of a WHO Expert Consultation Geneva.

WHO 2008b. WHO STEPwise approach to surveillance (STEPS). Geneva.

WILLER, C. J., SPELIOTES, E. K., LOOS, R. J., LI, S., LINDGREN, C. M., HEID, I. M., BERNDT, S. I., ELLIOTT, A. L., JACKSON, A. U., LAMINA, C., LETTRE, G., LIM, N., LYON, H. N., MCCARROLL, S. A., PAPADAKIS, K., QI, L., RANDALL, J. C., ROCCASECCA, R. M., SANNA, S., SCHEET, P., WEEDON, M. N., WHEELER, E., ZHAO, J. H., JACOBS, L. C., PROKOPENKO, I., SORANZO, N., TANAKA, T., TIMPSON, N. J., ALMGREN, P., BENNETT, A., BERGMAN, R. N., BINGHAM, S. A., BONNYCASTLE, L. L., BROWN, M., BURTT, N. P., CHINES, P., COIN, L., COLLINS, F. S., CONNELL, J. M., COOPER, C., SMITH, G. D., DENNISON, E. M., DEODHAR, P., ELLIOTT, P., ERDOS, M. R., ESTRADA, K., EVANS, D. M., GIANNINY, L., GIEGER, C., GILLSON, C. J., GUIDUCCI, C., HACKETT, R., HADLEY, D., HALL, A. S., HAVULINNA, A. S., HEBEBRAND, J., HOFMAN, A., ISOMAA, B., JACOBS, K. B., JOHNSON, T., JOUSILAHTI, P., JOVANOVIC, Z., KHAW, K. T., KRAFT, P., KUOKKANEN, M., KUUSISTO, J., LAITINEN, J., LAKATTA, E. G., LUAN, J., LUBEN, R. N., MANGINO, M., MCARDLE, W. L., MEITINGER, T., MULAS, A., MUNROE, P. B., NARISU, N., NESS, A. R., NORTHSTONE, K., O'RAHILLY, S., PURMANN, C., REES, M. G., RIDDERSTRALE, M., RING, S. M., RIVADENEIRA, F., RUOKONEN, A., SANDHU, M. S., SARAMIES, J., SCOTT, L. J., SCUTERI, A., SILANDER, K., SIMS, M. A., SONG, K., STEPHENS, J., STEVENS, S., STRINGHAM, H. M., TUNG, Y. C., VALLE, T. T., VAN DUIJN, C. M., VIMALESWARAN, K. S., VOLLENWEIDER, P., *et al.* 2009. Six new loci associated with body mass index highlight a neuronal influence on body weight regulation. *Nat Genet,* 41**,** 25-34.

WILLIAMS, G. M., IATROPOULOS, M. J., DJORDJEVIC, M. V. & KALTENBERG, O. P. 1993. The triphenylethylene drug tamoxifen is a strong liver carcinogen in the rat. *Carcinogenesis,* 14**,** 315-7.

WILLIAMS, S., DAVIE, G. & LAM, F. 1999. Predicting BMI in young adults from childhood data using two approaches to modelling adiposity rebound. *Int J Obes Relat Metab Disord,* 23**,** 348-54.

WILLIAMS, S. M. & GOULDING, A. 2009. Patterns of growth associated with the timing of adiposity rebound. *Obesity (Silver Spring),* 17**,** 335-41.

WISSE, B. E., KIM, F. & SCHWARTZ, M. W. 2007. Physiology. An integrative view of obesity. *Science,* 318**,** 928-9.

WOJCIECHOWSKI, P., LIPOWSKA, A., RYS, P., EWENS, K. G., FRANKS, S., TAN, S., LERCHBAUM, E., VCELAK, J., ATTAOUA, R., STRACZKOWSKI, M., AZZIZ, R., BARBER, T. M., HINNEY, A., OBERMAYER-PIETSCH, B., LUKASOVA, P., BENDLOVA, B., GRIGORESCU, F., KOWALSKA, I., GOODARZI, M. O., STRAUSS, J. F., 3RD, MCCARTHY, M. I. & MALECKI, M. T. 2012. Impact of FTO genotypes on BMI and weight in polycystic ovary syndrome: a systematic review and meta-analysis. *Diabetologia,* 55**,** 2636-45.

WOLFE, R. R. 2006. The underappreciated role of muscle in health and disease. *Am J Clin Nutr,* 84**,** 475-82.

WOOD, J. G., ROGINA, B., LAVU, S., HOWITZ, K., HELFAND, S. L., TATAR, M. & SINCLAIR, D. 2004. Sirtuin activators mimic caloric restriction and delay ageing in metazoans. *Nature,* 430**,** 686-9.

WRIGHT, W. S., LONGO, K. A., DOLINSKY, V. W., GERIN, I., KANG, S., BENNETT, C. N., CHIANG, S. H., PRESTWICH, T. C., GRESS, C., BURANT, C. F., SUSULIC, V. S. & MACDOUGALD, O. A. 2007. Wnt10b inhibits obesity in ob/ob and agouti mice. *Diabetes,* 56**,** 295-303.

WU, B., CRAMPTON, S. P. & HUGHES, C. C. 2007a. Wnt signaling induces matrix metalloproteinase expression and regulates T cell transmigration. *Immunity,* 26**,** 227-39.

WU, J., BOSTROM, P., SPARKS, L. M., YE, L., CHOI, J. H., GIANG, A. H., KHANDEKAR, M., VIRTANEN, K. A., NUUTILA, P., SCHAART, G., HUANG, K., TU, H., VAN MARKEN LICHTENBELT, W. D., HOEKS, J., ENERBACK, S., SCHRAUWEN, P. & SPIEGELMAN, B. M. 2012. Beige adipocytes are a distinct type of thermogenic fat cell in mouse and human. *Cell,* 150**,** 366-76.

WU, M., NEILSON, A., SWIFT, A. L., MORAN, R., TAMAGNINE, J., PARSLOW, D., ARMISTEAD, S., LEMIRE, K., ORRELL, J., TEICH, J., CHOMICZ, S. & FERRICK, D. A. 2007b. Multiparameter metabolic analysis reveals a close link between attenuated mitochondrial bioenergetic function and enhanced glycolysis dependency in human tumor cells. *Am J Physiol Cell Physiol,* 292**,** C125-36.

XIA, Q. & GRANT, S. F. 2013. The genetics of human obesity. *Ann N Y Acad Sci,* 1281**,** 178-90.

XIE, H., VALERA, V. A., MERINO, M. J., AMATO, A. M., SIGNORETTI, S., LINEHAN, W. M., SUKHATME, V. P. & SETH, P. 2009. LDH-A inhibition, a therapeutic strategy for treatment of hereditary leiomyomatosis and renal cell cancer. *Mol Cancer Ther,* 8**,** 626-35.

YAFFE, D. & SAXEL, O. 1977. Serial passaging and differentiation of myogenic cells isolated from dystrophic mouse muscle. *Nature,* 270**,** 725-7.

YAN, L., COLANDREA, V. J. & HALE, J. J. 2010. Prolyl hydroxylase domain-containing protein inhibitors as stabilizers of hypoxia-inducible factor: small molecule-based therapeutics for anemia. *Expert Opin Ther Pat,* 20**,** 1219-45.

YANG, J., LOOS, R. J., POWELL, J. E., MEDLAND, S. E., SPELIOTES, E. K., CHASMAN, D. I., ROSE, L. M., THORLEIFSSON, G., STEINTHORSDOTTIR, V., MAGI, R., WAITE, L., SMITH, A. V., YERGES-ARMSTRONG, L. M., MONDA, K. L., HADLEY, D., MAHAJAN, A., LI, G., KAPUR, K., VITART, V., HUFFMAN, J. E., WANG, S. R., PALMER, C., ESKO, T., FISCHER, K., ZHAO, J. H., DEMIRKAN, A., ISAACS, A., FEITOSA, M. F., LUAN, J., HEARD-COSTA, N. L., WHITE, C., JACKSON, A. U., PREUSS, M., ZIEGLER, A., ERIKSSON, J., KUTALIK, Z., FRAU, F., NOLTE, I. M., VAN VLIET-OSTAPTCHOUK, J. V., HOTTENGA, J. J., JACOBS, K. B., VERWEIJ, N., GOEL, A., MEDINA-GOMEZ, C., ESTRADA, K., BRAGG-GRESHAM, J. L., SANNA, S., SIDORE, C., TYRER, J., TEUMER, A., PROKOPENKO, I., MANGINO, M., LINDGREN, C. M., ASSIMES, T. L., SHULDINER, A. R., HUI, J., BEILBY, J. P., MCARDLE, W. L., HALL, P., HARITUNIANS, T., ZGAGA, L., KOLCIC, I., POLASEK, O., ZEMUNIK, T., OOSTRA, B. A., JUNTTILA, M. J., GRONBERG, H., SCHREIBER, S., PETERS, A., HICKS, A. A., STEPHENS, J., FOAD, N. S., LAITINEN, J., POUTA, A., KAAKINEN, M., WILLEMSEN, G., VINK, J. M., WILD, S. H., NAVIS, G., ASSELBERGS, F. W., HOMUTH, G., JOHN, U., IRIBARREN, C., HARRIS, T., LAUNER, L., GUDNASON, V., O'CONNELL, J. R., BOERWINKLE, E., CADBY, G., PALMER, L. J., JAMES, A. L., MUSK, A. W., INGELSSON, E., PSATY, B. M., BECKMANN, J. S., WAEBER, G., VOLLENWEIDER, P., HAYWARD, C., WRIGHT, A. F., RUDAN, I., *et al.* 2012. FTO genotype is associated with phenotypic variability of body mass index. *Nature,* 490**,** 267-72.

YEO, G. S. & HEISLER, L. K. 2012. Unraveling the brain regulation of appetite: lessons from genetics. *Nat Neurosci,* 15**,** 1343-9.

YUAN, H. X., XIONG, Y. & GUAN, K. L. 2013. Nutrient sensing, metabolism, and cell growth control. *Mol Cell,* 49**,** 379-87.

YUAN, S., LI, J., DIENER, D. R., CHOMA, M. A., ROSENBAUM, J. L. & SUN, Z. 2012. Target-of-rapamycin complex 1 (Torc1) signaling modulates cilia size and function through protein synthesis regulation. *Proc Natl Acad Sci U S A,* 109**,** 2021-6.

YUAN, S. & SUN, Z. 2012. TORC1-mediated protein synthesis regulates cilia size and function: implications for organelle size control by diverse signaling cascades. *Cell Cycle,* 11**,** 1750-2.

ZABENA, C., GONZALEZ-SANCHEZ, J. L., MARTINEZ-LARRAD, M. T., TORRES-GARCIA, A., ALVAREZ-FERNANDEZ-REPRESA, J., CORBATON-ANCHUELO, A., PEREZ-BARBA, M. & SERRANO-RIOS, M. 2009. The FTO obesity gene. Genotyping and gene expression analysis in morbidly obese patients. *Obes Surg,* 19**,** 87-95.

ZAN, Y., HAAG, J. D., CHEN, K. S., SHEPEL, L. A., WIGINGTON, D., WANG, Y. R., HU, R., LOPEZ-GUAJARDO, C. C., BROSE, H. L., PORTER, K. I., LEONARD, R. A., HITT, A. A., SCHOMMER, S. L., ELEGBEDE, A. F. & GOULD, M. N. 2003. Production of knockout rats using ENU mutagenesis and a yeast-based screening assay. *Nat Biotechnol,* 21**,** 645-51.

ZEGGINI, E., PANOUTSOPOULOU, K., SOUTHAM, L., RAYNER, N. W., DAY-WILLIAMS, A. G., LOPES, M. C., BORASKA, V., ESKO, T., EVANGELOU, E., HOFFMAN, A., HOUWING-DUISTERMAAT, J. J., INGVARSSON, T., JONSDOTTIR, I., JONNSON, H., KERKHOF, H. J., KLOPPENBURG, M., BOS, S. D., MANGINO, M., METRUSTRY, S., SLAGBOOM, P. E., THORLEIFSSON, G., RAINE, E. V., RATNAYAKE, M., RICKETTS, M., BEAZLEY, C., BLACKBURN, H., BUMPSTEAD, S., ELLIOTT, K. S., HUNT, S. E., POTTER, S. C., SHIN, S. Y., YADAV, V. K., ZHAI, G., SHERBURN, K., DIXON, K., ARDEN, E., ASLAM, N., BATTLEY, P. K., CARLUKE, I., DOHERTY, S., GORDON, A., JOSEPH, J., KEEN, R., KOLLER, N. C., MITCHELL, S., O'NEILL, F., PALING, E., REED, M. R., RIVADENEIRA, F., SWIFT, D., WALKER, K., WATKINS, B., WHEELER, M., BIRRELL, F., IOANNIDIS, J. P., MEULENBELT, I., METSPALU, A., RAI, A., SALTER, D., STEFANSSON, K., STYKARSDOTTIR, U., UITTERLINDEN, A. G., VAN MEURS, J. B., CHAPMAN, K., DELOUKAS, P., OLLIER, W. E., WALLIS, G. A., ARDEN, N., CARR, A., DOHERTY, M., MCCASKIE, A., WILLKINSON, J. M., RALSTON, S. H., VALDES, A. M., SPECTOR, T. D. & LOUGHLIN, J. 2012. Identification of new susceptibility loci for osteoarthritis (arcOGEN): a genome-wide association study. *Lancet,* 380**,** 815-23.

ZEGGINI, E., SCOTT, L. J., SAXENA, R., VOIGHT, B. F., MARCHINI, J. L., HU, T., DE BAKKER, P. I., ABECASIS, G. R., ALMGREN, P., ANDERSEN, G., ARDLIE, K., BOSTROM, K. B., BERGMAN, R. N., BONNYCASTLE, L. L., BORCH-JOHNSEN, K., BURTT, N. P., CHEN, H., CHINES, P. S., DALY, M. J., DEODHAR, P., DING, C. J., DONEY, A. S., DUREN, W. L., ELLIOTT, K. S., ERDOS, M. R., FRAYLING, T. M., FREATHY, R. M., GIANNINY, L., GRALLERT, H., GRARUP, N., GROVES, C. J., GUIDUCCI, C., HANSEN, T., HERDER, C., HITMAN, G. A., HUGHES, T. E., ISOMAA, B., JACKSON, A. U., JORGENSEN, T., KONG, A., KUBALANZA, K., KURUVILLA, F. G., KUUSISTO, J., LANGENBERG, C., LANGO, H., LAURITZEN, T., LI, Y., LINDGREN, C. M., LYSSENKO, V., MARVELLE, A. F., MEISINGER, C., MIDTHJELL, K., MOHLKE, K. L., MORKEN, M. A., MORRIS, A. D., NARISU, N., NILSSON, P., OWEN, K. R., PALMER, C. N., PAYNE, F., PERRY, J. R., PETTERSEN, E., PLATOU, C., PROKOPENKO, I., QI, L., QIN, L., RAYNER, N. W., REES, M., ROIX, J. J., SANDBAEK, A., SHIELDS, B., SJOGREN, M., STEINTHORSDOTTIR, V., STRINGHAM, H. M., SWIFT, A. J., THORLEIFSSON, G., THORSTEINSDOTTIR, U., TIMPSON, N. J., TUOMI, T., TUOMILEHTO, J., WALKER, M., WATANABE, R. M., WEEDON, M. N., WILLER, C. J., ILLIG, T., HVEEM, K., HU, F. B., LAAKSO, M., STEFANSSON, K., PEDERSEN, O., WAREHAM, N. J., BARROSO, I., HATTERSLEY, A. T., COLLINS, F. S., GROOP, L., MCCARTHY, M. I., BOEHNKE, M. & ALTSHULER, D. 2008. Meta-analysis of genome-wide association data and large-scale replication identifies additional susceptibility loci for type 2 diabetes. *Nat Genet,* 40**,** 638-45.

ZEGGINI, E., WEEDON, M. N., LINDGREN, C. M., FRAYLING, T. M., ELLIOTT, K. S., LANGO, H., TIMPSON, N. J., PERRY, J. R., RAYNER, N. W., FREATHY, R. M., BARRETT, J. C., SHIELDS, B., MORRIS, A. P., ELLARD, S., GROVES, C. J., HARRIES, L. W., MARCHINI, J. L., OWEN, K. R., KNIGHT, B., CARDON, L. R.,

WALKER, M., HITMAN, G. A., MORRIS, A. D., DONEY, A. S., MCCARTHY, M. I. & HATTERSLEY, A. T. 2007. Replication of genome-wide association signals in UK samples reveals risk loci for type 2 diabetes. *Science,* 316**,** 1336-41.

ZHANG, G., KARNS, R., NARANCIC, N. S., SUN, G., CHENG, H., MISSONI, S., DURAKOVIC, Z., RUDAN, P., CHAKRABORTY, R. & DEKA, R. 2010. Common SNPs in FTO gene are associated with obesity related anthropometric traits in an island population from the eastern Adriatic coast of Croatia. *PLoS One,* 5**,** e10375.

ZHANG, S. S., KIM, K. H., ROSEN, A., SMYTH, J. W., SAKUMA, R., DELGADO-OLGUIN, P., DAVIS, M., CHI, N. C., PUVIINDRAN, V., GABORIT, N., SUKONNIK, T., WYLIE, J. N., BRAND-ARZAMENDI, K., FARMAN, G. P., KIM, J., ROSE, R. A., MARSDEN, P. A., ZHU, Y., ZHOU, Y. Q., MIQUEROL, L., HENKELMAN, R. M., STAINIER, D. Y., SHAW, R. M., HUI, C. C., BRUNEAU, B. G. & BACKX, P. H. 2011. Iroquois homeobox gene 3 establishes fast conduction in the cardiac His-Purkinje network. *Proc Natl Acad Sci U S A,* 108**,** 13576-81.

ZHANG, Y., PROENCA, R., MAFFEI, M., BARONE, M., LEOPOLD, L. & FRIEDMAN, J. M. 1994. Positional cloning of the mouse obese gene and its human homologue. *Nature,* 372**,** 425-32.

ZHENG, G., DAHL, J. A., NIU, Y., FEDORCSAK, P., HUANG, C. M., LI, C. J., VAGBO, C. B., SHI, Y., WANG, W. L., SONG, S. H., LU, Z., BOSMANS, R. P., DAI, Q., HAO, Y. J., YANG, X., ZHAO, W. M., TONG, W. M., WANG, X. J., BOGDAN, F., FURU, K., FU, Y., JIA, G., ZHAO, X., LIU, J., KROKAN, H. E., KLUNGLAND, A., YANG, Y. G. & HE, C. 2013. ALKBH5 is a mammalian RNA demethylase that impacts RNA metabolism and mouse fertility. *Mol Cell,* 49**,** 18-29.

ZIMMERMANN, E., KRING, S. I., BERENTZEN, T. L., HOLST, C., PERS, T. H., HANSEN, T., PEDERSEN, O., SORENSEN, T. I. & JESS, T. 2009. Fatness-associated FTO gene variant increases mortality independent of fatness--in cohorts of Danish men. *PLoS One,* 4**,** e4428.

ZONCU, R., EFEYAN, A. & SABATINI, D. M. 2011. mTOR: from growth signal integration to cancer, diabetes and ageing. *Nat Rev Mol Cell Biol,* 12**,** 21-35.